BioMed Research International

Latest Treatment Option and Technology Advancement in Corneal and Ocular Surface Disease

Guest Editors: Ciro Costagliola, Mark Batterbury, Harminder Singh Dua, and Leonardo Mastropasqua

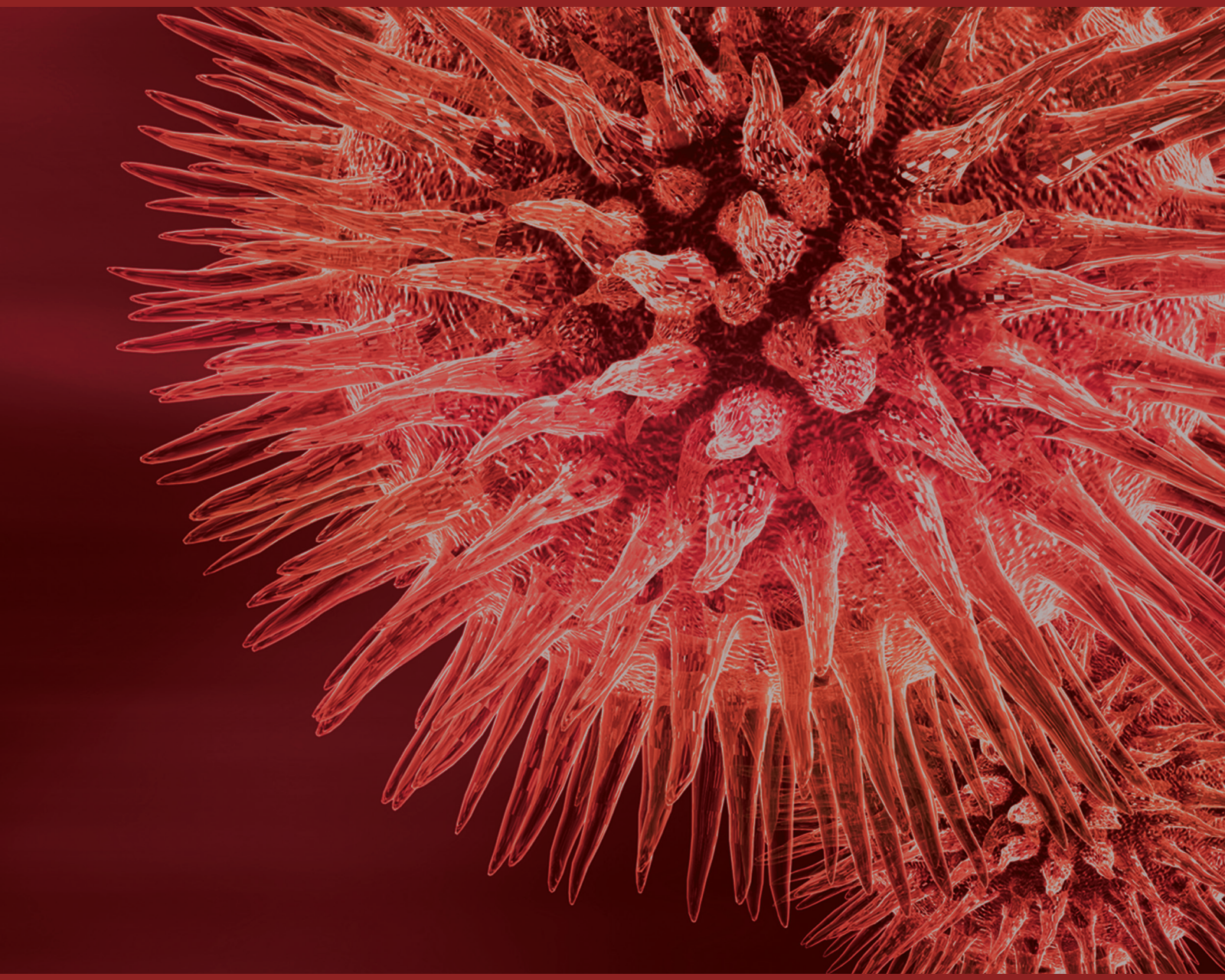

Latest Treatment Option and Technology Advancement in Corneal and Ocular Surface Disease

BioMed Research International

Latest Treatment Option and Technology Advancement in Corneal and Ocular Surface Disease

Guest Editors: Ciro Costagliola, Mark Batterbury, Harminder Singh Dua, and Leonardo Mastropasqu

Contents

Hindawi Publishing Corporation
BioMed Research International
Volume 2014, Article ID 203868, 2 pages
http://dx.doi.org/10.1155/2014/203868

Editorial

Latest Treatment Option and Technology Advancement in Corneal and Ocular Surface Disease

Ciro Costagliola,[1] Mark Batterbury,[2] Harminder Singh Dua,[3] and Leonardo Mastropasqua[4]

[1]*Department of Medicine and Health Sciences, University of Molise, Via F. De Sanctis 1, 86100 Campobasso, Italy*
[2]*Ophthalmology Department, St. Paul's Eye Unit, Royal Liverpool University Hospital, Prescot Street, Liverpool L7 8XP, UK*
[3]*Academic Ophthalmology, Division of Clinical Neuroscience, B Floor, Eye ENT Centre, Queens Medical Centre, University of Nottingham, Nottingham, UK*
[4]*Eye Clinic, University "G. D'Annunzio" Chieti-Pescara, Chieti, Italy*

Correspondence should be addressed to Ciro Costagliola; ciro.costagliola@unimol.it

Received 21 October 2014; Accepted 21 October 2014; Published 28 December 2014

This special issue was focused on the current approaches in the medical and surgical treatment of the most diffuse and important corneal and ocular surface diseases. In addition, the role of current available technologies in the diagnosis and follow-up of patients with ocular surface diseases was also included. We have invited many experts on this topic to highlight the understanding of corneal diseases.

Different topics were exhaustively treated. This allows improving the readers' knowledge on each theme, which is nowadays essential in the correct management of patients.

In detail, M. De Bernardo and coworkers described and discussed the different formulas to overcome the problem of calculating the intraocular lens power in patients that underwent corneal refractive surgery.

L. Mastropasqua and coworkers, focusing on glaucoma surgery, summarized the applications of time and spectral domain anterior segment-OCT in the conjunctival bleb assessment after filtrating surgery. The authors showed the utility of this technology in guiding the clinicians' decisions in the bleb management.

F. Semeraro and coworkers analyzed the potential etiopathogenetic mechanisms involved in the epithelial in growth after Descemet's stripping automated endothelial keratoplasty, reviewing the literature, and discussing the most appropriate therapeutic approaches.

T. Liu and coworkers proposed a relatively safe designed stromal bed thickness to avoid the endothelial damage following lamellar keratoplasty using an Allegretto WaveLight 3 FS200 femtosecond laser.

L. Ambrosone and coworkers evaluated the efficacy of topical verbascoside-based liposomal eye drops in the healing of alkali corneal wound. The authors reported that this approach reduced significantly the first stage of the process of wound healing of the corneal epithelium.

P. Vinciguerra and coworkers compared the biomechanical effect, the riboflavin penetration and distribution in 2 transepithelial corneal collagen cross-linking with iontophoresis (I-CXL), with standard cross-linking (S-CXL) and current transepithelial protocol (TE-CXL), in rabbits. The authors found that I-CXL induced a significant increase in corneal stiffness as well as better riboflavin penetration when compared to controls and TE-CXL, but not to S-CXL.

M. Lanza and coworkers evaluated the correlation between corneal biomechanical and morphological data in healthy eyes, eyes that underwent myopic photorefractive keratectomy (PRK), keratoconus affected eyes, and keratoconus affected eyes that underwent corneal collagen cross-linking (CCC). The authors suggested suggest that corneal curvature would have a greater influence on corneal deformation than corneal thickness.

L. Mastropasqua and coworkers quantified the effect of small incision lenticule extraction (SMILE) on the corneal biomechanics using Scheimpflug noncontact tonometer (CORVIS ST). The authors did not find significant modifications in biomechanical properties after SMILE, suggesting that this procedure could induce only minimal transient alterations of corneal biomechanics.

F. Semeraro and coworkers evaluated the efficacy of 50% autologous serum eye drops in ocular surface diseases not improved by conventional therapy reporting that this treatment effectively stabilized and improved signs and symptoms in patients' affected chemical burns, recurrent corneal erosion, neurotropic keratitis, and keratoconjunctivitis sicca.

A. Hill-Bator and coworkers reported a high cytoprotective ability of trehalose-based eye drops both in viable epithelial corneal cell number after the desiccation and in preservation of cellular functions.

Finally, D. Viswanathan and coworkers evaluated the efficacy of corneal collagen cross-linking for progressive keratoconus in pediatric patients, reporting the treatment as an effective option in stabilizing the condition and reducing the need for corneal grafting.

In summary, the papers published in this special issue confirm the progress in both research and treatment of corneal and ocular surface disease.

The guest editors wish to thank all the authors of this special issue for contributing the high quality papers. We would also like to thank the referees who have critically evaluated the papers.

Ciro Costagliola
Mark Batterbury
Harminder Singh Dua
Leonardo Mastropasqua

Hindawi Publishing Corporation
BioMed Research International
Volume 2014, Article ID 404587, 12 pages
http://dx.doi.org/10.1155/2014/404587

Research Article

Imaging Mass Spectrometry by Matrix-Assisted Laser Desorption/Ionization and Stress-Strain Measurements in Iontophoresis Transepithelial Corneal Collagen Cross-Linking

Paolo Vinciguerra,[1] Rita Mencucci,[2] Vito Romano,[3] Eberhard Spoerl,[4] Fabrizio I. Camesasca,[1] Eleonora Favuzza,[2] Claudio Azzolini,[5] Rodolfo Mastropasqua,[6] and Riccardo Vinciguerra[1,5]

[1] *Humanitas Clinical and Research Center, Via Manzoni 56, Rozzano, Italy*
[2] *Department of Surgery and Translational Medicine, Eye Clinic, University of Florence, Florence, Italy*
[3] *Department of Ophthalmology, Second University of Naples, Naples, Italy*
[4] *University Hospital Carl Gustav Carus, Dresden, Germany*
[5] *Department of Surgical and Morphological Sciences, Section of Ophthalmology, School of Medicine, University of Insubria, Via Guicciardini 9, Varese, Italy*
[6] *Ophthalmology Unit, Department of Neurological Neuropsychological, Morphological and Movement Sciences, University of Verona, Verona, Italy*

Correspondence should be addressed to Riccardo Vinciguerra; riccardovinciguerra@yahoo.it

Received 28 April 2014; Accepted 14 August 2014; Published 2 September 2014

Academic Editor: Leonardo Mastropasqua

Purpose. To compare biomechanical effect, riboflavin penetration and distribution in transepithelial corneal collagen cross-linking with iontophoresis (I-CXL), with standard cross linking (S-CXL) and current transepithelial protocol (TE-CXL). *Materials and Methods.* The study was divided into two different sections, considering, respectively, rabbit and human cadaver corneas. In both sections corneas were divided according to imbibition protocols and irradiation power. Imaging mass spectrometry by matrix-assisted laser desorption/ionization (MALDI-IMS) and stress-strain measurements were used. Forty-eight rabbit and twelve human cadaver corneas were evaluated. *Results.* MALDI-IMS showed a deep riboflavin penetration throughout the corneal layers with I-CXL, with a roughly lower concentration in the deepest layers when compared to S-CXL, whereas with TE-CXL penetration was considerably less. In rabbits, there was a significant increase (by 71.9% and $P = 0.05$) in corneal rigidity after I-CXL, when compared to controls. In humans, corneal rigidity increase was not significantly different among the subgroups. *Conclusions.* In rabbits, I-CXL induced a significant increase in corneal stiffness as well as better riboflavin penetration when compared to controls and TE-CXL but not to S-CXL. Stress-strain in human corneas did not show significant differences among techniques, possibly because of the small sample size of groups. In conclusion, I-CXL could be a valid alternative to S-CXL for riboflavin delivery in CXL, preserving the epithelium.

1. Introduction

Keratoconus is a slowly progressive, asymmetric, bilateral degenerative corneal disease [1]. The architecture of keratoconic cornea is characterized not only by a different distribution and expression of collagen fibrils, but also by an alteration of interfibrillary distance, therefore reducing corneal stability [2]. Corneal collagen cross-linking (CXL) is presently the only treatment that can relent or arrest progressive ectasia [3–5]. It is based on a photooxidative

reaction, catalyzed by riboflavin (vitamin B2), and it induces a biomechanical response that enhances corneal stiffness and blocks the progression of the disease [3, 5–7]. This bears consequences on corneal biomechanics, with visual acuity, morphological and functional indices improving up to 48 months postoperatively and possibly more [3–5]. Standard CXL (S-CXL) technique involves the removal of corneal epithelium to allow penetration of riboflavin. Epithelial debridement causes pain [8] and an increased risk of corneal infection [9] in the immediate postoperative period, as well as visual loss during the first months after treatment [4]. In the attempt to avoid these disadvantages, transepithelial CXL (TE-CXL) technique was introduced, with a protocol based on a specially formulated riboflavin solution, Ricrolin TE (Sooft, Montegiorgio, FM, Italy), featuring two enhancers, trometamol and sodium EDTA, in order to improve stromal penetration.

There are several long-term follow-up studies [3, 4, 6, 7, 10, 11], all adopting the standard technique, while there are only few reports on long-term results of TE-CXL, with controversial outcomes [12–16].

The use of enhancers is not the only way to increase riboflavin penetration through an intact epithelium. Another possibility is iontophoresis, a technique in which the drug is applied with an electrode of the same drug charge. A ground electrode, of opposite charge, is placed elsewhere on the body to complete the electric circuit. The drug serves as a conductor of the current through the tissue. Riboflavin penetration and distribution in the cornea using this technique remains controversial [17, 18].

The aim of this study was to evaluate corneal iontophoresis as a possible alternative to riboflavin corneal stromal impregnation without removing the epithelium, assessing riboflavin corneal penetration and distribution along with the best UV irradiation power to obtain adequate outcomes.

Initially, we evaluated riboflavin corneal penetration and distribution in rabbit eyes following different soaking protocols: standard, transepithelial, and iontophoresis-assisted corneal imbibition. Then we evaluated the biomechanical effect of iontophoresis corneal collagen cross-linking (I-CXL) with stress-strain measurements in rabbits and ex vivo human corneas.

2. Material and Methods

The study was divided in two different sections, one on pigmented rabbits (strain GD79b) and one on human cadaver corneas. One group of rabbit corneas was utilized to evaluate riboflavin distribution in the tissue with imaging mass spectrometry by matrix-assisted laser desorption/ionization (MALDI-IMS), whereas a second one, as well as the human corneas, was used for the evaluation of stress-strain.

The experiments were performed in the laboratory of Humanitas Clinical and Research Center, Rozzano, and in the Eye Clinic, University of Florence, Italy while the biomechanical assay was accomplished at the University Hospital Carl Gustav Carus, Dresden, Germany. Different riboflavin solutions and cross-linking techniques were evaluated.

We hereafter describe the different riboflavin solutions and cross-linking techniques adopted.

2.1. Riboflavin Solutions. Riboflavin preparations used were as follows: Riboflavin 0.1% with dextran T500 20% (Ricrolin, Sooft, Montegiorgio, FM, Italy); Riboflavin 0.1% with dextran T500 15%, plus EDTA and trometamol enhancers (Ricrolin TE, Sooft, Montegiorgio, FM, Italy); Riboflavin 0.1%, dextran free, with NaCl, plus EDTA and trometamol enhancers (Ricrolin preparation A, Sooft, Montegiorgio, FM, Italy); Riboflavin 0.1%, specifically formulated for iontophoresis, dextran free, without NaCl, plus EDTA and trometamol enhancers (Ricrolin +, Sooft, Montegiorgio, FM, Italy).

2.2. Standard Cross-Linking Technique

2.2.1. Imbibition. S-CXL was done according to the Dresden protocol [5]. The corneal epithelium was mechanically removed in a central 9-mm diameter area. A solution of riboflavin 0.1% and dextran 20% (Ricrolin Sooft, Montegiorgio, Italy) was instilled every minute for 30 minutes to fully irrigate the cornea.

2.2.2. Irradiation. A 7.5 mm diameter of the central cornea was then irradiated with an irradiance of 3 mW/cm^2 (VEGA CBM x-linker, C.S.O, Florence, Italy) for 30 minutes. The solution was instilled every 5 minutes during the UVA treatment.

2.3. Transepithelial Cross-Linking Technique

2.3.1. Imbibition. In TE-CXL, Ricrolin TE was applied on the corneas every minute for 30 minutes.

2.3.2. Irradiation. The central cornea was then similarly irradiated with an irradiance of 3 mW/cm^2 (VEGA CBM x-linker, C.S.O, Florence, Italy) for 30 minutes. The solution was instilled every 5 minutes during the UVA treatment.

2.4. Iontophoresis Cross-Linking Technique

2.4.1. Imbibition. Soaking time with iontophoresis in rabbit and human corneas was performed without the removal of the corneal epithelium, using the same iontophoretic device. This consists of two disposable components: an ocular applicator and a return electrode, both connected to a reusable generator. In rabbit corneas the ocular applicator consisted of a 10 mm wide—4.5 mm high round polycarbonate reservoir, filled with medical foam PUR (Advanced Medical Solutions BV, Etten-Leur, Netherlands) and a stainless steel electrode connected to the generator (cathode). The return electrode was a 25 G intradermic needle, inserted in the rabbit's neck (front side) and connected with a crocodile clip and lead to the generator (anode). A constant current generator (I-ON XL, Sooft, Montegiorgio, FM, Italy) was used, with a setting range of 1 mA for 5 minutes. The voltage applied during the study was measured with a multimeter.

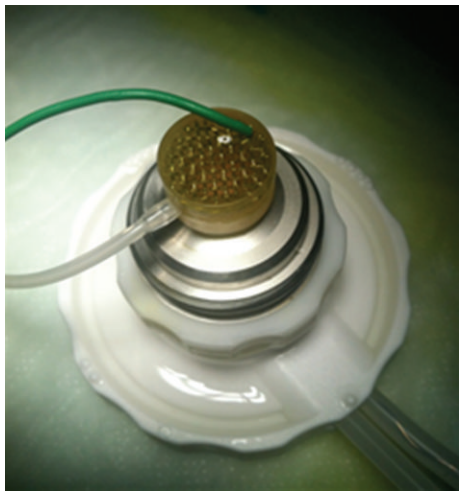

Figure 1: Iontophoresis applicator for human donor corneas.

In human corneas, a 8 mm-wide iontophoretic application device was placed on the corneal surface using an annular suction ring. The device was filled with approximately 0.5 mL solution from the open proximal side, until the electrode (stainless steel mesh) was covered. The device was connected to the constant current generator for 5 minutes (I-ON XL, Sooft, Montegiorgio, FM, Italy) set at 1 mA (the total dose of 5 mA/5 min was monitored by the generator). Human corneas were placed on an artificial anterior chamber (Moria USA, Doylestown, PA) and the return electrode was a stainless steel wire inserted into one of the pressure tubes, underneath the corneas, in the artificial anterior chamber. The two tubes were connected to a perfusion line allowing BSS circulation during the study (Figure 1). Attention was paid to eliminate any air bubble in the circuit.

2.4.2. Irradiation. Irradiation power in rabbits and human I-CXL corneas was either 3 mW for 30 minutes or 10 mW for 9 minutes (VEGA CBM x-linker, C.S.O, Florence, Italy) according to the group of randomization.

2.4.3. Rabbit Corneas. Twenty-four pigmented rabbits (twelve for the MALDI-IMS experiment and twelve for stress-strain measurements), aged 2 to 3 months, with a weight ranging from 2.0 kg to 2.5 kg, were used. All animals were healthy and free of ocular disease. Rabbits were handled according to the European Commission and the Association for Research in Vision and Ophthalmology (ARVO) Statement for the Use of Animals in Ophthalmic and Vision Research. Rabbits were anesthetized with a mixture of ketamine and xylazine hydrochloride. After the treatment, the animals were euthanized by an intravenous injection of overdosed pentobarbital and all efforts were made to minimize suffering.

In the MALDI-IMS study all rabbits eyes (24 eyes) were used for imbibition assessment, conversely in the stress-strain study (24 eyes) one eye of each rabbit was treated as randomized, the other eye was included in the sham group.

2.5. Imaging Mass Spectrometry by Matrix-Assisted Laser Desorption/Ionization (MALDI-IMS) Study. The experiments were performed in the Eye Clinic, University of Florence, Italy. In order to study tissue distribution of riboflavin, IMS was used. IMS is a relatively new technique that allows detecting the presence of a substance in a tissue without labelling it [19]. In particular, MALDI-IMS is able to identify a compound or its metabolites by detecting specific peaks in their mass spectra with a histologic resolution of about 50 μm. It has recently been used for pharmacokinetics studies of drug distribution in the eye [20].

MALDI ion source is formed by a nitrogen laser with UV emission. The laser gives energy to the matrix crystals causing desorption and ionization. Matrix and analytes (in ionic form) enter the mass spectrometer analyser and are detected.

Twenty-four rabbit eyes were evaluated. They were divided into three groups composed of eight eyes of four rabbits each, according to the different imbibition protocols: S-CXL, TE-CXL, and I-CXL. In order to evaluate riboflavin corneal penetration and distribution following different soaking protocols and differently from those involved in the stress-strain study, these eyes were not irradiated after the imbibition procedure.

After sacrifice, whole ocular globes were dissected and frozen with isopentane vapor at −80°C. Corneas of enucleated globes were cut in frontal sections (slice thickness about 20 μm) using a cryostat-microtome (Figure 2). Cornea sections were placed on a histology glass and dried under low vacuum inside a desiccator for 2 hours and then coated with a MALDI matrix: α-cyano-hydroxycinnamic acid 10 g/l solution in 50% acetonitrile, plus 0,1% TFA and equimolar quantity of aniline. Matrix coating was done by an automated spraying device (ImagePrep, Bruker Daltonics, Billerica, MA, USA). Every sample was then analysed using a high resolution hybrid MALDI-mass spectrometer. Sample analyses were conducted in raster mode at 50 μm raster size, collecting 20 laser shots at 5 μj laser energy, allowing the estimation of riboflavin localization and distribution inside the corneal layers. Riboflavin fragment ion at m/z 243.087 was used for detection into a tandem mass (product ion scan) experiment with 60.000 resolution power. The image was plotted into a colour scale related to the estimated riboflavin quantity for a single voxel (volume of approximately 5×10^{-5} mm^3) and it represents the riboflavin fragment ion distribution inside this tissue section (Figure 2(a)). The intensity of the ion signal (correlated with the colour scale) is proportional to the riboflavin amount in that given point. For the semiquantitative estimation of riboflavin we used a control tissue, spotted with riboflavin standard solution, running an external calibration curve. Every sample of every group was repeated on at least 5 tissue sections deriving from the same animals (technical replicates). The value presented

was averaged on these replicates. Every point of the plot is described by one tandem mass spectrum of the riboflavin (Figure 3(c)).

After IMS analysis, samples were washed with ethanol for matrix removal and prepared for haematoxylin-eosin staining following a standard staining protocol (Figure 3(b)).

Haematoxylin-eosin preparations permit to have an overview of the histological structure of the tissue and to visually locate the topographical distribution of the substance, overlapping it with the IMS images.

2.6. Biomechanical Study. The biomechanical study was divided in two different sections: a study on pigmented rabbits (twenty-four eyes) and one on human cadaver corneas (twelve). The experiments were performed in the laboratory of Humanitas Clinical and Research Center, Rozzano, while the biomechanical assay was performed at the University Hospital Carl Gustav Carus, Dresden, Germany.

2.6.1. Rabbit Corneas. Twelve pigmented rabbits were studied following the same procedure and handling specified above.

They were randomly divided into four groups of three animals each. The groups differed in type of riboflavin used and soaking time: TE-CXL, iontophoresis imbibition with Ricrolin TE, iontophoresis imbibition with Ricrolin prep A, and iontophoresis imbibition with Ricrolin + (see also Table 1). Randomization in the treatment groups was done using Excel software (Microsoft Office 2007). One eye of each rabbit was treated as randomized; the other eye was included in the sham group.

All treated eyes were irradiated with a power of 3 mW for 30 minutes.

Immediately after sacrifice, both eyes were quickly and carefully sampled, weighed, and stored in a wet chamber at 4°C (histological screw cap container filled with cotton soaked with 0,9% saline), until shipment for assay. The sampling time was equal for each rabbit (10 minutes). Central corneal thickness (CCT) was measured with a pachymeter (Pach-Pen XL; Mentor, Norwell, MA, USA) and mean CCT was 708.6 ± 52.9 μm. The corneoscleral ring was removed and the cornea was cut into 2 equal strips 5 mm wide and 7 mm long including 1 mm of sclera on both ends.

2.6.2. Human Corneas. Twelve single human corneal-scleral discs, and qualified for research use, were obtained by the biorepository of The Veneto Eye Bank Foundation, Venice (Italy). Before recovery, a written consent from donor's relatives was obtained, in order to get permission for surgical and alternative uses (i.e., education, training, and research purposes).

Corneas were collected after a mean postmortem interval of 6.3 hours (min 1.95, max 9.25 hours), and deemed unsuitable for transplantation because of donor contraindications, other than serology, or stromal abnormalities. These tissues were evaluated, stored in culture according to conventional eye banking procedures [21], and used for our protocols after a mean storage time of 120.4 hours (min 96, max 135.5 hours). All corneas (mean donor's age 63.1, min 43.2, max 73.5 years) displayed a healthy, uninterrupted epithelium. 24 hours before use, tissues were transferred in culture medium +6% dextran, according to conventional organ culture technique, to allow deturgescence. Central endothelial cell density and viability (tripan blu staining) were measured before use. The mean endothelial density was 2400 cells/mm^2 (min 2200, max 2800 cells/mm^2), with no evidence of cell mortality.

To reduce the variances in the stress-strain measurements due to different postmortem times and degrees of autolysis, the human corneas were uniformly divided into groups, taking account of the age of the donor values of post mortem interval and mean storage time.

The human corneas were randomly divided into four groups distinguished by method of impregnation and irradiation power, as reported in Table 2. Group A was the S-CXL treatment which entails epithelial debridement, passive soaking, and 3 mW UV-A power for 30 minutes; group B comprised 3 corneas treated with TE-CXL with passive transepithelial soaking and 3 mW UV-A power for 30 minutes; groups C and D were both impregnated with iontophoresis in 5 minutes, however group C was then irradiated with a power of 3 mW for 30 minutes whereas group D with 10 mW for 9 minutes. The randomization in two different irradiation powers for I-CXL was to evaluate if, giving the different impregnation method (I-CXL), the irradiance power had any influence in the results. Corneoscleral discs were gently grasped by the scleral rim and carefully mounted on a perfused artificial anterior chamber (Figure 1) (Moria USA, Doylestown, PA), with the endothelial side down. Once the disc was properly mounted, the epithelium was evaluated under microscope and CCT was determined using an ultrasound pachymeter (SP-2000; Tomey, Erlangen, Germany), showing a mean value of 572.6 ± 71.9 μm. Following treatment, each donor tissue was cut into two equal strips 4 mm wide and 14 mm long including 1 mm of sclera on both ends.

2.7. Static Stress-Strain Measurements. Static stress-strain measurements of the corneas were performed using a microcomputer-controlled biomaterial tester (Minimat, Rheometric Scientific GmbH) with a prestress of 5×10^3 Pa in the human corneas and 10×10^3 Pa in the rabbit corneas (1 Pa = 1 N/m^2). Vertical strips were clamped in the stress-strain device. The distance of the clamps was 7 mm, the load was 5 N, and the preload was 20 mN in the rabbit corneas, while in the human corneas the load was 5 N and the preload was 10 mN. The stress-stain curves were fitted with an exponential function $\sigma = A \exp(B \times \varepsilon)$ using the SPSS-calculation program (SPSS GmbH Software, Munich) and the Young's modulus (relation between tangential force and cross-sectional area) was calculated for 4%, 6%, 8%, and 10% strains as the gradient of the stress-strain graph.

2.8. Statistical Evaluation. Statistical analysis was performed using the STATA statistics software version 11.0 (STATA, Texas, USA). Data are described by mean and standard deviation. To test whether more than two independent

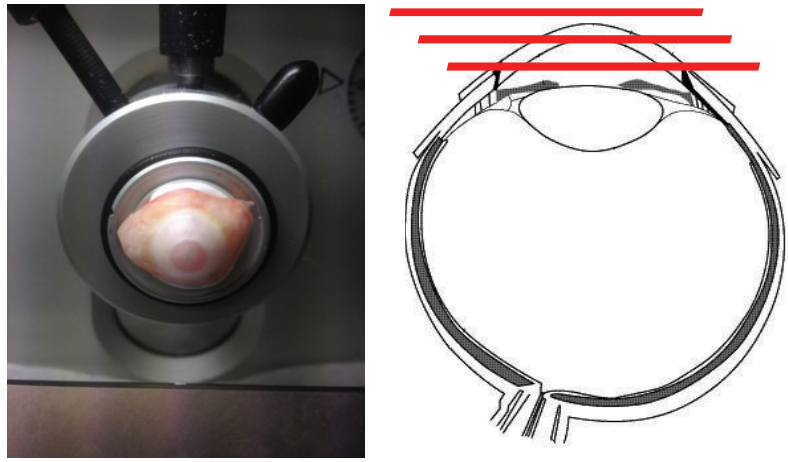

(a) (b)

Figure 2: Corneal section preparation for MALDI-IMS. Corneas of enucleated globes were cut in frontal sections (slice thickness about 20 μm) using a cryostat-microtome.

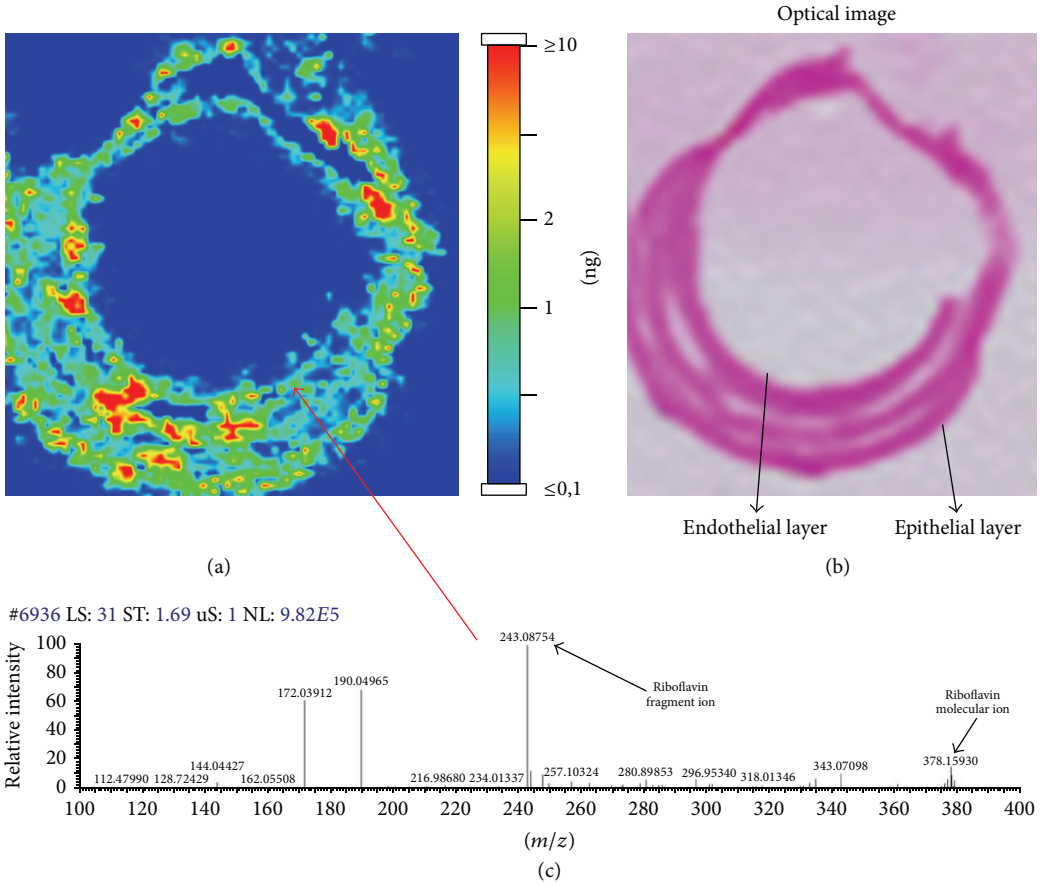

Figure 3: Example of a MALDI-MS imaging of a corneal section soaked with riboflavin, with the colour scale (a). Haematoxylin-eosin stained samples after MALDI-MS imaging and matrix removal (b). Example of MALDI-IMS spectrum of riboflavin that describe one point of the plot (c).

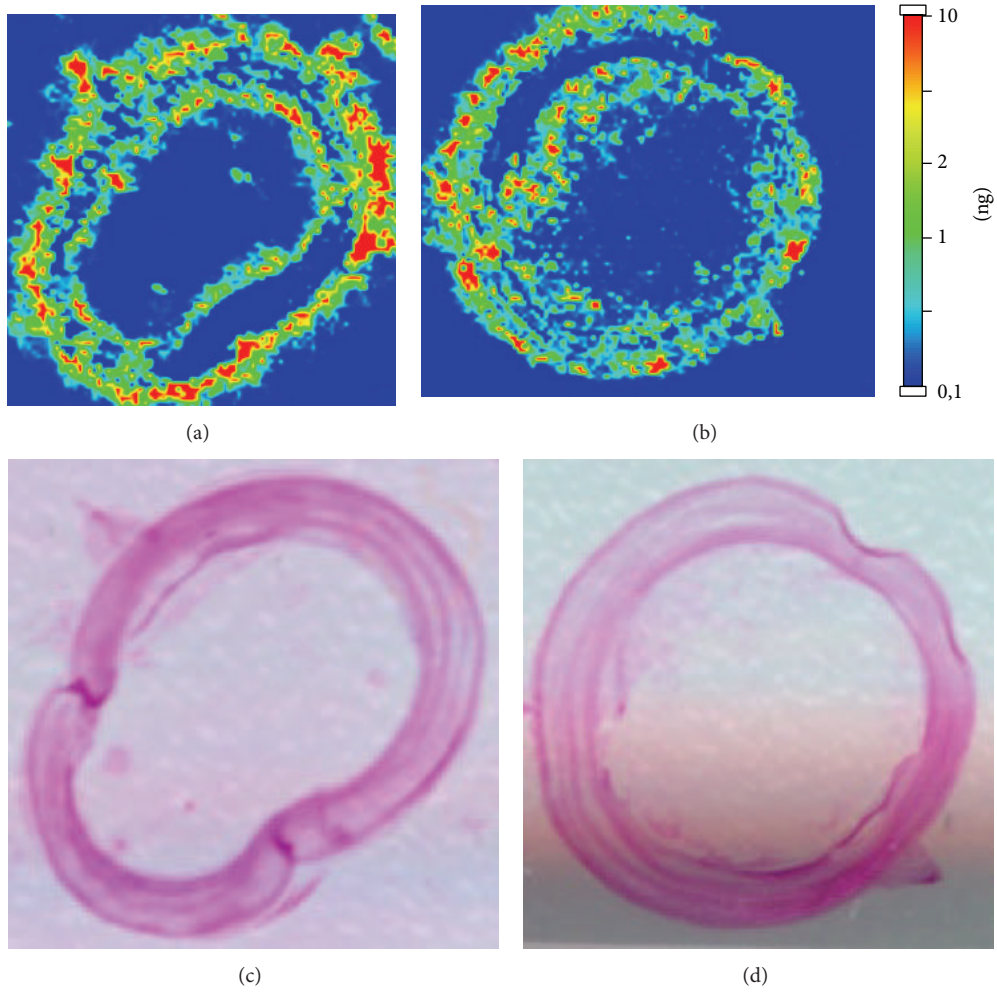

Figure 4: Standard group: MALDI-MS Imaging (a and b) and haematoxylin-eosin staining (c and d) of two corneal samples of two different eyes.

Table 1: Allocation of rabbits in the treatment groups, each rabbit showed right eye treated and left eye untreated.

	Group 1	Group 2	Group 3	Group 4
Number of corneas untreated	3	3	3	3
Number of corneas treated	3	3	3	3
Riboflavin	Ricrolin TE	Ricrolin Prep A	Ricrolin +	Ricrolin TE
Epithelium debridement	NO	NO	NO	NO
Soaking time (minutes)	5	5	5	30
Iontophoresis	YES	YES	YES	NO
Irradiation power (mW/cm^2)	3	3	3	3
Irradiation time (minutes)	30	30	30	30

samples originate from the same distribution we used a nonparametric method, the Kruskal-Wallis one-way analysis of variance by ranks. The Mann-Whitney test for unpaired data was applied to assess the significance of differences between control and treated data from the rabbits, using the same level of significance ($P \leq 0.05$) in all cases.

3. Results

3.1. MALDI-IMS Riboflavin Penetration. In the standard group, riboflavin was distributed throughout the cornea. Hot colour spots were detected in all corneal layers in depth and up to the limbus (Figure 4).

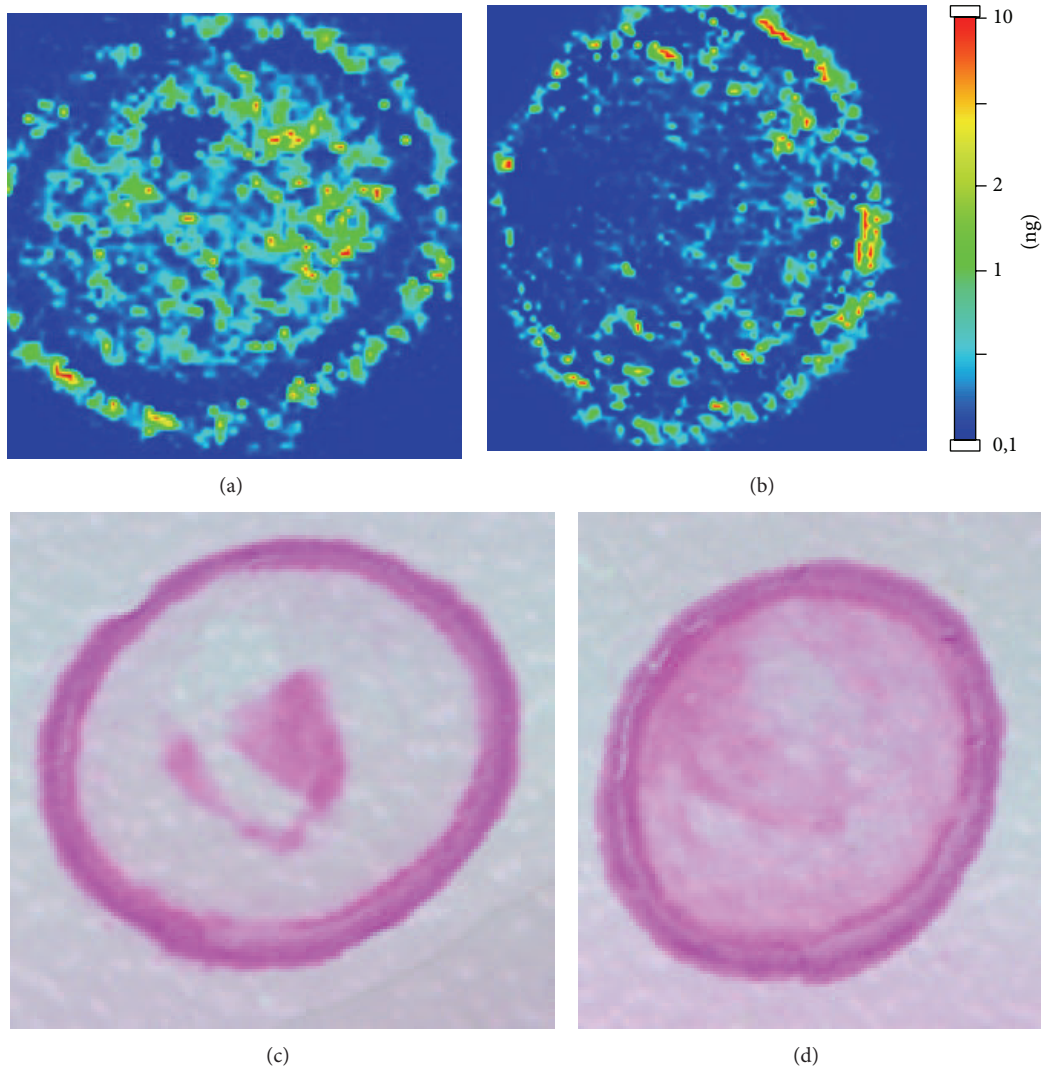

Figure 5: Transepithelial group: MALDI-MS imaging (a and b) and haematoxylin-eosin staining (c and d) of two corneal samples of two different eyes.

Conversely, in the transepithelial group the penetration of riboflavin was reduced in comparison with the standard group of almost 20%. Only faint hot spots can be detected (Figure 5).

Riboflavin in the iontophoresis group was distributed throughout the corneal layers, in depth, and up to the limbus, with a slightly lower concentration in the deepest layers compared to the standard group (Figure 6).

3.2. Biomechanical Essay

3.2.1. Stress-Strain Curve. The stress-strain curves in both experiments presented the typical exponential increase of a bioviscoelastic solid (Figures 7 and 8).

In rabbit corneas, there was no statistically significant difference between CCT between treated and untreated eyes in the four subgroups ($P = 0.8$, $P = 0.6$, $P = 0.5$, and $P = 0.4$). Stress-strain results of the different groups are summarized in Table 3. In Group 3 (I-CXL) the stress using 10% strain was $603,3 \pm 316,7 \times 10^3$ Pa in the treated corneas and $260,7 \pm 40,5 \times 10^3$ Pa in the untreated corneas, corresponding to a 71.9% increase (Figure 7). The difference was statistically significant ($P = 0.05$).

In human corneas, there was no statistically significant difference between CCT of several subgroups ($P = 0.06$). The stress using 4%, 6%, 8%, and 10% strains was not significantly different among subgroups ($P = 0.2$, $P = 0.2$, $P = 0.1$, and $P = 0.09$, resp.), but there was a tendency to a better result with S-CXL. However, one cornea of this group showed an abnormally high result. Stress values with a 10% strain are summarized in Table 4.

3.2.2. Young's Modulus. To calculate Young's modulus, the stress-strain values were fitted with an exponential function $\sigma = A \exp(B \times \varepsilon)$.

Table 2: Allocation of human corneas in the treatment groups.

	S-CXL (Group A)	TE-CXL (Group B)	I-CXL 3 mW (Group C)	I-CXL 10 mW (Group D)
Number of corneas	3	3	3	3
Riboflavin	Ricrolin	Ricrolin TE	Ricrolin +	Ricrolin +
Epithelium debridement	YES	NO	NO	NO
Soaking time (minutes)	30	30	10	10
Iontophoresis	NO	NO	YES	YES
Irradiation power (mW/cm^2)	3	3	30	10
Irradiation time (minutes)	30	30	30	9

Table 3: Stress value for 4%, 6%, 8%, and 10% strains in rabbit corneas.

Groups	Stress at 4% (10^3 Pa)	Stress at 6% (10^3 Pa)	Stress at 8% (10^3 Pa)	Stress at 10% (10^3 Pa)
Group 1				
Untreated	55.7 ± 17.16 ($E = 1.1 \times 10^6$ Pa)	101 ± 37.72 ($E = 1.8 \times 10^6$ Pa)	171.3 ± 73.89 ($E = 3 \times 10^6$ Pa)	270.3 ± 119.1 ($E = 4.8 \times 10^6$ Pa)
Treated	51.3 ± 11.8 ($E = 1 \times 10^6$ Pa)	93.7 ± 29.5 ($E = 1.7 \times 10^6$ Pa)	157.7 ± 59.7 ($E = 2.7 \times 10^6$ Pa)	249.0 ± 100.5 ($E = 4.3 \times 10^6$ Pa)
Group 2				
Untreated	57.3 ± 13.2 ($E = 1.2 \times 10^6$ Pa)	104.7 ± 31.0 ($E = 1.9 \times 10^6$ Pa)	181.0 ± 59.1 ($E = 3.2 \times 10^6$ Pa)	287.7 ± 88.9 ($E = 5.2 \times 10^6$ Pa)
Treated	56.3 ± 6.6 ($E = 1.1 \times 10^6$ Pa)	96.7 ± 12.7 ($E = 1.7 \times 10^6$ Pa)	164.0 ± 27.4 ($E = 2.8 \times 10^6$ Pa)	254.3 ± 37.8 ($E = 4.5 \times 10^6$ Pa)
Group 3				
Untreated	52.7 ± 9.6 ($E = 1.1 \times 10^6$ Pa)	94.7 ± 16.5 ($E = 1.8 \times 10^6$ Pa)	160 ± 25.2 ($E = 3 \times 10^6$ Pa)	260.7 ± 40.5 ($E = 4.9 \times 10^6$ Pa)
Treated	88.3 ± 26.3 ($E = 2 \times 10^6$ Pa)	184.3 ± 75.8 ($E = 3.6 \times 10^6$ Pa)	351.7 ± 171 ($E = 6.3 \times 10^6$ Pa)	603.3 ± 316.7 ($E = 11.0 \times 10^6$ Pa)
Group 4				
Untreated	63.7 ± 14.0 ($E = 1.1 \times 10^6$ Pa)	112.7 ± 22.4 ($E = 1.8 \times 10^6$ Pa)	187.3 ± 31.6 ($E = 2.8 \times 10^6$ Pa)	292.7 ± 45.5 ($E = 4.4 \times 10^6$ Pa)
Treated	51.7 ± 15.3 ($E = 0.9 \times 10^6$ Pa)	87.0 ± 26.9 ($E = 1.5 \times 10^6$ Pa)	134.0 ± 43.3 ($E = 2.3 \times 10^6$ Pa)	201.3 ± 60.2 ($E = 3.6 \times 10^6$ Pa)

Legenda. *E*: calculated Young's modulus.

Table 4: Stress value for 4%, 6%, 8%, and 10% strains in human corneas.

Groups	Stress at 4% (10^3 Pa)	Stress at 6% (10^3 Pa)	Stress at 8% (10^3 Pa)	Stress at 10% (10^3 Pa)
Group A				
S-CXL	194.3 ± 86.7 ($E = 3.2 \times 10^6$ Pa)	349.3 ± 193.8 ($E = 6 \times 10^6$ Pa)	574.3 ± 309.9 ($E = 11.3 \times 10^6$ Pa)	850.3 ± 487.4 ($E = 21.4 \times 10^6$ Pa)
Group B				
TE-CXL	114 ± 32.4 ($E = 1.8 \times 10^6$ Pa)	200.6 ± 50.8 ($E = 3.1 \times 10^6$ Pa)	308.6 ± 58.1 ($E = 5.2 \times 10^6$ Pa)	437.6 ± 53.4 ($E = 8.6 \times 10^6$ Pa)
Group C				
I-CXL 3 mW	123.6 ± 47.5 ($E = 2.2 \times 10^6$ Pa)	238.3 ± 57.2 ($E = 3.8 \times 10^6$ Pa)	388.3 ± 44.8 ($E = 6.7 \times 10^6$ Pa)	576 ± 45 ($E = 11.8 \times 10^6$ Pa)
Group D				
I-CXL 10 mW	150.3 ± 61.6 ($E = 2.9 \times 10^6$ Pa)	276.9 ± 115.4 ($E = 5.2 \times 10^6$ Pa)	449.7 ± 184.4 ($E = 9.3 \times 10^6$ Pa)	661.75 ± 280.9 ($E = 16.6 \times 10^6$ Pa)

Legenda. *E*: calculated Young's modulus.

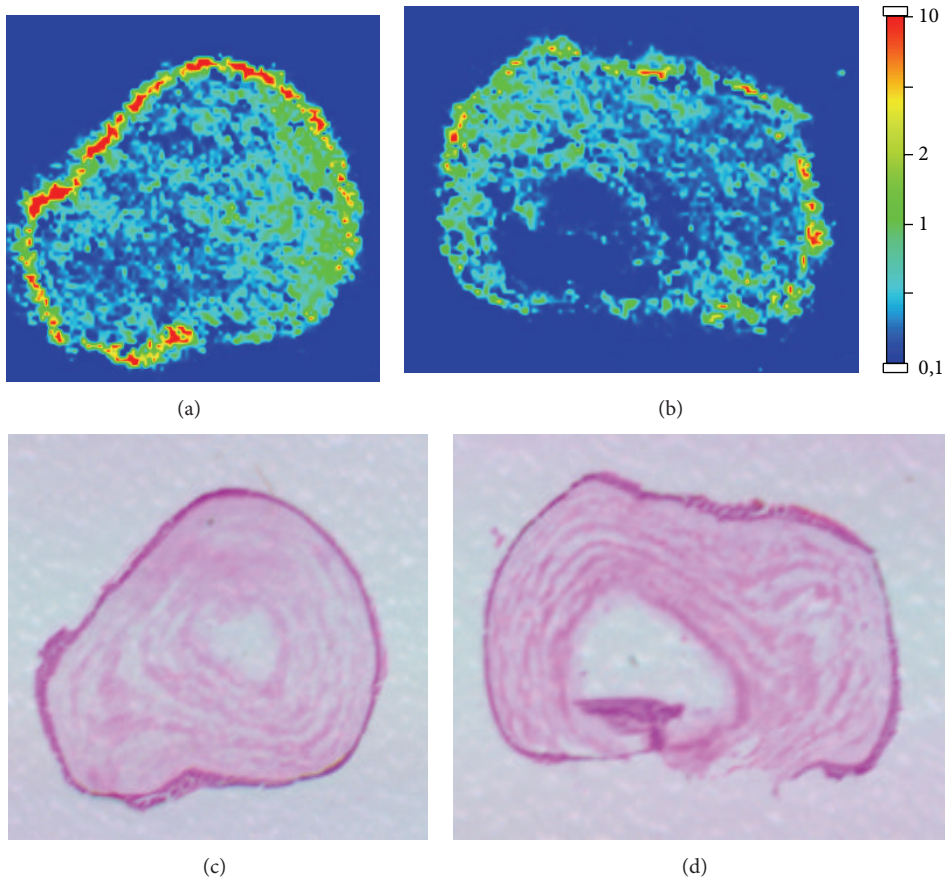

Figure 6: Iontophoresis group: MALDI-MS imaging (a and b) and haematoxylin-eosin staining (c and d) of two corneal samples of two different eyes.

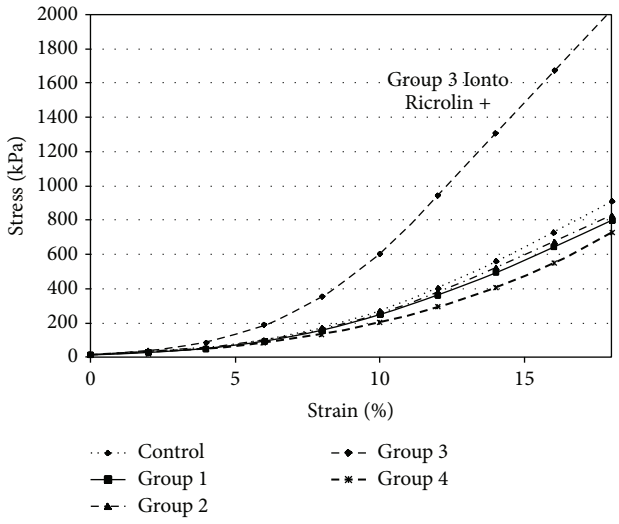

Figure 7: Stress-strain measurements of rabbit corneas.

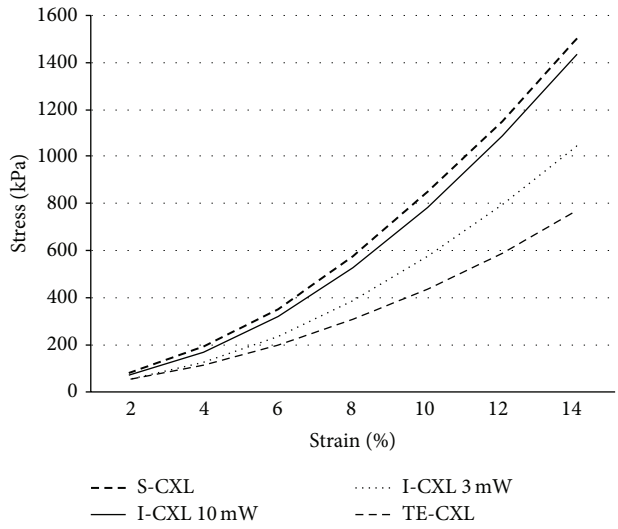

Figure 8: Stress-strain measurements of human corneas.

In rabbit corneas, in the group 3 at 10% strain, Young's modulus was $4,9 \times 10^6$ Pa in the untreated eyes and was $11,0 \times 10^6$ Pa in the treated eyes, with an increase factor of 0.8 (Figure 9).

In human corneas, stress-strain measurements showed an increase in corneal rigidity after CXL in the group treated with S-CXL when compared to other groups. This was shown by a rise in strain and in Young's modulus calculated at 10%

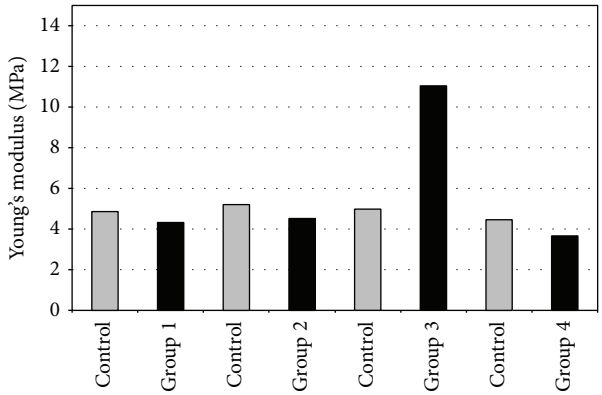

Figure 9: Young's modulus at 10% strain of rabbit corneas.

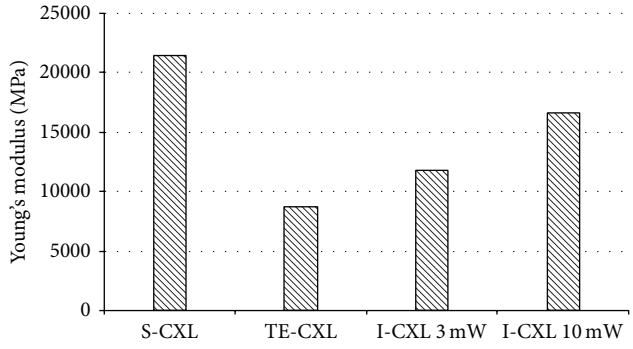

Figure 10: Young's modulus at 10% strain of human corneas.

strain (Figure 10). None of these differences were statistically significant, possibly because of the small sample size of each group.

4. Discussion

Corneal collagen cross-linking is a photochemical reaction aimed at increasing corneal rigidity via the formation intrafibrillar and interfibrillar covalent bonds. To achieve adequate riboflavin penetration in the corneal stroma, the standard cross-linking protocol includes epithelial removal. This induces discomfort [8], temporary vision reduction [4], and risk of infection [9]. In the last years, a cross-linking procedure warranting epithelial integrity but retaining maximal efficacy has been persistently sought for. Nevertheless results of TE-CXL are controversial, with evidences showing that treated patients continue to progress [13], while others show good results [14, 22, 23].

Both corneal epithelium blocking UV penetration and blockage of riboflavin penetration may be important factors for the reduced effect of TE-CXL [24, 25]. For years, the epithelium has been considered a physiological barrier to UV light [24, 25]. Nevertheless, as reported by Kolozsvári et al, epithelium and Bowman's layer mostly absorb UV-B light (up to 300 nm), while UV-A light is not absorbed [26]. Bottós et al. explained the reduced efficacy of TE-CXL with respect to S-CXL, with the hypothesis that the corneal epithelium, while not limiting UVA transmittance, reduces riboflavin penetration [27].

If corneal iontophoresis could increase photosensitizer penetration in the cornea, it could overcome the problem. In addition, riboflavin is theoretically a good candidate for ocular iontophoresis due to its negatively charged structure and low molecular weight.

In this study, we compared the changes induced by different CXL techniques in terms of tissue penetration and distribution of riboflavin, as well as of stress-strain. A secondary goal of our study was to evaluate if I-CXL is capable of inducing a good penetration of riboflavin and increase corneal rigidity, differently from TE-CXL.

The hystorical and most accepted approach for evaluating cross-linking efficacy in changing corneal elastic properties is measuring static stress-strain [25, 28]. Several reports in literature showed that S-CXL is able to induce significant increase in corneal stress-strain properties [25, 28–30], while there are only two studies measuring stress-strain after TE-CXL [25, 31]. Wollensak and Iomdina showed that TE-CXL does not induce any significant change in corneal rigidity [25], while Tao et al. reported the opposite [31].

Our biomechanical essay on rabbit corneas showed that I-CXL induces a significant increase in stress-strain when compared to untreated group. The best riboflavin solution for iontophoresis seemed to be the dextran and NaCl-free, with low osmolarity and the addition of enhancers, EDTA, and trometamol. Our findings are partly in agreement with those of Cassagne et al., which showed a significant increase in both stress-strain measurements and Young's modulus in I-CXL-treated rabbit corneas when compared to controls [17].

Rabbit corneas have been used in TE-CXL experiments because the rabbit epithelium is histologically quite similar to that of humans, and therefore recommended by past researchers as a reasonable approximation to clinical reality, avoiding the use of valuable nonhuman, primate research animals [32]. However, it is well known that rabbit corneas lack Bowman's membrane [32] and feature an epithelium which is centrally thicker than at the limbus [33], exactly the opposite of human beings [34]. For this reason, we decided to investigate the effect of I-CXL also in ex vivo human corneas. We did not observe a statistically significant difference between stress-strain values and Young's modulus among the different subgroups. Nevertheless, even if not significantly different, S-CXL treatment with epithelial removal and 10 mW I-CXL presented a tendency to better results when compared to TE-CXL and 3 mW I-CXL.

The increase in stress-strain measurement between TE-CXL, S-CXL, and I-CXL observed in our study differs from what was published by Wollensak et al. [28], who found an increase in biomechanical rigidity by a factor of 4.5. Possible reasons for this difference may be related to specimen preparation. Wollensak et al. treated human corneas within 1 to 2 hours after enucleation: fresh tissues could thus be the reason for their better results. In addition, even if in our study human corneas were grouped uniformly according to the age of donor and the time between death and sampling, variance among stress-strain measurements was noticed. This bias may be one limit of our study.

The second section of our study used MALDI-IMS. The combination of these two techniques in a single experiment offers a unique opportunity to understand the molecular arrangement of any tissue. Compared to the traditional biochemical procedures, based on antibodies or radiolabelling, and limited by the specificity of the used labels and by the number of compounds that can be studied at the same time, IMS recovers the sample molecular content without the need of any a-priori knowledge of the compound to be detected [35]. Another advantage of MALDI-MS imaging is the high sensitivity and specificity of the analysis. Even if this technique allows only a semiquantitative (not numerical) estimation of the concentration of a substance, it is able to give a vivid and clear spatial representation of the penetration and distribution of the compound in a tissue.

In the MALDI-IMS experiment we found different corneal penetrations and distributions of riboflavin solutions currently used in three cross-linking protocols: standard, transepithelial, and iontophoresis. In our study, corneas soaked with iontophoresis showed the presence of riboflavin in all corneal layers, even if with a lower concentration in the deeper stroma when compared with S-CXL protocol. The TE technique samples showed the lowest riboflavin concentration of all groups. Although every semiquantification value has variability between 20% and 30%, typical of IMS-imaging technique, the results of this semiquantitative analysis showed that the concentration of riboflavin among the three procedures was roughly different. Giving the semiquantitative method of analysis IMS should not be compared with the high-performance liquid chromatography (HPLC) analysis showed in other reports [17, 36] which are able to provide reliable concentrations. However, differently from HPLC, in MALDI-IMS the tissue is not homogenized but analysed in whole sections, so it is able to give a vivid and clear spatial representation of the penetration and distribution of the compound in a tissue.

Our findings are in agreement with the literature, even if with a different, semiquantitative technique, showing that iontophoresis imbibition is able to increase the stromal amount of riboflavin when compared to usual transepithelial administration (TE-CXL) [17, 36]. Nevertheless, it reached a lower concentration when compared to conventional, epi-off protocol [17, 36].

To summarize, the aim of transepithelial corneal collagen cross-linking is to reduce the risk of infections, allow faster vision recovery, and decrease treatment time, all without reducing the efficacy of the procedure. We observed that iontophoresis induced acceptable penetration of riboflavin in all corneal layers, which is the basis for an efficient cross-linking [27], even with an intact epithelium. The effective presence of riboflavin together with UV-A produced, as measured in our stress-strain measurements, a significant increase in corneal stiffness in the I-CXL group compared to controls, therefore partly confirming previous report [17].

Nevertheless, riboflavin concentration and stress-strain measurements after I-CXL were inferior to those obtained with the S-CXL. These findings are again in accordance with recent studies [17, 36]. A possible explanation of the reduced effect of I-CXL is that an intact epithelium soaked with riboflavin may partially arrest UV-A light. However, Zhang et al. showed that the epithelial cells are not enriched with riboflavin [37]. For that reason, only a small part of the UV light should be absorbed by the epithelium, approximately 15–20% [38, 39].

Furthermore, since the energy dose of I-CXL is the same as S-CXL protocol (5.4 J/cm^2), further studies are required to understand if more irradiance power is necessary to reach the standard protocol biomechanical effect, as well as if this lower stiffening effect may however be enough to stabilize an ectatic cornea.

In conclusion, even if more studies are needed to evaluate safety and efficacy, corneal cross-linking with iontophoresis is potentially a valid alternative to standard cross-linking in improving corneal biomechanical properties and reducing postoperative patient pain, risk of infection, and treatment time.

Conflict of Interests

The authors declare that there is no conflict of interests regarding the publishing of this paper.

References

[1] Y. S. Rabinowitz, "Keratoconus," *Survey of Ophthalmology*, vol. 42, no. 4, pp. 297–319, 1998.

[2] E. L. Cheng, I. Maruyama, N. SundarRaj, J. Sugar, R. S. Feder, and B. Y. J. T. Yue, "Expression of type XII collagen and hemidesmosome-associated proteins in keratoconus corneas," *Current Eye Research*, vol. 22, no. 5, pp. 333–340, 2001.

[3] F. Raiskup-Wolf, A. Hoyer, E. Spoerl, and L. E. Pillunat, "Collagen crosslinking with riboflavin and ultraviolet-A light in keratoconus: long-term results," *Journal of Cataract and Refractive Surgery*, vol. 34, no. 5, pp. 796–801, 2008.

[4] R. Vinciguerra, M. R. Romano, F. I. Camesasca et al., "Corneal cross-linking as a treatment for keratoconus: four-year morphologic and clinical outcomes with respect to patient age," *Ophthalmology*, vol. 120, no. 5, pp. 908–916, 2013.

[5] G. Wollensak, E. Spoerl, and T. Seiler, "Riboflavin/ultraviolet-A-induced collagen crosslinking for the treatment of keratoconus," *American Journal of Ophthalmology*, vol. 135, no. 5, pp. 620–627, 2003.

[6] A. Caporossi, C. Mazzotta, S. Baiocchi, and T. Caporossi, "Long-term results of riboflavin ultraviolet a corneal collagen cross-linking for keratoconus in Italy: the siena eye cross Study," *The American Journal of Ophthalmology*, vol. 149, no. 4, pp. 585–593, 2010.

[7] P. Vinciguerra, E. Albè, S. Trazza et al., "Refractive, topographic, tomographic, and aberrometric analysis of keratoconic eyes undergoing corneal cross-linking," *Ophthalmology*, vol. 116, no. 3, pp. 369–378, 2009.

[8] V. C. Ghanem, R. C. Ghanem, and R. de Oliveira, "Postoperative pain after corneal collagen cross-linking," *Cornea*, vol. 32, no. 1, pp. 20–24, 2013.

[9] S. Dhawan, K. Rao, and S. Natrajan, "Complications of corneal collagen cross-linking," *Journal of Ophthalmology*, vol. 2011, Article ID 869015, 5 pages, 2011.

[10] H. Hashemi, M. A. Seyedian, M. Miraftab, A. Fotouhi, and S. Asgari, "Corneal collagen cross-linking with riboflavin and

ultraviolet a irradiation for keratoconus: Long-term results," *Ophthalmology*, vol. 120, no. 8, pp. 1515–1520, 2013.

[11] Y. Goldich, Y. Barkana, O. W. Lior et al., "Corneal collagen cross-linking for the treatment of progressive keratoconus: 3-year prospective outcome," *Canadian Journal of Ophthalmology*, vol. 49, no. 1, pp. 54–59, 2014.

[12] A. Caporossi, C. Mazzotta, S. Baiocchi, T. Caporossi, and A. L. Paradiso, "Transepithelial corneal collagen crosslinking for keratoconus: qualitative investigation by in vivo HRT II confocal analysis," *European Journal of Ophthalmology*, vol. 22, supplement 7, pp. S81–S88, 2012.

[13] A. Caporossi, C. Mazzotta, A. L. Paradiso, S. Baiocchi, D. Marigliani, and T. Caporossi, "Transepithelial corneal collagen crosslinking for progressive keratoconus: 24-month clinical results," *Journal of Cataract and Refractive Surgery*, vol. 39, no. 8, pp. 1157–1163, 2013.

[14] M. Filippello, E. Stagni, and D. O'Brart, "Transepithelial corneal collagen crosslinking: bilateral study," *Journal of Cataract and Refractive Surgery*, vol. 38, no. 2, pp. 283–291, 2012.

[15] C. Koppen, K. Wouters, D. Mathysen, J. Rozema, and M.-J. Tassignon, "Refractive and topographic results of benzalkonium chloride-assisted transepithelial crosslinking," *Journal of Cataract and Refractive Surgery*, vol. 38, no. 6, pp. 1000–1005, 2012.

[16] Z. Y. Zhang and X. R. Zhang, "Efficacy and safety of transepithelial corneal collagen crosslinking," *Journal of Cataract & Refractive Surgery*, vol. 38, no. 7, pp. 1304–1305, 2012.

[17] M. Cassagne, C. Laurent, M. Rodrigues et al., "Iontophoresis transcorneal delivery technique for transepithelial corneal collagen crosslinking with riboflavin in a rabbit model," *Investigative Ophthalmology & Visual Science*, 2014.

[18] L. Mastropasqua, M. Nubile, R. Calienno et al., "Corneal cross-linking: intrastromal riboflavin concentration in iontophoresis-assisted imbibition versus traditional and transepithelial techniques," *The American Journal of Ophthalmology*, vol. 157, no. 3, pp. 623–630, 2014.

[19] B. Balluff, C. Schöne, H. Höfler, and A. Walch, "MALDI imaging mass spectrometry for direct tissue analysis: technological advancements and recent applications," *Histochemistry and Cell Biology*, vol. 136, no. 3, pp. 227–244, 2011.

[20] Y. Yamada, K. Hidefumi, H. Shion, M. Oshikata, and Y. Haramaki, "Distribution of chloroquine in ocular tissue of pigmented rat using matrix-assisted laser desorption/ionization imaging quadrupole time-of-flight tandem mass spectrometry," *Rapid Communications in Mass Spectrometry*, vol. 25, no. 11, pp. 1600–1608, 2011.

[21] D. Camposampiero, R. Tiso, E. Zanetti, A. Ruzza, A. Bruni, and D. Ponzin, "Cornea preservation in culture with bovine serum or chicken ovalbumin," *Cornea*, vol. 22, no. 3, pp. 254–258, 2003.

[22] A. Magli, R. Forte, A. Tortori, L. Capasso, G. Marsico, and E. Piozzi, "Epithelium-off corneal collagen cross-linking versus transepithelial cross-linking for pediatric keratoconus," *Cornea*, vol. 32, no. 5, pp. 597–601, 2013.

[23] A. G. Salman, "Transepithelial corneal collagen crosslinking for progressive keratoconus in a pediatric age group," *Journal of Cataract & Refractive Surgery*, vol. 39, no. 8, pp. 1164–1170, 2013.

[24] S. Baiocchi, C. Mazzotta, D. Cerretani, T. Caporossi, and A. Caporossi, "Corneal crosslinking: riboflavin concentration in corneal stroma exposed with and without epithelium," *Journal of Cataract and Refractive Surgery*, vol. 35, no. 5, pp. 893–899, 2009.

[25] G. Wollensak and E. Iomdina, "Biomechanical and histological changes after corneal crosslinking with and without epithelial debridement," *Journal of Cataract and Refractive Surgery*, vol. 35, no. 3, pp. 540–546, 2009.

[26] L. Kolozsvári, A. Nógrádi, B. Hopp, and Z. Bor, "UV absorbance of the human cornea in the 240- to 400-nm range," *Investigative Ophthalmology and Visual Science*, vol. 43, no. 7, pp. 2165–2168, 2002.

[27] K. M. Bottós, P. Schor, J. L. Dreyfuss, H. B. Nader, and W. Chamon, "Effect of corneal epithelium on ultraviolet-A and riboflavin absorption," *Arquivos Brasileiros de Oftalmologia*, vol. 74, no. 5, pp. 348–351, 2011.

[28] G. Wollensak, E. Spoerl, and T. Seiler, "Stress-strain measurements of human and porcine corneas after riboflavin-ultraviolet-A-induced cross-linking," *Journal of Cataract and Refractive Surgery*, vol. 29, no. 9, pp. 1780–1785, 2003.

[29] E. Spoerl, G. Wollensak, and T. Seiler, "Increased resistance of crosslinked cornea against enzymatic digestion," *Current Eye Research*, vol. 29, no. 1, pp. 35–40, 2004.

[30] S. Schumacher, L. Oeftiger, and M. Mrochen, "Equivalence of biomechanical changes induced by rapid and standard corneal cross-linking, using riboflavin and ultraviolet radiation," *Investigative Ophthalmology and Visual Science*, vol. 52, no. 12, pp. 9048–9052, 2011.

[31] X. Tao, H. Yu, Y. Zhang et al., "Role of corneal epithelium in riboflavin/ultraviolet-A mediated corneal cross-linking treatment in rabbit eyes," *BioMed Research International*, vol. 2013, Article ID 624563, 6 pages, 2013.

[32] T. F. Clarke, T. E. Johnson, M. B. Burton, B. Ketzenberger, and W. P. Roach, "Corneal injury threshold in rabbits for the 1540 nm infrared laser," *Aviation Space and Environmental Medicine*, vol. 73, no. 8, pp. 787–790, 2002.

[33] B. J. Reiser, T. S. Ignacio, Y. Wang et al., "In vitro measurement of rabbit corneal epithelial thickness using ultrahigh resolution optical coherence tomography," *Veterinary Ophthalmology*, vol. 8, no. 2, pp. 85–88, 2005.

[34] Y. Feng and T. L. Simpson, "Comparison of human central cornea and limbus in vivo using optical coherence tomography," *Optometry & Vision Science*, vol. 82, no. 5, pp. 416–419, 2005.

[35] M. Stoeckli, P. Chaurand, D. E. Hallahan, and R. M. Caprioli, "Imaging mass spectrometry: a new technology for the analysis of protein expression in mammalian tissues," *Nature Medicine*, vol. 7, no. 4, pp. 493–496, 2001.

[36] L. Mastropasqua, M. Nubile, R. Calienno et al., "Corneal cross-linking: intrastromal riboflavin concentration in iontophoresis-assisted imbibition versus traditional and transepithelial techniques," *American Journal of Ophthalmology*, vol. 157, no. 3, pp. 623–630.e1, 2014.

[37] Y. Zhang, P. Sukthankar, J. Tomich, and G. Conrad, "Effect of the synthetic NC-1059 peptide on diffusion of riboflavin across an intact corneal epithelium," *Investigative Ophthalmology & Visual Science*, vol. 53, no. 6, pp. 2620–2629, 2012.

[38] F. Raiskup, R. Pinelli, and E. Spoerl, "Riboflavin osmolar modification for transepithelial corneal cross-linking," *Current Eye Research*, vol. 37, no. 3, pp. 234–238, 2012.

[39] E. Spoerl, "Corneal collagen cross-linking epithelium-on versus epithelium-off treatments," in *Corneal Collagen Cross-Linking*, F. Hafezi and J. B. Randleman, Eds., pp. 139–142, SLACK Incorporated, Thorofare, NJ, USA, 2013.

Hindawi Publishing Corporation
BioMed Research International
Volume 2014, Article ID 906087, 8 pages
http://dx.doi.org/10.1155/2014/906087

Review Article

Etiopathogenesis and Therapy of Epithelial Ingrowth after Descemet's Stripping Automated Endothelial Keratoplasty

Francesco Semeraro, Attilio Di Salvatore, Alessandro Bova, and Eliana Forbice

Eye Clinic, Department of Neurological and Vision Sciences, University of Brescia, Piazzale Spedale Civili 1, 25123 Brescia, Italy

Correspondence should be addressed to Eliana Forbice; elianaforbice@email.it

Received 22 May 2014; Accepted 14 August 2014; Published 2 September 2014

Academic Editor: Leonardo Mastropasqua

Descemet's stripping endothelial keratoplasty is an emerging technique finalized to treat endothelial dysfunction replacing only the pathological portion of cornea. The advent of any new technique puts us in front of new complications. The epithelial ingrowth is a well-known complication already studied in case of ocular trauma and more recently in refractive surgery. This job analyzed the potential etiopathogenesis of epithelial ingrowth after DSAEK, reviewing the cases described in literature, and suggests the potential therapy.

1. Introduction

In the past decade, Descemet's stripping automated endothelial keratoplasty (DSAEK) has become the chosen procedure for the management of patients with endothelial dysfunction, overtaking penetrating keratoplasty (PK) in popularity for the treatment of these specific diseases [1]. The technique was originally described by Melles et al., [2] as "posterior lamellar keratoplasty," and was subsequently modified by Terry and Ousley [3] and renamed "deep lamellar endothelial keratoplasty." The technique of stripping Descemet's membrane was again described by Melles et al. [4] and termed "Descemet's stripping endothelial keratoplasty." The procedure was modified again to involve the use of an automated blade microkeratome to create a lamellar dissection of the donor cornea, as described by Gorovoy and Ratanasit [5], and was termed "Descemet's stripping automated endothelial keratoplasty" (DSAEK).

This technique has advantages such as minimal refractive changes and more rapid recovery compared to PK [6]. However, it is not free of complications, which include donor graft detachment, postoperative graft dislocation, pupillary block glaucoma, cataract development, aqueous misdirection syndrome, and epithelial ingrowth [7–10]. One of the most frequent DSAEK complications is the opacity that arises from interface abnormalities. Interface opacities are a well-documented phenomenon observed after DSAEK [10] caused by epithelial ingrowth, infection, inflammation, retention of Descemet's membrane, interface blood, calcium, interface fluid, retained viscoelastic material, or an irregular donor cut [11, 12]. Epithelial ingrowth has been reported to cause interface opacity within a lamellar graft after DSAEK [5, 8, 9, 11, 13–19].

Historically, epithelial ingrowth was described as an anterior chamber growth that rarely occurs after cataract extraction [20], penetrating keratoplasty (PKP) or other invasive ocular surgeries such as anterior chamber aspiration and glaucoma procedures [21]. In the recent literature, the most common experience with epithelial ingrowth into a lamellar interface follows laser in situ keratomileusis (LASIK). The reported incidence of intracorneal epithelial ingrowth after a corneal lamellar surgery such as LASIK is 20% [22, 23]. The reported frequency of epithelial ingrowth after DSAEK is very low.

Herein, we review the literature on epithelial ingrowth after DSAEK in order to better understand the risk factors,

generation mechanisms, and potential therapy associated with this complication of surgery. The results of our literature search on epithelial ingrowth, epithelial interface implantation, and epithelial ingrowth after DSAEK are shown in Table 1.

Although many authors use the term "downgrowth" [5, 9, 13, 14, 19] to describe this phenomenon, we prefer, as other have suggested, the term "ingrowth" to describe this grow into the interface [8, 11, 17, 18, 24].

2. Etiopathogenesis, Risk Factors, and Mechanism

Epithelial ingrowth is characterized by the migration and growth of corneal or conjunctival epithelial cells into the anterior chamber of the eye through a breach in the ocular surface or into the lamellar interface of the cornea itself after corneal lamellar or flap surgery [8].

The ingrowth observed after Descemet's keratoplasty generally develops at the interface, between the patient's stroma and the donor's lamella. In these cases, early epithelial ingrowth is seen as a haze during the slit-lamp examination, with a sharp demarcation representing multiple layers of corneal epithelium (resembling normal corneal epithelium), suggesting considerable proliferation. The late stage appears clinically as a homogenous white mass, which comprises clumps containing amorphous materials with scarce cellular elements or cellular debris, suggesting less proliferation [25]. In more severe cases, epithelial ingrowth may extend from the interface to a retrocorneal membrane with extension onto the iris surfaces, causing ectropion uveae, corneal decompensation, and glaucoma [18, 21]. However, not every case of suspected epithelial implantation leads to graft failure, and interface epithelial inclusions can remain static or even regress over time [8, 13, 16, 18, 19, 26].

Several groups have investigated the etiology of epithelial cells. Three main mechanisms were proposed as causes of epithelial ingrowth after DSAEK:

(1) dragging of loose epithelial cells intracamerally or onto the stromal surface during graft insertion [17, 19],

(2) migration of epithelial cells from the donor epithelium on eccentrically trephined grafts containing full-thickness cornea [27],

(3) introduction of epithelial cells from full-thickness cornel incisions (i.e., Venton incisions) [8].

Many reported cases of epithelial ingrowth involve intraoperative and/or postoperative complications (see Table 2). The first specific risk factor for the occurrence of epithelial ingrowth after DSAEK is graft dislocation or graft detachment, necessitating rebubbling or reattachment [8, 11, 14, 17, 19, 24]. Graft detachment/dislocation further exposes the area of denuded endothelium, which may facilitate the migration of loose epithelial cells. Seeded epithelial cells may proliferate within the denuded graft-host interface without the contact inhibition provided by endothelium [28, 29]. Reattachment procedures may subsequently trap the retained epithelial cells, allowing further proliferation at the interface. Another known risk factor is the combination of cataract extraction and IOL implantation along with DSAEK, which increases the amount of surgical manipulation and provides a portal of entry to the anterior chamber for host epithelial cells [5].

Wound leak and tissue incarceration are also considered risk factors for epithelial ingrowth; the presence of vitreous within the surgical wound can act as a scaffold for the migration of recipient epithelium [14, 21]. In a case report by Phillips et al. [14], histological examination of the failed DSAEK graft showed multilayered conjunctival epithelium; the ingrowth thus originated from the recipient conjunctiva. Possible causes of epithelial ingrowth in this case include the presence of vitreous within the surgical wound, which could provide a scaffold for the migration of conjunctival epithelium from the conjunctival tissue adjacent to a compromised wound. Furthermore, the location of the surgical incision may facilitate epithelial cell entry. Corneal or limbal incisions, as opposed to scleral tunnel incisions, allow loose epithelial cells at the cornea or limbus to be dragged and introduced into the anterior chamber, leading to epithelial ingrowth [18].

Preparation of the posterior lamellar disc manually or with use of a microkeratome is an important factor contributing to epithelial ingrowth. It is postulated that the donor epithelium may be implanted on the graft during preparation of the donor posterior lamellar disc and then introduced intraoperatively at the interface or in the anterior chamber [11, 16]. In a large series of patients with epithelial ingrowth Suh et al. [27] reported that epithelial cells originated from the full-thickness portion of the DSAEK graft after eccentric trephination of the donor tissue. In other cases, the donor epithelium was scraped off prior to use of the microkeratome during preparation of the DSAEK lenticule. Loose donor epithelial cells may thus be dragged across the stromal interface by the microkeratome and remain adherent to the stroma.

3. Diagnostic Procedures

During slit lamp biomicroscopy, epithelial ingrowth can appear as a flat haze that gradually increases in size with the development of epithelial pearls (see Figure 1), ultimately developing into a homogeneous whitish mass with a sharp demarcation, likely due to the fusion of epithelial pearls. Indirect slit-lamp illumination can sometimes help visualize this sheet-like proliferation. The use of fluorescein solution can also aid in diagnosis as well as in the prevention of postoperative recurrence by highlighting corneal abnormalities and epithelial fistulas, retracted tissue or an elevated wound edge.

Confocal microscopy permits noninvasive, in vivo microscopic examination of all layers of the cornea [19]. In cases of epithelial ingrowth, this technique may reveal an epithelial cell-like mass (large, polygonal cells suggestive of epithelial elements) at the graft-host interface, forming clusters or nests within fibrotic tissue [30]. Thus, epithelial ingrowth can be identified and distinguished from fibrous proliferation (see Figure 2). Confocal microscopy may also prove useful in

Table 1: Literature review of epithelial migration into anterior chamber after DSAEK.

Study	Numeber of eye(s)	Description	Diagnosis	Graft failure	Treatment
Culbertson [13]	1	Epithelial downgrowth	Confocal microscopy	No	PK
Koenig and Covert [17]	1	Epithelial ingrowth,interface	Histology	Yes	Repeat DSAEK
Walker et al. [19]	1	Epithelial downgrowth, at the interface	Confocal microscopy, histology	No	PK
Prasher et al. [9]	2	Case 1-epithelial downgrowth, interface Case 2-epithelial downgrowth, not at the interface	Histology	Yes	Case 1 had PK Case 2 had DSAEK
Phillips et al. [14]	1	Conjunctival epithelial downgrowth, over donor endothelium	Histology	Yes	Repeat DSAEK
Gorovoy and Ratanasit [5]	1	Epithelial downgrowth, not at the interface	Histology	Yes	Repeat DSAEK
Saelens et al. [11]	1	Epithelial ingrowth in the flap-graft interface	Histology		Posterior mushroom keratoplasty
Lee et al. [24]	1	Epithelial ingrowth at the interface	Histology	Yes	Repeat DSAEK
Suh et al. [18]	5	Epithelial ingrowth interface-1 Interface retrocorneal-4	AS-OCT-1, spectral domain Ultrahigh resolution OCT-3, histology-1	None documented	Observation in 4 cases Corneoscleral grafting in one case
Bansal et al. [8]	1	Epithelial ingrowth after stromal puncture	Clinical	No	Nil
Ghosh et al. [16]	1	Epithelial ingrowth interface	Histology	Yes	Repeat DSAEK
Wong et al. [34]	1	Interface haze (atypical presentation of epithelial ingrowth interface)	Slit lamp, translucent membrane whitened after argon laser photocoaugulation	Yes	3 DSAEKs intracameral 5-FU

DSAEK: Descemet stripping automated endothelial keratoplasty; PK: penetrating keratoplasty; AS-OCT: anterior segment optical coherence tomography; OCT: optical coherence tomography.

Table 2: Risk Factors of epithelial ingrowth.

Risk factors	Mechanism of ingrowth	Authors
Graft dislocation or graft detachment	Exposition of denuded endothelium areas, probable loss of the contact inhibition provided by the endothelium. Proliferation and migration of loose epithelial cells	Bansal et al. [8], Saelens et al. [11], Koenig and Covert [17], Phillips et al. [14], Walker et al. [19], Lee et al. [24], Sidrys and Demong [28], Cameron et al. [29]
Combination of cataract extraction and IOL implantation	Surgical manipulations may provide a portal of entry for host epithelial cells into the AC.	Gorovoy and Ratanasit [5]
Wound leak or tissue incarceration	Presence of vitreous within the surgical wound as a scaffold for the epithelial conjunctival cells migration, loss of endothelium cells inhibition	Phillips et al. [14], Chen and Pineda II [21]
Location of the surgery incision	Limbal or corneal incision would facilitate near loose epithelial cells to be dragged and introduced into the anterior chamber	Suh et al. [18]
Preparation of the posterior lamellar disc	The donor epithelium can be implanted on graft during the preparation of the donor posterior lamellar disc and then introduced intraoperatively at interface of AC. The loose donor epithelial cells may be mechanically dragged across the stromal interface by microkeratome and remain adherent to the stroma, developing epithelial ingrowth	Saelens et al. [11], Ghosh et al. [16], Suh et al. [27]

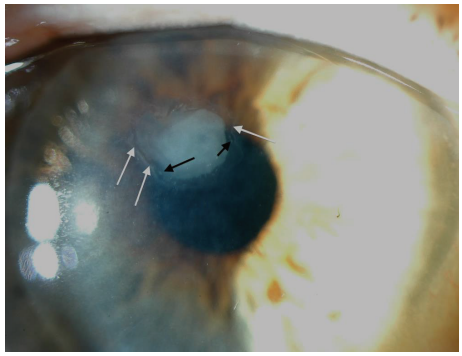

Figure 1: A case of epithelial ingrowth appeared two months after surgery. Epithelial pearls (black arrows) and a demarcation line (white arrow) could be seen.

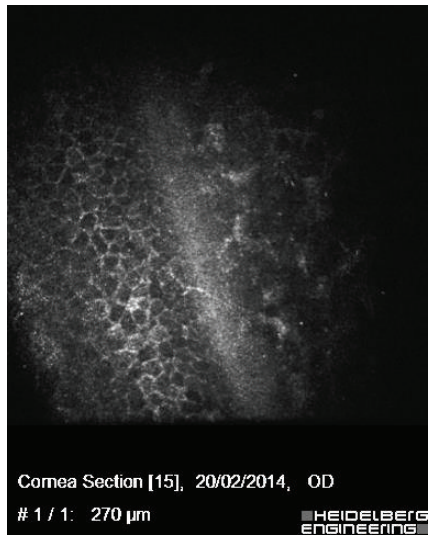

Figure 2: In vivo confocal micrographs showing microstructural changes (typically epithelial cells with prominent borders and distinctive nuclei) in the interface between the flap and stromal bed.

following the clinical course of epithelial ingrowth after treatment and may prove to be more sensitive than routine light microscopy for the detection of residual epithelial ingrowth [31, 32]. Prior to the advent of vivo confocal microscopy, the cellular changes associated with intraepithelial ingrowth were rarely described because PKP or flap removal was required for histological examination. We think that confocal microscopy may be the method of choice for evaluating epithelial ingrowth.

Through histopathology, scientists identified the extension of epithelium over donor endothelium as the cause of graft failure. The analysis of failed grafts after excision revealed epithelium on the posterior surface of the tissue [14]. XY karyotyping was performed to determine whether the tissue was of donor or host origins [5, 11, 19].

Optical coherence tomography (OCT) visualizes epithelial ingrowth at the interface as hyporeflective clefts and irregular, hyperreflective masses [18], which may represent different layers of epithelium trapped at the interface (see Figure 3). The predominance of hyporeflective clefts may represent the presence of basal epithelial layers, as would result from an early or arrested stage of epithelial ingrowth at the interface. These areas, however, may also represent fluid or debris trapped at the interface; histological confirmation

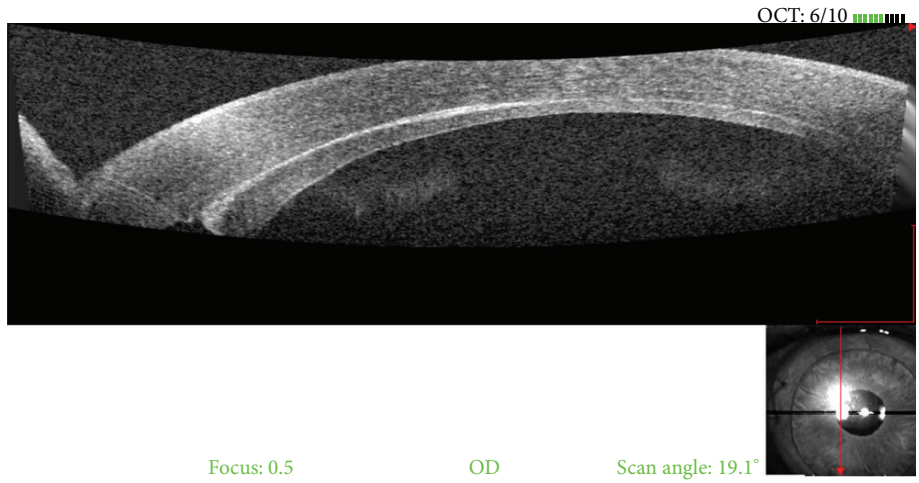

Figure 3: Optical coherence tomography (OCT) showing hyporeflective clefts and irregular, hyperreflective masses which may represent different layers of epithelium trapped at the interface between the flap and stromal bed in a case of epithelial ingrowth.

will be necessary for conclusive evidence that these layers represent various layers of epithelium. In a series of 5 eyes from Suh et al. [18], OCT was used to study the origins of epithelial ingrowth. In Cases 2 and 4, the hyperreflective layer was found to be contiguous with the temporal incision. In case 3, the hyperreflective layer was continuous with a full-thickness edge of the DSAEK graft, representing an eccentric trephination of the donor tissue. Hyperreflective layers contiguous with the temporal incisions, as shown by OCT in Cases 2 and 4, may delineate the track through which epithelial cells gained access during graft insertion. In case 3, the epithelium was likely derived from the full-thickness edge of the DSAEK graft, a mechanism of epithelial ingrowth reported in prior histopathological studies [28] of failed DSAEK grafts. In case 5, the fistulous tract from the limbal incision was likely the entryway through which epithelial cells gained access to the eye [18].

Pentacam technology has been used to measure reflectivity at the interface region between the graft and the host cornea in optically clear corneas at various time points after DSAEK [33]. However, no such report on epithelial ingrowth has been published to date. Furthermore, despite the utility of topographical technology in assessing the effects of ingrowth on astigmatism, this technique is not used to evaluate DSAEK patients.

4. Pathophysiology and Treatment

This review highlights the role of epithelial cells in epithelial ingrowth in order to clarify the associated pathophysiology and optimize treatment. Most of the risk factors for this condition can be minimized by performing DSAEK compared with standard PKP. It is therefore tempting to dismiss incidents of epithelial ingrowth as "chance" occurrences related to a history of multiple intraocular surgeries, the presence of vitreous in the wound, or the incidental implantation of epithelial cells at the time of surgery—rather than to the DSAEK procedure specifically.

As previously pointed out, the most common experience of epithelial ingrowth extending to the lamellar interface occurs in LASIK patients. Most cases of epithelial ingrowth after LASIK are self-limiting [22, 25]. Likewise, some cases of DSAEK-related ingrowth appear not to progress and sometimes they may even lead to gradual resolution spontaneously [8, 12, 26] (Table 1). In a series of 118 DSAEK patients, Suh et al. [26] found one case of presumed epithelial implantation at the interface, which had been documented clinically and by anterior segment OCT. In another case series, the same authors described five additional cases of epithelial ingrowth after DSAEK [18]. None of these cases developed into graft failure or deteriorated visual acuity, so no treatment was administered.

Bansal et al. [8] reported a case of epithelial ingrowth after DSAEK with stromal puncture for phakic bullous keratopathy, which they treated conservatively. The central visual axis was clear, and the epithelial ingrowth had not progressed at the end of followup (13 months). Bansal et al. [8] justified this low tendency to progress with the probability that the cells already present at the interface have limited proliferating potential and die after a few mitotic divisions, leaving amorphous debris seen clinically as a homogeneous white mass. While an intact corneal endothelium normally inhibits epithelial migration through contact inhibition, the loss of this protective effect would allow for the extension of ingrowth to the endothelium. It should be pointed that in these cases, which did not involve flap removal, no histological diagnosis was possible.

However, corneal graft failures and cases of severe interface abnormality attributed to epithelial ingrowth have recently been reported. In these cases, treatment typically involves surgical graft resection [5, 9–11, 14, 16–19, 24, 34]. Ghosh et al. [16] report a case of histologically proven epithelial ingrowth at the interface of graft and host tissue that

resulted in graft failure after uneventful DSAEK. The patient was treated successfully by stripping and careful aspirating the interface material, followed by a second DSAEK. Phillips et al. [14] reported a case of two failed DSAEKs where histological analysis of the failed graft after removal showed conjunctival epithelial cells over the surgical margin and even on the posterior surface. In both cases, a second DSAEK was performed. Lee et al. [24], in a retrospective histopathologic study of eight corneas, found one case of epithelial ingrowth at the interface resulting in graft failure. This case involved donor graft dislocation during the first DSAEK procedure. A second DSAEK was required after graft failure. Gorovoy and Ratanasit [5] documented one case of epithelial ingrowth that was confirmed histopathologically in a patient who had undergone DSAEK. In their case, the donor cells were growing along the iris as well as at the interface; the patient was treated with a repeat DSAEK, and no other treatment was necessary. Koenig and Covert [17] describe a case of epithelial ingrowth confirmed histopathologically after a rebubbling procedure for recurrent donor lenticule dislocation during DSAEK. Donor lenticule exchange, mechanical scraping, and irrigation-aspiration of the residual epithelial cells were performed, and a new graft was provided. Signs of epithelial ingrowth were not observed during the two-year followup. In each of the cases presented above, a repeat DSAEK was considered as sufficient treatment. No additional therapy or penetrating keratoplasty was necessary for resolution of the patient's ocular pathology. It should be noted that each of these cases involved a histological diagnosis of epithelial ingrowth.

However, in other published reports, a more invasive treatment approach was deemed necessary, and PKP was performed. Walker et al. [19] describe a case of epithelial ingrowth after DSAEK that required repositioning with an air bubble one week after surgery. Three months after DSAEK, multiple opacities were noted at the graft-host interface, and in vivo confocal microscopy revealed large, polygonal cells thought to be epithelial cells at the DSAEK interface. The patient underwent uneventful penetrating keratoplasty, and the diagnosis was confirmed histopathologically. Signs of recurrent epithelial ingrowth were not noted at the end of the 18-month followup.

Saelens et al. [11] documented epithelium-lined cysts at the interface after a DSAEK performed using tissue of donor origin, as revealed by XY karyotyping. The patient subsequently underwent PKP due to graft failure. Culbertson [13] documented a case of epithelial ingrowth treated with PKP using confocal microscopy. Prasher et al. [9] reported two cases of epithelial ingrowth after DSAEK. In the first, the ingrowth was limited to the endothelial surface of the donor cornea and was treated with a repeat DSAEK. In the second, interface epithelial ingrowth was histologically confirmed as the cause of graft failure in a patient treated with PKP.

The application of intracameral 5-fluorouracil (5-FU) is a conservative approach used rarely to treat epithelial ingrowth. In three cases of DSAEK reported by Lai and Haller, intracameral 5-FU was used safely to treat epithelial ingrowth and recalcitrant interface haze. Antimetabolites such as 5-FU inhibit cell proliferation, which allows the treatment to target epithelial cells in cases of ingrowth [35]. Wong et al. [36] describe the case of a 79-year-old woman who underwent DSAEK and subsequently presented with persistent interface haze. In this case, there was early evidence of a translucent membrane at the interface that extended over the peripheral iris inferotemporally. Argon laser photocoagulation was applied to the membranous growth, resulting in a whitening response characteristic of epithelial tissue. Epithelial ingrowth was diagnosed, and intracameral 5-FU was administered. One year after this single injection, the patient had a clear DSAEK graft without interface haze.

Aggressive surgical options may be considered in cases of epithelial ingrowth after DSAEK with extrainterface extension. Suh et al. [18] reported a case of epithelial ingrowth after DSAEK present at the interface and also as a retrocorneal membrane with extension onto the iris surface, causing ectropion uveae. This case of epithelial ingrowth was treated with block excision and corneoscleral grafting. However, Gorovoy and Ratanasit [5] suggested that the epithelial cells in patients who have undergone DSAEK cause less damage than expected. Observation may be indicated until symptomatic graft edema is accompanied by extensive diffusion. The authors go on to suggest a repeat DSAEK rather than PKP in cases of graft failure.

5. Conclusions

This review of the literature emphasizes that prevention is the mainstay treatment for epithelial ingrowth after DSAEK [37]. Prophylactic anterior vitrectomy should be performed in any case where posterior capsule integrity is in question and vitreous may be present in the anterior chamber. Wound construction and approximation with sutures should be prioritized, and excessive postoperative inflammation should be avoided. Every attempt should be made to avoid excessive endothelial cell damage, which might provide an easy path for the overgrowth of epithelial cells [14]. Extreme attention and meticulous technique are recommended at all stages of the DSAEK procedure [16]. Once intracorneal epithelial ingrowth is detected, careful evaluation by confocal microscopy and close followup are necessary.

In the case of progressive pathology leading to graft failure, early recognition, careful removal of the implanted epithelium, and repeat DSAEK may help achieve a successful outcome without the need for more invasive treatments [16]. Otherwise, disease progression can lead to severe opacity and graft failure involving the stroma, ultimately requiring PKP [9, 11, 13, 19]. However, it seems that even in the case of diffusion and extension over the interface observation is recommended over more aggressive approaches, because DSAEK-related ingrowth is less aggressive than commonly assumed. Even in severe cases, observation may be indicated until the appearance of symptomatic graft edema [5, 14].

Antimetabolites such as 5-FU may be used alone as a conservative approach to therapy.

In any case, a careful and noninvasive approach is advised. This stands in contrast with the common approaches taken by surgeons in case of ingrowth in penetrating surgery (PK,

glaucoma, and cataracts) that frequently results in extending pathology requiring early and aggressive treatment.

Conflict of Interests

The authors declare that there is noconflict of interests regarding the publication of this paper.

References

[1] N. Ghaznawi and E. S. Chen, "Descemet's stripping automated endothelial keratoplasty: innovations in surgical technique," *Current Opinion in Ophthalmology*, vol. 21, no. 4, pp. 283–287, 2010.

[2] G. R. J. Melles, F. A. Eggink, F. Lander et al., "A surgical technique for posterior lameliar keratoplasty," *Cornea*, vol. 17, no. 6, pp. 618–626, 1998.

[3] M. A. Terry and P. J. Ousley, "Deep lamellar endothelial keratoplasty in the first United States patients," *Cornea*, vol. 20, no. 3, pp. 239–243, 2001.

[4] G. R. J. Melles, R. H. J. Wijdh, and C. P. Nieuwendaal, "A technique to excise the descemet membrane from a recipient cornea (descemetorhexis)," *Cornea*, vol. 23, no. 3, pp. 286–288, 2004.

[5] M. S. Gorovoy and A. Ratanasit, "Epithelial downgrowth after descemet stripping automated endothelial keratoplasty," *Cornea*, vol. 29, no. 10, pp. 1192–1194, 2010.

[6] F. W. Price Jr. and M. O. Price, "Descemet's stripping with endothelial keratoplasty in 50 eyes: a refractive neutral corneal transplant," *Journal of Refractive Surgery*, vol. 21, no. 4, pp. 339–345, 2005.

[7] F. W. Price Jr. and M. O. Price, "Descemet's stripping with endothelial keratoplasty in 200 eyes: early challenges and techniques to enhance donor adherence," *Journal of Cataract & Refractive Surgery*, vol. 32, no. 3, pp. 411–418, 2006.

[8] R. Bansal, A. Ramasubramanian, P. Das, J. Sukhija, and A. K. Jain, "Intracorneal epithelial ingrowth after descemet stripping endothelial keratoplasty and stromal puncture," *Cornea*, vol. 28, no. 3, pp. 334–337, 2009.

[9] P. Prasher, O. Muftuoglu, M. L. Hsiao, R. W. Bowman, R. N. Hogan, and V. V. Mootha, "Epithelial downgrowth after descemet stripping automated endothelial keratoplasty," *Cornea*, vol. 28, no. 6, pp. 708–711, 2009.

[10] S. Vira, C. Y. Shih, N. Ragusa et al., "Textural interface opacity after descemet stripping automated endothelial keratoplasty: a report of 30 cases and possible etiology," *Cornea*, vol. 32, no. 5, pp. e54–e59, 2013.

[11] I. E. Y. Saelens, M. C. Bartels, G. van Rij, W. N. M. Dinjens, and C. M. Mooy, "Introduction of epithelial cells in the flap-graft interface during descemet stripping automated endothelial keratoplasty," *Archives of Ophthalmology*, vol. 127, no. 7, pp. 936–937, 2009.

[12] A. Anshu, B. Planchard, M. O. Price, C. D. R. Pereira, and F. W. Price Jr., "A cause of reticular interface haze and its management after descemet stripping endothelial keratoplasty," *Cornea*, vol. 31, no. 12, pp. 1365–1368, 2012.

[13] W. W. Culbertson, "Descemet stripping endothelial keratoplasty," *International Ophthalmology Clinics*, vol. 46, no. 3, pp. 155–168, 2006.

[14] P. M. Phillips, M. A. Terry, S. C. Kaufman, and E. S. Chen, "Epithelial downgrowth after Descemet-stripping automated endothelial keratoplasty," *Journal of Cataract and Refractive Surgery*, vol. 35, no. 1, pp. 193–196, 2009.

[15] A. D. S. Forseto, M. S. D. Santos, A. Sampaio, V. Mascaro, and W. Nosé, "Diagnosis of epithelial ingrowth after penetrating keratoplasty with confocal microscopy," *Cornea*, vol. 25, no. 9, pp. 1124–1127, 2006.

[16] S. Ghosh, R. Bonshek, and S. J. Morgan, "Histologically proven epithelial ingrowth in failed Descemet stripping automated endothelial keratoplasty (DSAEK) managed by repeat DSAEK," *Clinical Ophthalmology*, vol. 7, pp. 1035–1040, 2013.

[17] S. B. Koenig and D. J. Covert, "Epithelial ingrowth after descemet-stripping automated endothelial keratoplasty," *Cornea*, vol. 27, no. 6, pp. 727–729, 2008.

[18] L. H. Suh, M. A. Shousha, R. U. Ventura et al., "Epithelial ingrowth after descemet stripping automated endothelial keratoplasty: description of cases and assessment with anterior segment optical coherence tomography," *Cornea*, vol. 30, no. 5, pp. 528–534, 2011.

[19] B. M. Walker, H. B. Hindman, K. B. Ebrahimi et al., "Epithelial downgrowth following Descemet's-stripping automated endothelial keratoplasty," *Archives of Ophthalmology*, vol. 126, no. 2, pp. 278–280, 2008.

[20] A. E. Maumenee and C. R. Shannon, "Epithelial invasion of the anterior chamber," *The American Journal of Ophthalmology*, vol. 41, no. 6, pp. 929–942, 1956.

[21] S. H. Chen and R. Pineda II, "Epithelial and fibrous downgrowth: mechanisms of disease," *Ophthalmology Clinics of North America*, vol. 15, no. 1, pp. 41–48, 2002.

[22] H. V. Gimbel, E. E. Anderson Penno, J. A. Van Westenbrugge, M. Ferensowicz, and M. T. Furlong, "Incidence and management of intraoperative and early postoperative complications in 1000 consecutive laser in situ keratomileusis cases," *Ophthalmology*, vol. 105, no. 10, pp. 1839–1848, 1998.

[23] M. Y. Wang and R. K. Maloney, "Epithelial ingrowth after laser in situ keratomileusis," *The American Journal of Ophthalmology*, vol. 129, no. 6, pp. 746–751, 2000.

[24] J. A. Lee, A. R. Djalilian, K. M. Riaz et al., "Clinical and histopathologic features of failed descemet stripping automated endothelial keratoplasty grafts," *Cornea*, vol. 28, no. 5, pp. 530–535, 2009.

[25] N. Asano-Kato, I. Toda, Y. Hori-Komai, Y. Takano, and K. Tsubota, "Epithelial ingrowth after laser in situ keratomileusis: clinical features and possible mechanisms," *The American Journal of Ophthalmology*, vol. 134, no. 6, pp. 801–807, 2002.

[26] L. H. Suh, S. H. Yoo, A. Deobhakta et al., "Complications of descemet's stripping with automated endothelial keratoplasty. Survey of 118 eyes at one institute," *Ophthalmology*, vol. 115, no. 9, pp. 1517–1524, 2008.

[27] L. H. Suh, D. G. Dawson, L. Mutapcic et al., "Histopathological examination of failed grafts in Descemet's stripping with automated endothelial keratoplasty," *Ophthalmology*, vol. 116, no. 4, pp. 603–608, 2009.

[28] L. A. Sidrys and T. Demong, "Epithelial downgrowth after penetrating keratoplasty," *Canadian Journal of Ophthalmology*, vol. 17, no. 1, pp. 29–31, 1982.

[29] J. D. Cameron, B. A. Flaxman, and M. Yanoff, "In vitro studies of corneal wound healing: epithelial endothelial interactions," *Investigative Ophthalmology & Visual Science*, vol. 13, no. 8, pp. 575–579, 1974.

[30] S. C. Kaufman, D. C. Musch, M. W. Belin et al., "Confocal microscopy: a report by the American Academy of Ophthalmology," *Ophthalmology*, vol. 111, no. 2, pp. 396–406, 2004.

[31] Y. Hara, A. Shiraishi, M. Yamaguchi, T. Uno, and Y. Ohashi, "Diagnosis and clinical course of epithelial ingrowth after Descemet-stripping automated endothelial keratoplasty followed by in vivo confocal microscopy," *Clinical and Experimental Ophthalmology*, vol. 39, no. 7, pp. 710–712, 2011.

[32] M. J. Weiner, J. Trentacoste, D. M. Pon, and D. M. Albert, "Epithelial downgrowth: a 30-year clinicopathological review," *The British Journal of Ophthalmology*, vol. 73, no. 1, pp. 6–11, 1989.

[33] S. Heinzelmann, D. Böhringer, P. C. Maier, and T. Reinhard, "Correlation between visual acuity and interface reflectivity measured by pentacam following DSAEK," *Acta Ophthalmologica*, vol. 92, no. 1, pp. 1–4, 2014.

[34] R. K. Wong, D. P. Greene, D. R. Shield, C. G. Eberhart, J. J. Huang, and A. Shayegani, "5-Fluorouracil for epithelial downgrowth after descemet stripping automated endothelial keratoplasty," *Cornea*, vol. 32, no. 12, pp. 1610–1612, 2013.

[35] M. M. Lai and J. A. Haller, "Resolution of epithelial ingrowth in a patient treated with 5-fluorouracil," *The American Journal of Ophthalmology*, vol. 133, no. 4, pp. 562–564, 2002.

[36] R. K. Wong, D. P. Greene, D. R. Shield, C. G. Eberhart, J. J. Huang, and A. Shayegani, "5-Fluorouracil for epithelial downgrowth after descemet stripping automated endothelial keratoplasty," *Cornea*, vol. 32, no. 12, pp. 1610–1612, 2013.

[37] R. A. Latkany, F. E. Haq, and M. G. Speaker, "Advanced epithelial ingrowth 6 months after laser in situ keratomileusis," *Journal of Cataract and Refractive Surgery*, vol. 30, no. 4, pp. 929–931, 2004.

Hindawi Publishing Corporation
BioMed Research International
Volume 2014, Article ID 290619, 8 pages
http://dx.doi.org/10.1155/2014/290619

Clinical Study

Evaluation of Corneal Biomechanical Properties Modification after Small Incision Lenticule Extraction Using Scheimpflug-Based Noncontact Tonometer

Leonardo Mastropasqua,[1] Roberta Calienno,[1] Manuela Lanzini,[1] Martina Colasante,[1] Alessandra Mastropasqua,[2] Peter A. Mattei,[1] and Mario Nubile[1]

[1] *Ophthalmic Clinic, University "G d'Annunzio" of Chieti-Pescara, Via dei Vestini, 66100 Chieti, Italy*
[2] *Ophthalmic Clinic, Campus Biomedico, University of Rome, 00185 Rome, Italy*

Correspondence should be addressed to Roberta Calienno; roberta.calienno@gmail.com

Received 8 April 2014; Accepted 7 August 2014; Published 31 August 2014

Academic Editor: Ciro Costagliola

Purpose. To quantify the effect of small incision lenticule extraction (SMILE) on the corneal biomechanics using Scheimpflug noncontact tonometer (Corvis ST). *Methods.* Twenty eyes of twenty patients, evaluated as eligible for surgery, with high myopia and/or moderate myopic astigmatism, underwent small incision lenticule extraction (SMILE). All patients underwent Corvis ST preoperatively and postoperatively after 1 week, and 1 and 3 months to observe alterations of corneal biomechanical properties. The main outcome measures were Deformation Amplitude, 1st-AT, and 2nd-AT. The relationship between the amount of stroma removed and the percentage variation of the measured parameters from baseline was evaluated with generalized linear model from each time point. For completeness also intraocular pressure (IOP), central corneal thickness (CCT), and their variations after surgery were evaluated. *Results.* The ratio between the amount of removed refractive error and, respectively, changes of Deformation Amplitude, 1st-AT, and 2nd-AT were significantly modified at the 1st week after surgery ($P = 0.005$; $P = 0.001$; $P = 0.024$). At 1 and 3 months these values did not show statistically significant alterations. Intraocular pressure and central corneal thickness showed statistically significant changes during follow-up. *Conclusions.* No significant modifications in biomechanical properties were observed after SMILE so this procedure could induce only minimal transient alterations of corneal biomechanics.

1. Introduction

The structural and reparative properties of the cornea are essential to its function as a resilient, yet transparent, barrier to intraocular injury. Because the cornea is also the scaffold for the major refractive surface of the eye, any mechanical or biological response to injury will also influence optical performance. Consequently, the same mechanisms responsible for preserving ocular integrity can undermine the goals of achieving predictable and stable visual outcomes after keratorefractive surgery [1].

While empirical modifications to algorithms and major advances in laser delivery platforms have improved the statistical predictability of refractive surgery currently most widespread procedures (LASIK, PRK), the ability to anticipate confounding biological responses at the level of the individual patient remains limited. In fact, a predisposition to mechanical instability or abnormal regulation of healing can lead to serious complications such as keratectasia [1]. Previous studies already reported a significant reduction of corneal resistance after LASIK surgery [2–5].

The goal of research in this setting is to improve outcomes and reduce complications by discerning details of the biomechanical and wound healing pathways, identifying measurable predictors of individual responses [1].

In this context the possibility of standardizing the measurement of corneal tissue deformation degree, induced by refractive surgery procedures, would be essential to determine the predictability in the development of complications such as keratectasia and to compare different surgical procedures in terms of biomechanical and tissue stability.

The Oculus Corvis ST (Oculus Optikgeräte, OCULUS, Wetzlar, Germany) is a noncontact High-Speed (UHS ST) tonometer, supported by Scheimpflug Technology, designed to obtain in vivo measurements of corneal biomechanical properties; this device allows monitoring corneal deformation response to a symmetrically metered air pulse (Figure 1).

The device depicts the time required to applanate the cornea with the air puff, and the time of the first inward applanation is directly proportional to the IOP, which ranges from 1 mm Hg to 60 mm Hg. IOP and CCT are obtained during one measurement process. Additional Corvis ST parameters are measured in time in milliseconds, length in millimetres, and velocity in metres/second of the first (air puff flattens cornea) and second (interruption of air puff results in "reformation" of cornea) corneal applanation; furthermore, peak distance, radius, and deformation amplitude in millimetres of the highest corneal concavity during the measurement process are measured [6] (Figure 2).

Different previous studies demonstrated that corneal parameters measured by Corvis ST are repeatable and reproducible [6–9]; in particular Hon and Lam recently defined the central corneal thickness (CCT) as the most repeatable corneal parameter measured by Corvis and the deformation amplitude (DA) as an indicator of corneal biomechanical properties, followed by the first applanation time (1st-AT) [8].

With the introduction of the VisuMax femtosecond laser (Carl ZeissMeditec AG, Jena, Germany) in 2006 [10, 11], keratorefractive surgery was revolutionized and intrastromal keratomileusis was reinvented in the shape of refractive lenticule extraction [12]. A new procedure, small-incision lenticule extraction (SMILE), was developed, totally without excimer laser support.

During SMILE procedure, first a stromal lenticule, with characteristics defined on the basis of the refractive defect of the patient, is cut within the corneal stroma by the femtosecond laser, using ultrafast [13–18] pulses to create photo disruption. Afterwards, a surface cut is made to allow access to dissect and manually remove the lenticule [11]. In SMILE, only a small incision is made without the creation of a flap, minimizing trauma to the corneal surface if compared with other surgical procedures (PRK or LASIK) [19–22] (Figure 3).

In a recent paper, Hassan and coll. carried out a comparison of the corneal biomechanical parameters variation between PRK and LASIK using Corvis; they observed that most of these biomechanical parameters remained unchanged after one month of LASIK and PRK compared to the preoperative data [23].

Also a recent study of Reinstein et al., developing a mathematical model to estimate the relative differences in postoperative corneal stromal tensile strength following PRK, LASIK, and SMILE, defined that the postoperative stromal tensile strength is higher after SMILE if compared with other procedures, as expected given that the strongest anterior lamellae remain intact in SMILE [24].

However, little is known regarding the biomechanical effects of SMILE. Provided that all types of keratorefractive surgery induce a variable degree of corneal deformation with consequences on tissue stability, it is interesting to assess the possible biomechanical alterations induced by SMILE procedure.

So the aim of this study was to quantify the effect of SMILE on the corneal biomechanical properties, for the first time, by means of Corvis ST.

2. Materials and Methods

This prospective, nonrandomized, and comparative clinical trial comprised 20 eyes of 20 patients (age from 25 to 43 years, DS 34 ± 12), scheduled for refractive surgery at the Ophthalmic Clinic of the "SS. Annunziata" Hospital of Chieti (Italy) for myopic and/or astigmatic correction between May 2010 and October 2012, that underwent SMILE. The protocol adhered to the tenets of the Declaration of Helsinki and received approval from an institution review board. Informed consent was obtained from all participants and possible consequences of taking part were explained.

Inclusion criteria were a moderate to high myopia, stability for at least 1 year, a corrected distance visual acuity (CDVA) of 20/25 or better, spherical equivalent refraction from −3.00 to −7.00 diopters (D), and a refractive astigmatism from 0.50 to 1.50 D.

A central corneal thickness (CCT) less than 480 μm, a calculated postoperative residual stromal bed of less than 250 μm, a presence of keratoconus, pregnancy, or breast-feeding, and all other ocular pathological conditions meant exclusion from surgery.

Patients underwent eye examination including objective and manifest visual acuity, intraocular pressure (Canon tonometer, TX10, NY, USA), pupil size (Sirius, CSO, Firenze Italy), keratometric measurements, slit-lamp examination, and fundoscopy (Slit lamp BM900, Haag-Streit, Koeniz Switzerland). Regular topographic patterns of both the corneal front and back and normal CCT were confirmed with a Pentacam-HR Scheimpflug camera (Oculus, Germany). This included the usage of the Pentacam Ambrósio/Belin module to exclude also a subclinical keratoconus. We decided to consider the most repeatable indicators of corneal biomechanical properties measured by Corvis ST and already validated from scientific literature [8]: the deformation amplitude (DA) and the first applanation time (1st-AT). We also voluntarily considered, for study completeness, the second applanation time (2nd-AT). Also IOP and CCT values were evaluated before surgery and at every step of follow-up in order to identify modifications of these parameters induced by SMILE.

All patients before surgery underwent Corvis ST measurement preoperatively to evaluate DA that represents the maximum amplitude at the corneal apex (highest concavity), 1st-AT, that is, the time from starting until the first corneal applanation, and 2nd-AT, that is, time from starting until the second applanation, according to the mode previously described in literature [24] and described below.

The patient can be comfortably positioned due to the proper placement of the chin and forehead and is asked to focus at the central red light emitting diode (LED).

The UHS Scheimpflug camera takes over 4,300 frames per second in order to monitor corneal response to a metered,

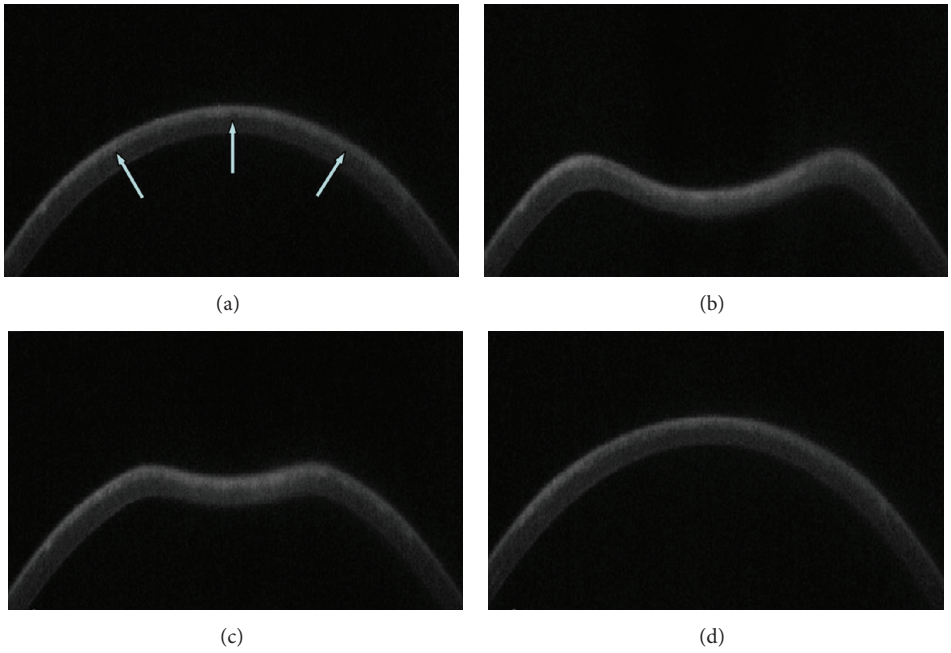

Figure 1: Corvis UHS Scheimpflug camera frames of corneal response to a metered, collimated air pulse: air pulse forces cornea that underwent SMILE procedure (a) inwards through applanation into a concavity phase until it achieves the highest concavity (b). An oscillation period precedes the outgoing or returning phase. The cornea undergoes a second applanation (c) before achieving its natural shape with possible oscillation (d). White arrows indicate femtosecond laser cutting surface interface after SMILE procedure.

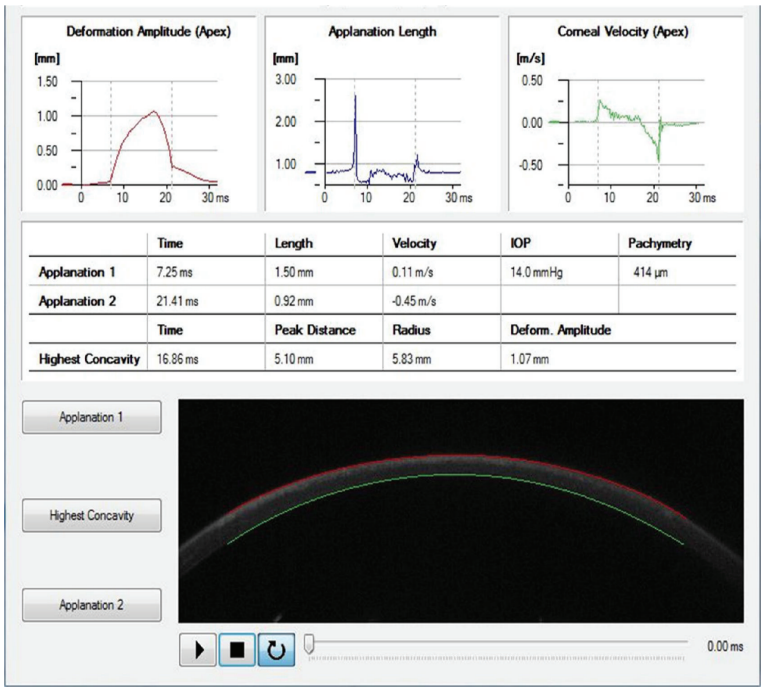

Figure 2: Measurements obtained by Corvis immediately upon air impulse after SMILE procedures. Real-time informations recorded after SMILE: corneal highest concavity, IOP, pachymetry, and first and second time applanation. A high-speed Scheimpflug camera recorded the cornea movements and then displayed them on the control panel in an ultraslow motion (not shown).

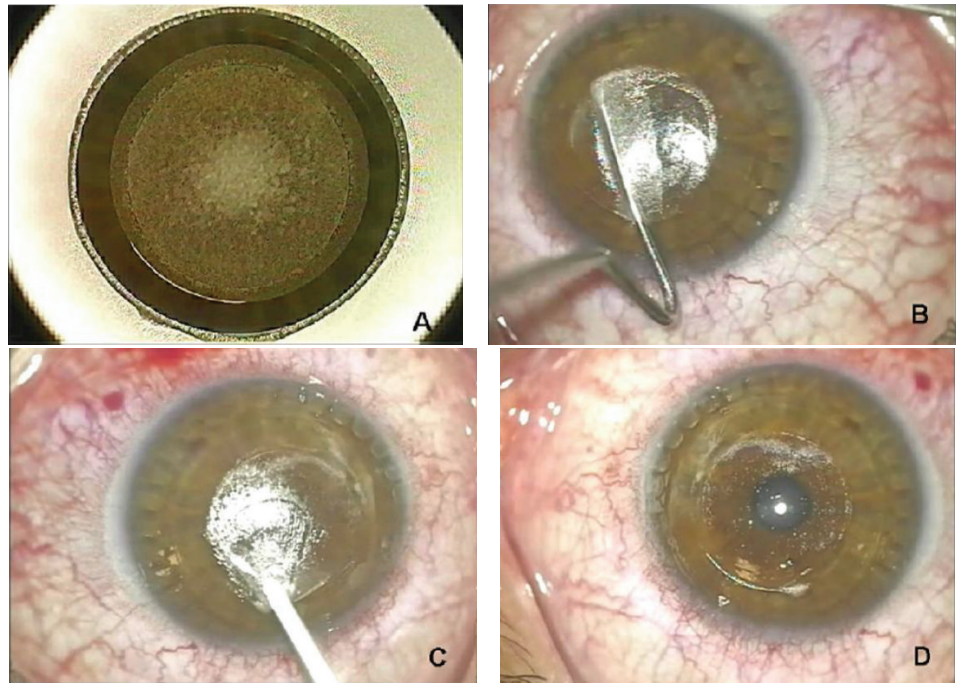

Figure 3: Femtosecond laser SMILE procedure: a stromal lenticule, with characteristics defined on the basis of the refractive defect of the patient, is cut within the corneal stroma by the femtosecond laser (a). Afterwards, only a small incision is made to allow access to dissect (b) and manually remove the lenticule (c-d).

collimated air pulse with symmetrical fixed profile and a fixed maximal internal pump pressure of 25 kPa.

This imaging system permits the dynamic inspection of the actual deformation process during noncontact tonometry. The recording starts with the cornea at the natural convex shape. The air pulse forces the cornea inwards (i.e., the ingoing phase) through applanation (i.e., the first or ingoing applanation) into a concavity phase until it achieves the highest concavity (HC). An oscillation period precedes the outgoing or returning phase. The cornea undergoes a second applanation before achieving its natural shape with possible oscillation (Figure 1). The timing and corresponding pressure of the air pulse at the first and second applanation and at the HC moments are identified. IOP is calculated based on the timing of the first applanation event. The deformation amplitude (DA) is measured as the highest displacement of the apex in the HC moment image. The radius of curvature at the HC is recorded. The lowest value is displayed. The Corvis ST measurements were repeated on the patients three times subsequently on the same patient by the same operator (Roberta Calienno)

Two surgeons performed all surgical procedures (Leonardo Mastropasqua and Mario Nubile).

Visumax (Carl Zeiss Meditec, Jena, Germany) femtosecond laser platform was used to realize SMILE procedure. The procedures were performed as previously described and illustrated in detail [22, 25, 26].

Briefly, laser cut energy index range was approximately from 125 to 170 mJ and spot spacing ranged from 2.5 to 4.5 μm. Then a 40° to 60° incision located at the 12-o'clock position was created to allow the lenticule extraction. Lenticule diameter (optical zone) was 6.0 to 6.5 mm, and the cap diameter was 7.3 mm. Intended cap thickness was 110 to 120 μm.

After surgery, all patients received one drop of Netilmicin 0,3% (Nettacin, SIFI, Catania, Italy) and one drop of dexamethasone phosphate 0,15% (Etacortilen, SIFI, Catania, Italy); then a soft contact lens was applied.

The postoperative regimen included the same eye drops four times a day for 1 week, followed by two times a day for 1 week and lubricating drops four times a day. On the first day after surgery, the soft contact lens was removed; then visual acuity was measured and slit-lamp examination was performed. On the first week and 1 month and 3 months after surgery, patients returned for a follow-up examination with measurement of the same parameters and Corvis ST parameters.

2.1. Statistical Analysis. Parameters were summarized as mean and standard deviation of the percentage difference from baseline values. The presence of statistically significant differences in the percentage variation from baseline for each of the three variables was evaluated with a paired t-test. The relationship between the amount of stroma removed and the percentage variation of each of the measured parameters from baseline was evaluated with linear regression for each time point.

Statistical analysis was performed using SPSS 20.0 (IBM, Armonk, NY). Statistical significance was assigned at $P \leq 0.05$.

In addition IOP and CCT values were considered to identify if a statistically significant difference was present

Table 1: Percentage variation from baseline values of the three parameters measured (millisecond (ms) in applanation times and millimeter (mm) for deformation amplitude) expressed as mean and standard deviation (S.D.) for each of the three time points. The three time points were compared using a two-tailed paired t-test.

	N	Mean ± S.D	Paired t-test P (versus 7 days)	Paired t-test P (versus 30 days)
DA (mm)				
7 Days	20	60.0 ± 10.4	0.005	
30 Days	20	−3.6 ± 11.2	0.021	
90 Days	20	−1.7 ± 8.4		0.576
TA1 (ms)				
7 Days	20	14.8 ± 21.7	0.001	
30 Days	20	−10.7 ± 18.9	0.014	
90 Days	20	−6.0 ± 21.9		0.263
TA2 (ms)				
7 Days	20	13.2 ± 18.1	0.024	
30 Days	20	−4.0 ± 28.3	0.049	
90 Days	20	2.4 ± 18.6		0.385

between preoperative time and all follow-up times with an ordinary one way ANOVA test.

3. Results

The surgical procedure was successfully completed in all patients, no complications occurred, and no patients were lost to follow-up. Mean correction was 5.5 ± 1.2 D (range 3.5 to 7 D) at each of the three follow-ups.

Table 1 shows the percentage variation from baseline values of the three parameters expressed as mean and standard deviation (S.D.) for each of the three time points that were compared using paired t-tests. The differences between seven days and 30 and 90 days were statistically significant for all three parameters while those between 30 and 90 days were not.

Figure 4 presents a scatterplot of the percentage variation from baseline values of DA (a), TA1 (b), and TA2 (c) for each subject against the correction performed with SMILE. These relationships were evaluated with linear regression analysis that showed a statistically significant relationship was present only at 7 days postoperatively. The coefficient of determination ($r2$) was 0.502 for D ($P < 0.001$), 0.347 for TA1 ($P = 0.004$), and 0.583 for TA2 ($P < 0.001$) at seven days postoperatively. The regression lines also demonstrated that there was a pattern for less structural integrity with progressively higher corrections at seven days postoperatively but not at the later follow-ups.

The variation from preoperative values of the IOP and CCT and all time of follow-up, compared using ordinary one way ANOVA, showed a statistically significant difference (reduction) ($P = 0.0082$ and $P = 0.0084$, resp.).

4. Discussion

Corneal biomechanical properties involve, besides elasticity and viscosity, thickness and hydration, mostly dominated by the stroma that constitutes 90% of the total corneal thickness and determines mechanical response of the cornea to injury [27].

Despite the recent progress and the technological advances that are obtained in refractive surgery, particularly in improved understanding of the refractive errors basic science and the biomechanics of corneal wound healing, currently complications still happen [28].

In fact, the unpredictable nature of corneal wound healing and the biomechanical response to surgery can lead to postoperative refractive surprises, discrepancies between attempted and achieved visual outcomes, and biomechanical and wound healing problems with particular importance for keratectasia [28]. During LASIK, PRK, or any other procedure involving central ablation, an immediate circumferential severing of corneal lamellae is produced. In simple elastic shell models, this results in a forward herniation that would result in corneal steepening and thickening [29]. It is already known that LASIK flap creation may induce astigmatism and higher order aberrations [30, 31] because the flap itself is subject to shape changes induced by the circumferential keratotomy of flap creation.

Furthermore, the risk of developing post-LASIK ectasia increases in patients with preexisting keratoconus, deep flaps, high myopia, deep laser ablation [32], a corneal thickness lower than 500 μm, and residual stromal bed thickness lower than 250 μm.

Since refractive surgery decreases collagen tension, by disrupting cornea biomechanics, and may lead to corneal ectasia that favors decreased visual acuity [33], determining risk factors which lead corneal ectasia and understanding what kind of refractive surgical procedure can reduce ectasia incidence are indispensable.

Femtosecond laser seems to imply biomechanical advantages in LASIK flap creation [18].

SMILE procedure theoretically may have biomechanical benefits over LASIK because it does not involve the creation of a flap and leaves the stroma over the lenticule untouched. However, there are not many published studies regarding the biomechanical effects of SMILE.

Recently Agca et al. performed an analysis of corneal biomechanical properties (corneal hysteresis as CH and corneal resistance factor as CRF) after SMILE, comparing these values with the same ones obtained after femto-LASIK procedure with the support of the Ocular Response Analyzer (ORA; Reichert Inc., Buffalo, NY, USA) [34].

They concluded that there were no differences between the two compared procedures in terms of biomechanical properties and that CH and CRF decreased after SMILE.

They also hypothesized that, although not statistically significant, differences in postoperative CH and CRF values between the femto-LASIK and SMILE groups were found; this did not mean that the corneas in both groups were biomechanically similar to each other after these surgical procedures because CH and CRF values only reflected some

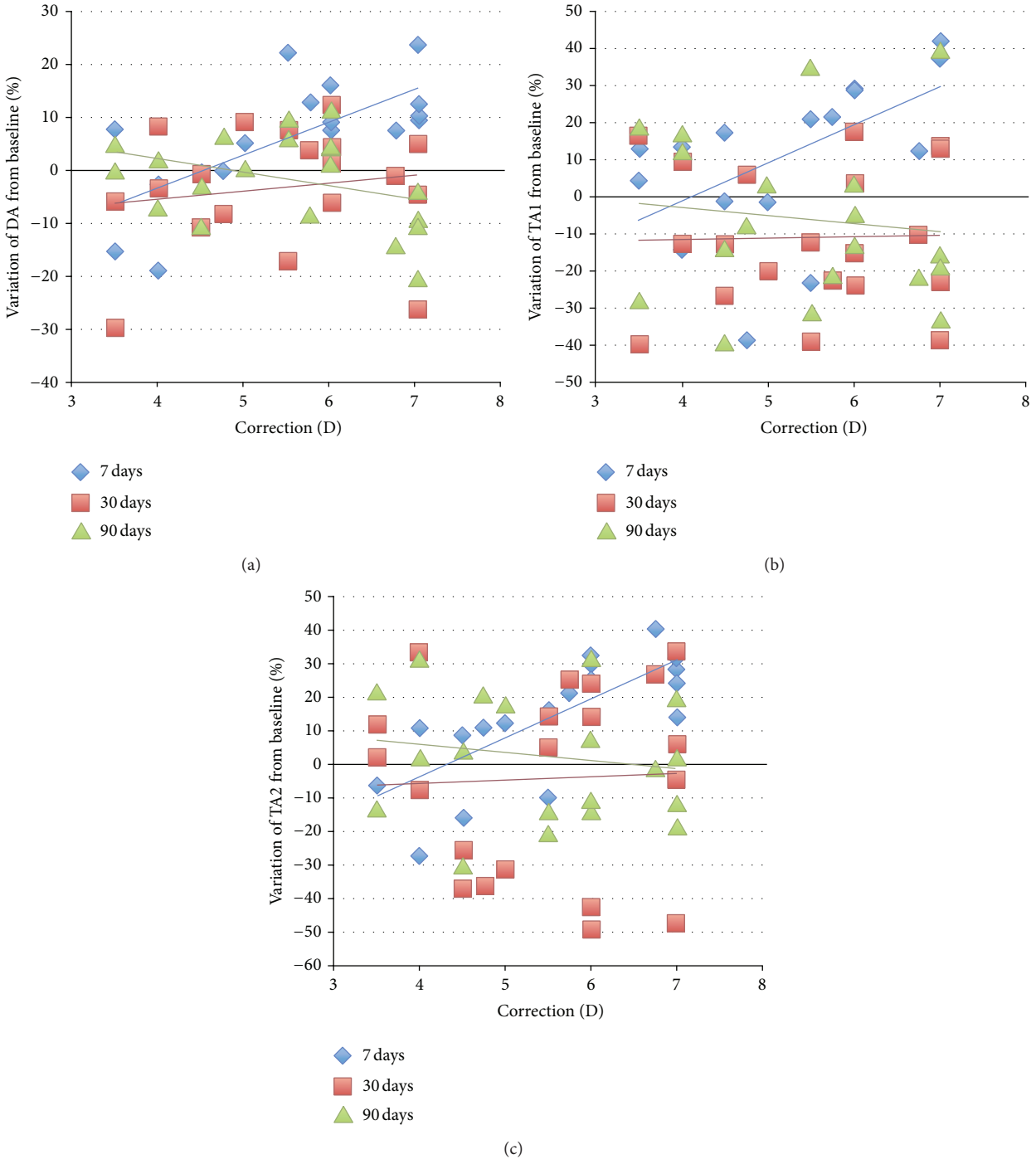

Figure 4: The figure presents a scatterplot of the percentage variation from baseline values of DA (a), TA1 (b), and TA2 (c) for each subject against the correction performed with SMILE.

clinically significant aspects of corneal biomechanical structure and the absence of difference did not mean that the corneas in both groups are biomechanically similar [34].

In order to investigate these critical points, our study aims to assess changes induced on corneal biomechanical parameters after SMILE to understand the impact of this new surgical procedure on corneal biomechanical stability.

We decided to consider the most currently validated CORVIS parameters by the scientific literature: DA and applanation times [8]. In addition, IOP and CCT were considered because it is already known by scientific literature that these parameters are fundamental in corneal deformation response evaluation and could influence the CORVIS biomechanical values [35].

In particular we identify a statistically significant difference for both parameters between the preoperative period and all the follow-up period as might be expected after SMILE treatment.

Such significance certainly makes our biomechanical results more valid and reliable.

Moreover, as described in the results section, DA and 1st and 2nd applanation times were increased 7 days after surgery. This is easily understood since the procedure SMILE, causing the removal of a corneal tissue lenticule, reduces the stiffness and the structural compactness of the cornea and consequently involves an increase of applanation times.

In fact, as it is guessed, thinner and therefore less rigid corneas have more applanation time because when a load force is applied over it, the corresponding response force is reduced as it is directly related to the decreased tissue stiffness.

Consequently also the amplitude of deformation will increase by increasing the corneal deformability. However at the other follow-up controls (30 and 90 days) all the three parameters presented no statistically significant modifications.

So, based on our results, a substantial modification of corneal biomechanics occurs only in the very first follow-up time after SMILE (7 days).

This is certainly related to the lenticule removal and the subsequent rebuilding of a new biomechanical balance dominated by different tensile forces related to the residual stromal bed. Otherwise, these differences from baseline were evident, and a statistically significant relationship was present, only at 7 days postoperatively but not between 30 and 90 days; this probably means that this new biomechanical balance is relatively quickly determined, and this despite the removed lenticule thickness that is directly proportional to the corrected refractive errors.

This would mean that corneal biomechanical stability is only relatively and temporarily modified after SMILE, when stromal lenticule removal, graven by femtosecond laser, happens. So probably tensile forces that allow and encourage corneal stability are altered only minimally after SMILE procedure.

On the basis of the most recent scientific literature that defined SMILE as a minimally invasive and inflammatory surgical procedure for corneal tissue if compared to the other refractive surgery procedures [36], we could also hypothesize that even a low level of induced inflammation may perhaps encourage a more rapid reestablishment of a stable biomechanical corneal balance.

However the study presents limits of a reduced sample size and the use of Corvis ST, that is, an innovative imaging system that allows obtaining in vivo biomechanical information and avoids the limitations of previous in vivo and in vitro techniques but is only recently emerging as a clinical instrument used to investigate in vivo biomechanical properties of the cornea.

Probably other prospective studies supported by the use of this new technology are needed to confirm our data and to imply the corneal biomechanical properties knowledge. Furthermore, as already reported in literature [33], the average appearance timing of corneal ectasia is about 12–60 months after LASIK; so it will be interesting to conduct a more extensive follow-up (up to 3 months) in order to consider possible late changes of corneal biomechanics after SMILE.

Finally, a comparison on the corneal biomechanical changes after SMILE among patients who presented a variability of myopia and astigmatism degree (from minimum to high) will certainly be an additional element of assessment (our patients presented only high level of myopia and/or moderate myopic astigmatism).

In conclusion, from these results we could define SMILE as a procedure that determines only minimum alterations of corneal biomechanics but we need to overcome our limitations by broadening and deepening the study in order to well define the benefits of this new and increasingly diffuse refractive surgery procedure.

Conflict of Interests

The authors declare that there is no conflict of interests regarding the publication of this paper.

References

[1] W. J. Dupps Jr. and S. E. Wilson, "Biomechanics and wound healing in the cornea," *Experimental Eye Research*, vol. 83, no. 4, pp. 709–720, 2006.

[2] D. A. Luce, "Determining in vivo biomechanical properties of the cornea with an ocular response analyzer," *Journal of Cataract & Refractive Surgery*, vol. 31, no. 1, pp. 156–162, 2005.

[3] D. Ortiz, D. Piñero, M. H. Shabayek, F. Arnalich-Montiel, and J. L. Alió, "Corneal biomechanical properties in normal, post-laser in situ keratomileusis, and keratoconic eyes," *Journal of Cataract and Refractive Surgery*, vol. 33, no. 8, pp. 1371–1375, 2007.

[4] J. S. Pepose, S. K. Feigenbaum, M. A. Qazi, J. P. Sanderson, and C. J. Roberts, "Changes in corneal biomechanics and intraocular pressure following LASIK using static, dynamic, and noncontact tonometry," *American Journal of Ophthalmology*, vol. 143, no. 1, pp. 39–47, 2007.

[5] C. Kirwan and M. O'Keefe, "Corneal hysteresis using the Reichert ocular response analyser: findings pre- and post-LASIK and LASEK," *Acta Ophthalmologica*, vol. 86, no. 2, pp. 215–218, 2008.

[6] L. Reznicek, D. Muth, A. Kampik, A. S. Neubauer, and C. Hirneiss, "Evaluation of a novel Scheimpflug-based non-contact tonometer in healthy subjects and patients with ocular hypertension and glaucoma," *British Journal of Ophthalmology*, vol. 97, no. 11, pp. 1410–1414, 2013.

[7] G. Nemeth, Z. Hassan, A. Csutak, E. Szalai, A. Berta, and L. Modis Jr., "Repeatability of ocular biomechanical data measurements with a scheimpflug-based noncontact device on normal corneas," *Journal of Refractive Surgery*, vol. 29, no. 8, pp. 558–563, 2013.

[8] Y. Hon and A. K. C. Lam, "Corneal deformation measurement using Scheimpflug noncontact tonometry," *Optometry and Vision Science*, vol. 90, no. 1, pp. 1–8, 2013.

[9] J. Hong, J. Xu, A. Wei et al., "A new tonometer—the corvis ST tonometer: clinical comparison with noncontact and goldmann applanation tonometers," *Investigative Ophthalmology and Visual Science*, vol. 54, no. 1, pp. 659–665, 2013.

[10] W. Sekundo, K. Kunert, C. Russmann et al., "First efficacy and safety study of femtosecond lenticule extraction for the correction of myopia: six-month results," *Journal of Cataract & Refractive Surgery*, vol. 34, no. 9, pp. 1513–1520, 2008.

[11] M. Blum, K. Kunert, M. Schröder, and W. Sekundo, "Femtosecond lenticule extraction for the correction of myopia: preliminary 6-month results," *Graefe's Archive for Clinical and Experimental Ophthalmology*, vol. 248, no. 7, pp. 1019–1027, 2010.

[12] A. H. Vestergaard, K. T. Grønbech, J. Grauslund, A. R. Ivarsen, and J. Ø. Hjortdal, "Subbasal nerve morphology, corneal sensation, and tear film evaluation after refractive femtosecond laser lenticule extraction," *Graefe's Archive for Clinical and Experimental Ophthalmology*, vol. 251, no. 11, pp. 2591–2600, 2013.

[13] R. Ambrósio Jr., T. Tervo, and S. E. Wilson, "LASIK-associated dry eye and neurotrophic epitheliopathy: pathophysiology and strategies for prevention and treatment," *Journal of Refractive Surgery*, vol. 24, no. 4, pp. 396–407, 2008.

[14] S. E. Wilson, "Laser in situ keratomileusis-induced (presumed) neurotrophic epitheliopathy," *Ophthalmology*, vol. 108, no. 6, pp. 1082–1087, 2001.

[15] D. T. Vroman, H. P. Sandoval, L. E. Fernández de Castro, T. J. Kasper, M. P. Holzer, and K. D. Solomon, "Effect of hinge location on corneal sensation and dry eye after laser in situ keratomileusis for myopia," *Journal of Cataract and Refractive Surgery*, vol. 31, no. 10, pp. 1881–1887, 2005.

[16] H. K. Lee, K. S. Lee, H. C. Kim, S. H. Lee, and E. K. Kim, "Nerve growth factor concentration and implications in photorefractive keratectomy vs laser in situ keratomileusis," *The American Journal of Ophthalmology*, vol. 139, no. 6, pp. 965–971, 2005.

[17] E. Y. W. Yu, A. Leung, S. Rao, and D. S. C. Lam, "Effect of laser in situ keratomileusis on tear stability," *Ophthalmology*, vol. 107, no. 12, pp. 2131–2135, 2000.

[18] I. Ratkay-Traub, T. Juhasz, C. Horvath et al., "Ultra-short pulse (femtosecond) laser surgery: initial use in LASIK flap creation," *Ophthalmology Clinics of North America*, vol. 14, no. 2, pp. 347–355, 2001.

[19] S. Wei and Y. Wang, "Comparison of corneal sensitivity between FS-LASIK and femtosecond lenticule extraction (ReLEx flex) or small-incision lenticule extraction (ReLEx smile) for myopic eyes," *Graefe's Archive for Clinical and Experimental Ophthalmology*, vol. 251, no. 6, pp. 1645–1654, 2013.

[20] W. Sekundo, K. S. Kunert, and M. Blum, "Small incision corneal refractive surgery using the small incision lenticule extraction (SMILE) procedure for the correction of myopia and myopic astigmatism: results of a 6 month prospective study," *British Journal of Ophthalmology*, vol. 95, no. 3, pp. 335–339, 2011.

[21] R. Shah, S. Shah, and S. Sengupta, "Results of small incision lenticule extraction: all-in-one femtosecond laser refractive surgery," *Journal of Cataract and Refractive Surgery*, vol. 37, no. 1, pp. 127–137, 2011.

[22] A. Vestergaard, A. R. Ivarsen, S. Asp, and J. Ø. Hjortdal, "Small-incision lenticule extraction for moderate to high myopia: predictability, safety, and patient satisfaction," *Journal of Cataract and Refractive Surgery*, vol. 38, no. 11, pp. 2003–2010, 2012.

[23] Z. Hassan, L. Modis Jr., E. Szalai, A. Berta, and G. Nemeth, "Examination of ocular biomechanics with a new Scheimpflug technology after corneal refractive surgery," *Contact Lens & Anterior Eye*, vol. 37, no. 5, pp. 337–341, 2014.

[24] D. Z. Reinstein, T. J. Archer, and J. B. Randleman, "Mathematical model to compare the relative tensile strength of the cornea after PRK, LASIK, and small incision lenticule extraction," *Journal of Refractive Surgery*, vol. 29, no. 7, pp. 454–460, 2013.

[25] J. O. Hjortdal, A. H. Vestergaard, A. Ivarsen, S. Ragunathan, and S. Asp, "Predictors for the outcome of small-incision lenticule extraction for myopia," *Journal of Refractive Surgery*, vol. 28, no. 12, pp. 865–871, 2012.

[26] M. Rosman, R. C. Hall, C. Chan et al., "Comparison of efficacy and safety of laser in situ keratomileusis using 2 femtosecond laser platforms in contralateral eyes," *Journal of Cataract and Refractive Surgery*, vol. 39, no. 7, pp. 1066–1073, 2013.

[27] BF. Valbon, R. Ambrósio Jr., B. M. Fontes, and M. R. Alves, "Effects of age on corneal deformation by non-contact tonometry integrated with an ultra-high-speed (UHS) Scheimpflug camera," *Arquivos Brasileiros de Oftalmologia*, vol. 76, no. 4, pp. 229–232, 2013.

[28] D. T. Azar, J.-H. Chang, and K. Y. Han, "Wound healing after keratorefractive surgery: review of biological and optical considerations," *Cornea*, vol. 31, supplement 1, pp. S9–S19, 2012.

[29] M. R. F. D. Bryant, M. Campos, and P. J. McDonnell, "Finite element analysis of corneal topographic changes after excimer laser phototherapeutic keratectomy," *Investigative Ophthalmology and Vision Science*, vol. 31, p. 804, 1993.

[30] J. L. Güell, F. Velasco, C. Roberts, M. T. Sisquella, and A. Mahmoud, "Corneal flap thickness and topography changes induced by flap creation during laser in situ keratomileusis," *Journal of Cataract and Refractive Surgery*, vol. 31, no. 1, pp. 115–119, 2005.

[31] I. G. Pallikaris, G. D. Kymionis, S. I. Panagopoulou, C. S. Siganos, M. A. Theodorakis, and A. I. Pallikaris, "Induced optical aberrations following formation of a laser in situ keratomileusis flap," *Journal of Cataract and Refractive Surgery*, vol. 28, no. 10, pp. 1737–1741, 2002.

[32] P. S. Binder, "Ectasia after laser in situ keratomileusis," *Journal of Cataract and Refractive Surgery*, vol. 29, no. 12, pp. 2419–2429, 2003.

[33] M. G. Tatar, F. A. Kantarci, A. Yildirim et al., "Risk factors in post-LASIK corneal ectasia," *Journal of Ophthalmology*, vol. 2014, Article ID 204191, 4 pages, 2014.

[34] A. Agca, E. B. Ozgurhan, A. Demirok et al., "Comparison of corneal hysteresis and corneal resistance factor after small incision lenticule extractionand femtosecond laser-assisted LASIK: a prospective fellow eye study," *Contact Lens and Anterior Eye*, vol. 37, no. 2, pp. 77–80, 2014.

[35] T. Huseynova, G. O. Waring IV, C. Roberts, R. R. Krueger, and M. Tomita, "Corneal biomechanics as a function of intraocular pressure and pachymetry by dynamic infrared signal and scheimpflug imaging analysis in normal eyes," *American Journal of Ophthalmology*, vol. 157, no. 4, pp. 885–893, 2014.

[36] Z. Dong, X. Zhou, J. Wu et al., "Small incision lenticule extraction (SMILE) and femtosecond laser LASIK: comparison of corneal wound healing and inflammation," *British Journal of Ophthalmology*, vol. 98, no. 2, pp. 263–269, 2014.

Hindawi Publishing Corporation
BioMed Research International
Volume 2014, Article ID 471642, 8 pages
http://dx.doi.org/10.1155/2014/471642

Research Article

Corneal Epithelial Wound Healing Promoted by Verbascoside-Based Liposomal Eyedrops

Luigi Ambrosone,[1] Germano Guerra,[2] Mariapia Cinelli,[3] Mariaelena Filippelli,[2] Monica Mosca,[1] Francesco Vizzarri,[4] Dario Giorgio,[2] and Ciro Costagliola[2]

[1] *Department of Bioscience and Territory (DIBT), University of Molise, Contrada Lappone, Pesche, 86090 Isernia, Italy*
[2] *Department of Medicine and Health Sciences, University of Molise, Via F. De Sanctis, 86100 Campobasso, Italy*
[3] *Department of Public Health, University of Naples Federico II, Via S. Pansini 5, 80131 Naples, Italy*
[4] *Department of Agriculture, Environment and Food (AAA), University of Molise, Via F. De Sanctis, 86100 Campobasso, Italy*

Correspondence should be addressed to Germano Guerra; germano.guerra@unimol.it

Received 3 May 2014; Accepted 8 July 2014; Published 6 August 2014

Academic Editor: Leonardo Mastropasqua

Different liposomal formulations were prepared to identify those capable of forming eyedrops for corneal diseases. Liposomes with neutral or slightly positive surface charge interact very well with the cornea. Then these formulations were loaded with verbascoside to heal a burn of corneal epithelium induced by alkali. The cornea surface affected involved in wound was monitored as a function of time. Experimental results were modeled by balance equation between the rate of healing, due to the flow of phenylpropanoid, and growth of the wound. The results indicate a latency time of only three hours and furthermore the corneal epithelium heals in 48 hours. Thus, the topical administration of verbascoside appears to reduce the action time of cells, as verified by histochemical and immunofluorescence assays.

1. Introduction

Epidemiological, chemical, and clinical studies have provided various evidences that free-radical-induced oxidative damage of cellular membrane plays a causative role in aging and several degenerative diseases such as cancer, atherosclerosis, age related macular degeneration, and cataract formations [1–4]. *In vitro* and *in vivo* evidence seem to indicate that antioxidants might have beneficial effects in protecting against these diseases. Thus it is not surprising that inhibition of free-radicals-induced oxidative damage, by means of antioxidant supplementations, has become a therapeutic strategy to reduce the risk of these diseases [5, 6]. The degree of oxidation and extent of the oxidative damage depend on the physical phase in which antioxidants are located and on the presence of interfaces [7–9]. Among others, phenyl-propanoid glycosides have been found to play important roles in protection against oxidative stress [10, 11]. Phenylpropanoid glycosides are water-soluble derivatives of natural polyphenols widely distributed in the plant kingdom. Verbascoside belongs to the phenylpropanoid glycoside group and is structurally characterized by caffeic acid and 4,5-hydroxyphenylethanol bound to a β-(D)-glucopyranoside, with a rhamnose in sequence (1–3) to the glucose molecule. Although there are many studies concerning the biological activity of verbascoside, its molecular mechanism and target are uncertain. Recently, we showed that a prolonged verbascoside-based diet improves both health status and the oxidative state of the different eye tissues in rabbits and hares [12, 13]. In these experiments verbascoside was administered in the form of tiny capsules of lipids for effectively protecting the antioxidant during its passage in the digestive tract [13]. It is well documented that verbascoside promotes skin repair and ameliorates skin inflammation [14]. Traditionally, ocular drug therapies have been administrated in the form of topical eyedrops. However, using this means of delivery, the drug may be quickly eliminated due to overflow and tear drainage [15]. Following the instillation of a normal 50 μL eyedrop, approximately

20–30 μL is immediately lost to overflow since the maximum volume that can be retained in the eye is 20–30 mL when blinking is prohibited or 10 μL when blinking is permitted [15, 16]. In order to improve the therapeutic benefit and to confer to liposome a specificity for a certain cell or organ macromolecules such as antibodies, peptides and ligands of natural receptors are conjugated on liposome [17, 18]. The aim of this study has been to verify the efficacy of a verbascoside-based liposomal eyedrops in alkali corneal wound and to ascertain the corneal retention liposomal affinity toward liposomes by modulating their surface charge.

2. Material and Methods

2.1. Chemicals. Soy lecithin (phosphatidylcholine-enriched fraction, Epikuron 200), composed of phosphatidylcholine (min. 92%), lysophosphatidylcholine (max. 3%), other phospholipids (max. 2%), and fatty acid (approximately 1%),was kindly offered by Cargill, Inc. The average fatty acid composition of this lecithin says that the linoleic acid is the most abundant (≈60%) followed by palmitic and oleic acid. Phospholipids Epikuron 130 P composed of phosphatidylcholine (33%), phosphatidylethanolamine (15%), phosphatidylinositol (16%), and phosphatidic acid (6%) was kindly offered by Cargill. Cholesterol from lanolin was purchased from Fluka Analytical. Any other reagent used was of analytical grade of purity.

2.2. Preparation of Liposomal Encapsulated Verbascoside. Liposomes with different sizes and surface charges were used. They were prepared from lecithin and conventional rotary evaporation-sonication method [19]. Appropriate amounts of lecithin (40 mg) were dissolved in chloroform. The mixture was dried to a thin film under vacuum. The film was then hydrated with phosphate buffer (10 mM, pH 7.4) to make a 20 mL of lipid coarse dispersion. Cholesterol was added in a 4 : 1 lecithin-cholesterol molar ratio, PC/C liposomes. Sonication was carried out at 15°C and under N_2 (water bath sonicator, P-Selecta Ultrasons, 60 Hz) on 3 mL aliquots of the coarse dispersion. Then, 300 μL of this sonicated dispersion was diluted to 3 mL in phosphate buffer and sonicated for 10 min at 15°C in N_2 to obtain liposomes with a size of about 200 nm. The final lecithin concentration of all the final dispersions is 0.2 mg/mL. This procedure of preparation by sonicator was found by monitoring the size and z-potential with sonication time through preliminary experiments. The method described above was used to prepare two types of liposomes useful for formulations of eyedrops. The first contains lecithin Epikuron 200 (EP200); the other one contains phospholipids Epikuron 130 P (EP130).

2.3. Size Measurement and z-Potential. Liposomes size was measured by a dynamic light scattering (DLS) particle size analyzer which has a measuring range from 0.6 nm to 6 μm (Zetasizer Nano ZS90, Malvern Instruments Ltd., Worcestershire, UK). Dynamic light scattering, also known as photon correlation spectroscopy (PCS), measures Brownian motion in relation to the particles size: by illuminating the particles with a laser and analyzing the intensity fluctuations in the scattered light. The relationship between the size of a particle and its speed due to Brownian motion is defined by the Stokes-Einstein equation. The final particle diameter was calculated from a mean of at least three measurements. DLS measurements also provide the polydispersity index (PDI), which allows us to evaluate how the size of liposome population is distributed around a mean diameter [20]. The z-potential was measured using the Zetasizer Nano ZS90, which measures the distribution of the electrophoretic mobility of particles with a size range from 3 nm to 10 μm using the laser Doppler velocity technique. Since the z-potential is related to the electrophoretic mobility of the particles, the analyzer calculates the z-potential from the measured velocity using the Smoluchowski approximation, valid in the case of aqueous solutions.

2.4. Encapsulation Efficacy. Encapsulation efficiency was determined as the percentage verbascoside encapsulated in liposome to the original amount of verbascoside added. To determine drug release efficiency of liposome, lipid vesicles were lysed using 100% Triton X-100. Briefly, 100 μL of liposomal suspension was added to 100 μL 100% Triton X-100 and vortexed for 5 min to ease lysis of the liposomal encapsulated verbascoside. Free verbascoside was separated from liposome by centrifugation. Concentrations of the verbascoside in the filtrate, total drug, and free drug were quantitatively analyzed using spectrophotometric peak at 328 nm. The encapsulation efficacy was calculated using the following formula:

$$\eta = \frac{T - F}{T} \cdot 100, \tag{1}$$

where η is the efficiency of encapsulation, T the total verbascoside for encapsulation, and F free drug in the sample.

2.5. Alkali Burn Procedure. Adult hares of either sex weighing 3.0–3.5 kg were used in this study. All procedures were performed according to the ARVO Statement for the Use of Animals in Ophthalmic and Vision Research. Hares eyes were anesthetized topically with two drops of proparacaine hydrochloride (Alcon Laboratories, Ft. Worth, TX). One eye of each animal received a corneal burn by pipetting 0.5 mL of 2 N NaOH [21]. External examinations of each hares cornea were performed daily. Examinations of the alkali burns were performed every morning controlling the presence of corneal defects, ulceration, perforation, vascularization, or infection. Generally, corneal opacity is classified under a dissociation microscope as follows: 0, no opacity; 1, less than one-third of the corneal surface being clouded; 2, less than two-thirds of the corneal surface being clouded; 3, more than two-thirds of the corneal surface being clouded; and 4, almost all the corneal surface being clouded, and the opacity prevents visualization of the pupil margins. According to this classification, our system is of class 1. However such a classification is not necessary for kinetic analysis performed in this research so that it has not been used. For each animal just one eye was used for analysis. Animals were randomly assigned into two groups; one group of three hares received one treatment with liposomal eyedrop containing verbascoside daily, while

Table 1: Experimental results of different liposomal formulations.

	EP130			EP200		
	z_{av} (nm)	z-Potential (mV)	PDI	z_{av} (nm)	z-Potential (mV)	PDI
Liposomes	135	−25.0	0.117	107	−7.5	0.104
Liposomes containing verbascoside	113	−26.2	0.152	112	+4.8	0.095

the other group (three animals) received treatment with liposomal eyedrop without verbascoside as controls. Eyes of both groups were followed morphologically with taking photos of the corneas.

2.6. Histochemistry. Corneal fragments obtained from hares were fixed in buffered 10% formalin, embedded in paraffin, and sectioned. 5 μm thick serial sections of corneal specimens were deparaffinized and treated for hematoxylin and eosin (H&E) routine staining (haematoxylin: Fluka, AG, Switzerland, Buchs SG-Eosin Y: alcohol and water soluble, Winlap, UK).

2.7. Apoptosis Assay. In corneal epithelium apoptotic cells were detected using a commercially available fluorescence kit (ApopTag Plus Fluorescein *in situ* Apoptosis Detection Kit, Chemicon International, Temecula, CA, USA) based on the TUNEL method, which detects and labels the free 3′-OH end of DNA strand breaks in apoptotic nuclei. According to the manufacturer's protocol, sections were fixed in 1% PFA solution after washing with PBS. Digoxigenin-labeled nucleotides in reaction buffer and terminal deoxynucleotidyl transferase enzyme (TdT) were applied to the sections for one hour at 37°C to catalyze the template-independent addition of nucleotide triphosphates to the 3′-OH ends of double-stranded or single-stranded DNA. After termination of the reaction, fluorescent-labeled antidigoxigenin antibodies were applied to visualize the nucleotides added to DNA free ends. Sections were counterstained with DAPI and visualized using fluorescence microscopy [22, 23]. Microscopic analysis was performed with a Leica DMLB microscope equipped with epifluorescence EL6000 system (Leica Microsystems, Solms, Germany). Images were captured with a CCD camera (DC 200, Leica Microsystems, Solms, Germany) and image analysis software Quantimet 520 (Leica Microsystems, Solms, Germany). The number of apoptotic nuclei that stained intensely green was expressed relative to total number of nuclei stained by DAPI.

2.8. Analysis of Data. Image analysis involves the conversion of features and objects in image data into quantitative information about these measured features and attributes. Digital images of corneas were acquired using a CCD camera (DC 200, Leica, Solms, Germany). The contours in the images appeared to be always well-distinguishable so that any filtering was not necessary; then we applied computational techniques to extract the corneal-wound area from the images. MATLAB tools have been used to measure the area of the regions affected by the alkali burn. The area of the corneas of untreated eyes was used to calibrate the method and determine the scaling factor.

3. Results

3.1. Size Measurement and z-Potential. Size, PDI, and z-potential were measured for liposomes EP200 and EP130, both before and after the encapsulation of verbascoside. Results are collected in Table 1.

As one can see, for both formulations liposomes size is reduced after the inclusion of verbascoside and this indicates that the phenylpropanoid is involved in the assembly process. PDI values in Table 1 suggest that the size distribution of liposomes is very narrow and this monodipersity does not vary for the inclusion of guest molecules. Liposomes EP130 exhibit a net negative charge whilst EP200 liposomes are positive and become practically neutral after the inclusion of verbascoside. For this reason, we decided to prepare eyedrops with Liposomes EP200. For these formulations a further filtering step was performed (Whatman filters) and the residual moisture was removed in laminar-flow-hood to avoid contamination.

3.2. Morphological Analysis. Figure 1 shows the morphology of the corneal wound at time zero (i.e., just formed) and after four days, for both groups of hares.

It can be seen that the wound is almost circular in shape and occupies 15% about of cornea surface and involves only epithelial layers. After four days animals treated with verbascoside-based eyedrops have a perfectly healthy cornea; on the contrary animals treated with only liposomes exhibit an unchanged wound both in shape and in size. Since the extension of a wound is directly proportional to the degree of inflammation, we decided to monitor the evolution of corneal burning with measuring wound surface, A, as a function of time. However, the measured surface is not planar and therefore one should introduce corrective terms to take into account the true shape. To avoid the introduction of unknown parameters, it is useful to define the ratio A/A_c, being A_c the surface area of entire and healthy cornea. In other words we monitor the fraction of cornea surface involved in the ulceration process. Results are displayed in Figure 2, for both groups of hares. It is evident that the treatment with only liposomes has no effect and then A/A_c remains constant. For animal treated with verbascoside-based liposome the ratio remains constant only for the first 2-3 hours and then decreases to become zero.

3.3. Histochemistry. The hematoxylin and eosin (H&E) combination is the most common staining technique used in histology. Hematoxylin has a deep blue-purple color and stains nucleic acids by a complex, incompletely understood reaction. Eosin is pink and stains proteins nonspecifically. In a typical tissue, nuclei are stained blue, whereas

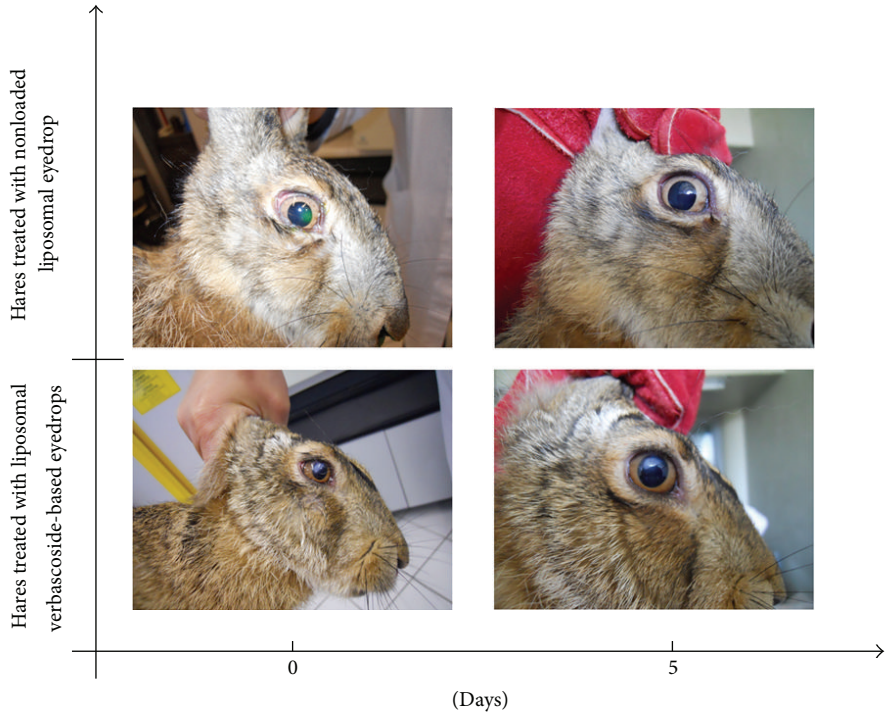

Figure 1: Morphological comparison between alkali burns in hares treated with verbascoside loaded liposomal eyedrops and hares treated only with liposomes, as a function of time.

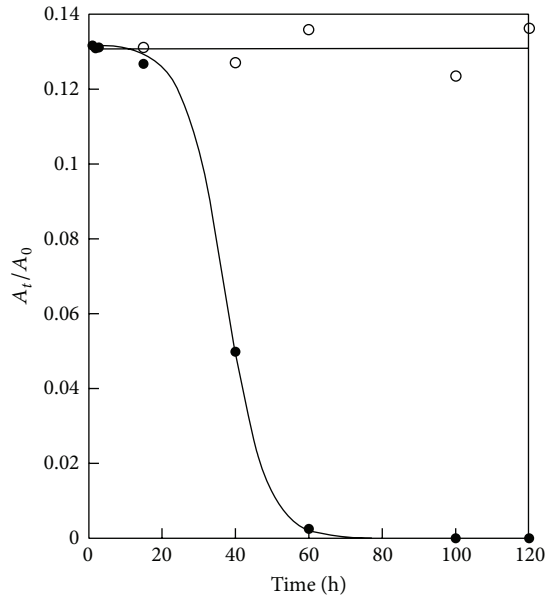

Figure 2: Fraction of cornea burned as a function of time for hares treated with verbascoside loaded liposomal eyedrops (•) and hares treated only with liposomes (○).The curve is the fit of (5) to the experimental data.

the cytoplasm and extracellular matrix have varying degrees of pink staining. H&E staining shows in corneal samples obtained from hare's eye injured by alkali burn a completely damaged epithelial layer. In Figures 3(a) and 3(c) superficial layer appears completely removed and polygonal cell of deep layer reduced in number and disorganized. After treatment with verbascoside-based eyedrop epithelial layer looked completely reorganized. Epithelial layer observed using H&E staining showed normal thickness and architecture (Figure 3(b)). In untreated hare's eye corneal epithelium looks still damaged with a superficial as well as deep layer being thinner and unorganized (Figure 3(d)).

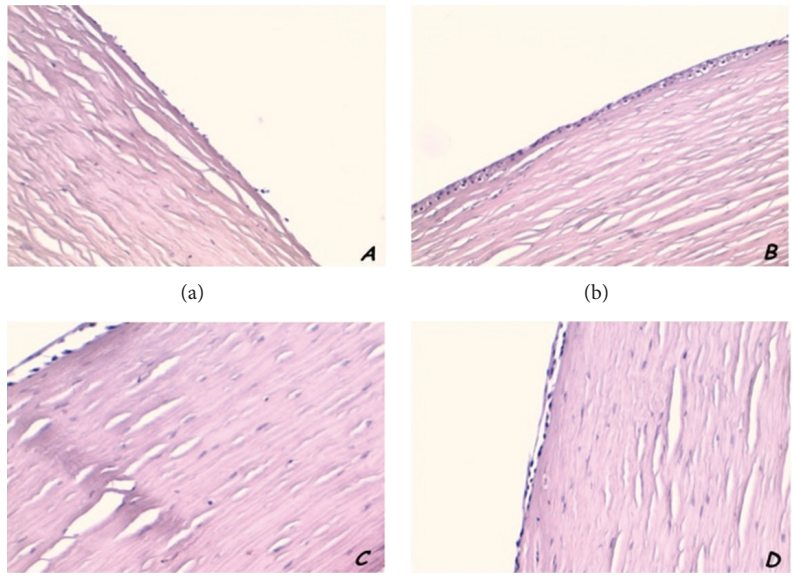

(a) (b)

(c) (d)

Figure 3: H&E staining in hares treated with verbascoside loaded liposomal eyedrops and hares treated only with liposomes. After alkali burn corneal epithelium appears thinner than normal and with superficial layer completely removed ((a)–(c)). Epithelial layer shows a restored normal thickness after treatment (b) but in untreated animals appears still thinner (d). Original magnification ×20.

3.4. Apoptosis Assay. *In situ* ApopTag Plus Fluorescein *in situ* Apoptosis Detection Kit (Chemicon International, Temecula, CA, USA) based on terminal transferase dUTP nick end labeling was used to evaluate the apoptosis of corneal epithelial cells. The number of apoptotic nuclei that stained intensely green was expressed relative to total number of nuclei stained by DAPI. In corneal samples obtained from hare's eye injured by alkali burn a large number of intensely green stained cells were described (Figures 4(a)–4(c)). Treatment by verbascoside-based eyedrop induced a large reduction of apoptotic phenomenon in corneal epithelium. Figures 4(d)–4(f) show only few green stained cells. In untreated samples no changes in apoptosis assay were observed.

4. Discussion

Following trauma to the corneal epithelium, the restoration of epithelial cell layers is crucial to the maintenance of normal visual acuity. Experimental study on corneal epithelial wound closure suggests that the process includes two distinct phases, an initial (or *latent*) phase followed by a closure wound phase. The latent phase, which has been found to last between 5 and 6 hours in both rabbit and monkey, is characterized by wounded-triggered cellular reorganization processes, including desquamation, loss of columnar appearance of the basal layers of cells, and breakdown of hemidesmosomes at the basal membrane [15, 16, 24]. During this phase little or no wound closure is observed. At the onset of the closure phase, the leading edge of the transformed epithelium is composed of a single layer of cells. Epidermal growth factor (EGF), keratinocyte growth factor, vascular endothelial factor (VEGF), and platelet derived growth factor (PDGF) are some of the growth factors known to stimulate corneal wound healing. These factors have been shown to promote corneal epithelial cell migration and wound closure *in vivo*. Epidermal growth factor (EGF) is also used to treat alkali-burned corneas. However, EGF-induced corneal angiogenesis, which is currently untreatable, is a side effect of this therapy. It has been recently demonstrated that blockade of the intermediate-conductance (Ca^{2+}) activated K^+ channel inhibits the angiogenesis induced by epidermal growth factor in the treatment of corneal alkali burn [25]. Ca^{2+} plays a master role in the complex and multistep process of angiogenesis by regulating endothelial proliferation, migration, adhesion to the substrate, contractility, and organization into capillary-like structures in normal [25–29] and neoplastic conditions [30–34]. Results displayed in Figure 2 seem to confirm a two-stage mechanism of wound healing also for hares. Moreover, it should be noted that the latency exhibited in Figure 2 is due to not only the cellular reorganization, but also the accumulation of liposomes on the wound boundary. To interpret the results displayed in Figure 2, we assume that the rate of wound healing contributes gain and loss factors. Schematically, we write

$$\frac{dx}{dt} = \text{gain} - \text{loss}, \tag{2}$$

where $x = A/A_c$. The left side of (2) represents the rate of healing. The gain depends both on the migration of epithelial cells from periphery of the wound into the wound region and on the diffusion of liposomes which release verbascoside. Therefore, we can assume the gain to be a second-order process:

$$\text{gain} = k_2 x^2, \tag{3}$$

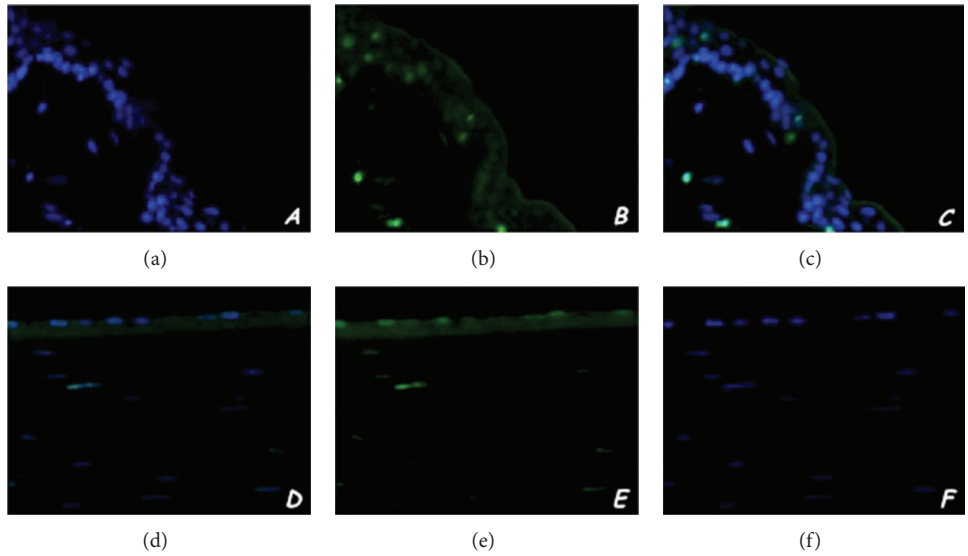

(a) (b) (c)

(d) (e) (f)

Figure 4: Representative images of nick end-incorporated nucleotides (for evaluation of apoptosis) immunofluorescent green staining in hares treated with verbascoside loaded liposomal eyedrops. Alkali burn induces in epithelial cell an increasing intensely green nuclear apoptotic staining (a) comparing normal nuclear staining with DAPI (b); merge image shows a plastic picture of this phenomenon (c). Verbascoside treatment shows a large reduction of intensely green apoptotic epithelial cells (d) with respect to nonapoptotic cells stained with DAPI (e); merge image represents clearly this condition (f). Original magnification ×20.

where k_2 is a kinetic constant. The loss, however, being proportional to verbascoside molecules reacting, is a process of first order:

$$\text{loss} = \frac{x}{\tau}, \tag{4}$$

where τ is the lifetime [35, 36] of the closure process.

Therefore (2) becomes

$$\frac{dx}{dt} = -\frac{x}{\tau} + k_2 x^2. \tag{5}$$

Which, solved with the initial condition $x(0) = x_0$, provides

$$x(t) = \frac{x_0 (1 + B)}{1 + Be^{-t/\tau}}, \tag{6}$$

where

$$B = \frac{1}{\tau k_2 x_0} - 1. \tag{7}$$

In computational terms, parameters τ and B were calculated by nonlinear fitting of (5) to experimental data while x_0 was directly measured. The values of chi-square ($\chi^2 = 2.6 \cdot 10^{-5}$) and correlation coefficient ($R = 0.9995$) indicate that the model fits very well the experimental data. By applying this procedure we get $\tau = (12.1 \pm 0.7)$ h and $k_2 = 0.60 \pm 0.05\,\text{h}^{-1}$. As seen from (5), when wound surface is such that $x_0 \ll 1/\tau k_2$, $x(t)$ remains constant. Furthermore, for both groups of animals, the experimental curves start from the same values so that we deduce that phenylpropanoid molecules reduce the latency time by lowering the lifetime τ. Using these parameters one obtains that in 48 hours the wound heals. This result is remarkable when compared with the value of 40 hours obtained under continuous delivery of EGF [24]. Damage to the corneal epithelium can be caused by trauma, microbial insult, or chemical insult, during contact lens wear or by surgery such as photorefractive keratectomy or laser *in situ* keratomileusis. Moreover, degenerative corneal disease such keratoconus is characterized by a thinning of the central part of epithelium [37]. Most corneal epithelial wounds heal promptly. However, under certain clinical conditions, such as chemical injury, healing of the corneal epithelium is delayed, leaving the underlying stroma vulnerable to infection and ulceration. Alkali injuries are of particular concern and cause acute inflammation characterized by rapid infiltration of neutrophils into the cornea followed by chronic inflammation involving the migration and recruitment of inflammatory cells over extended periods, further damaging the corneal surface. Oxidative stress plays an important role in pathogenesis of several corneal diseases. Corneas are characterized by the disturbed lipid peroxidation and nitric oxide pathways. Malfunctioning of these pathways may lead to accumulation of their toxic by-products inducing several detrimental effects, along with apoptosis of the epithelial corneal cells. Reactive oxygen species (ROS) are the prime initiators of the angiogenic response after alkali injury of the cornea. Light microscopy histochemical analysis performed using H&E routine staining showed in corneal samples obtained from hare's eye injured by alkali burn an epithelial layer almost completely destroyed. Epithelial cells of superficial layer appeared completely removed. A large reduction in number and a loss of regular organization and connections of epithelial polygonal cell of deep layer were also observed. Nevertheless, in our samples alkali burn induced in epithelial cells an increasing intensely green nuclear apoptotic staining comparing normal nuclear staining with DAPI

observed in nonapoptotic cells. Nanotechnology provides the opportunity to design and develop drug delivery systems able to target and treat several diseases, including those mediated by inflammation. Up to date, several delivery systems have been designed to deliver drugs to the retina. Drug delivery strategies may be classified into 3 groups: noninvasive techniques, implants, and colloidal carriers. Colloidal systems (liposomes, nanoparticles, etc.) can be easily administrated in a liquid form. Nanostructured nanolipids carriers are biocompatible, are easy to produce at large scale, and may be autoclaved or sterilized.

5. Conclusion

The positive influence of a prolonged diet supplemented with the powerful antioxidant verbascoside on the oxidative state in hares was recently demonstrated by our group. The research established that verbascoside supplementation is able to protect ocular tissue and fluids from naturally occurring oxidation and that its protective effect depends on the daily dose, being maximum up to 3 μg/die. Feed administration of verbascoside exerts higher antioxidant capacity in retina, lenses, and optic nerve. In present research we utilized topic administration of verbascoside-based eyedrops. After treatment we performed H&E staining to demonstrate a complete reorganization of epithelial layer. Corneal epithelium showed normal thickness and restored architecture of all layer. Histochemical analysis of untreated hare's eye displayed a corneal epithelium which is still damaged with a superficial as well as deep layer being thinner and unorganized. In treated animals nick end-incorporated nucleotides immunefluorescent green staining for evaluation of apoptosis showed a large reduction of intensely green apoptotic epithelial cells with respect to nonapoptotic cells stained with DAPI. The number of apoptotic corneal epithelial cells does not change in comparison to number of cells died by apoptosis induced by alkali burn in untreated animals. The results show that neutral liposomes interact well with the cornea and fail to deliver suitable amounts of verbascoside relatively quickly. A mathematical model based on the idea that the area burned by alkali is proportional both to the number of cells that arrives from the periphery and to the amount of verbascoside that, loaded in liposomes, is suggested. The model fits well experimental data and the curves obtained indicate that topical administration of verbascoside reduces significantly the first stage of the process of wound healing of the corneal epithelium.

Conflict of Interests

The authors declare that they do not have conflict of interests (political, personal, religious, ideological, academic, intellectual, commercial, or otherwise) regarding the publication of the paper.

Authors' Contribution

Luigi Ambrosone and Germano Guerra contributed equally to this work.

References

[1] C. Costagliola, G. Iuliano, M. Menzione, A. Nesti, F. Simonelli, and E. Rinaldi, "Systemic human diseases as oxidative risk factors in cataractogenesis. I. Diabetes," *Ophthalmic Research*, vol. 20, no. 5, pp. 308–316, 1988.

[2] F. Cattaneo, A. Iaccio, G. Guerra, S. Montagnani, and R. Ammendola, "NADPH-oxidase-dependent reactive oxygen species mediate EGFR transactivation by FPRL1 in WKYMVm-stimulated human lung cancer cells," *Free Radical Biology and Medicine*, vol. 51, no. 6, pp. 1126–1136, 2011.

[3] R. Dell'omo, F. Semeraro, G. Guerra et al., "Short-time prone posturing is well-tolerated and reduces the rate of unintentional retinal displacement in elderly patients operated on for retinal detachment," *BMC Surgery*, vol. 13, supplement 2, article S55, 2013.

[4] V. Conti, G. Russomanno, G. Corbi et al., "Aerobic training workload affects human endothelial cells redox homeostasis," *Medicine and Science in Sports and Exercise*, vol. 45, no. 4, pp. 644–653, 2013.

[5] M. C. Haigis and B. A. Yankner, "The Aging Stress Response," *Molecular Cell*, vol. 40, no. 2, pp. 333–344, 2010.

[6] C. Blanquicett, B. Kang, J. D. Ritzenthaler, D. P. Jones, and C. M. Hart, "Oxidative stress modulates PPARγ in vascular endothelial cells," *Free Radical Biology and Medicine*, vol. 48, no. 12, pp. 1618–1625, 2010.

[7] M. Mosca, A. Ceglie, and L. Ambrosone, "Antioxidant dispersions in emulsified olive oils," *Food Research International*, vol. 41, no. 2, pp. 201–207, 2008.

[8] L. Ambrosone, M. Mosca, and A. Ceglie, "Impact of edible surfactants on the oxidation of olive oil in water-in-oil emulsions," *Food Hydrocolloids*, vol. 21, no. 7, pp. 1163–1171, 2007.

[9] M. Mosca, A. Diantom, F. Lopez, L. Ambrosone, and A. Ceglie, "Impact of antioxidants dispersions on the stability and oxidation of water-in-olive-oil emulsions," *European Food Research and Technology*, vol. 236, no. 2, pp. 319–328, 2013.

[10] L. G. Korkina, "Phenylpropanoids as naturally occurring antioxidants: from plant defense to human health," *Cellular and Molecular Biology*, vol. 53, no. 1, pp. 15–26, 2007.

[11] V. A. Kurkin, "Phenylpropanoids from medicinal plants: distribution, classification, structural analysis, and biological activity," *Chemistry of Natural Compounds*, vol. 39, no. 2, pp. 123–153, 2003.

[12] D. Casamassima, M. Palazzo, F. Vizzarri, C. Costagliola, M. Mosca, and L. Ambrosone, "Effects of verbascoside-based diet on blood plasma constituents of rabbits," *The Journal of the American College of Nutrition*, vol. 32, no. 6, pp. 391–398, 2013.

[13] M. Mosca, L. Ambrosone, F. Semeraro, D. Casamassima, F. Vizzarri, and C. Costagliola, "Ocular tissue and fluids oxidative stress in hares fed on verbascoside," *International Journal of Food Sciences and Nutrition*, vol. 65, no. 2, pp. 235–240, 2014.

[14] S. Vertuani, E. Beghelli, E. Scalambra et al., "Activity and stability studies of verbascoside, a novel antioxidant, in dermocosmetic and pharmaceutical topical formulations," *Molecules*, vol. 16, no. 8, pp. 7068–7080, 2011.

[15] C. E. Crosson, "Cellular changes following epithelial abrasion," in *Healing of Cornea*, C. E. Crosson, R. W. Beuerman, and H. E. Kaufman, Eds., Gulf Press, Houston, Tex, USA, 1989.

[16] C. E. Crosson, S. D. Klyce, and R. W. Beuerman, "Epithelial wound closure in the rabbit cornea. A biphasic process," *Investigative Ophthalmology and Visual Science*, vol. 27, no. 4, pp. 464–473, 1986.

[17] M. H. Vingerhoeds, G. Storm, and D. J. A. Crommelin, "Immunoliposomes in vivo," *ImmunoMethods*, vol. 4, no. 3, pp. 259–272, 1994.

[18] M. C. Woodle, M. S. Newman, and J. A. Cohen, "Sterically stabilized liposomes: physical and biological properties," *Journal of Drug Targeting*, vol. 2, no. 5, pp. 397–403, 1994.

[19] M. Mosca, A. Ceglie, and L. Ambrosone, "Effect of membrane composition on lipid oxidation in liposomes," *Chemistry and Physics of Lipids*, vol. 164, no. 2, pp. 158–165, 2011.

[20] L. Ambrosone, A. Ceglie, G. Colafemmina, and G. Palazzo, "General methods for determining the droplet size distribution in emulsion systems," *Journal of Chemical Physics*, vol. 110, no. 2, pp. 797–804, 1999.

[21] J.-H. Chung, P. Fagerholm, and B. Lindstrom, "The behaviour of corneal epithelium following a standardized alkali wound," *Acta Ophthalmologica*, vol. 65, no. 5, pp. 529–537, 1987.

[22] F. Lopez, F. Cuomo, A. Ceglie, L. Ambrosone, and G. Palazzo, "Quenching and dequenching of pyrene fluorescence by nucleotide monophosphates in cationic micelles," *Journal of Physical Chemistry B*, vol. 112, no. 24, pp. 7338–7344, 2008.

[23] L. Ambrosone, G. D'Errico, and R. Ragone, "Interaction of tryptophan and N-acetyltryptophanamide with dodecylpentaoxyethyleneglycol ether micelles," *Spectrochimica Acta A: Molecular and Biomolecular Spectroscopy*, vol. 53, no. 10, pp. 1615–1620, 1997.

[24] H. Sheardown and Y. L. Cheng, "Mechanisms of corneal epithelial wound healing," *Chemical Engineering Science*, vol. 51, no. 19, pp. 4517–4529, 1996.

[25] H. Yang, X. Li, J. Ma et al., "Blockade of the intermediate-conductance Ca^{2+}-activated K^+ channel inhibits the angiogenesis induced by epidermal growth factor in the treatment of corneal alkali burn," *Experimental Eye Research*, vol. 110, pp. 76–87, 2013.

[26] Y. Sánchez-Hernández, U. Laforenza, E. Bonetti et al., "Store-operated Ca^{2+} entry is expressed in human endothelial progenitor cells," *Stem Cells and Development*, vol. 19, no. 12, pp. 1967–1981, 2010.

[27] S. Dragoni, U. Laforenza, E. Bonetti et al., "Vascular endothelial growth factor stimulates endothelial colony forming cells proliferation and tubulogenesis by inducing oscillations in intracellular Ca^{2+} concentration," *Stem Cells*, vol. 29, no. 11, pp. 1898–1907, 2011.

[28] R. Berra-Romani, J. E. Avelino-Cruz, A. Raqeeb et al., "Ca^{2+}-dependent nitric oxide release in the injured endothelium of excised rat aorta: a promising mechanism applying in vascular prosthetic devices in aging patients," *BMC Surgery*, vol. 13, p. S40, 2013.

[29] F. Moccia, S. Dragoni, M. Cinelli et al., "How to utilize Ca^{2+} signals to rejuvenate the repairative phenotype of senescent endothelial progenitor cells in elderly patients affected by cardiovascular diseases: a useful therapeutic support of surgical approach?" *BMC Surgery*, vol. 13, p. S46, 2013.

[30] S. Dragoni, U. Laforenza, E. Bonetti et al., "Canonical Transient Receptor Potential 3 channel triggers VEGF-induced intracellular ca2+ oscillations in endothelial progenitor cells isolated from umbilical cord blood," *Stem Cells and Development*, vol. 22, no. 19, pp. 2561–2580, 2013.

[31] F. Moccia, S. Dragoni, F. Lodola et al., "Store-dependent Ca^{2+} entry in endothelial progenitor cells as a perspective tool to enhance cell-based therapy and adverse tumour vascularization," *Current Medicinal Chemistry*, vol. 19, no. 34, pp. 5802–5818, 2012.

[32] F. Moccia, F. Lodola, S. Dragoni et al., "Ca^{2+} signalling in endothelial progenitor cells: a novel means to improve cell-based therapy and impair tumour vascularisation," *Current Vascular Pharmacology*, vol. 12, no. 1, pp. 87–105, 2014.

[33] F. Lodola, U. Laforenza, E. Bonetti et al., "Store-operated ca^{2+} entry is remodelled and controls *in vitro* angiogenesis in endothelial progenitor cells isolated from tumoral patients," *PLoS ONE*, vol. 7, no. 9, Article ID e42541, 2012.

[34] S. Dragoni, U. Laforenza, E. Bonetti et al., "Enhanced expression of stim, orai, and TRPC transcripts and proteins in endothelial progenitor cells isolated from patients with primary myelofibrosis," *PLoS ONE*, vol. 9, no. 3, Article ID e91099, 2014.

[35] F. Venditti, G. Bufalo, F. Lopez, and L. Ambrosone, "Pollutants adsorption from aqueous solutions: the role of the mean lifetime," *Chemical Engineering Science*, vol. 66, no. 23, pp. 5922–5929, 2011.

[36] F. Venditti, F. Cuomo, A. Ceglie, L. Ambrosone, and F. Lopez, "Effects of sulfate ions and slightly acidic pH conditions on Cr(VI) adsorption onto silica gelatin composite," *Journal of Hazardous Materials*, vol. 173, no. 1–3, pp. 552–557, 2010.

[37] K. A. Wojcik, J. Blasiak, J. Szaflik, and J. P. Szaflik, "Role of biochemical factors in the pathogenesis of keratoconus," *Acta Biochimica Polonica*, vol. 61, no. 1, pp. 55–62, 2014.

Hindawi Publishing Corporation
BioMed Research International
Volume 2014, Article ID 826970, 11 pages
http://dx.doi.org/10.1155/2014/826970

Clinical Study

Evaluation of the Efficacy of 50% Autologous Serum Eye Drops in Different Ocular Surface Pathologies

Francesco Semeraro,[1] Eliana Forbice,[1] Osvaldo Braga,[1] Alessandro Bova,[1] Attilio Di Salvatore,[1] and Claudio Azzolini[2]

[1] *Eye Clinic, Department of Neurological and Vision Sciences, University of Brescia, Piazzale Spedale Civili 1, 25123 Brescia, Italy*
[2] *Department of Surgical and Morphological Sciences, Section of Ophthalmology, University of Insubria, Ospedale di Circolo, Via F. Guicciardini 9, 21100 Varese, Italy*

Correspondence should be addressed to Eliana Forbice; elianaforbice@email.it

Received 27 March 2014; Accepted 18 May 2014; Published 22 July 2014

Academic Editor: Ciro Costagliola

Purpose. This study evaluated the efficacy of 50% autologous serum eye drops in ocular surface diseases not improved by conventional therapy. *Methods*. We analyzed two groups: (1) acute eye pathologies (e.g., chemical burns) and (2) chronic eye pathologies (e.g., recurrent corneal erosion, neurotropic keratitis, and keratoconjunctivitis sicca). The patients were treated for surface instability after conventional therapy. The patients received therapy 5 times a day until stabilization of the framework; they then reduced therapy to 3 times a day for at least 3 months. We analyzed the best corrected visual acuity, epithelial defects, inflammation, corneal opacity, and corneal neovascularization. We also analyzed symptoms such as tearing, burning, sense of foreign body or sand, photophobia, blurred vision, and difficulty opening the eyelids. *Results*. We enrolled 15 eyes in group 1 and 11 eyes in group 2. The average therapy period was 16 ± 5.86 weeks in group 1 and 30.54 ± 20.33 weeks in group 2. The epithelial defects all resolved. Signs and symptoms improved in both groups. In group 2, the defect recurred after the suspension of therapy in 2 (18%) patients; in group 1, no defects recurred. *Conclusions*. Autologous serum eye drops effectively stabilize and improve signs and symptoms in eyes previously treated with conventional therapy.

1. Introduction

The ocular surface is a morphofunctional unit that owes its action to the perfect cooperation of all its structures (i.e., conjunctival and corneal epithelium, lacrimal apparatus, and eyelids) [1]. In particular, tears are important in maintaining the stability of the ocular surface because of its lubricant, mechanical, epitheliotropic, and antimicrobial functions [2]. A qualitative and quantitative deficiency of tears can lead to the persistent and progressive damage of the ocular surface with a compromised wound-healing process [3–5]. In this situation, the conventional therapeutic options are intensive artificial tears, punctual occlusion, contact lenses, and appropriate management of adnexa diseases [2]. However, these therapies are limited in supplying the neurotrophic factors, vitamins, and immunoglobulins necessary for the health of the ocular surface [2]. Just with this target arises the use of autologous serum (AS) eye drops. In 1970, the use of AS for treating ocular surface disorders began when it was used to treat ocular alkali burns [6]. However, only later—first with Fox et al. [7] and then with Tsubota et al. [8]—did this therapy enter clinical practice for the treatment of different ocular surface diseases. Since its introduction, this treatment has become increasingly popular and the indications for its use have expanded rapidly [9]. To date, AS is used for the treatment of persistent epithelial defects [10–15], dry eyes [1, 8, 16–27], neurotrophic keratopathy [28], recurrent erosion syndrome [29, 30], superior limbic keratoconjunctivitis [31], and chemical injuries [32, 33].

The rationale for the use of AS arises from its strong similarity to tears, which contains growth factors, cytokines, vitamins, and bactericidal components that provide the necessary nutritional factors to maintain cellular tropism

Table 1: Inclusion and exclusion criteria of the study.

Criteria	Inclusion criteria	Exclusion criteria
General		Inability of venous blood sampling because of (i) venous access being not available,, (ii) anemia, (iii) cerebrovascular or cardiovascular disorders, (iv) being positive for viral markers (HBV, HCV, and HIV), (v) being bacterial active, (vi) women who are pregnant or breast-feeding, (vii) patients unable to provide informed consent, (viii) age under 18 years.
Chemical eye burn	(i) Persistent epithelial defect (ii) Inflammation and/or opacity and/or corneal neovascularization	
Severe dry eye syndrome	(i) Symptoms of dry eye with daily activity limitation (ii) Time to break-up <5 sec (iii) Schirmer's test without anaesthesia <5 mm after 5 minutes (iv) Fluorescein staining positive with or without epithelial defect (v) Patients refractory to conventional therapy	(i) Corneal perforation/melting (ii) Limbal stem cell deficit (iii) Patients with active infections of the eye or eyelid (iv) Abnormalities of the eyelid
Neurotrophic keratitis	(i) Patients with persistent epithelial defects (ii) Patients refractory to conventional therapy	

HBV = hepatitis B virus; HCV = hepatitis C virus; HIV = human immunodeficiency virus.

and reduce the risk of contamination and infection during epithelial repair processes [2]. In fact, human serum contains substances such as epithelial growth factor (EGF), which speeds epithelial cell migration and has antiapoptotic effects [34]; transforming growth factor β (TGF-β), which is involved in the epithelial and stromal repair process [35]; vitamin A, which seems to prevent epithelium squamous metaplasia [36] and modulates the expression of thrombospondin 1 (TSP1) [37], thrombospondin 2 (TSP2), vascular endothelial growth factor A (VEGF-A), metallopeptidase 9, and TGF-β to promote wound healing [38]; albumin, which has antiapoptotic activity [39]; α-2 macroglobulin, which exhibits anticollagenase activity; and fibronectin, which is important in cell migration [11, 40]. Autologous serum also contains neuronal factors such as substance P (SP) and insulin-like growth factor 1 (IGF-1), which seem to have a role in corneal epithelium migration and adhesion [41]. In addition, AS contains immunoglobulins (Ig) such as IgG and IgA and lysozyme that provide bactericidal and bacteriostatic effects [2, 42]. Furthermore, AS is superior to artificial tears in maintaining corneal epithelium health because it is free of preservatives [43] (which potentially induce toxic or allergic reactions [44]) and its osmolality and biomechanical properties are similar to those of natural tears. The aim of this study was to evaluate the efficacy of 50% autologous serum eye drops in the treatment of symptoms and objective signs in different ocular surface diseases that are not improved by conventional therapy.

2. Materials and Methods

This single-center prospective study was conducted from January 2008 to January 2013. We enrolled patients who came to our department because of ocular surface dysfunction related to trophic deficiency (e.g., recurrent corneal erosion, neurotrophic keratitis, and keratoconjunctivitis sicca [Sjögren and non-Sjögren-related]) and chemical burns. Table 1 lists the inclusion and exclusion criteria of the study.

Written informed consent was obtained from all subjects before their enrollment after they received an explanation of the nature and possible consequences of the study. The institutional review board of the Spedali Civili Hospital (Brescia, Italy) ethics committee approved the study. The Declaration of Helsinki was followed. All patients had a screening visit. The best corrected visual acuity (BCVA) was measured using a Snellen-type acuity in all patients.

Specialized ophthalmologists collected clinical data by slit-lamp examination (using corneal fluorescein staining to study epithelial defects) and evaluated epithelial defects, inflammation, corneal opacity, and corneal neovascularization. A grading scale of 1 to 3 was used to identify the severity

of these signs in which grade 1 was "absence of signs"; grade 2 was "slight"; and grade 3 was "severe."

A similar scale was used for subjective symptoms. We recorded data on tearing, burning, sense of foreign body or sand, photophobia, blurred vision, and difficulty in opening the eyelids on a scale graded from 1 to 4 in which grade 1 was "no symptom," grade 2 was "slight," grade 3 was "moderate," and grade 4 was "severe." When possible, a picture of the anterior segment of the eye was obtained.

Patients were divided into 2 groups: (1) patients with an acute illness (e.g., chemical burns) and (2) patients with chronic disease (e.g., recurrent corneal erosion, neurotropic keratitis, and keratoconjunctivitis sicca (non-Sjögren and Sjögren-related)).

Group 1 eyes had chemical burns [grades II and III chemical injuries (based on the Dua classification [45])]. We treated the eyes with first-aid therapy, which included irrigation with normal saline or glucose to normalize the ocular surface pH, topical anti-inflammatory drugs, and antibiotic with eye bandage or contact lens. The treatment with AS eye drops was initiated after an average of 7 days of corticosteroid therapy in patients with persistent inflammation, epithelial defects, or any type of ocular surface instability without significant stem cell deficiency (i.e., more than one quadrant). The group was treated 5–6 times per day for 1 month in association with anti-inflammatory therapy (which was progressively decreased during the month) and then was reduced to 3 times daily until the absence of symptoms for at least 3 months without support therapy.

Group 2 included patients with chronic diseases that were unresponsive to conventional therapy (e.g., lubricating drops and ointments, punctal plug, bandage contact lenses, tarsorrhaphy, and gold eyelid weight). The treatment in this group was 5 times a day for 3 months and then was reduced progressively to 3 times a day for 3 months until the absence of symptoms. An antibiotic (moxifloxacin/netilmicin/tobramycin) was administered 4 times a day until the closing of the epithelial defect. No other supportive therapies were used during the treatment period. For each patient, the specialist could modify the therapy whenever necessary. The change was registered and justified.

Autologous serum drops were produced in the following manner. A total of 200 mL of blood was procured by venipuncture and collected in a sterile container. The blood was allowed to stand for 24–48 h at 4°C to allow clotting. The blood was centrifuged at 4000 rpm for 10 min. The serum was separated from the blood and diluted with saline to 50% in a laminar flow cabinet. At this point, the product was quarantined until the outcome of the sterility test performed by the Laboratory of Microbiology of the AO Civil Hospital of Brescia (Brescia, Italy). The final product was formed from an average of 288 single-dose eye drops for venipuncture. Single-application packs were packed in bags of 20 and marked with a label plate.

At −30°C, the product is preserved for 6 months from the date of withdrawal. From the time of delivery, the product is stored at a destination (e.g., home freezer) at −20°C for a period not exceeding 3 months from the date of delivery and no later than the expiration date stated on the label. If the entire production process is successful, the eye drops are validated, which takes into account negative serology examinations, group control transmitted and validated by the Emonet management system (i.e., computer system with records of the personal data of patients and the procedure to be performed), and negative results of sterility control.

Statistical Analysis. The data were recorded on a predesigned pro forma and managed on a spreadsheet using the Microsoft Excel 2013 software (Microsoft Corp., Redmond, WA). All entries were checked for errors. Appropriate statistical tests were applied to analyze the results. The t-test was used to determine the significance of changes in subjective symptoms, BCVA, epithelial defects, corneal neovascularization, opacity, and inflammation before and after AS eye inoculation therapy in the 2 groups of patients. The significance (p) was defined as a probability of error <0.01.

3. Results

3.1. Patients. In this study 28 eyes of 28 patients were enrolled. Two patients dropped out of the study because of the impossibility of obtaining blood samples: the first patient was seropositive for the human immunodeficiency virus and the second patient did not have venous access.

Of the 26 eyes of the 26 patients treated with AS, 18 patients were men and 8 were women. The mean age was 39.6 ± 16.47 years (range, 19–81 years) in group 1 and 57.63 ± 16.59 years (range, 37–80 years) in group 2 (Table 2).

Group 1 consisted of 15 eyes (58% of all patients in the study) injured by chemical agents of different natures. Group 2 (i.e., patients with chronic eye diseases) consisted of 11 eyes as follows: 6 eyes with neurotrophic keratopathy, 3 eyes with keratoconjunctivitis sicca not Sjögren, and 2 eyes with keratoconjunctivitis sicca, Sjögren-related.

The average therapy period was 22.15 ± 15.44 weeks (range, 12–72 weeks), 16 ± 5.86 weeks in group 1 and 30.54 ± 20.33 weeks in group 2. Two patients, both in group 2, remain under treatment.

3.2. Clinical Data. The *visual acuity* in group 1 went from 2.4/10 ± 1.91/10 (mean ± standard deviation) to 6.25/10 ± 3.25/10 ($P < 0.01$) after treatment with an average gain of 4 Snellen lines. In group 2, visual acuity went from 2.96/10 ± 2.04/10 to 4.7/10 ± 3.37/10 ($P < 0.01$) with an average gain of 2 Snellen lines. The visual acuity improved in 100% of patients (Figures 3(a) and 3(b)). The 55% percent of patients with chronic eye diseases had associated eye pathologies affecting the final visual acuity such as maculopathy, cataracts, and diabetic retinopathy, whereas no acute patient had concomitant pathology. The signs that were evaluated in the clinical examination were the presence of epithelial defects, neovascularization, corneal opacity, and the degree of inflammation.

In group 1 before treatment, 100% of patients had inflammation (it extended to the entire eye in 73% of patients and was grade 2 in 27% of patients); 100% of patients had corneal opacity (grade 3 in 93% of patients and grade 2 in 7% of

Table 2: Summary of the 26 eyes treated with autologous serum eye drops.

Eye	Sex	Age (y)	Etiology	Weeks of serum therapy	Comorbidity
1	M	41	CB	24	None
2	M	22	CB	24	None
3	M	59	CB	12	None
4	F	81	CB	12	Diabetes mellitus
5	M	29	CB	24	None
6	M	41	CB	12	None
7	M	30	CB	48	None
8	M	32	CB	12	None
9	M	38	CB	12	None
10	M	55	CB	12	None
11	M	31	CB	12	None
12	M	50	CB	24	None
13	M	19	CB	24	None
14	M	23	CB	12	None
15	M	43	CB	12	None
16	F	71	SS	24	None
17	F	37	NK	24	s/p PK
18	F	64	NK	12	s/p trabeculectomy
19	M	71	DE	12	None
20	M	80	DE	24	None
21	M	60	NK	12	Trigeminal neuralgia
22	F	79	SS	48	None
23	F	44	NK	48	s/p trabeculectomy
24	M	37	NK	72	Acoustic neuroma
25	F	40	NK	12	None
26	F	51	NK	48	Lagophthalmos

CB = chemical burn; DE = dry eye syndrome; NK = neurotrophic keratopathy; s/p PK = status postpenetrating keratoplasty; s/p trabeculectomy = status posttrabeculectomy; SS = Sjogren's syndrome.

patients); and 60% of patients had neovascularization (grade 3 in 33% of patients and grade 2 in 27% of patients).

In group 2 before treatment, 100% of patients had corneal inflammation (grade 3 in 64% of patients and grade 2 in 36% of patients); 82% of patients had corneal opacity (grade 3 in 60% of patients and grade 2 in 40% of patients); and 55% of patients had corneal neovascularization (grade 3 in 36% of patients, grade 2 in 27% of patients, and grade 1 in 37% of patients) (Table 3).

Evolution of the Clinical Data (Figure 2)

Epithelial Defects. Epithelial defects were completely resolved (grade 1) by the end of followup in all patients. In 2 patients in group 2, the epithelial defect recurred after the suspension of therapy. One patient was administered a new cycle of AS eye drops that resolved the defect. In the second patient, a tarsorrhaphy was necessary owing to the severity of the ocular disease and the impossibility of restarting AS therapy because of the inability to perform blood sampling due to the patient's worsening condition.

Inflammation. After treatment in group 1, the inflammation was grade 1 (i.e., absent) in 87% of patients and grade 2 in 13% of patients with an improvement of 2 degrees in 58% of patients and 1 degree in 42% of patients. In group 2, inflammation was grade 1 (i.e., absent) in 81% of patients and grade 2 in 19% of patients with an improvement of 2 degrees in 55% of patients and 1 degree in 45% of patients. All patients improved. The average improvement was 1.60 ± 0.49 degrees in group 1 ($P < 0.01$) and 1.54 ± 0.50 degrees in group 2 ($P < 0.01$).

Opacity. After treatment in group 1, opacity became grade 1 in 60% of patients and grade 2 in the remaining 40% with an improvement of 2 degrees in 35% of patients and 1 degree in 54% of patients. In group 2, opacity became grade 1 in 55% of patients and grade 2 in 45% of patients. The improvement was 2 degrees in 18% of patients and 1 degree in 64% of patients; by contrast, 2 patients remained stable at grade 2 (these were diabetic patients with neurotrophic keratopathy).

The average improvement was 1.53 degrees ± 0.52 in group 1 ($P < 0.01$) and 0.82 degrees ± 0.60 in group 2 ($P < 0.01$).

Neovascularization. After treatment in group 1, neovascularization became grade 1 in 73% of patients and grade 2 in 27% of patients with an improvement of 2 degrees in 29% of patients and 1 degree in 64% of patients. In group 2,

Table 3: Summary of the distribution and evolution of the clinical signs in the 2 groups of patients.

Signs	Presence of sign PRE-AS gr 1	Presence of sign POST-AS gr 1	Distribution of grades	Distribution of grades	Average of the grades PRE-AS GR.1	Average of the grades POST-AS GR.1	P value
Epithelial defect	100%	0%	GRADE 3: 73% GRADE 2: 27% GRADE 1: 0%	GRADE 3: 0% GRADE 2: 0% GRADE 1: 100%	**2.73** ± 0.46	1	<0.01
Inflammation	100%	14%	GRADE 3: 73% GRADE 2: 27% GRADE 1: 0%	GRADE 3: 0% GRADE 2: 13% GRADE 1: 87%	**2.73** ± **0.46**	1.13 ± 0.35	<0.01
Corneal opacity	100%	27%	GRADE 3: 84% GRADE 2: 6% GRADE 1: 0%	GRADE 3: 0% GRADE 2: 40% GRADE 1: 60%	**2.93** ± **0.26**	1.40 ± 0.51	<0.01
Neovascularization	60%	40%	GRADE 3: 33% GRADE 2: 27% GRADE 1: 40%	GRADE 3: 0% GRADE 2: 27% GRADE 1: 73%	**1.93** ± **0.88**	1.20 ± 0.41	<0.01
Epithelial defect	100%	0%	GRADE 3: 73% GRADE 2: 27% GRADE 1: 0%	GRADE 3: 0% GRADE 2: 0% GRADE 1: 100%	**2.73** ± 0.46	1	<0.01
Inflammation	100%	10%	GRADE 3: 64% GRADE 2: 36% GRADE 1: 0%	GRADE 3: 0% GRADE 2: 19% GRADE 1: 81%	**2.64** ± **0.51**	1.09 ± 0.30	<0.01
Corneal opacity	88%	28%	GRADE 3: 45% GRADE 2: 36% GRADE 1: 19%	GRADE 3: 0% GRADE 2: 45% GRADE 1: 55%	**2.27** ± **0.79**	1.27 ± 0.47	<0.01
Neovascularization	55%	45%	GRADE 3: 36% GRADE 2: 18% GRADE 1: 46%	GRADE 3: 0% GRADE 2: 27% GRADE 1: 73%	**1.67** ± **0.52**	1.18 ± 0.40	<0.01

Post-AS = postautologous serum treatment; pre-AS = preautologous serum treatment.

neovascularization became grade 1 in 73% of patients and grade 2 in 27% of patients with an improvement of 2 degrees in 27% of patients and 1 degree in 45% of patients, whereas there was no change in 1 diabetic patient with neurotrophic keratopathy. The average improvement was 1.11 degrees ±0.60 in group 1 ($P < 0.01$) and 1.17 degrees ±0.75 in group 2 ($P < 0.01$).

3.3. Symptoms. The symptoms reported in group 1 were (in decreasing frequency) burning, feeling a foreign body/sand in the eyes, tearing, photophobia, and blurred vision.

Tearing was present in 42% of patients at the first visit: 73% of patients had grade 4 and 27% of patients had grade 3.

Burning was present in 73% of patients at first visit: 79% of patients had grade 4, 11% of patients had grade 3, and 10% of patients had grade 2.

The sense of sand in the eyes was present in 78% of patients at the first visit: 55% of patients had grade 4 and 45% of patients had grade 3.

Photophobia was present in 65% of patients at the first visit: 53% of patients had grade 4, 37% of patients had grade 3, and 10% of patients had grade 2.

Blurred vision was present in 73% of patients at the first visit: 48% of patients had grade 4, 48% of patients had grade 3, and 4% of patients had grade 2.

Difficulty opening *the eyelids* was present in 42% of patients at the first visit: 64% of patients had grade 4, 27% of patients had grade 3, and 9% of patients had grade 2.

The most severe symptom was eye burning. The symptoms reported in group 2 (in decreasing frequency) were a sense of a foreign body in the eyes, blurred vision, burning, and photophobia. The feeling of sand in the eyes and blurred vision were the most severe symptoms (Table 3).

Evolution of Symptoms. Tearing at the end of followup was grade 1 in 55% of patients and grade 2 in 45% of patients. There was an improvement of 3 degrees in 36% of patients, 2 degrees in 55% of patients, and 1 degree in 9% of patients. All patients improved. The average improvement was 2.43 ± 0.49 degrees in group 1 ($P < 0.01$) and 2 ± 0.70 degrees in group 2 ($P < 0.01$).

Burning at the end of followup was grade 1 in 74% of patients, grade 2 in 21% of patients, and grade 3 in 5% of patients. There was an improvement of 3 degrees in 53% of patients, 2 degrees in 32% of patients, and 1 degree in 15%

of patients (i.e., 100% of patients improved). The average improvement was 2.42 ± 0.76 degrees in group 1 ($P < 0.01$) and 2.28 ± 0.70 degrees in group 2 ($P < 0.01$).

The sense of sand in the eyes at the end of followup was grade 1 in 75% of patients, grade 2 in 15% of patients, and grade 3 in 10% of patients. There was an improvement of 3 degrees in 40% of patients, 2 degrees in 45% of patients, and 1 degree in 10% of patients; however, 1 (5%) patient with neurotrophic keratopathy showed no improvement. The average improvement was 2.45 ± 0.50 degrees in group 1 ($P < 0.01$) and 1.89 ± 0.99 degrees in group 2 ($P < 0.01$).

Photophobia at the end of followup was grade 1 in 71% of patients and grade 1 in 29% of patients.

There was an improvement of 3 degrees in 35% of patients, 2 degrees in 47% of patients, and 1 degree in 18% of patients (i.e., 100% of patients improved). The average improvement was 2.36 ± 0.77 degrees in group 1 ($P < 0.01$) and 1.83 ± 037 degrees in group 2 ($P < 0.01$).

Blurred vision at the end of followup was grade 1 in 63% of patients, grade 2 in 21% of patients, and grade 3 in 16% of patients. There was an improvement of 3 degrees in 32% of patients, 2 degrees in 37% of patients, 1 degree in 21% of patients, and no improvement in only 2 (10%) patients (the first patient had a chemical eye injury with a slight degree of injury and the second patient had Sjögren syndrome eye with a mild degree of injury). The average improvement was 1.91 ± 0.99 degrees in group 1 ($P < 0.01$) and 1.87 ± 0.92 degrees in group 2 ($P < 0.01$).

Difficulty opening *the eyelids* at the end of followup was grade 1 in 91% of patients and grade 2 in 9% of patients. There was an improvement of 3 degrees in 64% of patients, 2 degrees in 18% of patients, and 1 degree in 18% of patients (i.e., 100% of patients improved). The average improvement was 2.5 ± 0.76 degrees in group 1 ($P < 0.01$) and 2.25 ± 0.83 degrees in group 2 ($P < 0.01$).

4. Discussion

Autologous serum eye drops are actually used in the treatment of many ocular diseases, and many studies have demonstrated the effectiveness of AS eye drops in treating different conditions such as superior limbic keratoconjunctivitis [31], recurrent corneal erosion [12, 30], neurotropic keratopathy [10], and Sjogren's syndrome [8].

Despite clinical evidence of the efficacy of AS, a shared protocol for the preparation and the administration of this therapy is lacking because of the bureaucratic and technical difficulties of handling biological materials. The European Union (European Parliament and Council) has issued several directives concerning AS eye drops (1965/65, 1975/139, and 1975/318). However, in the European Union, individual countries regulate the manufacture and distribution of pharmaceuticals, and the use of serum eye drops remains an experimental approach [20]. The marketing authorization for a drug normally depends on proof of efficacy in clinical trials, implementation of quality control, reports of adverse effects, evidence of expert knowledge, and other regulatory issues. A doctor who makes or prescribes a specific medical product to treat a patient on a nominal basis is exempt from the requirement to obtain authorization as a "professional authorized by law to prescribe or administer drugs or devices so the responsibility in preparation and administration is entirely of the prescriber." This has justified the limited use of AS eye drops [20, 46–48].

In addition, there have been few reports that show the efficacy of some blood products such as platelet-rich plasma (PRP) in treating chemical burns [32, 49]. Hence, we started using AS eye drops for different ocular surface diseases that were not responding to conventional therapies. Our study investigated a heterogeneous group of pathologies with different pathogeneses to understand better the role and potentialities of AS.

We chose to use 50% AS eye drops instead of other concentrations (e.g., 20% or 100%) used in some works in the literature [48]. This decision is based on the significant effect that 50% AS has shown in several studies [1, 14, 50] and on the hypothesis that at higher concentrations some components can become harmful. In fact, the concentration of biologically active molecules is different in serum and tear fluids. There are no data on which concentration of AS is most appropriate for treating ocular surface diseases. For example, Gupta et al. [51] report that the TGF-β concentration in human serum is approximately 50 ng/mL, which is 5 times higher than the amount in tears, and TGF-β has antiproliferative effects and high concentrations of this molecule may suppress wound healing of the epithelium [51, 52]. Jeng and Dupps Jr. [14] say that in their series 100% AS has a very high concentration of serum proteins that could alter the osmolality and pH of the preparation; in addition, patients enjoy the extra viscosity of 50% AS, compared to 20% AS. In addition, we must consider that the frequency of venipuncture and the amount of blood needed are doubled with the use of 100% AS drops [11]. Therefore, even if 100% AS drops were more effective, we believed 50% AS eye drops were safer and more manageable.

The main focus of the study was to show the clinical success of AS eye drops in the treatment of different ocular surface diseases. All collected data were analyzed complexly and subsequently in 2 distinct groups of pathologies—acute eye pathology (i.e., group 1) and chronic eye pathology (i.e., group 2)—with the aim of understanding the potential and the efficacy of this therapy.

The data analysis showed that all patients achieved a significant improvement in symptoms and all patients had excellent compliance with the treatment. No patient in the current study has reported any adverse effects to date; however, some studies have reported adverse effects [39]. In our patients, the treatment was safe and no patients reported allergy intolerance, deposits, or infection.

Best corrected visual acuity improved in all patients, which was in contrast to the study of Ziakas et al. [30] (Figures 3(a) and 3(b)). The average improvement was greater in patients with acute diseases, but this difference occurred because of a higher rate of eye comorbidity, which was also influenced by the age of the patients.

In primary or secondary tear deficiency, the AS supplies the lacking factors and reestablishes a correct ocular surface balance. This is the situation with dry eyes, Sjögren and non-Sjögren-related. For mild dry eyes, artificial tears, when

frequently applied, are usually effective since they are able to reduce symptoms and prevent complications and the progression of damage [53, 54]. However, in more severe cases, artificial tears may be unable to stabilize the framework, and the damage to the ocular surface worsens with dramatic consequences such as eye ulcers to eye perforation [55]. In 1984, Fox et al. [7] were the first to report the beneficial effects of applying AS eye drops to dry eye in Sjogren's syndrome. Tsubota et al. [8] later revealed increased numbers of goblet cells and decreased squamous epithelium metaplasia after AS therapy. Compared to patients treated with nonpreserved artificial tears, Kojima et al. [39] found a significant improvement in tear stability, ocular surface vital staining scores, and pain symptom scores in patients treated with AS.

In our study, the patients with dry eye syndrome started therapy with AS eye drops because the symptom had not resolved with conventional therapy and they had a long history of chronic inflammation and recurrent epithelial defects leading to infection, opacity, and visual capacity damage [56]. All patients improved in objective and subjective symptoms. Four patients are currently without AS treatment but maintain artificial tears therapy. They are all followed up regularly and show a stable framework with no recurrence. However, the therapy suspension period remains short and does not allow stating the stability of the framework. It seems that, in cases of medium to serious ocular dryness, AS therapy is able to give stability, even if the duration must be verified.

In neurotropic keratopathy, a different mechanism occurs [57]. In this disease, there is not a single deficiency of tears but rather an imbalance with the production of harmful substance and an increased need for trophic factors. Numerous ocular and systemic diseases may lead to neurotropic keratopathy. In these diseases, neural factors such as acetylcholine or SP are depleted from the cornea. Nishida et al. [41] emphasize the importance of SP and IGF for a normal wound-healing response and Matsumoto et al. [28] report efficiency in the treatment of neurotropic keratopathy with 20% AS eye drops. Matsumoto showed that AS contains nerve growth factor and SP levels that are several times higher than the levels in tears and harbors IGF-1. It is their belief that AS helps healing in neurotropic keratopathy by providing lubrication and nerve healing and epithelialization. In another study, López-García et al. [58] report that, in aniridic keratopathy, AS eye drops improve the ocular surface and give more comfort compared to artificial tears. In our neurotropic keratopathy series patients, 3 patients had postherpetic keratitis, 2 patients had trigeminal nerve injury, and 1 patient had aniridic keratopathy. All patients had long-term therapy with tear substitutes and a history of recurrent trophic ulcers, significant neovascularization, and corneal scarring. On average, these patients had frameworks more severe than previous cases of dry eye, particularly when the deficit involved facial paralysis and anomalies in the dynamics of the eyelids. In all patients, we obtained stabilization of the framework, which was characterized by epithelial stability (i.e., more regular epithelium without defects) and a reduction in neovascularization, inflammation, and corneal opacity (Figure 1). One patient with trigeminal injury remains in therapy after 2 years, whereas the other patient, after discontinuing AS therapy, has relapsed with a trophic ulcer at risk of perforation. This experience allows us to believe that, especially in severe cases of neurotropic damage, the contribution of AS factors should be continuous and a program of chronic therapy can be scheduled.

The patients with ocular burn represent a different framework in which a single traumatic event, the acid burn, leads to an ocular surface injury with an action at term, but persistent damage. Few studies are available in the literature on chemical burns, and used as a treatment PRP [32], umbilical cord serum [33], or amniotic membranes [59]. Corneal chemical burns cause corneal infection, ulceration, opacity, and

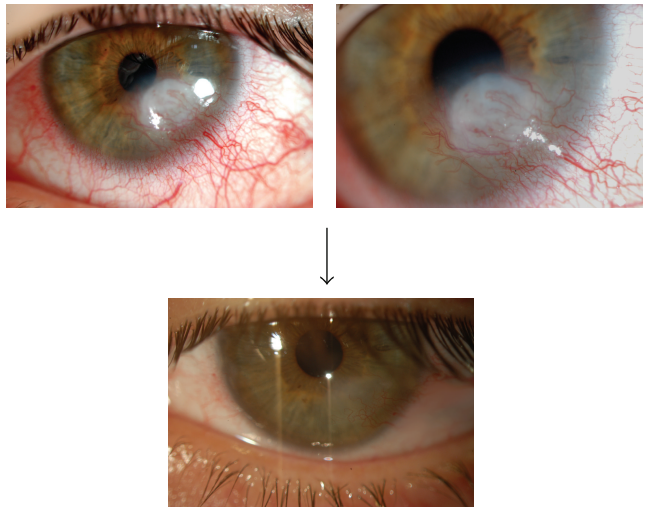

Figure 1: Clinical evolution of a patient with neurotrophic keratitis due to trigeminal nerve injury that occurred during acoustic neuroma excision.

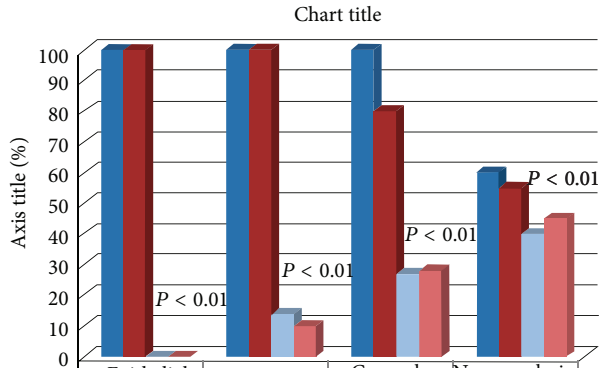

	Epithelial defect	Inflammation	Corneal opacity	Neovascularization
Before group 1	100%	100%	100%	60%
Before group 2	100%	100%	80%	55%
After group 1	0%	14%	27%	40%
After group 2	0%	10%	28%	45%

Figure 2: Evolution of clinical signs in group 1 and group 2. All data significantly improved.

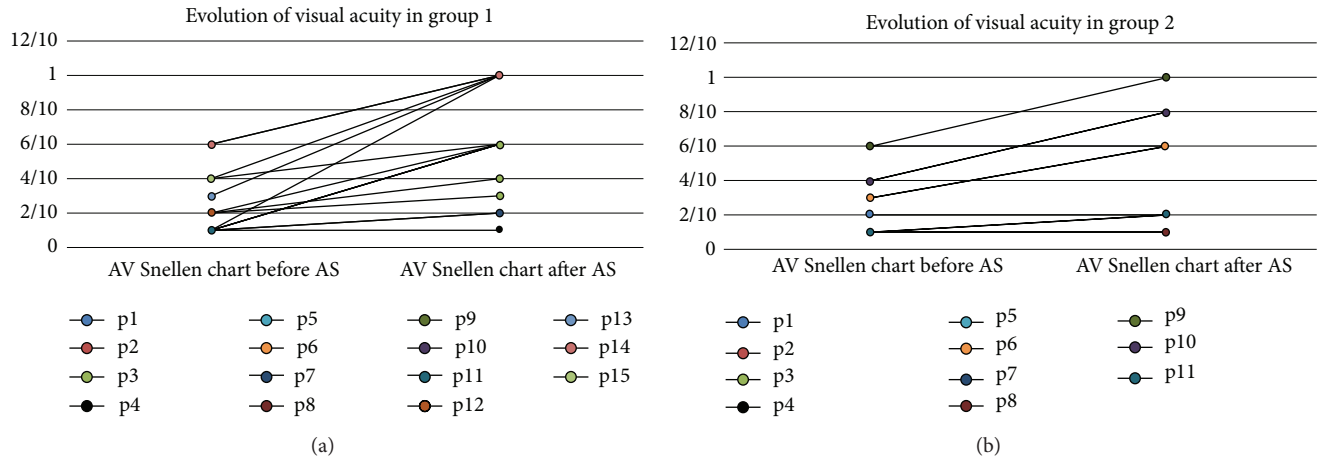

Figure 3: Evolution of visual acuity in the patients in the 2 groups. AS = autologous serum; p1–p15 = patient 1–patient 15.

neovascularization. Irrespective of the source of regenerating epithelium, the rate of migration after chemical injury is reduced [60–63]. Therefore, the primary aims of therapy are the promotion of epithelialization as fast as possible, reduction of inflammation, support of reparative processes, and prevention of complications with the least permanent damage. Subconjunctival autologous regenerative factor-rich plasma in ocular alkali burns is able to appreciably reduce corneal and conjunctival epithelialization time, sick leave duration, and healing time [64]. In a small sample, Panda et al. [32] showed significant improvement in the healing of epithelial defects, corneal clarity, and BCVA with the inoculation of PRP. Márquez-de-Aracena et al. [65] showed a shorter corneal healing time with the use of subconjunctival platelet concentrate autologous injection in comparison to conventional therapy. They also state that it is unnecessary to activate PRP and suggest using it topically [65, 66].

The rationale of using AS in chemical burns derives from the fact that it contains antiproteases such as alpha 2 macroglobulin (which reduces collagenase) and vitamin A (which modulates the normal growth and differentiation of the epithelium) [38, 67]. It modulates the expression of TSP1 to accelerate epithelialization [65] and inhibits VEGF-A [38, 68].

In our casuistry, 5–7 days after injury, all patients had evident signs of corneal suffering with epithelial instability and inflammation that was caused by trophic damage on the cornea and conjunctiva, despite limited limbal deficiency. The study of clinical signs showed that in each patient we attained the primary objective, which was the stabilization of the condition in the absence of inflammation, and a complete restitution of epithelial integrity. The regression of neovascularization in most patients may be because of an increase in trophic factors and a decrease in inflammatory factors. In fact, neovascularization that is formed to provide nourishment disappears quickly if the stimulus ceases. Opacity declined because of the reduction of inflammation and because of stromal remodeling supported by serum factors such as EGF, fibronectin, TGF-β, retinoic acid, and nerve growth factor that are able to promote proliferation and differentiation of limbal corneal epithelium cells.

All our patients obtained these results, although with different timings between acute and chronic diseases. Chemical burns had a shorter average treatment time. This suggests that chemical injury is reversible and the ocular surface stability can be self-maintained if inflammation is properly reduced and growth factors are rebalanced. We suggest that our patients had a limited limbal ischemia with a largely preserved limbus. None of the chemically burned patients remain in therapy and all patients have a healthy ocular surface.

A limitation of our study is the lack of a control arm for the acute group patients. A future goal will be to followup with a control arm treated with anti-inflammatory drugs and artificial tears to make direct comparisons between both therapies in chemical injury.

5. Conclusions

In our casuistry, AS eye drops have been effective in improving and stabilizing signs and symptoms in patients who do not improve with conventional therapy. We believe that a reconfirmation of our findings will be desirable in a larger group of patients in a prospective controlled trial setting. Studies aimed at clarifying the beneficial effects and risks of prolonged application of AS drops at different AS concentrations should also be the subject of future investigations.

In addition, a future goal will be to conduct examinations, especially in the composition of tears. This can help scientists understand what factors are decreased in the tears of these patients and how they are decreased and how long AS components can effectively remain in tears after therapy.

Conflict of Interests

The authors declare that there is no conflict of interests regarding the publication of this paper.

References

[1] B. A. Noble, R. S. K. Loh, S. MacLennan et al., "Comparison of autologous serum eye drops with conventional therapy in a randomised controlled crossover trial for ocular surface disease," *British Journal of Ophthalmology*, vol. 88, no. 5, pp. 647–652, 2004.

[2] G. G. Quinto, M. Campos, and A. Behrens, "Autologous serum for ocular surface diseases," *Arquivos Brasileiros de Oftalmologia*, vol. 71, no. 6, pp. 47–54, 2009.

[3] M. E. Stern, R. W. Beuerman, R. I. Fox, J. Gao, A. K. Mircheff, and S. C. Pflugfelder, "The pathology of dry eye: the interaction between the ocular surface and lacrimal glands," *Cornea*, vol. 17, no. 6, pp. 584–589, 1998.

[4] M. E. Stern, J. Gao, K. F. Siemasko, R. W. Beuerman, and S. C. Pflugfelder, "The role of the lacrimal functional unit in the pathophysiology of dry eye," *Experimental Eye Research*, vol. 78, no. 3, pp. 409–416, 2004.

[5] M. Rolando, "Sjögren's syndrome as seen by an ophthalmologist," *Scandinavian Journal of Rheumatology, Supplement*, vol. 30, no. 115, pp. 27–33, 2001.

[6] R. A. Ralph, M. G. Doane, and C. H. Dohlman, "Clinical experience with a mobile ocular perfusion pump," *Archives of Ophthalmology*, vol. 93, no. 10, pp. 1039–1043, 1975.

[7] R. I. Fox, R. Chan, J. B. Michelson, J. B. Belmont, and P. E. Michelson, "Beneficial effect of artificial tears made with autologous serum in patients with keratoconjunctivitis sicca," *Arthritis and Rheumatism*, vol. 27, no. 4, pp. 459–461, 1984.

[8] K. Tsubota, E. Goto, H. Fujita et al., "Treatment of dry eye by autologous serum application in Sjogren's syndrome," *British Journal of Ophthalmology*, vol. 83, no. 4, pp. 390–395, 1999.

[9] B. H. Jeng, "Use of autologous serum in the treatment of ocular surface disorders," *Archives of Ophthalmology*, vol. 129, no. 12, pp. 1610–1612, 2011.

[10] K. Tsubota, E. Goto, S. Shimmura, and J. Shimazaki, "Treatment of persistent corneal epithelial defect by autologous serum application," *Ophthalmology*, vol. 106, no. 10, pp. 1984–1989, 1999.

[11] A. C. Poon, G. Geerling, J. K. G. Dart, G. E. Fraenkel, and J. T. Daniels, "Autologous serum eyedrops for dry eyes and epithelial defects: clinical and in vitro toxicity studies," *British Journal of Ophthalmology*, vol. 85, no. 10, pp. 1188–1197, 2001.

[12] A. L. Young, A. C. O. Cheng, H. K. Ng, L. L. Cheng, G. Y. S. Leung, and D. S. C. Lam, "The use of autologous serum tears in persistent corneal epithelial defects," *Eye*, vol. 18, no. 6, pp. 609–614, 2004.

[13] S. Schrader, T. Wedel, R. Moll, and G. Geerling, "Combination of serum eye drops with hydrogel bandage contact lenses in the treatment of persistent epithelial defects," *Graefe's Archive for Clinical and Experimental Ophthalmology*, vol. 244, no. 10, pp. 1345–1349, 2006.

[14] B. H. Jeng and W. J. Dupps Jr., "Autologous serum 50% eyedrops in the treatment of persistent corneal epithelial defects," *Cornea*, vol. 28, no. 10, pp. 1104–1108, 2009.

[15] J. A. Choi and S.-H. Chung, "Combined application of autologous serum eye drops and silicone hydrogel lenses for the treatment of persistent epithelial defects," *Eye and Contact Lens*, vol. 37, no. 6, pp. 370–373, 2011.

[16] E. M. Rocha, F. Pelegrino, C. S. De Paiva, A. C. Vigorito, and Ç. A. De Souza, "GVHD dry eyes treated with autologous serum tears," *Bone Marrow Transplantation*, vol. 25, no. 10, pp. 1101–1103, 2000.

[17] N. Tananuvat, M. Daniell, L. J. Sullivan et al., "Controlled study of the use of autologous serum in dry eye patients," *Cornea*, vol. 20, no. 8, pp. 802–806, 2001.

[18] E. Takamura, K. Shinozaki, H. Hata, J. Yukari, and S. Hori, "Efficacy of autologous serum treatment in patients with severe dry eye," *Advances in Experimental Medicine and Biology*, vol. 506, pp. 1247–1250, 2002.

[19] Y. Ogawa, S. Okamoto, T. Mori et al., "Autologous serum eye drops for the treatment of severe dry eye in patients with chronic graft-versus-host disease," *Bone Marrow Transplantation*, vol. 31, no. 7, pp. 579–583, 2003.

[20] G. Geerling, S. MacLennan, and D. Hartwig, "Autologous serum eye drops for ocular surface disorders," *British Journal of Ophthalmology*, vol. 88, no. 11, pp. 1467–1474, 2004.

[21] T. Kojima, R. Ishida, M. Dogru et al., "The effect of autologous serum eyedrops in the treatment of severe dry eye disease: a prospective randomized case-control study," *American Journal of Ophthalmology*, vol. 139, no. 2, pp. 242–246, 2005.

[22] S. C. Leite, R. S. de Castro, M. Alves et al., "Risk factors and characteristics of ocular complications, and efficacy of autologous serum tears after haematopoietic progenitor cell transplantation," *Bone Marrow Transplantation*, vol. 38, no. 3, pp. 223–227, 2006.

[23] T. Noda-Tsuruya, N. Asano-Kato, I. Toda, and K. Tsubota, "Autologous serum eye drops for dry eye after LASIK," *Journal of Refractive Surgery*, vol. 22, no. 1, pp. 61–66, 2006.

[24] K.-C. Yoon, H. Heo, S.-K. Im, I.-C. You, Y.-H. Kim, and Y.-G. Park, "Comparison of autologous serum and umbilical cord serum eye drops for dry eye syndrome," *American Journal of Ophthalmology*, vol. 144, no. 1, pp. e86–e92, 2007.

[25] G. A. Lee and S. X. Chen, "Autologous serum in the management of recalcitrant dry eye syndrome," *Clinical and Experimental Ophthalmology*, vol. 36, no. 2, pp. 119–122, 2008.

[26] C. A. Urzua, D. H. Vasquez, A. Huidobro, H. Hernandez, and J. Alfaro, "Randomized double-blind clinical trial of autologous serum versus artificial tears in dry eye syndrome," *Current Eye Research*, vol. 37, no. 8, pp. 684–688, 2012.

[27] N. Phasukkijwatana, P. Lertrit, S. Liammongkolkul, and P. Prabhasawat, "Stability of epitheliotrophic factors in autologous serum eye drops from chronic Stevens-Johnson syndrome dry eye compared to non-autoimmune dry eye," *Current Eye Research*, vol. 36, no. 9, pp. 775–781, 2011.

[28] Y. Matsumoto, M. Dogru, E. Goto et al., "Autologous serum application in the treatment of neurotrophic keratopathy," *Ophthalmology*, vol. 111, no. 6, pp. 1115–1120, 2004.

[29] J. M. del Castillo, J. M. de la Casa, R. C. Sardiña et al., "Treatment of recurrent corneal erosions using autologous serum," *Cornea*, vol. 21, no. 8, pp. 781–783, 2002.

[30] N. G. Ziakas, K. G. Boboridis, C. Terzidou et al., "Long-term follow up of autologous serum treatment for recurrent corneal erosions," *Clinical and Experimental Ophthalmology*, vol. 38, no. 7, pp. 683–687, 2010.

[31] E. Goto, S. Shimmura, J. Shimazaki, and K. Tsubota, "Treatment of superior limbic keratoconjunctivitis by application of autologous serum," *Cornea*, vol. 20, no. 8, pp. 807–810, 2001.

[32] A. Panda, M. Jain, M. Vanathi, T. Velpandian, S. Khokhar, and T. Dada, "Topical autologous platelet-rich plasma eyedrops for acute corneal chemical injury," *Cornea*, vol. 31, no. 9, pp. 989–993, 2012.

[33] N. Sharma, M. Goel, T. Velpandian, J. S. Titiyal, R. Tandon, and R. B. Vajpayee, "Evaluation of umbilical cord serum therapy in

acute ocular chemical burns," *Investigative Ophthalmology and Visual Science*, vol. 52, no. 2, pp. 1087–1092, 2011.

[34] S. E. Wilson, L. Chen, R. R. Mohan, Q. Liang, and L. Janice, "Expression of HGF, KGF, EGF and receptor messenger RNAs following corneal epithelial wounding," *Experimental Eye Research*, vol. 68, no. 4, pp. 377–397, 1999.

[35] N. Kokawa, C. Sotozono, K. Nishida, and S. Kinoshita, "High total TGF-β2 levels in normal human tears," *Current Eye Research*, vol. 15, no. 3, pp. 341–343, 1996.

[36] S. C. G. Tseng, M. Farazdaghi, and A. A. Rider, "Conjunctival transdifferentiation induced by systemic vitamin A deficiency in vascularized rabbit corneas," *Investigative Ophthalmology and Visual Science*, vol. 28, no. 9, pp. 1497–1504, 1987.

[37] K. Uno, M. Kuroki, H. Hayashi, H. Uchida, M. Kuroki, and K. Oshima, "Impairment of thrombospondin-1 expression during epithelial wound healing in corneas of vitamin A-deficient mice," *Histology and Histopathology*, vol. 20, no. 2, pp. 493–499, 2005.

[38] E. C. Kim, T. K. Kim, S. H. Park, and M. S. Kim, "The wound healing effects of vitamin A eye drops after a corneal alkali burn in rats," *Acta Ophthalmologica*, vol. 90, no. 7, pp. e540–e546, 2012.

[39] T. Kojima, A. Higuchi, E. Goto, Y. Matsumoto, M. Dogru, and K. Tsubota, "Autologous serum eye drops for the treatment of dry eye diseases," *Cornea*, vol. 27, no. 1, pp. S25–S30, 2008.

[40] C. Costagliola, V. Romano, E. Forbice et al., "Corneal oedema and its medical treatment," *Clinical and Experimental Optometry*, vol. 96, no. 6, pp. 529–535, 2013.

[41] T. Nishida, M. Nakamura, K. Ofuji, T. Reid, M. Mannis, and C. Murphy, "Synergistic effects of substance P with insulin-like growth factor-1 on epithelial migration of the cornea," *Journal of Cellular Physiology*, vol. 169, no. 1, pp. 159–166, 1996.

[42] L. Liu, D. Hartwig, S. Harloff et al., "Corneal epitheliotrophic capacity of three different blood-derived preparations," *Investigative Ophthalmology and Visual Science*, vol. 47, no. 6, pp. 2438–2444, 2006.

[43] G. Geerling, J. T. Daniels, J. K. G. Dart, I. A. Cree, and P. T. Khaw, "Toxicity of natural tear substitutes in a fully defined culture model of human corneal epithelial cells," *Investigative Ophthalmology and Visual Science*, vol. 42, no. 5, pp. 948–956, 2001.

[44] R. Noecker, "Effects of common ophthalmic preservatives on ocular health," *Advances in Therapy*, vol. 18, no. 5, pp. 205–215, 2001.

[45] H. S. Dua, A. J. King, and A. Joseph, "A new classification of ocular surface burns," *British Journal of Ophthalmology*, vol. 85, no. 11, pp. 1379–1383, 2001.

[46] L. Liu, D. Hartwig, S. Harloff, P. Herminghaus, T. Wedel, and G. Geerling, "An optimised protocol for the production of autologous serum eyedrops," *Graefe's Archive for Clinical and Experimental Ophthalmology*, vol. 243, no. 7, pp. 706–714, 2005.

[47] J. S. López-García and I. García-Lozano, "Use of containers with sterilizing filter in autologous serum eyedrops," *Ophthalmology*, vol. 119, no. 11, pp. 2225–2230, 2012.

[48] Y. K. Cho, W. Huang, G. Y. Kim, and B. S. Lim, "Comparison of autologous serum eye drops with different diluents," *Current Eye Research*, vol. 38, no. 1, pp. 9–17, 2013.

[49] R. Marquez De Aracena Del Cid and I. Montero De Espinosa Escoriaza, "Subconjunctival application of regenerative factor-rich plasma for the treatment of ocular alkali burns," *European Journal of Ophthalmology*, vol. 19, no. 6, pp. 909–915, 2009.

[50] K. R. Fischer, A. Opitz, M. Böeck, and G. Geerling, "Stability of serum eye drops after storage of 6 months," *Cornea*, vol. 31, no. 11, pp. 1313–1318, 2012.

[51] A. Gupta, D. Monroy, Z. Ji, K. Yoshino, A. Huang, and S. C. Pflugfelder, "Transforming growth factor beta-1 and beta-2 in human tear fluid," *Current Eye Research*, vol. 15, no. 6, pp. 605–614, 1996.

[52] K. Terai, M. K. Call, H. Liu et al., "Crosstalk between TGF-β and MAPK signaling during corneal wound healing," *Investigative Ophthalmology and Visual Science*, vol. 52, no. 11, pp. 8208–8215, 2011.

[53] P. Aragona, V. Papa, A. Micali, M. Santocono, and G. Milazzo, "Long term treatment with sodium hyaluronate-containing artificial tears reduces ocular surface damage in patients with dry eye," *British Journal of Ophthalmology*, vol. 86, no. 2, pp. 181–184, 2002.

[54] K. Jirsova, K. Brejchova, I. Krabcova et al., "The application of autologous serum eye drops in severe dry eye patients; subjective and objective parameters before and after treatment," *Current Eye Research*, vol. 39, no. 1, pp. 21–30, 2014.

[55] F. Mantelli, L. Tranchina, A. Lambiase, and S. Bonini, "Ocular surface damage by ophthalmic compounds," *Current Opinion in Allergy and Clinical Immunology*, vol. 11, no. 5, pp. 464–470, 2011.

[56] A. Tincani, L. Andreoli, I. Cavazzana et al., "Novel aspects of Sjögren's syndrome in 2012," *BMC Medicine*, vol. 11, no. 1, article 93, 2013.

[57] F. Semeraro, M. Angi, M. Romano, M. Filippelli, R. Di Iorio, and C. Costagliola, "Neurotrophic keratitis," *Ophthalmologica*, vol. 231, no. 4, pp. 191–197, 2014.

[58] J. S. López-García, L. Rivas, I. García-Lozano, and J. Murube, "Autologous serum eyedrops in the treatment of aniridic keratopathy," *Ophthalmology*, vol. 115, no. 2, pp. 262–267, 2008.

[59] G. Clare, H. Suleman, C. Bunce, and H. Dua, "Amniotic membrane transplantation for acute ocular burns," *Cochrane Database of Systematic Reviews*, vol. 9, Article ID CD009379, 2012.

[60] M. D. Wagoner, K. R. Kenyon, and I. K. Gipson, "Polymorphonuclear neutrophils delay corneal epithelial wound healing in vitro," *Investigative Ophthalmology and Visual Science*, vol. 25, no. 10, pp. 1217–1220, 1984.

[61] R. R. Pfister and N. Burstein, "The effects of ophthalmic drugs, vehicles, and preservatives on corneal epithelium: a scanning electron microscope study," *Investigative Ophthalmology*, vol. 15, no. 4, pp. 246–259, 1976.

[62] M. Berman, E. Manseau, M. Law, and D. Aiken, "Ulceration is correlated with degradation of fibrin and fibronectin at the corneal surface," *Investigative Ophthalmology and Visual Science*, vol. 24, no. 10, pp. 1358–1366, 1983.

[63] K. Hayashi, M. Berman, D. Smith, A. El-Ghatit, S. Pease, and K. R. Kenyon, "Pathogenesis of corneal epithelial defects: role of plasminogen activator," *Current Eye Research*, vol. 10, no. 5, pp. 381–398, 1991.

[64] M. Berman, R. Leary, and J. Gage, "Evidence for a role of the plasminogen activator-plasmin system in corneal ulceration," *Investigative Ophthalmology and Visual Science*, vol. 19, no. 10, pp. 1204–1221, 1980.

[65] R. Márquez-de-Aracena, I. Montero-de-Espinosa, M. Muñoz, and G. Pereira, "Subconjunctival application of plasma platelet concentrate in the treatment of ocular burns. Preliminary results," *Archivos de la Sociedad Espanola de Oftalmologia*, vol. 82, no. 8, pp. 475–481, 2007.

[66] A. Granelli-Piperno, J. D. Vassalli, and E. Reich, "Secretion of plasminogen activator by human polymorphonuclear leukocytes. Modulation by glucocorticoids and other effectors," *Journal of Experimental Medicine*, vol. 146, no. 6, pp. 1693–1706, 1977.

[67] J. Imanishi, K. Kamiyama, I. Iguchi, M. Kita, C. Sotozono, and S. Kinoshita, "Growth factors: importance in wound healing and maintenance of transparency of the cornea," *Progress in Retinal and Eye Research*, vol. 19, no. 1, pp. 113–129, 2000.

[68] T. K. Kobayashi, K. Tsubota, E. Takamura, M. Sawa, Y. Ohashi, and M. Usui, "Effect of retinol palmitate as a treatment for dry eye: a cytological evaluation," *Ophthalmologica*, vol. 211, no. 6, pp. 358–361, 1997.

Hindawi Publishing Corporation
BioMed Research International
Volume 2014, Article ID 658350, 9 pages
http://dx.doi.org/10.1155/2014/658350

Review Article

IOL Power Calculation after Corneal Refractive Surgery

Maddalena De Bernardo,[1] Luigi Capasso,[2] Luisa Caliendo,[1] Francesco Paolercio,[3] and Nicola Rosa[1]

[1] *Department of Medicine and Surgery, University of Salerno, Via Salvatore Allende1, Baronissi, 84081 Salerno, Italy*
[2] *U.O.C. Corneal Transplant Unit, Pellegrini Hospital, 80100 Naples, Italy*
[3] *U.O.C. Eye Day Surgery, De Luca e Rossano Hospital, 80069 Vico Equense, Italy*

Correspondence should be addressed to Nicola Rosa; nrosa@unisa.it

Received 23 May 2014; Accepted 3 July 2014; Published 21 July 2014

Academic Editor: Ciro Costagliola

Purpose. To describe the different formulas that try to overcome the problem of calculating the intraocular lens (IOL) power in patients that underwent corneal refractive surgery (CRS). *Methods*. A Pubmed literature search review of all published articles, on keyword associated with IOL power calculation and corneal refractive surgery, as well as the reference lists of retrieved articles, was performed. *Results*. A total of 33 peer reviewed articles dealing with methods that try to overcome the problem of calculating the IOL power in patients that underwent CRS were found. According to the information needed to try to overcome this problem, the methods were divided in two main categories: 18 methods were based on the knowledge of the patient clinical history and 15 methods that do not require such knowledge. The first group was further divided into five subgroups based on the parameters needed to make such calculation. *Conclusion*. In the light of our findings, to avoid postoperative nasty surprises, we suggest using only those methods that have shown good results in a large number of patients, possibly by averaging the results obtained with these methods.

1. Introduction

Since the introduction of excimer laser treatment in the field of refractive surgery, several problems such as incorrect measurement of the intraocular pressure and intraocular lens (IOL) power calculation, have been pointed out [1–12].

It is well known that the calculation of the power of the IOL to be implanted in patients undergoing cataract surgery is mainly based on the measurement of corneal power, on axial length, and on the forecast of the actual position of the lens after surgery [13–21].

In eyes that underwent corneal refractive surgery (CRS), all the routinely used methods to measure corneal power do not guarantee the same accuracy compared to the same measurements in naive eyes. It has been extensively demonstrated that after myopic refractive surgery (PRK, LASIK, RK) both keratometry and corneal topography tend to overestimate the corneal power [22–35].

For this reason, if a patient develops a cataract after these procedures, using the current values of keratometry readings (K), the IOL power could be underestimated and the patient may have a considerable risk of becoming hyperopic [36–42].

Hyperopia after cataract surgery is not only a surprising result, but also a real disaster in terms of refractive outcome as pseudophakic eyes have lost their accommodative ability. In severe cases it may be necessary to remove and to replace the implanted IOL.

The purpose of the present paper is to describe the different available techniques to improve the accuracy of the IOL power calculation after refractive procedures.

2. Methods

An accurate Pubmed database search review of the recent literature from 2000 to nowadays was performed to identify all potentially relevant published studies. The search strategy used the following keywords: IOL power calculation and refractive surgery. The literature search was conducted between January and the march 2014. The references cited

in retrieved articles were also scanned for any additional relevant studies.

From this research 33 papers have been found.

All the authors of these papers agree that the main problem in the IOL power calculation after CRS is due to the incorrect keratometry readings.

After an accurate reading of these papers the collected methods have been divided in two main categories: methods based on the knowledge of the patient clinical history and methods that do not require the patient's medical history.

Moreover the methods based on the knowledge of the patient clinical history have been further divided into four subgroups based on the parameters needed to make such a calculation:

(1) the preoperative refraction and keratometry plus the postrefractive surgery refraction,

(2) the pre- and postrefractive surgery refractions,

(3) the preoperative keratometry,

(4) the preoperative keratometry and refraction,

(5) the prerefractive surgery refraction.

3. Results

According to this classification, the papers assigned to the different categories were as follows.

3.1. Methods Based on the Knowledge of the Patient Clinical History

3.1.1. Knowledge of the Preoperative Keratometry and Refraction and Postrefractive Surgery Refraction. The so-called "Medical history method", described in 1989 by Eiferman [43] and Holladay [44], which later was modified by Hoffer [45], belongs to this group. With this method the K value is calculated subtracting the change in refraction, induced by the treatment, to the mean preoperative corneal power:

$$K_{\text{eff}} = K_{\text{pre}} - \Delta\text{Ref}, \tag{1}$$

where K_{eff} is corneal power to be included in calculation formulas, K_{pre} is preoperative mean corneal power, and ΔRef is change of refraction measured as spherical equivalent.

For many years this method has been considered to be the gold standard, but today it is considered outdated.

3.1.2. Knowledge of the Preoperative and Postrefractive Surgery Refraction. The following methods belong to this group.

Camellin and Calossi [46] proposed two formulas, according to the different treatment (PRK or RK) in which the IOL power is calculated utilizing a corneal radius, function of the preoperative one, modified taking into account the surgically induced refractive change. The formulas are the following:

$$P = \frac{1336\left(4R_{\text{adj}} - L\right)}{\left(L - \text{ACD}_{\text{post}}\right)\left(4R_{\text{adj}} - \text{ACD}_{\text{post}}\right)}, \tag{2}$$

where P is power of the IOL to be implanted, L is axial length, ACD_{post} represents the actual position of the IOL, and R_{adj} is radius of curvature after refractive surgery, modified depending on whether the individual has undergone incisional surgery:

$$R_{\text{adj}} = \frac{0.3319 \times R}{n_{\text{adj}} - 1} = \frac{0.3319 \times R}{0.00096 \times \text{SIRC} + 0.3319} \tag{3}$$

or photorefractive surgery:

$$R_{\text{adj}} = \frac{0.3316 \times R}{n_{\text{rel}} - 1} = \frac{0.3319 \times R}{0.0013 \times \text{SIRC} + 0.3319}, \tag{4}$$

where SIRC is refractive changes induced by surgery.

The authors tested the formula in 15 eyes undergoing IOL implantation after cataract surgery, with a mean postoperative error of $+0.28D \pm 0.66D$ ranging from $-1.04D$ to $+1.58D$ with 9 eyes in the range of $\pm 0.5D$, 12 eyes in the range of $\pm 1D$, and 15 eyes in the range of $\pm 2D$.

Chen and Hu [47] proposed two formulas, for two different devices utilized for measuring the corneal power, namely, (1) the Topcon CR 3000 autokeratometer and (2) the TMS1 Corneal topographer.

(1) consider

$$\Delta\text{Auto}\, K = 0.7397 \times \Delta\text{ES} + 0.3778, \tag{5}$$

where ΔAuto K is change in corneal power after corneal refractive surgery, ΔES is pre- and postoperative refractive change.

(2) consider

$$\Delta K \text{ Central} = 0.9183 \times \Delta\text{ES} - 0.0204, \tag{6}$$

where ΔK Central is change in Central keratometry, ΔES is change in pre- and postoperative refraction.

In both cases the change in corneal power after refractive surgery is based on a linear correlation with the change in refraction induced by refractive surgery. The difference between these two values is then subtracted from the postoperative K to obtain the actual K.

Diehl et al. [48, 49] suggest a formula where the change in refraction is utilized to calculate the target refractive error to achieve emmetropia:

$$\begin{aligned}&\text{Target postoperative refractive error } (D) \text{ to}\\ &\quad\text{achieve emmetropia during IOL power calculation}\\ &= -0.018 * (\text{MRSE Change}) * (\text{MRSE Change})\\ &\quad + 0.192 * (\text{MRSE Change}) - 0.062,\end{aligned} \tag{7}$$

where MRSE change is manifest refraction spherical equivalent change in diopters.

The outcomes in 97% of the 32 examined eyes fell within ± 1.00 D of the value predicted by this formula.

Feiz et al. [50, 51] suggested two different regression formulas to be used depending on whether the patient underwent a myopic or hyperopic LASIK treatment, in which the difference in refraction induced by the treatment is subtracted from the IOL power traditionally calculated:

Myopic LASIK:

$$\text{IOL imp} = \text{IOL calc} - 0.231 + (0.595 \times \Delta\text{ES}), \quad (8)$$

Hyperopic LASIK:

$$\text{IOL imp} = \text{IOL calc} + 0.751 - (0.862 \times \Delta\text{ES}), \quad (9)$$

where IOL imp is power of IOL to be implanted, IOL calc is the power of IOL calculated by the traditional method, and ΔES is difference in refraction before and after refractive surgery.

The authors tested the formula in 19 eyes undergoing IOL implantation after cataract surgery, with a mean postoperative refractive error of $-0.375 \pm 2.3D$ ranging from $-2D$ to $+1.25D$ with 12 eyes (63.2%) in the range of $\pm 0.5D$, 16 eyes (84.2%) in the range of $\pm 1D$, and 19 eyes (100%) in the range of $\pm 1.5D$.

Hamed et al. [52] proposed two formulas, for two different devices utilized for measuring the corneal power, namely, the Bausch and Lomb keratometer and the EyeSys topographer: in both cases the corneal power is calculated with a regression formula, subtracting the RS-induced change in refraction from the mean postoperative corneal power:

(a)

$$K_{\text{post-adj}} = K_{\text{post}} - 0.24 \times (\Delta\text{Rif}) + 0.15, \quad (10)$$

(b)

$$\text{EffRP}_{\text{post-adj}} = \text{EffRP}_{\text{post}} - 0.15\,(\Delta\text{Rif}) - 0.05, \quad (11)$$

where $K_{\text{post-adj}}$ is corneal power to be included in calculation formulas, K_{post} is average postoperative corneal power obtained by keratometry, ΔRif is pre- and postoperative refractive change measured as spherical equivalent, $\text{EffRP}_{\text{post-adj}}$ is corneal power to be included in calculation formulas, and $\text{EffRP}_{\text{post}}$ is average postoperative corneal power using the parameter EffRP from EyeSys topographer.

The authors do not provide data to support the reliability of their method.

Jarade et al. [53] suggested a formula in which the K value is calculated from the ratio between the effective treatment and the anterior corneal radius of curvature:

$$K\text{-reading} = \frac{(rN - 1)}{R_a}, \quad (12)$$

where R_a is radius of anterior corneal curvature measured in meters, $rN = 0.0014 * \Delta + 1.3375$, and Δ is amount of myopic ablation.

The authors do not provide data to support the reliability of their method.

S. Masket and S. E. Masket [54] suggested a formula related to the effective treatment at the corneal apex, to calculate a factor to be added to the calculated IOL power:

$$\text{IOL power add} = (\text{LSE} * -0.326) + 0.101, \quad (13)$$

where IOL power add is power of IOL to be added and LSE is effective treatment at the corneal apex.

The author provides no data to support the reliability of the method.

Rosa et al. [42] proposed the following formula: $y = 0.7615x - 0.6773$, where x is difference in refraction at the corneal plane and y is keratometric difference evaluated with the IOL Master. To obtain the corrected K the difference between x and y has to be subtracted from the values of measured postoperative K. The authors do not provide data to support the reliability of their method.

Stakheev and Balashevich [55] described a formula in which there is a linear correlation between the corneal power correcting factor and the effective treatment, utilizing different constants, varying depending on the performed treatment and the device used to measure the corneal power:

$$Y = aX - b, \quad (14)$$

where Y is corneal power correcting factor, X is effective treatment, and a and b vary depending on the type of refractive surgery performed and the equipment used to measure the corneal power.

In the case of LASIK one has the following:

(i) Humphrey autokeratometer:

(1) $a = 0.225$,
(2) $b = 0.3893$,

(ii) Grand Seiko GR3100 autokeratometer:

(1) $a = 0.3356$,
(2) $b = 0.453$,

(iii) Sim K with the Humphrey topographer:

(1) $a = 0.2876$,
(2) $b = 0.5402$,

(iv) Average Corneal Power with the Humphrey topographer:

(1) $a = 0.1468$,
(2) $b = 0.4468$.

In the case of PRK one has the following:

(i) Humphrey autokeratometer:

(1) $a = 0.2537$,
(2) $b = 0.5322$,

(ii) Grand Seiko GR3100 autokeratometer:

(1) $a = 0.3701$,
(2) $b = 0.89$,

(iii) Sim K with the Humphrey topographer:

(1) $a = 0.3341$,
(2) $b = 0.7857$,

(iv) Average Corneal Power Humphrey topographer:

(1) $a = 0.2325$,
(2) $b = 0.643$.

In the case of RK one has the following:

(i) Humphrey autokeratometer:

(1) $a = 0.0256$,
(2) $b = 1.0957$,

(ii) Grand Seiko GR3100 autokeratometer:

(1) $a = 0.2572$,
(2) $b = 1.3328$,

(iii) Sim K with the Humphrey topographer:

(1) $a = 0.2189$,
(2) $b = 1.4481$,

(iv) Average Corneal Power Humphrey topographer:

(1) $a = 0.0479$,
(2) $b = 0.7457$.

3.1.3. Knowledge of the Preoperative Keratometry. The following methods belong to this group.

Aramberri [56, 57], assuming that the error in the calculation is due to an incorrect estimation of the actual position of the IOL, suggested the so-called double-K method, which relies on the use of both preoperative and postoperative K, which are needed to calculate the effective lens position:

$$\mathrm{IOL}_{\mathrm{emme}} = \frac{\left[1000 * n_a * \left(n_a * r_{\mathrm{post}} - 0.333 * \mathrm{LOPT}\right)\right]}{\left[\left(\mathrm{LOPT} - \mathrm{ACD}_{\mathrm{est}}\right) * \left(n_a * r_{\mathrm{post}} - 0.333 * \mathrm{ACD}_{\mathrm{est}}\right)\right]}, \quad (15)$$

where $n_a = 1.336$, r_{post} is radius of curvature after refractive surgery, $\mathrm{LOPT} = L + (0.65696 - 0.02029 * L)$, and L is axial length; $\mathrm{ACD}_{\mathrm{est}}$ is estimated anterior chamber depth that requires knowledge of preoperative radius of curvature.

To prove the validity of the formula the author tested it in 9 eyes undergoing IOL implantation after cataract surgery, obtaining a mean postoperative refractive error of $0.43D \pm 0.44D$ with a range from -0.56 to$1.47D$ with 6 eyes (66.66%) in the range of $\pm 0.5D$ and 8 eyes (88.88%) in the range of $\pm 1D$.

Jarade and Tabbara [58] suggested, to calculate the corneal power, the following formula:

$$K_{\mathrm{postop}} = K_{\mathrm{prepop}} - \left[\frac{\left(N_c - 1\right) * \left(R_{a\text{-postop}} - R_{a\text{-preop}}\right)}{\left(R_{a\text{-postop}} * R_{a\text{-preop}}\right)}\right], \quad (16)$$

where K_{postop} is corneal power to be included in the formula to calculate the IOL, K_{prepop} is corneal power before corneal refractive surgery, N_c is cornea's index of refraction (1.376), $R_{a\text{-postop}}$ is radius of curvature of the anterior surface of the cornea after refractive surgery, and $R_{a\text{-preop}}$ is radius of curvature of the anterior surface of the cornea before refractive surgery.

The authors do not provide data to support the reliability of their method.

Seitz et al. [59] suggested calculating the corneal power by subtracting from the preoperative corneal power a number derived from the inverse of the pre- and postoperative keratometric values:

$$K_{\mathrm{calc\text{-}ex}} = K_{\mathrm{pre}} - \left[\frac{0.376}{\left(0.3313 * K_{\mathrm{pre}}\right)} - \frac{0.376}{\left(0.3313 * K_{\mathrm{post}}\right)}\right], \quad (17)$$

where $K_{\mathrm{calc\text{-}ex}}$ is keratometric value to be included in the formula; K_{pre} is keratometric value prior to corneal refractive surgery; K_{post} is keratometric value after corneal refractive surgery.

The authors do not provide data to support the reliability of their method.

3.1.4. Knowledge of the Preoperative Keratometry and Refraction. Walter et al. [60] recommend using RPRE (patient refraction before surgery) as $\mathrm{RX}_{\mathrm{TARG}}$ (i.e., the target refraction) utilizing AL (axial length) and K_{PRE} (i.e., keratometry before surgery).

The authors tested this method in 9 eyes undergoing IOL implantation after cataract surgery, obtaining a mean refractive error of $+0.03D \pm 0.42D$ ranging from $-0.625D$ to $+0.75D$; 8 eyes where in the range of $\pm 0, 5D$ and 9 eyes in the range of $\pm 1D$.

3.1.5. Knowledge of the Prerefractive Surgery Refraction. Latkany et al. [61] suggested different methods, among which is the use of the flattest keratometry value to calculate the IOL power, using the SRK-T formula:

$$\text{IOL implanted} = \text{IOL calc} - (0.47x + 0.85), \quad (18)$$

where x is preoperative refractive error.

However, since they found a hypocorrection with this method, they suggest modifying the result taking into account the preoperative refractive error.

3.2. Methods That Do Not Require the Knowledge of the Patient's Clinical History. Borasio et al. [62] suggested measuring the corneal thickness and the anterior and posterior corneal power with a Pentacam, together with a corneal refractive index, related to the corneal thickness. These data should be inserted in the so-called BESSt formula, to calculate the K values to be used with the SRK/T or with the Hoffer Q formula, depending on the axial length:

$$\begin{aligned}\text{BESSt } K &= \left\{\left[\frac{1}{rF} * \left(n_{\text{adj}} - n_{\text{air}}\right)\right] + \left[\frac{1}{rB} * \left(n_{\text{acq}} - n_{\text{adj}}\right)\right] \right. \\ &\quad \left. - \left[d * \frac{1}{r} * \left(n_{\text{adj}} - n_{\text{air}}\right) * \frac{1}{rB} * \left(n_{\text{acq}} - n_{\text{adj}}\right)\right]\right\} \\ &\quad * 1000, \end{aligned} \tag{19}$$

where rF is anterior radius of curvature, n_{adj} is refractive index modified according to corneal thickness, n_{air} is refractive index of air (1), n_{acq} is aqueous index of refraction (1.336), and rB is posterior radius of curvature; $d = d_{\text{cct}}/1.3265$; d_{cct} = CCT/1000000; CCT is central corneal thickness.

The authors tested their formula in 13 eyes (7 myopic, 6 hyperopic) undergoing IOL implantation after cataract, with a mean postoperative refractive error of $0.08D \pm 0.62D$, with 46% of the eyes in the range of $\pm 0.5D$ and 100% in the range of $\pm 1D$.

Ferrara et al. [63], assuming that the index of refraction changes in relation with the corneal refractive treatment, proposed a second-order regression formula based on the axial length, to calculate a new index of refraction to be used to calculate the K values:

$$\text{IR} = -0.0006 * (\text{AL} * \text{AL}) + 0.0213 * \text{AL} + 1.1572, \tag{20}$$

where IR is the index of refraction and AL is the axial length.

The authors tested the formula in 5 eyes with the following results: $\pm 0.50D$ in 2 eyes, $\pm 1.00D$ in 4 eyes, and $\pm 1.50D$ in 5 eyes (range $-0.25D$ to $-1.50D$).

Haigis [64] suggested a formula to calculate the corrected corneal radius that is inversely related to the one measured with the IOL Master:

$$r_{\text{corr}} = \frac{331.5}{\left(-5.1625 \times r_{\text{meas}} + 82.2603 - 0.35\right)}, \tag{21}$$

where r_{corr} is corrected radius of curvature and r_{meas} is radius of curvature after corneal refractive surgery measured with the IOL Master.

The author tested the formula in 117 eyes undergoing IOL implant after cataract surgery with a mean postoperative refractive error of $-0.04D \pm 0.7$ ranging from $-2.3D$ to $+2.4D$, with 61 eyes in the range of $\pm$ 0, $5D$, 84 eyes in the range of $\pm 1D$, 98.4 eyes in the range of $\pm 2D$.

Ianchulev et al. [65] proposed a method which requires no special calculations; in fact, they suggested to perform phacoemulsification and measure the patient refraction on the operating table; this refraction, in terms of spherical equivalent, is multiplied for a constant, to obtain the IOL power to be implanted: IOL = 2.01449 × intraoperative spherical equivalent.

The authors tested the formula in 16 eyes undergoing IOL implantation after cataract extraction, and 83% of eyes were in the range of $\pm 1D$.

Kim et al. [66] proposed a formula in which the calculated corneal power is derived from a linear correlation with the mean corneal power after refractive surgery:

$$K_M = 0.715 * K_C + 11.998, \tag{22}$$

where K_M is average corneal power measured after refractive surgery. K_C is average corneal power recalculated by the formula.

The authors do not provide data to support the reliability of their method.

Latkany et al. [61] suggested different methods; among these they suggested to use the flattest keratometry value to calculate the IOL power, together with the SRK-T formula:

$$\text{IOL implanted} = \text{IOL calc} - (0.47x + 0.85), \tag{23}$$

where x is preoperative refractive error.

However, since they found a hypocorrection with this method, they suggest modifying the result utilizing also the preoperative refractive error.

The authors do not provide data to support the reliability of their method.

Mackool and Ko [67] suggested to perform phacoemulsification and measure the refraction 30 minutes later; the patient is then brought to the operating room for secondary IOL implantation. The IOL power is calculated multiplying the obtained refraction for a constant:

$$P = 1.75 * \text{AR}, \tag{24}$$

where P is IOL power to be implanted and AR is aphakic refraction.

The authors tested the formula in 12 eyes undergoing IOL implantation after cataract surgery, with a mean postoperative refractive error of $-0.3125 \pm 1.15D$ ranging from $-1.125D$ to $+0.5D$.

Rosa et al. [68, 69] were the first authors to publish a method that does not require the knowledge of the clinical history for the calculation of the IOL power in patients after excimer laser refractive surgery. The method is based on the following formula:

$$K_{\text{eff}} = \frac{337.5}{R_{\text{mis}}} * (0.0276 * \text{AL} + 0.3635), \tag{25}$$

where K_{eff} is corneal power to be included in calculation formulas, R_{mis} is patient mean radius of curvature measured with a common keratometry, and AL is axial length.

They suggest to use the K_{eff} with SRK T formula in eyes with axial length <30 mm and an average between the values of SRKT and SRK II in eyes with axial length over 30 mm.

The formula was tested in 62 eyes undergoing IOL implantation after cataract surgery with a mean postoperative

refractive error of $-0.41 \pm 0.75D$ with a range running from $-3.25D$ to $+1D$, with 37 eyes (60%) in the range of $\pm 0.5D$, 53 eyes (85%) in the range of $\pm 1D$, and 61 eyes (98%) in the range of $\pm 2D$.

The same authors, recently, proposed a modification to this method [70]: the power of the IOL should be calculated using the SRKT formula for all axial lengths utilizing the correction factor described above, but in case the product of AL (axial length) $*$ K_{mis} (corneal power measured with a common keratometer) is >1060, the IOL power obtained shall be reduced using the following regression formula:

$$Y = -\left(-0.0157 * \text{AL} * K_{\text{mis}} + 16.437\right), \tag{26}$$

where Y is refractive error to insert in the IOL power calculation to obtain emmetropia.

(For instance, if $Y = 5$, to obtain emmetropia, the calculation should aim to $+5D$.)

This new formula is more reliable than the first because it takes into account any hypocorrection or regressions that may be present in these patients after cornea refractive surgery.

Saiki et al. [71] proposed a modified double K method, also called anterior posterior (A-P) method, in patients that underwent laser in situ Keratomileusis (LASIK), utilizing a linear regression formula that requires the postoperative posterior corneal power evaluated with the Pentacam to calculate the preoperative Km to be used to calculate the ELP, similarly to the double K method:

$$y = -4.907x + 12.371, \tag{27}$$

where y is preoperative Km evaluated with the Pentacam and x is posterior postoperative Km evaluated with the Pentacam.

The authors tested their formula in 28 eyes of 19 patients: the median values of the arithmetic and absolute prediction errors using the A-P method were $0.16D$ and $0.54D$, respectively. The prediction errors were within $\pm 0.50D$ in 46.4% of eyes and within $\pm 1.00D$ in 75.0%.

Savini et al. [72] suggested to calculate the corneal power utilizing a refractive index deriving from a regression formula related to the attempted correction:

$$P^{\text{post}} = \frac{\left(n^{\text{post}} - 1\right)}{r}, \tag{28}$$

where P^{post} is the corneal power after corneal refractive surgery, n^{post} is the postoperative index of refraction = 1.338 + 0.0009856 $*$ attempted correction, and r is radius of curvature.

The formula is the result of a retrospective analysis of 98 eyes that underwent myopic refractive surgery, utilizing the TMS 2 corneal topographer. The authors do not provide data to support the reliability of their method.

Shammas et al. [73, 74] proposed a formula in which the calculated mean corneal power is derived from a linear correlation with the mean corneal power after refractive surgery:

$$K_{\text{c.cd}} = 1.14 * K_{\text{post}} - 6.8, \tag{29}$$

where $K_{\text{c.cd}}$ is mean corneal power recalculated by the formula and K_{post} is mean corneal power after refractive surgery.

The formula was tested in 15 eyes undergoing IOL implantation after cataract surgery, with a mean postoperative refractive error of $0.55 \pm 0.31D$ ranging from $-0.89D$ to $+1.05D$ with 14 eyes (93.3%) in the range of $\pm 1D$.

Soper and Goffman [75] described the contact lens method, later modified by Holladay, which consists of three phases: measurement of refraction in diopters before contact lens application, application of a neutral contact lens with known curvature, and measurement of the refraction with the contact lens. After measuring the refraction before and after application of the contact lens, the change in refraction is added to the value of the contact lens curvature.

This method is slightly less accurate than the standard keratometry for determining corneal power in people with normal and transparent corneas, and with good visual acuity, and can be used in patients whose preoperative parameters are unknown, but unfortunately it is not reliable in case of media opacities which reduce the visual acuity below 20/70 and it is suggested after radial keratotomy but not after excimer laser corneal refractive surgery.

4. Conclusion

It is said that when there are too many ways to solve a problem it means that none of them is reliable. We think the real problem is that so far, as it is evident from the above, only few methods have been tested in a sufficient number of patients, while most of them are just theoretical and have been verified in few patients; in many of them, in fact, the studied group does not reach the number of twenty subjects.

The other problem is that several methods are clinical history based and, unfortunately, in most of the patients the preoperative keratometry values and the exact refractive treatment are not available, so we can conclude that methods that require knowledge of medical history are difficult to use.

With some of these methods, the authors report to have achieved 100% results in the range of 1 diopter, but we believe this is only due to the limited number of patients tested: in fact, even in patients without a story of previous refractive surgery, these results would be described as impressive. If these methods were in fact so precise, it would be probably convenient to treat them first with refractive surgery and later to perform the cataract surgery, but obviously this is illogical. Therefore we recommend, to avoid postoperative nasty surprises, using only those methods that have shown good results in a large number of patients, possibly by averaging the results obtained with these methods.

Conflict of Interests

The authors declare that there is no conflict of interests regarding the publication of this paper.

References

[1] N. Rosa, "Standards for reporting results of refractive surgery," *Journal of Refractive Surgery*, vol. 17, no. 4, pp. 473–474, 2001.

[2] N. Rosa, L. Capasso, M. Lanza, and A. Romano, "Axial eye length evaluation before and after myopic photorefractive keratectomy," *Journal of Refractive Surgery*, vol. 21, no. 3, pp. 281–287, 2005.

[3] M. de Bernardo, L. Capasso, and N. Rosa, "Algorithm for the estimation of the corneal power in eyes with previous myopic laser refractive surgery," *Cornea*, vol. 33, no. 6, article e2, 2014.

[4] G. Cennamo, N. Rosa, E. Guida, A. Del Prete, and A. Sebastiani, "Evaluation of corneal thickness and endothelial cells before and after excimer laser photorefractive keratectomy," *Journal of Refractive and Corneal Surgery*, vol. 10, no. 2, pp. 137–141, 1994.

[5] G. Ambrosio, G. Cennamo, R. de Marco, L. Loffredo, N. Rosa, and A. Sebastiani, "Visual function before and after photorefractive keratectomy for myopia.," *Journal of Refractive and Corneal Surgery*, vol. 10, no. 2, pp. 129–136, 1994.

[6] N. Rosa, G. Cennamo, A. Del Prete, B. Pastena, and A. Sebastini, "Effects on the corneal endothelium six months following photorefractive keratectomy," *Ophthalmologica*, vol. 209, no. 1, pp. 17–20, 1995.

[7] G. Cennamo, N. Rosa, A. La Rana, S. Bianco, and A. Sebastiani, "Non-contact tonometry in patients that underwent photorefractive keratectomy," *Ophthalmologica*, vol. 211, no. 6, pp. 341–343, 1997.

[8] N. Rosa, G. Cennamo, A. del Prete, S. Bianco, and A. Sebastiani, "Endothelial cells evaluation two years after photorefractive keratectomy," *Ophthalmologica*, vol. 211, no. 1, pp. 32–39, 1997.

[9] N. Rosa and G. Cennamo, "Noncontact tonometry after LASIK," *Journal of Cataract & Refractive Surgery*, vol. 27, no. 8, pp. 1146–1147, 2001.

[10] N. Rosa, G. Cennamo, and J. A. Sanchis Gimeno, "Goldmann applanation tonometry after PRK and LASIK," *Cornea*, vol. 20, no. 8, pp. 905–906, 2001.

[11] G. Cennamo and N. Rosa, "Noncontact tonometry after LASIK," *Journal of Cataract and Refractive Surgery*, vol. 28, no. 12, pp. 2069–2070, 2002.

[12] M. Lanza, N. Rosa, L. Capasso, G. Iaccarino, S. Rossi, and A. Romano, "Can we utilize photorefractive keratectomy to improve visual acuity in adult amblyopic eyes?" *Ophthalmology*, vol. 112, no. 10, pp. 1684–1691, 2005.

[13] N. Rosa, D. Furgiuele, M. Lanza, L. Capasso, and A. Romano, "Correlation of changes in refraction and corneal topography after photorefractive keratectomy," *Journal of Refractive Surgery*, vol. 20, no. 5, pp. 478–483, 2004.

[14] N. Rosa, M. Lanza, L. Capasso, M. Lucci, B. Polito, and A. Romano, "Anterior Chamber depth measurement before and after PRK: comparison between IOL master and Orbscan II," *Ophthalmology*, vol. 113, no. 6, pp. 962–969, 2006.

[15] N. Rosa, L. Capasso, and M. Lanza, "Power calculation after laser refractive surgery," *Journal of Cataract and Refractive Surgery*, vol. 35, no. 9, article 1653, 2009.

[16] N. Rosa, L. Capasso, M. de Bernardo, and M. Lanza, "IOL power calculation after refractive surgery," *Ophthalmology*, vol. 118, no. 11, p. 2309, 2011.

[17] N. Rosa, M. de Bernardo, and M. Lanza, "Axial eye length evaluation before and after hyperopic photorefractive keratectomy," *Journal of Refractive Surgery*, vol. 29, article 80, 2013.

[18] N. Rosa, M. Lanza, M. Borrelli, B. Polito, M. L. Filosa, and M. de Bernardo, "Comparison of central corneal thickness measured with Orbscan and Pentacam," *Journal of Refractive Surgery*, vol. 23, no. 9, pp. 895–899, 2007.

[19] M. De Bernardo, L. Zeppa, M. Cennamo, S. Iaccarino, and N. Rosa, "Prevalence of corneal astigmatism before cataract surgery in Caucasian patients," *European Journal of Ophthalmology*, vol. 24, no. 4, pp. 494–500, 2014.

[20] M. de Bernardo and N. Rosa, "Letters to the editor: re: alveolar bone loss associated with age-related macular degeneration in males," *Journal of Periodontology*, vol. 85, no. 1, pp. 11–12, 2014.

[21] N. Rosa, M. De Bernardo, S. Iaccarino, and M. Cennamo, "Intraocular lens power calculation: a challenging case," *Optometry & Vision Science*, vol. 91, pp. e29–e31, 2014.

[22] G. Cennamo, N. Rosa, G. O. D. Rosenwasser, and A. Sebastiani, "Phototherapeutic keratectomy in the treatment of Avellino dystrophy," *Ophthalmologica*, vol. 208, no. 4, pp. 198–200, 1994.

[23] N. Rosa, G. Cennamo, A. Pasquariello, F. Maffulli, and A. Sebastiani, "Refractive outcome and corneal topographic studies after photorefractive keratectomy with different-sized ablation zones," *Ophthalmology*, vol. 103, no. 7, pp. 1130–1138, 1996.

[24] G. Cennamo, N. Rosa, A. del Prete, M. A. Breve, and A. Sebastiani, "The corneal endothelium 12 months after photorefractive keratectomy in high myopia," *Acta Ophthalmologica*, vol. 75, no. 2, pp. 128–130, 1997.

[25] N. Rosa, D. Greer, C. J. Rapuano, and D. D. Koch, "Excimer laser photorefractive keratectomy," *Ophthalmology*, vol. 107, no. 1, pp. 6–8, 2000.

[26] N. Rosa, G. Cennamo, and A. Sebastiani, "Classification of corneal topographic patterns after PRK [1]," *Journal of Refractive Surgery*, vol. 16, no. 4, pp. 481–483, 2000.

[27] N. Rosa, G. Cennamo, and M. Rinaldi, "Correlation between refractive and corneal topographic changes after photorefractive keratectomy for myopia," *Journal of Refractive Surgery*, vol. 17, no. 2, pp. 129–133, 2001.

[28] N. Rosa and D. Huang, "Multiple regression and vector analysis of LASIK for myopia and astigmatism," *Journal of Refractive Surgery*, vol. 17, no. 5, article 620, 2001.

[29] N. Rosa and G. Cennamo, "Phototherapeutic keratectomy for relief of pain in patients with pseudophakic corneal edema," *Journal of Refractive Surgery*, vol. 18, no. 3, pp. 276–279, 2002.

[30] N. Rosa, A. Iura, M. Romano, G. Verolino, and A. Romano, "Correlation between automated and subjective refraction before and after photorefractive keratectomy," *Journal of Refractive Surgery*, vol. 18, no. 4, pp. 449–453, 2002.

[31] N. Rosa, M. Lanza, G. De Rosa, and A. Romano, "Anterior corneal surface after Nidek EC-5000 multipass and multizone photorefractive keratectomy for myopia," *Journal of Refractive Surgery*, vol. 18, no. 4, pp. 460–462, 2002.

[32] N. Rosa and L. Capasso, "Intraocular lens power calculation after photorefractive keratectomy for myopia," *Archives of Ophthalmology*, vol. 121, article 584, no. 4, 2003.

[33] G. Cennamo, N. Rosa, M. A. Breve, and M. di Grazia, "Technical improvements in photorefractive keratectomy for correction of high myopia," *Journal of Refractive Surgery*, vol. 19, no. 4, pp. 438–442, 2003.

[34] N. Rosa, L. Capasso, and M. Lanza, "New formula for calculating intraocular lens power after LASIK," *Journal of Cataract and Refractive Surgery*, vol. 31, no. 10, pp. 1854–1855, 2005.

[35] N. Rosa and L. Capasso, "IOL power calculation after corneal refractive surgery," *Journal of Refractive Surgery*, vol. 22, no. 8, pp. 735–736, 2006.

[36] N. Rosa, M. Lanza, and L. Capasso, "IOL power calculations for eyes with previous myopic LASIK," *Journal of Refractive Surgery*, vol. 22, no. 4, p. 847, 2006.

[37] N. Rosa, L. Capasso, and M. Lanza, "IOL calculations after refractive surgery," *Journal of Cataract and Refractive Surgery*, vol. 32, no. 12, p. 1984, 2006.

[38] N. Rosa, L. Capasso, M. Lanza, and M. Borrelli, "Clinical results of a corneal radius correcting factor in calculating intraocular lens power after corneal refractive surgery," *Journal of Refractive Surgery*, vol. 25, no. 7, pp. 599–603, 2009.

[39] N. Rosa, M. de Bernardo, M. Borrelli, M. L. Filosa, E. Minutillo, and M. Lanza, "Reliability of the IOLMaster in measuring corneal power changes after hyperopic photorefractive keratectomy," *Journal of Refractive Surgery*, vol. 27, no. 4, pp. 293–298, 2011.

[40] N. Rosa, M. Borrelli, M. de Bernardo, and M. Lanza, "Corneal morphological changes after myopic excimer laser refractive surgery," *Cornea*, vol. 30, no. 2, pp. 130–135, 2011.

[41] N. Rosa, M. de Bernardo, M. R. Romano et al., "Analysis of photoastigmatic keratectomy with the cross-cylinder ablation," *Indian Journal of Ophthalmology*, vol. 60, no. 4, pp. 283–287, 2012.

[42] N. Rosa, L. Capasso, M. Lanza, D. Furgiuele, and A. Romano, "Reliability of the IOLMaster in measuring corneal power changes after photorefractive keratectomy," *Journal of Cataract and Refractive Surgery*, vol. 30, no. 2, pp. 409–413, 2004.

[43] R. C. Eiferman, "Corneal wound healing and the future of refractive surgery," *Refractive and Corneal Surgery*, vol. 5, no. 2, pp. 73–74, 1989.

[44] J. T. Holladay, "Consultations in refractive surgery," *Refractive Corneal surgery*, vol. 5, p. 203, 1989.

[45] K. J. Hoffer, "Intraocular lens power calculation for eyes after refractive keratotomy," *Journal of Refractive Surgery*, vol. 11, no. 6, pp. 490–493, 1995.

[46] M. Camellin and A. Calossi, "A new formula for intraocular lens power calculation after refractive corneal surgery," *Journal of Refractive Surgery*, vol. 22, no. 2, pp. 187–199, 2006.

[47] S. Chen and F. R. Hu, "Correlation between refractive and measured corneal power changes after myopic excimer laser photorefractive surgery," *Journal of Cataract and Refractive Surgery*, vol. 28, no. 4, pp. 603–610, 2002.

[48] J. W. Diehl, F. Yu, M. D. Olson, J. N. Moral, and K. M. Miller, "Intraocular lens power adjustment nomogram after laser in situ keratomileusis," *Journal of Cataract and Refractive Surgery*, vol. 35, no. 9, pp. 1587–1590, 2009.

[49] M. De Bernardo and N. Rosa, "Diehl-Miller nomogram for intraocular lens power calculation," *Journal of Cataract & Refractive Surgery*, vol. 39, no. 11, p. 1791, 2013.

[50] V. Feiz, M. J. Mannis, F. Garcia-Ferrer et al., "Intraocular lens power calculation after laser in situ keratomileusis for myopia and hyperopia: a standardized approach," *Cornea*, vol. 20, no. 8, pp. 792–797, 2001.

[51] V. Feiz, M. Moshirfar, M. J. Mannis et al., "Nomogram-based intraocular lens power adjustment after myopic photorefractive keratectomy and LASIK: a new approach," *Ophthalmology*, vol. 112, no. 8, pp. 1381–1387, 2005.

[52] A. M. Hamed, L. Wang, M. Misra, and D. D. Koch, "A comparative analysis of five methods of determining corneal refractive power in eyes that have undergone myopic laser in situ keratomileusis," *Ophthalmology*, vol. 109, no. 4, pp. 651–658, 2002.

[53] E. F. Jarade, F. C. Abi Nader, and K. F. Tabbara, "Intraocular lens power calculation following LASIK: determination of the new effective index of refraction," *Journal of Refractive Surgery*, vol. 22, no. 1, pp. 75–80, 2006.

[54] S. Masket and S. E. Masket, "Simple regression formula for intraocular lens power adjustment in eyes requiring cataract surgery after excimer laser photoablation," *Journal of Cataract and Refractive Surgery*, vol. 32, no. 3, pp. 430–434, 2006.

[55] A. A. Stakheev and L. J. Balashevich, "Corneal power determination after previous corneal refractive surgery for intraocular lens calculation," *Cornea*, vol. 22, no. 3, pp. 214–220, 2003.

[56] J. Aramberri, "Intraocular lens power calculation after corneal refractive surgery: double-K method," *Journal of Cataract and Refractive Surgery*, vol. 29, no. 11, pp. 2063–2068, 2003.

[57] N. Rosa, L. Capasso, and M. Lanza, "Double-K method to calculate IOL power after refractive surgery," *Journal of Cataract and Refractive Surgery*, vol. 31, no. 2, pp. 254–256, 2005.

[58] E. F. Jarade and K. F. Tabbara, "New formula for calculating intraocular lens power after laser in situ keratomileusis," *Journal of Cataract & Refractive Surgery*, vol. 30, no. 8, pp. 1711–1715, 2004.

[59] B. Seitz, A. Langenbucher, N. X. Nguyen, M. M. Kus, and M. Küchle, "Underestimation of intraocular lens power for cataract surgery after myopic photorefractive keratectomy," *Ophthalmology*, vol. 106, no. 4, pp. 693–702, 1999.

[60] K. A. Walter, M. R. Gagnon, P. C. Hoopes Jr., and P. J. Dickinson, "Accurate intraocular lens power calculation after myopic laser in situ keratomileusis, bypassing corneal power," *Journal of Cataract and Refractive Surgery*, vol. 32, no. 3, pp. 425–429, 2006.

[61] R. A. Latkany, A. R. Chokshi, M. G. Speaker, J. Abramson, B. D. Soloway, and G. Yu, "Intraocular lens calculations after refractive surgery," *Journal of Cataract and Refractive Surgery*, vol. 31, no. 3, pp. 562–570, 2005.

[62] E. Borasio, J. Stevens, and G. T. Smith, "Estimation of true corneal power after keratorefractive surgery in eyes requiring cataract surgery: BESSt formula," *Journal of Cataract & Refractive Surgery*, vol. 32, no. 12, pp. 2004–2014, 2006.

[63] G. Ferrara, G. Cennamo, G. Marotta, and E. Loffredo, "New formula to calculate corneal power after refractive surgery," *Journal of Refractive Surgery*, vol. 20, no. 5, pp. 465–471, 2004.

[64] W. Haigis, "Intraocular lens calculation after refractive surgery for myopia: haigis-L formula," *Journal of Cataract and Refractive Surgery*, vol. 34, no. 10, pp. 1658–1663, 2008.

[65] T. Ianchulev, J. Salz, K. Hoffer, T. Albini, H. Hsu, and L. LaBree, "Intraoperative optical refractive biometry for intraocular lens power estimation without axial length and keratometry measurements," *Journal of Cataract and Refractive Surgery*, vol. 31, no. 8, pp. 1530–1536, 2005.

[66] J.-H. Kim, D.-H. Lee, and C.-K. Joo, "Measuring corneal power for intraocular lens power calculation after refractive surgery: comparison of methods," *Journal of Cataract & Refractive Surgery*, vol. 28, no. 11, pp. 1932–1938, 2002.

[67] R. J. Mackool and W. Ko, "Intraocular lens power calculation after laser in situ keratomileusis: aphakic refraction technique," *Journal of Cataract and Refractive Surgery*, vol. 32, no. 3, pp. 435–437, 2006.

[68] N. Rosa, L. Capasso, and A. Romano, "A new method of calculating intraocular lens power after photorefractive keratectomy," *Journal of Refractive Surgery*, vol. 18, no. 6, pp. 720–724, 2002.

[69] N. Rosa, L. Capasso, M. Lanza, G. Iaccarino, and A. Romano, "Reliability of a new correcting factor in calculating intraocular lens power after refractive corneal surgery," *Journal of Cataract and Refractive Surgery*, vol. 31, no. 5, pp. 1020–1024, 2005.

[70] N. Rosa, M. de Bernardo, M. Borrelli, and M. Lanza, "New factor to improve reliability of the clinical history method for intraocular lens power calculation after refractive surgery," *Journal of Cataract and Refractive Surgery*, vol. 36, no. 12, pp. 2123–2128, 2010.

[71] M. Saiki, K. Negishi, N. Kato et al., "Modified double-K method for intraocular lens power calculation after excimer laser corneal refractive surgery," *Journal of Cataract and Refractive Surgery*, vol. 39, no. 4, pp. 556–562, 2013.

[72] G. Savini, P. Barboni, and M. Zanini, "Correlation between attempted correction and keratometric refractive index of the cornea after myopic excimer laser surgery," *Journal of Refractive Surgery*, vol. 23, no. 5, pp. 461–466, 2007.

[73] H. J. Shammas, M. C. Shammas, A. Garabet, J. H. Kim, A. Shammas, and L. Labree, "Correcting the corneal power measurements for intraocular lens power calculations after myopic laser in situ keratomileusis," *American Journal of Ophthalmology*, vol. 136, no. 3, pp. 426–432, 2003.

[74] H. J. Shammas and M. C. Shammas, "No-history method of intraocular lens power calculation for cataract surgery after myopic laser in situ keratomileusis," *Journal of Cataract and Refractive Surgery*, vol. 33, no. 1, pp. 31–36, 2007.

[75] J. W. Soper and J. Goffman, "Contact lens fitting by retinoscopy," in *Contact Lenses*, J. W. Soper, Ed., pp. 99–108, Stratton Intercontinental Medical Book, Miami, Fla, USA, 1974.

Hindawi Publishing Corporation
BioMed Research International
Volume 2014, Article ID 610623, 11 pages
http://dx.doi.org/10.1155/2014/610623

Review Article

Anterior Segment Optical Coherence Tomography Imaging of Conjunctival Filtering Blebs after Glaucoma Surgery

Rodolfo Mastropasqua,[1] Vincenzo Fasanella,[2] Luca Agnifili,[2] Claudia Curcio,[3] Marco Ciancaglini,[4] and Leonardo Mastropasqua[2]

[1] *Ophthalmology Unit, Department of Neurological, Neuropsychological, Morphological and Movement Sciences, University of Verona, 53593 Verona, Italy*
[2] *Ophthalmic Clinic, Department of Medicine and Aging Science, Ophthalmic Clinic, University G. d'Annunzio of Chieti-Pescara, Via dei Frentani 114, 66100 Chieti, Italy*
[3] *Excellence Eye Research Center, CeSI, G. d'Annunzio University of Chieti-Pescara, 66100 Chieti, Italy*
[4] *Ophthalmic Clinic, Department of Surgical Science, University of L'Aquila, 67100 L'Aquila, Italy*

Correspondence should be addressed to Luca Agnifili; l.agnifili@unich.it

Received 23 May 2014; Accepted 25 June 2014; Published 20 July 2014

Academic Editor: Ciro Costagliola

Time domain (TD) and spectral domain (SD) optical coherence tomography (OCT) are cross-sectional, noncontact, high-resolution diagnostic modalities for posterior and anterior segment (AS) imaging. The AS-OCT provides tomographic imaging of the cornea, iris, lens, and anterior chamber (AC) angle in several ophthalmic diseases. In glaucoma, AS-OCT is utilized to evaluate the morphology of AS structures involved in the pathogenesis of the disease, to obtain morphometric measures of the AC, to evaluate the suitability for laser or surgical approaches, and to assess modifications after treatment. In patients undergoing surgery, AS-OCT is crucial in the evaluation of the filtering bleb functionality, permitting a combined qualitative and quantitative analysis. In this field, AS-OCT may help clinicians in distinguishing between functioning and nonfunctioning blebs by classifying their macroscopic morphology, describing bleb-wall features, bleb cavity, and scleral opening. This information is critical in recognizing signs of filtration failure earlier than the clinical approach and in planning the appropriate timing for management procedures in failing blebs. In this review, we summarize the applications of AS-OCT in the conjunctival bleb assessment.

1. Introduction

The only treatment of proven efficacy in glaucoma is still the reduction of intraocular pressure (IOP) [1]. However, several patients do not achieve the required target IOP despite maximum tolerated medical therapy or may become intolerant to medication because of adverse events thus reducing compliance [2]. In these cases, a surgical approach is warranted in order to control IOP and reduce the rate of damage progression [3]. Surgical filtration procedures for glaucoma may be classified as either penetrating or nonpenetrating, depending on the removal or preservation of the trabeculo-Descemet membrane, respectively. Trabeculectomy represents the most common and effective penetrating surgical procedure for glaucoma and is still the gold standard surgery. Deep sclerectomy and viscocanalostomy were proposed as nonpenetrating filtration procedures, with the aim of reducing the occurrence of postoperative complications [4]. All filtration procedures lead to an elevation of the conjunctiva at the site of surgery, which is commonly referred to as a filtering bleb. A filtering bleb is considered a cornerstone of IOP control after glaucoma filtration surgery [5–8] and, to a lesser degree, after drainage device implantation. This critical structure allows aqueous humor (AH) to drain from the anterior chamber (AC) into the subconjunctiva, lowering the IOP. However, in a significant number of cases AH filtration fails [9] subsequent to conjunctival fibrosis within the bleb wall.

New imaging diagnostic methods such as anterior segment-optical coherence tomography (AS-OCT) [10] and

in vivo laser scanning confocal microscopy (LSCM) [11–15] can be used in conjunction with clinical evaluation to assess morphology and function of blebs and to distinguish functioning from nonfunctioning blebs. These techniques can identify precocious signs of conjunctival fibrosis prior to identification with clinical assessment.

The aim of this review was to summarize the application of the AS-OCT on morphofunctional assessment of conjunctival filtering blebs after glaucoma surgery.

2. Methods of Literature Search

PubMed searches were performed on April 22, 2014, using the phrases "anterior segment-optical coherence tomography or AS-OCT and blebs," "anterior segment-optical coherence tomography or AS-OCT and glaucoma filtration surgery," and "filtering blebs and anterior segment-optical coherence tomography or AS-OCT" for publications from 1980 to April 2014. Articles in English were fully reviewed; articles in other languages were reviewed using their English abstracts when available.

3. Platforms and Technical Characteristics of the AS-OCT

AS-OCT is a noncontact method that provides cross-sectional, three-dimensional, high-resolution images of the anterior segment of the eye, with an axial resolution ranging from 3 to 20 μm. It provides qualitative and quantitative assessment of the most important structures involved in the pathogenesis of glaucoma, such as those defining the iridocorneal angle. Moreover, AS-OCT is used to evaluate anatomical variations of these structures after glaucoma surgery to determine the position of tubes within the AC and to assess bleb features and functionality.

Two OCT platforms are currently available: time domain (TD-OCT) and spectral domain (SD-OCT). The most diffuse and studied anterior segment TD-OCT for glaucoma is the Visante OCT (Carl Zeiss Meditec, Inc., Dublin, CA). Visante has a scanning speed of 4,000 axial scans per image and image acquisition rate of 8 frames/sec with an axial resolution of 18 μm and a lateral resolution of 60 μm.

SD-OCT systems include the RTVue (Optovue, Inc., CA), the Cirrus (Carl Zeiss Meditec), the Spectralis (Heidelberg Engineering, Inc.), and the Casia SS-1000 OCT (Tomey, Nagoya, Japan) [17]. SD-OCT platforms have several advantages over TD-OCT. First, this imaging modality yields high-resolution images that are almost similar to those obtainable with histological preparations. Second, in SD-OCT the scanning speed is much higher than in TD-OCT (ranging from 26.000 to 40.000 A-scans per second); thus, measurement time and overall exam duration are reduced, with better patient comfort. Third, SD-OCT platforms assess both the posterior and anterior pole of the eye (with the cornea/anterior segment modules). Finally, dedicated software permits a three-dimensional assessment of AC structures and conjunctival bleb.

On the other hand, the optical cross-sections obtained with SD-OCT have less tissue penetration than TD-OCT. Therefore, while SD-OCT is able to show features of the bleb wall such as the optically empty cystic spaces and scarring processes, this imaging technique is less adapt in imaging deep structures such as the scleral flap, intrascleral lake, and internal ostium [18] (Figure 1).

4. AS-OCT of Filtering Blebs after Penetrating Filtration Surgery

4.1. Trabeculectomy. The macroscopic appearance and the microscopic features of conjunctival blebs have predictive implications for surgical outcomes of trabeculectomy. The clinical evaluation of the filtering ability of a bleb incorporates well-established parameters such as the extent, elevation, and vascularity of the conjunctiva at the site of surgery. Unfortunately, in some cases, there is no correlation between the bleb appearance and the IOP. This can lead to difficulty in assessing the filtering ability with slit-lamp evaluation and in recognizing the signs of failure in time.

Different bleb classification systems were proposed [19–21]. According to these systems, a functioning bleb presents a diffuse or cystic shape, with a mild elevation over the scleral flap, few conjunctival vessels, and evidence of microcysts within the conjunctival epithelium. On the other hand, failed blebs are characterized by a small superficial extension without elevation at the site of surgery (flat shape) or with a high degree of elevation with excessive and irregular vascularization (encapsulated shape). However, these systems present some limitations such as assignment of a single vascularity grading and coarse grading scales and are unable to describe blebs with mixed morphology. Currently, the most used grading systems, which for the most part overcome these limitations, are the Moorfields bleb grading system (MBGS) and the Indiana bleb appearance grading scale (IBAGS) [22]. The MBGS defines the bleb functionality by considering the area, height, and vascularity, whereas the IBAGS considers also the AH leakage with Seidel test.

Wells et al. [23] reported that both systems performed adequately in defining the bleb morphology, were clinically reproducible, and had generally high levels of interobserver agreement. MBGS performed similarly to the IBAGS for reproducibility, had higher intraclass correlation coefficient values for morphologic characteristics, and captured extra vascularity data. However, both systems presented minor deficiencies with possible loss of information.

In cases in which slit-lamp examination cannot provide clear and complete information, advanced imaging technologies may help clinicians in defining the exact morphological bleb type and in differentiating between functioning from failing or failed blebs.

LSCM was used to study the conjunctiva before and after different surgical and medical therapies for glaucoma to analyze AH outflow pathways modifications [16, 24–26]. In filtration surgery, LSCM proved valuable in assessing the drainage capability of conjunctival blebs by assessing microcysts density and area within the epithelium, and the collagen

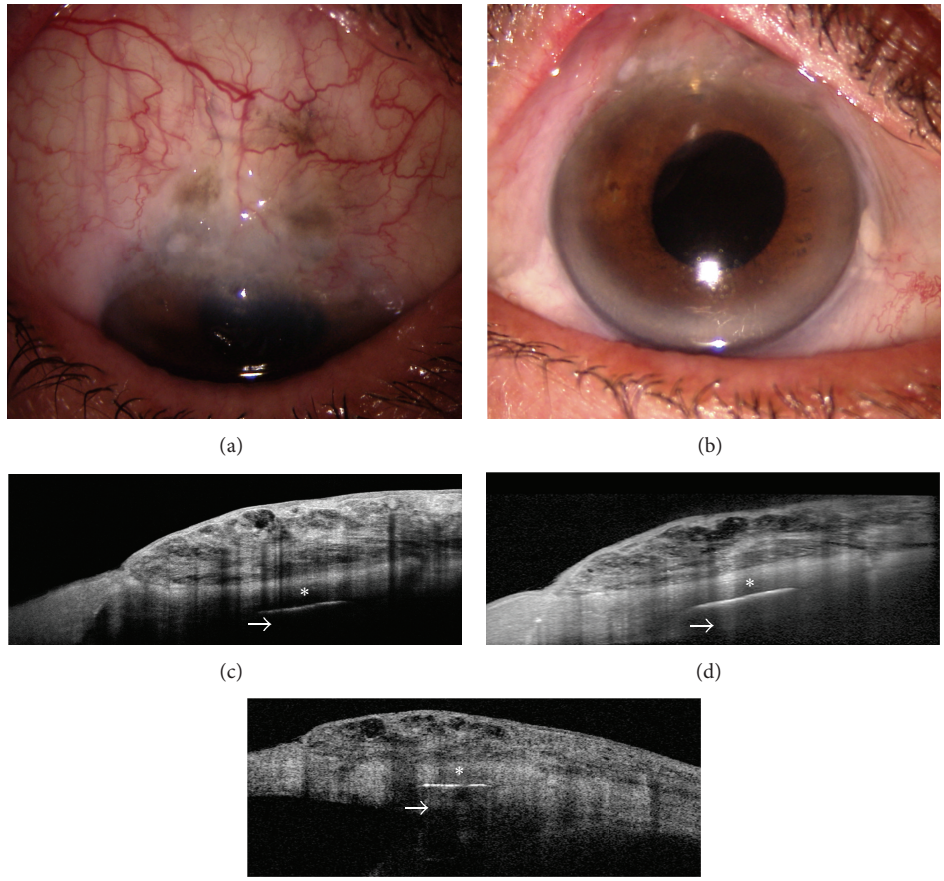

Figure 1: Spectral domain- (SD-) and time domain- (TD-) OCT assessment of a cystic filtering bleb. Slit-lamp biomicroscopy of a functioning cystic bleb after Ex-PRESS implant (a and b). Bleb images (taken at the same point) as obtained with SD-OCT (Optovue and Spectralis, resp.) (c and d) and TD-OCT (Visante OCT) (e). SD-OCT presents a higher resolution with a more detailed visualization of bleb-wall layers, inner cystic spaces, and the limit between scleral bed and bleb, with respect to TD-OCT. On the other hand, SD platforms seem to have less tissue penetration than TD- OCT (arrows).

deposition within the stroma [12–15]. While LSCM permits a microscopic analysis, with the advantage of analyzing tissue at a cellular level, AS-OCT allows a macroscopic analysis, useful to classify blebs according to their morphology.

Several studies have analyzed if TD-OCT (Visante OCT) can be used to distinguish between functioning and nonfunctioning filtering blebs [27, 28]. Leung et al. [27] differentiated blebs according to their global appearance: diffuse or cystic blebs were classified as functioning, whereas encapsulated or flattened blebs were classified as nonfunctioning. Additionally, while functioning blebs presented a low to medium reflectivity of the external wall with a wide inner fluid-filled cavity, failed blebs presented with opposite features (Figures 2 and 3). Pfenninger et al. [29] reported a significant direct correlation between the reflectivity of the fluid-filled cavity and the IOP, whereas Tominaga et al. [30] found a significant inverse correlation between the bleb-wall thickness and IOP. On the contrary, the same authors did not find significant correlation between the height and extent of the filtering bleb cavity and the IOP.

Generally, AS-OCT features are in agreement with microscopic findings as seen with LSCM: in functioning trabeculectomy, the bleb wall appears low reflective and thick at AS-OCT, with numerous intraepithelial microcysts and a loosely arranged stroma at LSCM. Conversely, failed blebs show the opposite features (Figures 2 and 3) [12]. Ciancaglini et al., [12] in a study that proposed a combined clinical and instrumental approach to evaluate the filtering bleb functionality, found a good degree of concordance between the clinical and AS-OCT bleb classification, particularly for the cystic (100%) and diffuse (74%) patterns. Thus, AS-OCT may support clinicians in correctly classifying blebs. In the same study, the use of MMC produced a significantly higher mean longitudinal radial length, indicative of a diffuse functioning bleb, compared to eyes that had not received antimetabolites.

The introduction of SD-OCT yielded obtaining additional or more defined information of the bleb morphology. Kawana et al. [31] studied the internal structures of blebs after trabeculectomy using a 3-dimensional cornea

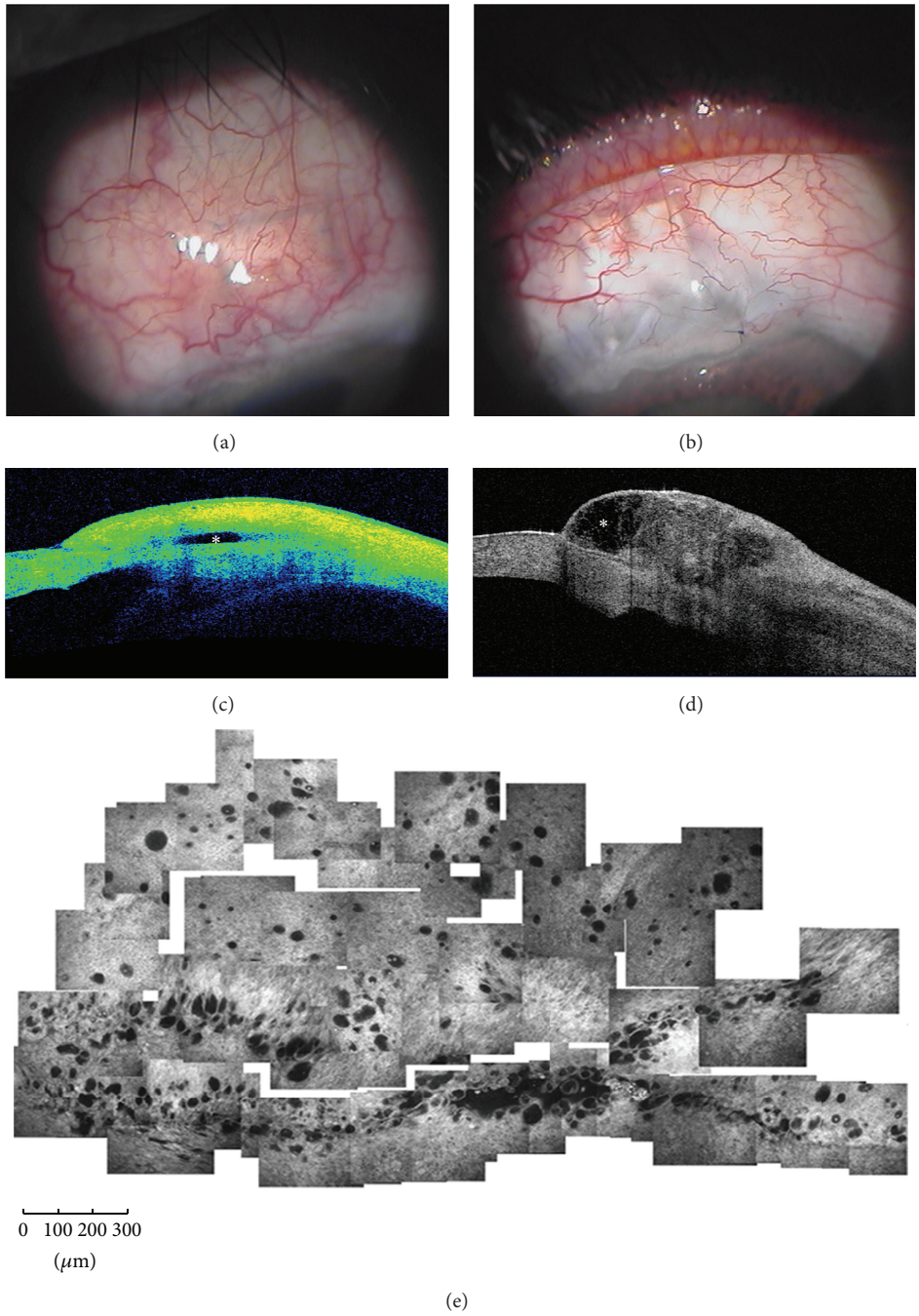

Figure 2: Functioning filtering blebs. Functioning blebs, after MMC-augmented trabeculectomy, present a diffuse (a) or a cystic shape (b) at clinical evaluation. At AS-OCT (Visante OCT) these blebs show a patent and low reflective inner cavity (asterisks) (c and d), multilobed in the cystic shape, and a thick and low reflective bleb wall. In vivo laser scanning confocal microscopy (e) shows numerous intraepithelial microcysts in a glaucomatous patient after successful MMC-augmented trabeculectomy (planar reconstruction of the superior bulbar conjunctiva 6 weeks after surgery). (e: from Ciancaglini et al., [15] with permission from the publisher).

AS-OCT (3-D CAS OCT) reporting that AH intrableb drainage routes, bleb-wall microcysts, and the scleral flap could be visualized in more than 90% of the cases. Successful blebs presented a large internal fluid-filled cavity, a wide hyporeflective area, and thicker walls with a higher number of microcysts. The 3D AS-OCT proved valuable also in identifying the exact filtration openings after trabeculectomy, where AH flows through the sclera into the bleb cavity [32]. Particularly, filtration openings were identified in the 95% of cases and were mostly located in the middle third of the scleral flap margins; moreover, 24% of blebs presented two or more scleral openings.

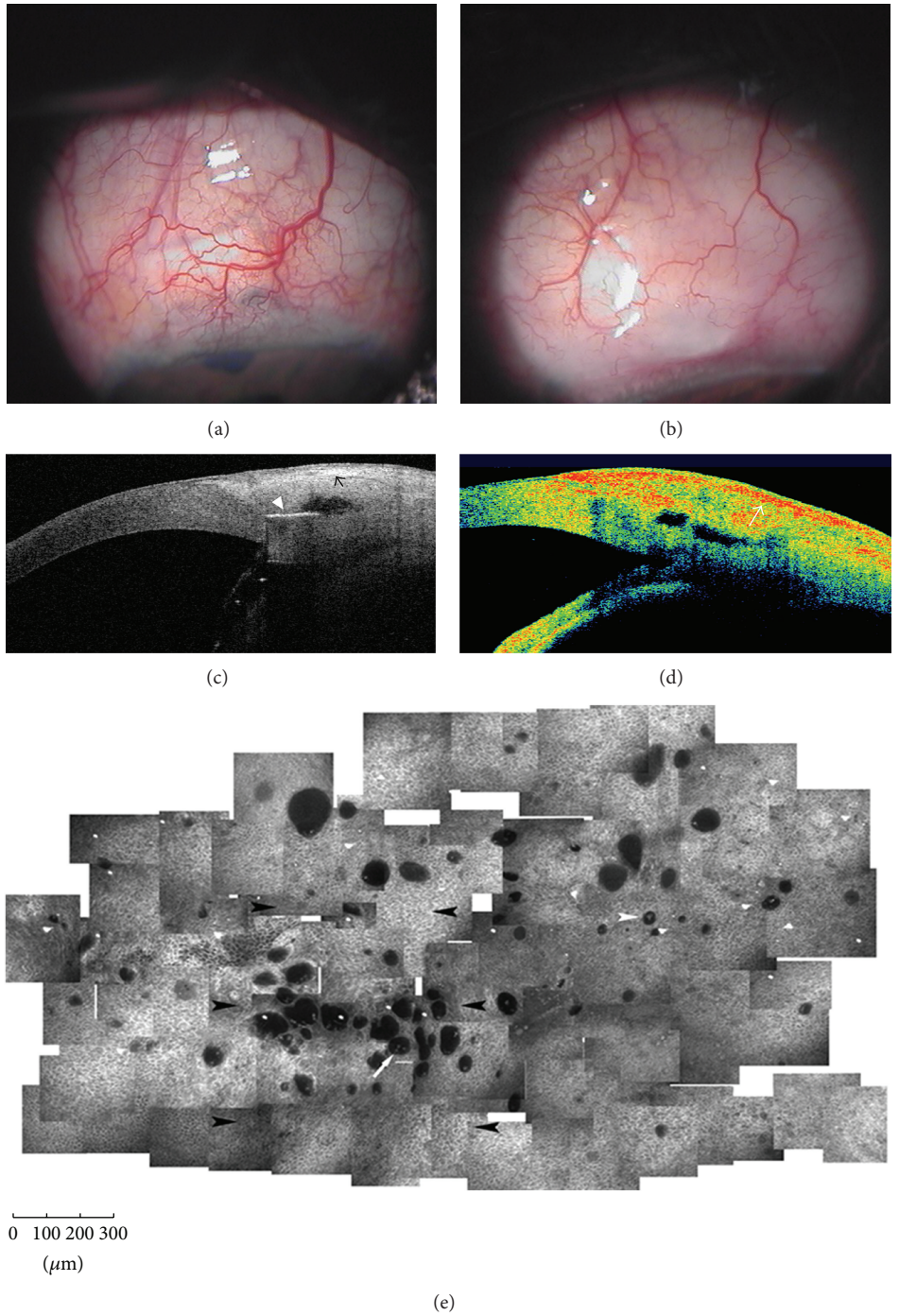

Figure 3: Failed filtering blebs. Nonfunctioning blebs, after MMC-augmented trabeculectomy, appear flat (a) or encapsulated (b) at clinical evaluation. At AS-OCT (Visante OCT) (c and d) these blebs present a patent and low reflective inner cavity but with a thick and hyperreflective bleb wall (arrows). In vivo laser scanning confocal microscopy (e) shows scattered and markedly less numerous intraepithelial microcysts in a glaucomatous patient who underwent failed MMC-augmented trabeculectomy (planar reconstruction of the superior bulbar conjunctiva 6 weeks after surgery). Arrowhead indicates the Ex-PRESS implantation. (e: from Mastropasqua et al., [16] with permission from the publisher).

4.2. Ex-PRESS Implant. AS-OCT also provides high-resolution imaging in eyes implanted with glaucoma drainage devices, helping clinicians in identifying the position and patency of tubes in AC, AH outflow pathways, and the occurrence of complications such as corneal- or iris-tube contact. The Ex-PRESS glaucoma filtration device (Alcon Laboratories, Fort Worth, Texas, USA) is a small stainless steel, nonvalved, MRI-compatible implant (available with a 50 or 200 μm lumen). It lowers IOP by shunting AH from the AC into the subconjunctiva, creating a bleb similar to

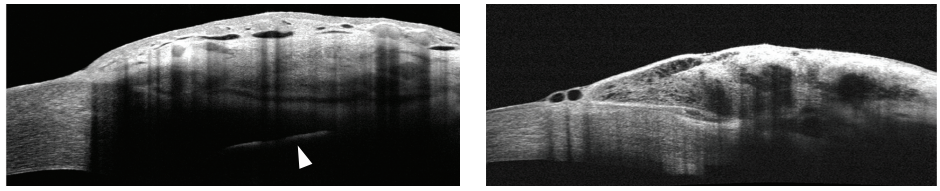

(a) (b)

Figure 4: Filtering bleb features after trabeculectomy and Ex-PRESS implantation. Conjunctival filtering bleb after successful MMC/Ex-PRESS (P200) implantation (arrowhead) (a) shows a uniform and regular diffuse pattern, with AH drainage well extended posteriorly to the scleral flap. Differently, bleb after MMC/trabeculectomy (b) presents a cystic pattern with a less regular shape (RTVue, Optovue, Inc, CA).

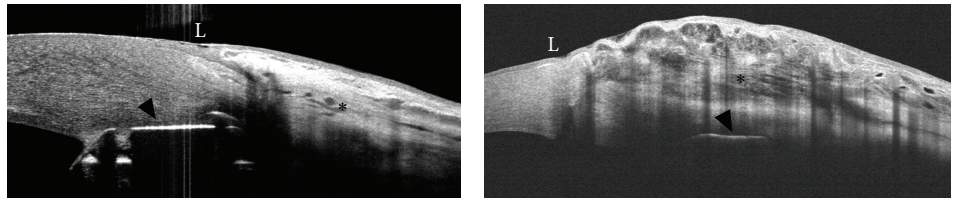

(a) (b)

Figure 5: Filtering bleb features after Ex-PRESS implantation according to the position of the device. Bleb morphology may be significantly affected by the position of the device within the scleral bed. In anteriorly positioned Ex-PRESS implant (a) (0-1 mm from the limbal margin (L); arrowhead), the bleb presents features of a failed filtration, with a flat shape (asterisk), limited subconjunctival area (scattered cysts), and a hyperreflective bleb wall. Conversely, in posteriorly positioned Ex-PRESS implant (b) (1 to 2-3 mm from the limbal margin (L); arrowhead), the bleb presents features of an effective filtration, with a cystic multilobed shape (asterisk), a wide subconjunctival filtration area, and a low reflective bleb wall (RTVue, Optovue, Inc, CA).

that produced by trabeculectomy. The procedure, in fact, is an alternative to trabeculectomy. Very recently, the XTV study [33] reported that mean IOP, medication use, and surgical success were similar at 2 years after EX-PRESS implantation or trabeculectomy, with fewer complications in eyes that received the Ex-PRESS device. Verbraak et al. [34] used an experimental AS-OCT to evaluate porcine eye after Ex-PRESS implantation ex vivo, clearly visualizing the entire outline and position of the implant. However, to date, studies that evaluated filtering blebs characteristics in human eyes implanted with Ex-PRESS, and studies that analyzed differences in bleb morphology after trabeculectomy or Ex-PRESS implantation, are still lacking.

It can be hypothesized that blebs after Ex-PRESS implantation present some morphological differences with respect to blebs after trabeculectomy since the AH flows through artificial scleral channels with different lumen sizes and morphology. In the case of Ex-PRESS implant, a regular tube creates the scleral channel; in trabeculectomy, a transscleral channel extending from the position formerly occupied by trabecular meshwork to the subconjunctiva is formed. The channel formed following trabeculectomy is irregular, since it is a network of extended fibroblasts with loosely arranged collagenous tissue and a large number of vessels [35]. Thus, the difference in hydrodynamic effects that AH undergoes in order to reach the subconjunctival space may lead to a different modulation and a final different shape of the bleb.

In large case series of patients implanted with Ex-PRESS (P200 model)/MMC or who underwent trabeculectomy/MMC (unpublished data), we observed with SD-OCT (RTVue, Optovue, Inc., CA) that blebs after Ex-PRESS implants presented a diffuse shape, with a uniform and posteriorly directed AH filtration, probably expression of a regulated AH passage toward the subconjunctiva (Figure 4(a)). Conversely, filtering blebs derived from trabeculectomy were more commonly cystic with a less extended (even though higher) subconjunctival area, probably expression of a more turbulent AH passage toward the subconjunctiva (Figure 4(b)). On this basis, further structured studies assessing bleb morphology with AS-OCT in patients undergoing trabeculectomy or Ex-PRESS device are warranted.

Also the position of the device, in relation to the limbal margin, may have a significant effect on bleb morphology and final surgical success. In the same case, series blebs showed a smaller subconjunctival area, a hyperreflective wall with a flat shape (Figure 5(a)) when the device was placed anteriorly (arrowhead, 0 to 1 mm from the limbus). Oppositely, a higher subconjunctival filtration area, a lower reflective wall, and a more diffuse or cystic shape were evident when Ex-PRESS was implanted more posteriorly in the scleral bed (1 to 2 mm from the limbus) (Figure 5(b)) (RTVue, Optovue, Inc., CA). When comparing the overall surgical success (six-month follow-up, one third reduction of IOP from baseline), the Ex-PRESS devices implanted posteriorly presented a significantly

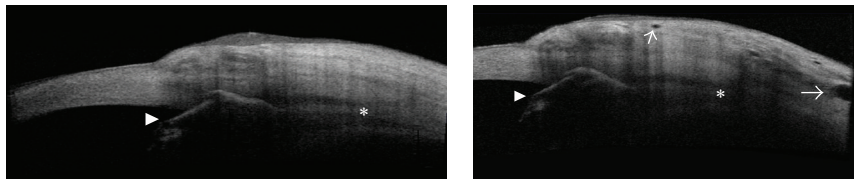

(a) (b)

Figure 6: Effects of the digital ocular massage on filtering bleb morphology. Sixty seconds after bulbar digital massage of an eye implanted with Ex-PRESS (arrowhead), the fluid-filled cavity area extended posteriorly (asterisks), bleb-wall thickness increased, and several intraepithelial cysts appeared (arrows) compared to baseline (b and a, resp.) (RTVue, Optovue, Inc, CA).

higher success rate compared to devices implanted anteriorly (75% versus 38%; $P < 0.001$). By hypothesizing, this could be due to the fact that a device implanted too anteriorly do not allow a useful posterior AH outflow, which is critical to promote the formation of a diffuse and functioning filtering bleb.

5. AS-OCT of Conjunctival Bleb in Nonpenetrating Filtration Surgery

Nonpenetrating filtration surgery was proposed as an alternative to trabeculectomy with the aim of reducing intra- and postoperative complications [36]. Nonpenetrating deep sclerectomy and viscocanalostomy, which have now abandoned the clinical scenario, were the two proposed nonpenetrating procedures. Aptel et al. [37] used the AS-OCT to study filtering blebs after deep sclerectomy with collagen implant, reporting that lower IOP values correlated with a thinner and lower reflective bleb wall and with larger subconjunctival fluid spaces.

6. AS-OCT of Filtering Blebs after Glaucoma Drainage Device Implantation

In a recent study, [38] Jung et al. reported that Visante OCT proved valuable in the morphological assessment of blebs in patients who underwent Ahmed glaucoma valve (AGV) implantation. The authors observed a significantly lower maximum bleb-wall thickness in successful compared to unsuccessful AGV implants. This aspect, which was the opposite to that found in filtering blebs of successful trabeculectomy, could be determined by the presence of silicone drainage device, which impedes direct absorption of AH by the conjunctiva. Moreover, AS-OCT did not identify microcysts and collections of multiloculated fluid cavities within the bleb wall above the plate of the valves, which, conversely, are common in trabeculectomy [27, 31]. No significant differences were found between successful and failed AGV concerning the bleb-wall reflectivity, which presented a high signal in all cases. Therefore, the bleb morphology above the drainage valve plate was quite similar to that of encapsulated blebs after unsuccessful filtration surgery with a fluid-filled space surrounded by a connective tissue with a high reflectivity [27]. Therefore, conjunctiva blebs after glaucoma valve are morphologically different from blebs formed after filtration surgery, suggesting that AH reabsorption is only in part linked to the bleb drainage ability.

7. AS-OCT in the Bleb Management Procedures

The early postoperative period represents the most critical period for the bleb survival and the long-term surgical success. Frequently, several procedures are required to reduce the scarring processes and maintain an effective AH filtration through the scleral flap margins and the layers of conjunctival bleb wall. Various procedures may be adopted to preserve the bleb functionality. The AS-OCT could be a useful tool to support the decision-making process for the timing and choice of the most appropriate procedure to adopt in failing blebs.

Finger Massage. Finger massage is a common technique employed after filtering surgery to aid the AH flow through the artificially created pathway. This procedure promotes the patency of the scleral channel, with the subsequent expansion of the subconjunctival space. Bulbar massage can be done with fingers or with an ocular massage device. In a pilot study, Gouws et al. [39] compared these two techniques but did not find a statistically significant difference in terms of IOP between methods. On the other hand, the use of the device presented a greater ease of use and lower pain scores.

No previous studies were conducted on the application of AS-OCT for studying bleb modifications before and after bulbar massage. In a prospective case series study (unpublished data) conducted with SD-OCT (RTVue, Optovue, Inc., CA), we evaluated the modification of the fluid-filled cavity area, bleb-wall thickness, and scleral opening before and after bulbar digital massage (60 seconds of duration). We observed a significant decrease of IOP with an increase of the bleb-wall thickness, intraepithelial microcysts, and the fluid-filled cavity area more extended posteriorly (Figure 6). Of note, all these variables returned to baseline values after 120 minutes.

Subconjunctival Injections of Antimetabolites. To date, studies on the application of AS-OCT after subconjunctival antimetabolites injections are not available. Our group recently conducted a prospective randomized, double blind, six-month study (unpublished data, currently under peer review) to compare the long-term effect of peribleb injection of 5-fluorouracil (5-FU; three weekly injections for three

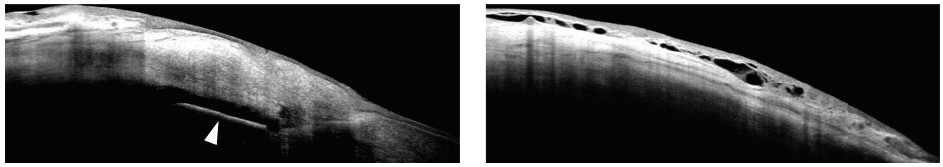

(a) (b)

Figure 7: Effects of 5-FU injections on filtering bleb morphology. Blebs injected with subconjunctival 5-FU (extrableb injection) showed a less reflective and thicker bleb wall, with multiple intra- and subepithelial fluid filled cavities (b), compared to eyes treated with PBS, which presented opposite signs without evidence of filtration (a). Arrowhead represents Ex-PRESS device (RTVue, Optovue, Inc, CA).

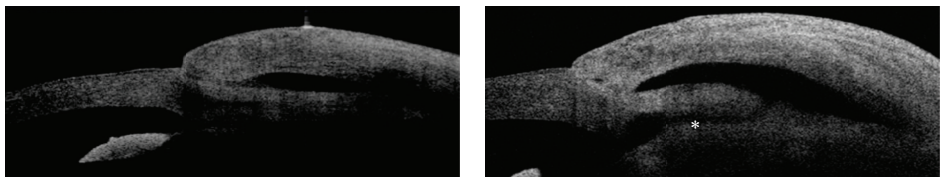

(a) (b)

Figure 8: Filtering bleb morphology modifications after laser suture lysis (LSL). Nonfunctioning encapsulated filtering bleb (a) showing a subconjunctival fluid filled cavity isolated from the anterior chamber because of the tight contact of the flap with the surrounding sclera. After LSL the scleral flap appears separated from the surrounding sclera, with restoration of the access (asterisk) with the anterior chamber (b) (Visante OCT).

weeks) versus phosphate buffered solution (PBS; three weekly injections for three weeks) in patients with failing blebs (progressive IOP increase in the last two weeks, flattening or encapsulation of the conjunctiva at slit lamp, decrease of the density of intraepithelial microcysts and stromal scarring at LSCM, bleb-wall hyper-reflectivity at AS-OCT). In blebs injected with 5-FU the SD-OCT (RTVue, Optovue, Inc., CA) showed a less reflective and thicker bleb wall, with multiple intra- and subepithelial fluid filled cavities, compared to eyes treated with PBS (Figure 7).

Bleb Needling. The bleb-wall fibrosis is the more common long-term complication and the first cause of failure of filtration surgery. In addition, the intra- and episcleral fibrosis is also involved in the final blockage of the AH outflow. The needling procedure is aimed at mechanically removing the connective capsule under the bleb wall and the fibrotic adhesion in the bleb cavity in failing encapsulated blebs, by using a needle. During procedure, a needle is moved in a side-to-side motion, breaking episcleral adhesions over the scleral flap and within the bleb cavity. To improve the efficacy of the bleb needling, revisions with 5-FU were proposed by Ewing and Stamper [40]. Guthoff et al. [41] analyzed the bleb modifications with AS-OCT before and after needling, reporting a collapse of the intrableb cysts in five patients out of nine; notably, only those patients in whom cysts collapsed presented a controlled IOP without glaucoma medication after six months.

Laser Suture Lysis (LSL). In a prospective observational case series study Singh et al. [42] reported that AS-OCT significantly affected the decision-making process concerning LSL after trabeculectomy. In this study, LSL was recommended in 100.0% of cases based on clinical findings of elevated IOP, deep AC, and a poorly formed bleb. When AS-OCT was used to decide whether to perform LSL or not, this procedure was recommended in 71.4% of cases, particularly in blebs showing opposed scleral flaps, absent subflap spaces, and thin bleb wall. Moreover, AS-OCT can also be used to assess bleb modifications after LSL. In successful treatments, a separation of the scleral flap from the scleral bed is evident (Figure 8), with facilitation of the AH drainage and the elevation of the conjunctiva at the site of bleb [43, 44].

Filling Implants. The insertion of filling implants within the bleb or the scleral lake may be considered as an intraoperative bleb management procedure, aimed at reducing the rate of failure after penetrating or nonpenetrating filtration surgery. In penetrating surgery, these implants act as space maintainers between the scleral flap and conjunctiva in the early postoperative period, facilitating the AH passage through the conjunctival layers, and limiting fibrotic processes. In addition, such implants reduce the incidence of hypotony, acting as mechanical compressors over the scleral flap. In nonpenetrating surgery, filling implants also promote the preservation of the intrascleral lake. Space filling implants can be differentiated in absorbable and nonabsorbable. The HEALA flow (a slowly absorbable viscoelastic implant), the SK-gel (SKGEL 3.5 (Corneal Laboratories, Paris, France); sodium hyaluronate implant), and the Ologen (a disc-shaped porcine-derived biodegradable collagen matrix) are absorbable implants. The T-flux (T-Flux device; IOLTECH Laboratories, La Rochelle, France) used during deep sclerectomy is nonabsorbable.

To date, their utility is still controversial [45, 46]. In a prospective randomized trial Cillino et al. [47] compared

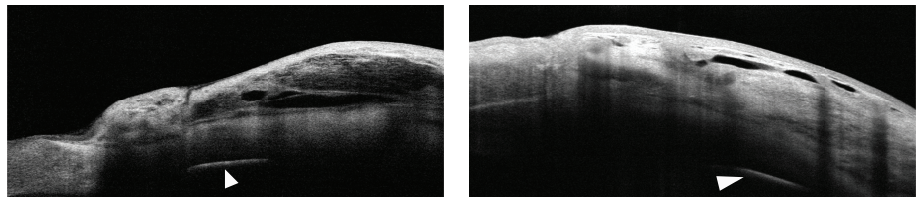

(a) (b)

Figure 9: Filtering bleb morphology after biodegradable collagen matrix implantation. Three months after the subconjunctival implantation of the Ologen (a), no significant morphological differences in the macroscopic bleb structure are evident (except for a thicker bleb wall) compared to eyes that did not receive the implant (b).

the Ologen implant as adjuvant versus low-dosage MMC in trabeculectomy and used AS SD-OCT (Topcon 3DOCT-1000, Topcon Corporation, Tokyo, Japan) to evaluate bleb morphology. The authors reported that SD-OCT did not show qualitative differences in the bleb-wall appearance between groups, indicating that the Ologen implant did not enhance or modify the morphology of the bleb wall. Nevertheless, SD-OCT documented a thicker bleb wall in successful Ologen-augmented trabeculectomy with respect to MMC-augmented successful trabeculectomy. In consistence with these results, in our case series (unpublished data) Optovue did not document significant differences of bleb morphology in patients implanted with Ologen compared to patients who did not receive the device (Figure 9).

8. Limitations

One of the shortcomings of AS-OCT in assessing filtering blebs is that it does not provide microscopic information (as all imaging modalities), which is essential for detecting the very early signs of failure, such as the stromal collagen deposition and the reduction of AH filled epithelial microcysts. Moreover, features indicative of bleb inflammation (dendritic cell activation and lymphocyte infiltration) or infection (infiltration of mononucleate inflammatory cells) cannot be detected. Therefore, AS-OCT may probably identify failing blebs in a later time with respect to microscopic methods of analysis such as LSCM. Further prospective studies evaluating the ability of these methods in detecting the early signs of failure over time are warranted.

9. Discussion and Conclusion

The main challenge in the management of filtration surgery is the preservation of the AH outflow through the scleral ostium and the bleb in order to maintain a good IOP control. Therefore, a careful postoperative clinical evaluation is strongly recommended because the bleb filtering ability may decrease over time. In several cases, the slit-lamp appearance may not be indicative of the bleb functionality because the clinical analysis is a qualitative assessment affected by the intra- and interobservers variability. In addition, the presence of collagen fibers within the bleb wall, especially in cases of florid connective deposition, may impede the visualization of the deeper layers of the bleb wall, the inner cavity, and the scleral flap. Therefore, clinical assessment cannot permit a timely identification of signs of filtration failure.

AS-OCT may contribute to overcome these problems by allowing a detailed structural assessment of bleb-wall layers, bleb cavity, and scleral opening. Moreover, this methodology provides essential biometric parameters such as the bleb-wall reflectivity and thickness, the inner cavity diameters and area, which may help the clinician in distinguishing between functioning from nonfunctioning blebs. In addition, AS-OCT proved valuable in the early identification of signs of failure, critical for the bleb management. This is essential to preserve AH filtration since bleb management procedures are much more effective when administered very early. Therefore, a postsurgical follow-up that also considers the routinely use of AS-OCT with the clinical evaluation is recommended in order to obtain detailed information concerning bleb functionality.

In closing, a combined diagnostic approach that comprehends the standard clinical evaluation and an imaging technique such the AS-OCT may improve the clinician's ability in the understanding bleb functionality, in planning the correct timing for bleb management procedures, and in the evaluation of their efficacy.

Conflict of Interests

None of the authors have a proprietary interest in the development or marketing of any of the products mentioned in this paper. The authors declare that there is no conflict of interests regarding the publication of this paper.

Authors' Contribution

Rodolfo Mastropasqua and Vincenzo Fasanella equally contributed to this work and share primary authorship.

References

[1] The AGIS Investigators, "The Advanced Glaucoma Intervention Study (AGIS): 7. The relationship between control of intraocular pressure and visual field deterioration," *The American Journal of Ophthalmology*, vol. 130, no. 4, pp. 429–440, 2000.

[2] D. S. Friedman, C. O. Okeke, H. D. Jampel et al., "Risk factors for poor adherence to eyedrops in electronically monitored

patients with glaucoma," *Ophthalmology*, vol. 116, no. 6, pp. 1097–1105, 2009.

[3] P. G. Watson, "When to operate on open angle glaucoma," *Eye*, vol. 1, pp. 51–54, 1987.

[4] E. Rulli, E. Biagioli, I. Riva et al., "Efficacy and safety of trabeculectomy vs nonpenetrating surgical procedures: a systematic review and meta-analysis," *JAMA Ophthalmology*, vol. 131, no. 12, pp. 1573–1582, 2013.

[5] G. W. Abrams, M. A. Thomas, G. A. Williams, and T. C. Burton, "Management of postoperative suprachoroidal hemorrhage with continuous-infusion air pump," *Archives of Ophthalmology*, vol. 104, no. 10, pp. 1455–1458, 1986.

[6] F. D'Ermo, L. Bonomi, and D. Doro, "A critical analysis of the long term results of trabeculectomy," *American Journal of Ophthalmology*, vol. 88, no. 5, pp. 829–835, 1979.

[7] R. Z. Levene, "Glaucoma filtering surgery: factors that determine pressure control," *Ophthalmic Surgery*, vol. 15, no. 6, pp. 475–483, 1984.

[8] R. Z. Levene, "Glaucoma filtering surgery factors that determine pressure control," *Transactions of the American Ophthalmological Society*, vol. 82, pp. 282–301, 1984.

[9] A. Azuara-Blanco and L. J. Katz, "Dysfunctional filtering blebs," *Survey of Ophthalmology*, vol. 43, no. 2, pp. 93–126, 1998.

[10] R. Sharma, A. Sharma, T. Arora et al., "Application of anterior segment optical coherence tomography in glaucoma," *Survey of Ophthalmology*, vol. 59, no. 3, pp. 311–327, 2014.

[11] A. Labbé, B. Dupas, P. Hamard, and C. Baudouin, "In vivo confocal microscopy study of blebs after filtering surgery," *Ophthalmology*, vol. 112, no. 11, pp. 1979.e1–1979.e9, 2005.

[12] M. Ciancaglini, P. Carpineto, L. Agnifili et al., "Filtering bleb functionality: a clinical, anterior segment optical coherence tomography and in vivo confocal microscopy study," *Journal of Glaucoma*, vol. 17, no. 4, pp. 308–317, 2008.

[13] L. Mastropasqua, L. Agnifili, R. Mastropasqua, and V. Fasanella, "Conjunctival modifications induced by medical and surgical therapies in patients with glaucoma," *Current Opinion in Pharmacology*, vol. 13, no. 1, pp. 56–64, 2013.

[14] P. Carpineto, L. Agnifili, M. Nubile et al., "Conjunctival and corneal findings in bleb-associated endophthalmitis: an in vivo confocal microscopy study," *Acta Ophthalmologica*, vol. 89, no. 4, pp. 388–395, 2011.

[15] M. Ciancaglini, P. Carpineto, L. Agnifili et al., "Conjunctival characteristics in primary open-angle glaucoma and modifications induced by trabeculectomy with mitomycin C: an in vivo confocal microscopy study," *The British Journal of Ophthalmology*, vol. 93, no. 9, pp. 1204–1209, 2009.

[16] L. Mastropasqua, L. Agnifili, M. L. Salvetat et al., "In vivo analysis of conjunctiva in canaloplasty for glaucoma," *British Journal of Ophthalmology*, vol. 96, no. 5, pp. 634–639, 2012.

[17] S. Radhakrishnan, A. M. Rollins, J. E. Roth et al., "Real-time optical coherence tomography of the anterior segment at 1310 nm," *Archives of Ophthalmology*, vol. 119, no. 8, pp. 1179–1185, 2001.

[18] M. Singh, J. L. S. See, M. C. Aquino, L. S. Y. Thean, and P. T. K. Chew, "High-definition imaging of trabeculectomy blebs using spectral domain optical coherence tomography adapted for the anterior segment," *Clinical & Experimental Ophthalmology*, vol. 37, no. 4, pp. 345–351, 2009.

[19] P. C. Kronfeld, "Functional characteristics of surgically produced outflow channels," *Transactions—American Academy of Ophthalmology and Otolaryngology*, vol. 73, no. 2, pp. 177–193, 1969.

[20] C. Migdal and R. Hitchings, "The developing bleb: effect of topical antiprostaglandins on the outcome of glaucoma fistulising surgery," *British Journal of Ophthalmology*, vol. 67, no. 10, pp. 655–660, 1983.

[21] G. Picht and F. Grehn, "Classification of filtering blebs in trabeculectomy: biomicroscopy and functionality," *Current Opinion in Ophthalmology*, vol. 9, no. 2, pp. 2–8, 1998.

[22] L. B. Cantor, A. Mantravadi, D. WuDunn, K. Swamynathan, and A. Cortes, "Morphologic classification of filtering blebs after glaucoma filtration surgery: the Indiana Bleb Appearance Grading Scale," *Journal of Glaucoma*, vol. 12, no. 3, pp. 266–271, 2003.

[23] A. P. Wells, N. N. Ashraff, R. C. Hall, and G. Purdie, "Comparison of two clinical bleb grading systems," *Ophthalmology*, vol. 113, no. 1, pp. 77–83, 2006.

[24] L. Mastropasqua, L. Agnifili, M. Ciancaglini et al., "In vivo analysis of conjunctiva in gold micro shunt implantation for glaucoma," *British Journal of Ophthalmology*, vol. 94, no. 12, pp. 1592–1596, 2010.

[25] L. Mastropasqua, L. Agnifili, R. Mastropasqua et al., "In vivo laser scanning confocal microscopy of the ocular surface in glaucoma," *Microscopy and Microanalysis*, vol. 20, no. 3, pp. 879–894, 2014.

[26] R. Mastropasqua, V. Fasanella, E. Pedrotti et al., "Trans-conjunctival aqueous humor outflow in glaucomatous patients treated with prostaglandin analogues: an in vivo confocal microscopy study," *Graefe's Archive for Clinical and Experimental Ophthalmology*, 2014.

[27] C. K. Leung, D. W. Yick, Y. Y. Kwong et al., "Analysis of bleb morphology after trabeculectomy with Visante anterior segment optical coherence tomography," *British Journal of Ophthalmology*, vol. 91, no. 3, pp. 340–344, 2007.

[28] M. Singh, P. T. K. Chew, D. S. Friedman et al., "Imaging of trabeculectomy blebs using anterior segment optical coherence tomography," *Ophthalmology*, vol. 114, no. 1, pp. 47–53, 2007.

[29] L. Pfenninger, F. Schneider, and J. Funk, "Internal reflectivity of filtering blebs versus intraocular pressure in patients with recent trabeculectomy," *Investigative Ophthalmology & Visual Science*, vol. 52, no. 5, pp. 2450–2455, 2011.

[30] A. Tominaga, A. Miki, Y. Yamazaki, K. Matsushita, and Y. Otori, "The assessment of the filtering bleb function with anterior segment optical coherence tomography," *Journal of Glaucoma*, vol. 19, no. 8, pp. 551–555, 2010.

[31] K. Kawana, T. Kiuchi, Y. Yasuno, and T. Oshika, "Evaluation of trabeculectomy blebs using 3-dimensional cornea and anterior segment optical coherence tomography," *Ophthalmology*, vol. 116, no. 5, pp. 848–855, 2009.

[32] T. Inoue, R. Matsumura, U. Kuroda, K. Nakashima, T. Kawaji, and H. Tanihara, "Precise identification of filtration openings on the scleral flap by three-dimensional anterior segment optical coherence tomography," *Investigative Ophthalmology and Visual Science*, vol. 53, no. 13, pp. 8288–8294, 2012.

[33] P. A. Netland, S. R. Sarkisian Jr., and M. R. Moster, "Randomized, prospective, comparative trial of EX-PRESS glaucoma filtration device versus trabeculectomy (XVT study)," *American Journal of Ophthalmology*, vol. 157, no. 2, pp. 433–440, 2014.

[34] F. D. Verbraak, D. M. de Bruin, M. Sulak et al., "Optical coherence tomography of the Ex-PRESS miniature glaucoma implant," *Lasers in Medical Science*, vol. 20, no. 1, pp. 41–44, 2005.

[35] E. Van der Zypen, F. Fankhauser, and S. Kwasniewska, "The mechanism of aqueous outflow following trabeculectomy.

A light and electron microscopic study," *International Ophthalmology*, vol. 13, no. 3, pp. 219–228, 1989.

[36] A. Ambresin, T. Shaarawy, and A. Mermoud, "Deep sclerectomy with collagen implant in one eye compared with trabeculectomy in the other eye of the same patient," *Journal of Glaucoma*, vol. 11, no. 3, pp. 214–220, 2002.

[37] F. Aptel, S. Dumas, and P. Denis, "Ultrasound biomicroscopy and optical coherence tomography imaging of filtering blebs after deep sclerectomy with new collagen implant," *European Journal of Ophthalmology*, vol. 19, no. 2, pp. 223–230, 2009.

[38] K. I. Jung, S. A. Lim, H. L. Park, and C. K. Park, "Visualization of blebs using anterior-segment optical coherence tomography after glaucoma drainage implant surgery," *Ophthalmology*, vol. 120, no. 5, pp. 978–983, 2013.

[39] P. Gouws, Y. M. Buys, R. Rachmiel, G. E. Trope, and B. B. Fresco, "Finger massage versus a novel massage device after trabeculectomy," *Canadian Journal of Ophthalmology*, vol. 43, no. 2, pp. 222–224, 2008.

[40] R. H. Ewing and R. L. Stamper, "Needle revision with and without 5-fluorouracil for the treatment of failed filtering blebs," *American Journal of Ophthalmology*, vol. 110, no. 3, pp. 254–259, 1990.

[41] R. Guthoff, T. Guthoff, D. Hensler, F. Grehn, and T. Klink, "Bleb needling in encapsulated filtering blebs: evaluation by optical coherence tomography," *Ophthalmologica*, vol. 224, no. 4, pp. 204–208, 2010.

[42] M. Singh, T. Aung, M. C. Aquino, and P. T. K. Chew, "Utility of bleb imaging with anterior segment optical coherence tomography in clinical decision-making after trabeculectomy," *Journal of Glaucoma*, vol. 18, no. 6, pp. 492–495, 2009.

[43] M. Singh, T. Aung, D. S. Friedman et al., "Anterior segment optical coherence tomography imaging of trabeculectomy blebs before and after laser suture lysis," *American Journal of Ophthalmology*, vol. 143, no. 5, pp. 873–875, 2007.

[44] C. C. A. Sng, M. Singh, P. T. K. Chew et al., "Quantitative assessment of changes in trabeculectomy blebs after laser suture lysis using anterior segment coherence tomography," *Journal of Glaucoma*, vol. 21, no. 5, pp. 313–317, 2012.

[45] M. Rękas, K. Lewczuk, B. Fuksińska, J. Rudowicz, R. Pawlik, and A. Stankiewicz, "Combined surgery for cataract and glaucoma: PDS with absorbable SK-gel implant compared with PDS with non-absorbable T-flux implant medium-term results," *Current Medical Research and Opinion*, vol. 26, no. 5, pp. 1131–1137, 2010.

[46] E. Ravinet, E. Bovey, and A. Mermoud, "T-Flux Implant versus Healon GV in Deep Sclerectomy," *Journal of Glaucoma*, vol. 13, no. 1, pp. 46–50, 2004.

[47] S. Cillino, F. Di Pace, G. Cillino, and A. Casuccio, "Biodegradable collagen matrix implant vs mitomycin-C as an adjuvant in trabeculectomy: a 24-month, randomized clinical trial," *Eye*, vol. 25, no. 12, pp. 1598–1606, 2011.

Hindawi Publishing Corporation
BioMed Research International
Volume 2014, Article ID 731565, 10 pages
http://dx.doi.org/10.1155/2014/731565

Research Article

Comparative Study of Corneal Endothelial Cell Damage after Femtosecond Laser Assisted Deep Stromal Dissection

Ting Liu, Jingjing Zhang, Dapeng Sun, Wenjie Sui, Yangyang Zhang, Dongfang Li, Zhaoli Chen, and Hua Gao

State Key Laboratory Cultivation Base, Shandong Provincial Key Laboratory of Ophthalmology, Shandong Eye Institute, Shandong Academy of Medical Sciences, No. 5 Yan'erdao Road, Qingdao 266071, China

Correspondence should be addressed to Hua Gao; gaohua100@126.com

Received 12 May 2014; Accepted 24 June 2014; Published 10 July 2014

Academic Editor: Ciro Costagliola

Purpose. To find a relatively safe designed stromal bed thickness to avoid endothelial damage for lamellar keratoplasty with an Allegretto Wavelight FS200 femtosecond laser. *Methods.* Twelve rabbits were randomly divided into 50 μm and 150 μm groups according to the anticipated residue stromal bed thickness preparation with a femtosecond laser. Six rabbits without laser cutting were used as a control group. Central endothelial images were analyzed with in vivo confocal microscopy and scanning electron microscopy. The apoptosis of endothelium was evaluated with Hoechst 33342 staining and a TUNEL assay. *Results.* The endothelium of the 50 μm group had extensive injuries upon in vivo confocal and scanning electron microscopic observation, and minor injuries were observed in the 150 μm group. Moreover, more apoptotic cells were observed in the 50 μm group. *Conclusions.* When using a FS200 femtosecond laser assisted anterior lamellar keratoplasty, there was minor endothelium damage with a 150 μm stromal bed, and a more than 150 μm thickness stromal bed design may prevent the damage of corneal endothelium.

1. Introduction

Penetrating keratoplasty has been widely used in patients with corneal blindness [1, 2]. But the risk of immune rejection and postoperative astigmatism following penetrating keratoplasty still affect postoperative prognosis [3]. With the deepening understanding of the anatomical structure of the cornea and the development of modern microsurgical techniques, an increasing number of ophthalmologists tend to use split keratoplasty, which only replaces the diseased part of cornea. So, anterior lamellar keratoplasty was used to treat corneal stromal lesions without apparent endothelial cell damage, and lamellar posterior keratoplasty was applied in patients with endothelial decompensation. During the split keratoplasty procedure, the two primary concerns are cutting the diseased stroma precisely and protecting the host's endothelium [4, 5].

The femtosecond laser was a modern transition medical instrument, and it presented remarkable prospects in various medical fields. In the field of ophthalmology, femtosecond lasers provide advantages for the modern corneal surgeon and have been rapidly adopted to create corneal flaps of predetermined depth during LASIK. The femtosecond laser is now capable of dissecting a thin, of uniform thickness, lamellar disk of cornea not only to be used for lamellar posterior but also to be used for anterior lamellar keratoplasty [6, 7]. With the use of proprietary software, a femtosecond laser can create a better graft-host fit with less postoperative astigmatism and can increase graft-host interface surface area and fit. However, femtosecond lasers are long wavelength lasers, and a light burst will damage the surrounding corneal tissue [8, 9]. Corneal endothelial cells comprise one of the most important layers of the corneal cells and cannot be regenerated when injury results in corneal endothelial cell decompensation. During the femtosecond laser cutting, the laser energy was generated for photodisruption of tissue, which may be absorbed by the cornea tissue and damage the nearby corneal endothelial cells. Therefore, there are still

some concerns about the use of a femtosecond laser to create a <100 μm thick stromal bed, in which the endothelium may be damaged when cutting close to the delicate cells.

Although the femtosecond laser was a delicate and accurate machine in cutting, there still existed deviation during the cutting procedure. The predictability of the cutting was an important factor to consider when we need a femtosecond laser assisted deep stromal dissection. In the present study, we used FS200 femtosecond laser to make designed 50 μm and 150 μm recipient stromal bed and observe its effects on the corneal endothelium. Our aim was to find a relatively safe designed stromal bed thickness to avoid endothelial damage for lamellar keratoplasty with an Allegretto Wavelight FS200 femtosecond laser.

2. Materials and Methods

2.1. Animals. All animal experiments were carried out in accordance with The Chinese Ministry of Science and Technology Guidelines on the Humane Treatment of Laboratory Animals (vGKFCZ-2006-398) and the Association for Research in Vision and Ophthalmology (ARVO) Statement for the Use of Animals in Ophthalmic and Vision Research. This study was approved by the Animal Care and Use Committee on the Ethics of the Shandong Eye Institute. Eighteen male or female New Zealand White rabbits (2–2.5 kg) were used in this study. Rabbits were anaesthetized with a combination of ketamine and xylazine (ketamine 40 mg/kg, xylazine 20 mg/kg; IM). Proparacaine drops were used for topical anesthesia during surgery. Animals were sacrificed with an overdose intravenous injection of pentobarbital.

2.2. Groups. In accordance with planting bed thickness, the animals were subdivided into three groups: a residual bed thickness of 50 μm or 150 μm and a control group, with 6 rabbits in each group. The right eye of each rabbit was used, and central corneal thickness was measured with anterior segment ocular coherence tomography (AS-OCT) before surgery.

2.3. Femtosecond Laser Cutting Procedure. Lamellar cutting was performed using an Allegretto Wavelight FS200 femtosecond laser (Wavelight AG, Erlangen, Germany). A lamellar keratoplasty cut configuration was chosen for the graft with diameters of 8.5 mm and an angle of 90°. ASOCT was used to help guide the desired thickness of the graft. The femtosecond laser settings included a bed cut energy of 1.0 μJ and a side cut energy of 0.1 μJ. The spot separation at the bed cut was 6.0 μm, and the line separation was 6.0 μm. The spot/line separation of the bed cut was 10.0/10.0 μm. The surgical procedure was as follows: the speculum was placed adjacent to the rabbit's eye, the eyelid was opened, and the suction ring was positioned on the right eye. After the suction ring had an appropriate vacuum pressure (500 mmHg), the applanation cone was guided into the suction ring using the laser joystick, and the laser pedal was pressed [10]. In the rabbits in control group, suction rings were also put on the right eye and vacuum pressure was added, but the laser pedal was not pressed.

2.4. Slit-Lamp Photography and Optical Coherence Tomography (OCT) of Rabbit Corneas. Before the animals were sacrificed, slit-lamp photographs (Nikon FS-3V; Nikon, Tokyo, Japan) were captured. Corneal cross-sectional visualization in the rabbits was performed using a Visante ASOCT unit (Carl Zeiss Meditec) 12 hours after surgery.

2.5. In Vivo Scanning Confocal Microscopy of Rabbit Corneas. Confocal microscopy images were obtained before surgery and 12 hours after surgery. Before the examination, each rabbit was anaesthetized as described above. A lid speculum was placed to separate the eyelids of the right eye of each rabbit. After one drop of 0.5% proparacaine hydrochloride (Alcon Laboratories, Fort Worth, Texas, USA) was applied, the central cornea was examined with a scanning confocal microscope (Heidelberg HRT III, German). The center and four quadrant points within 6 mm of the central cornea were examined. Approximately 100 sequential images were obtained from the endothelium to the epithelium during a single examination.

2.6. Evaluation of the Corneal Endothelium. Endothelial cell damage was assessed in the right eyes of rabbits, and corneal buttons were excised for endothelial staining and electron microscopy after 12 hours. The corneas were collected, and divided equally into 3 parts. One-third of the cornea was examined by alizarin red and Hoechst staining (Beyotime Institute of Biotechnology, Shanghai, China). The other two parts were used for scanning electron microscopy and histopathology assay. Briefly, 1% alizarin red was added to the cornea, which was incubated for 2 minutes at room temperature and washed three times in normal saline. Next, Hoechst 33342 stain was added to the cornea and incubated for 15–20 minutes at 4°C in the dark. Endothelial cells were observed using a Fluorescence E800 microscope (Nikon, Tokyo, Japan) [11]. Hoechst 33342 staining showed that the nucleus of apoptotic cells was uneven and shrinking. Six microscopy fields (400x) were randomly chosen in each cornea of three groups, and average apoptosis positive cells per high power field were counted for statistical analysis.

2.7. Scanning Electron Microscopy (SEM). The corneal buttons were half cut and fixed in 4% glutaraldehyde in 0.05 M cacodylate buffer for 1 h, washed in a buffered solution of 0.2% sucrose-cacodyl for 4–10 h, postfixed in 1% osmium tetroxide in veronal acetate buffer for 1 h, and dehydrated through a series of ethanol. The samples were then dried and mounted on SEM stubs using carbon adhesive tabs. They were then sputter-coated with a 10 nm thick layer of gold (Bal-Tec) and examined with a scanning electron microscope (JSM-840; JEOL, Tokyo, Japan).

2.8. Histopathology and TUNEL Assay. The corneal buttons were half cut along the central line. Serially graded ethanol baths followed by xylene were used to dehydrate the tissues

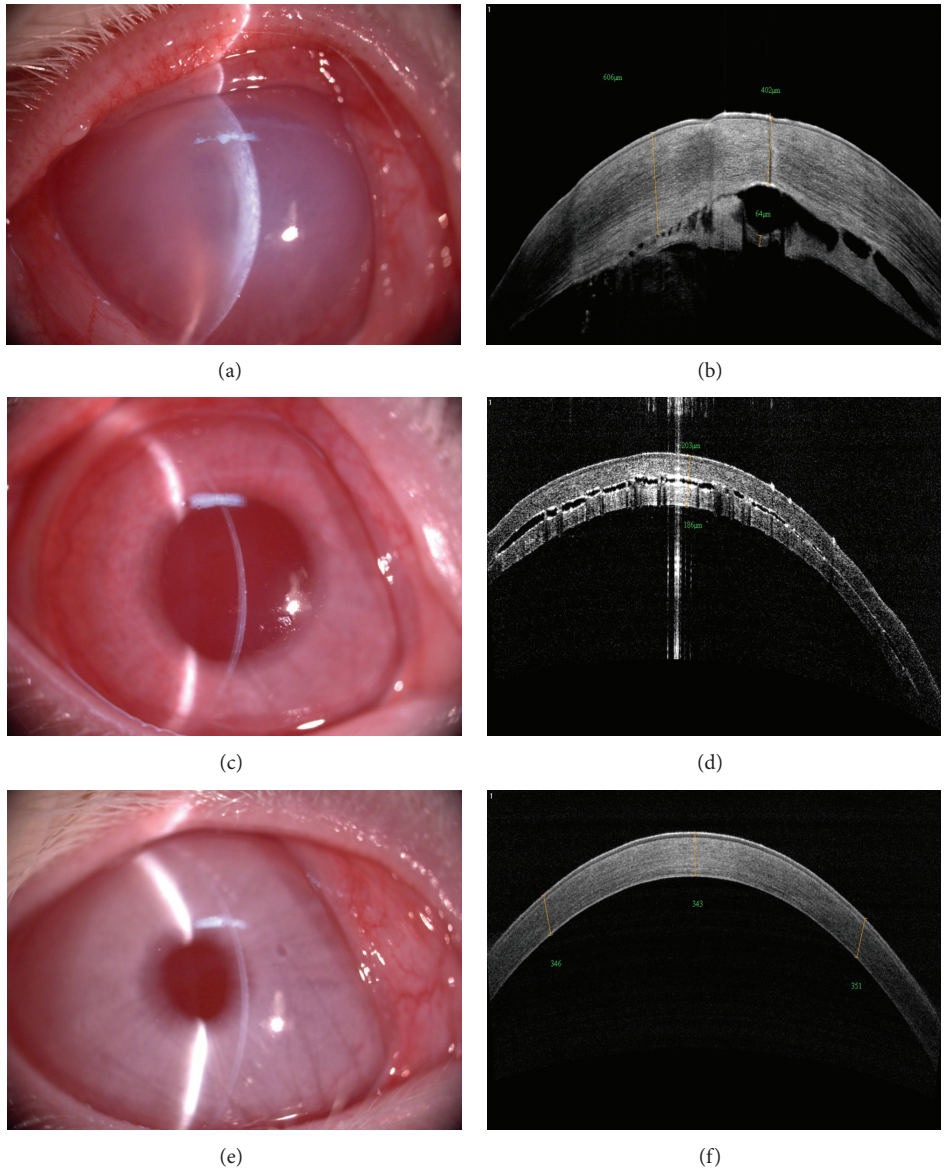

Figure 1: Rabbit slit-lamp microscopic examination and OCT images after femtosecond laser cutting. (a) The obvious corneal edema can be observed. (b) The irregular interlamellar space can be seen in the 50 μm group and connected to the anterior chamber. (c) No obvious corneal edema can be observed. (d) There was a relatively regular interlamellar space in the 150 μm group. (e) A clear cornea can be observed. (f) No interlamellar space was present in the control group.

before they were immersed in paraffin wax. The samples were embedded in paraffin molds, sectioned at 4 μm thickness, and mounted on glass slides. A hematoxylin-eosin stain was used for microscopic examination and evaluation.

Free 3′-OH DNA ends were detected in situ by the terminal deoxyribonucleotidyl transferase-mediated (TUNEL) labeling method according to the manufacturer's instructions using the in situ cell death detection kit, POD (Roche, Mannheim, Germany). Briefly, the sections were incubated with terminal deoxynucleotidyl transferase (TDT) and a nucleotide mixture in a reaction buffer and then incubated with an anti-FITC antibody conjugated with horseradish peroxidase. Peroxidase activity was detected by exposure of the sections to 3-amino-9-ethylcarbazole (AEC) solution (Maxin, Fujian, China), which were finally counterstained with hematoxylin. For negative controls, the nucleotide mixture was used instead of the TDT enzyme solution. Positive cells stained red in high-magnification fields were counted [12]. Six high power fields (400x) were randomly chosen in each slide of three groups, and average positive cells were counted per high power field for statistical analysis.

2.9. Statistical Analysis. Significant differences between endothelium counts and apoptotic cell counts among the three groups were evaluated with the Student-Newman-Keuls one-way ANOVA using SPSS 17.0 software. The mean ± standard deviation is shown, and P values < 0.05 were considered to be statistically significant.

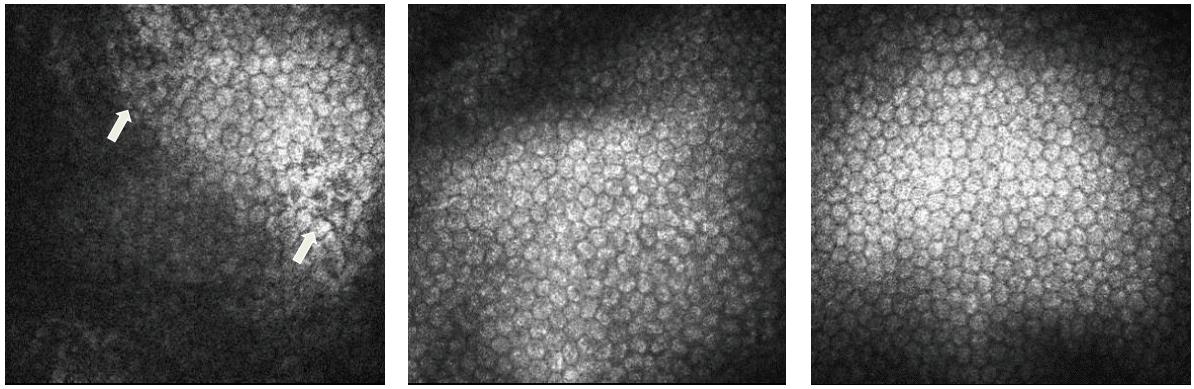

(a) (b) (c)

Figure 2: Representative images of the endothelium from in vivo confocal microscopy after femtosecond laser cutting. (a) Many lost hexagonal endothelium cells could be observed in the 50 μm group. ((b) and (c)) The endothelium had a regular hexagonal structure in the 150 μm group and the control group.

3. Results

3.1. Femtosecond Laser Cutting Accuracy. The femtosecond laser is a near infrared laser, and it causes photodisruption of tissue. The generation and confluence of plasma cavitations in a plane will result in tissue dissection. After the femtosecond laser cutting, corneal edema occurred in the 50 μm group. The corneas of two rabbits in the 50 μm group were unexpectedly penetrated by the laser, and obvious corneal edema still could be observed after 12 hours. The irregular interlamellar space could be seen in the 50 μm group and was connected to the anterior chamber. In the 150 μm group, there were regular shallow interlamellar space in the cornea and no obvious edema could be observed after 12 hours. In the control group, the corneas of rabbits were clear throughout the experiment (Figure 1).

No differences were found in the corneal thickness before surgery. The corneal thicknesses of three groups were 351.3 ± 12.9 μm (50 μm group), 345.7 ± 11.9 μm (150 μm group), and 353.2 ± 12.1 μm (control group), respectively. The cutting thickness was calculated by subtracting the anticipated stromal bed thickness. After laser cutting, the achieved residual bed thickness was 40.0 ± 34.8 μm (range: 0–77 μm) in the 50 μm group and 175.2 ± 6.3 μm (range: 167–185 μm) in the 150 μm group.

The expected cutting depth is 301.2±13.0 μm (range: 293–327 μm) for 50 μm group, 195.7±11.8 μm (range: 179–215 μm) for 150 μm group, and 0 μm for control group.

The average deviation from expected target results was 30.0 ± 14.6 μm (range: 14–50 μm) in the 50 μm group and 25.2±6.3 μm (range: 17–35 μm) in the 150 μm group, and there was no significant difference ($P = 0.413$).

3.2. Evaluation of the Endothelial Cell Density In Vivo. There were no differences in the endothelium cells density between each group before surgery. After the laser cutting, there were many lost hexagonal endothelium cells in the 50 μm group, as observed with in vivo confocal microscopy, which was not found in the 150 μm group or the control group (Figure 2). The endothelium count of 1691.3 ± 277.9 cells/mm^2 in the 50 μm group was significantly poorer when compared with 2797.5±238.1 cells/mm^2 in the 150 μm group and 2912±273.1 cells/mm^2 in the control group ($P = 0.000$ and $P = 0.000$, resp.).

3.3. Evaluation of Corneal Endothelium Apoptosis. Apoptosis was a main mechanism involved in corneal endothelium loss. The endothelium decreased with aging, and less than 500 cells/mm^2 in human will induce the endothelium decompensation. With alizarin red staining, the endothelial cell borders of the corneal buttons in the 50 μm group were not clear, and in some places the endothelial cells were completely lost (Figure 3(a)). The endothelial cell borders of the 150 μm group and control group were clear and maintained a hexagonal structure (Figures 3(c) and 3(e)). Hoechst staining showed that the nucleus was uneven and shrinking, with many apoptotic cells present in the 50 μm group (Figure 3(b)). No apoptotic cells could be detected in the 150 μm group or the control group (Figures 3(d) and 3(f)).

3.4. Scanning Electron Microscopy (SEM). SEM images of endothelial cells were analyzed in the cutting area. The laser created substantial endothelial damage areas in the 50 μm group (Figures 4(a) and 4(b)). The damaged endothelium presented with many small cavities resembling holes in a sponge, and the normal hexagonal structure was destroyed. Only sporadic cells presented with swollen changes in the 150 μm group (Figures 4(c) and 4(d)), and no obvious damage was noted in the control group (Figures 4(e) and 4(f)).

3.5. Histological Evaluation and TUNEL Assay. In the 50 μm group, the corneal stroma was edematous and only a small number of keratocytes and endothelial cells could be found (Figure 5(a)). Most of the deep stromal cells and endothelial cells of the 150 μm group were intact, and only swollen changes could be seen in the 150 μm group (Figure 5(c)). No endothelium damage or swollen changes could be observed

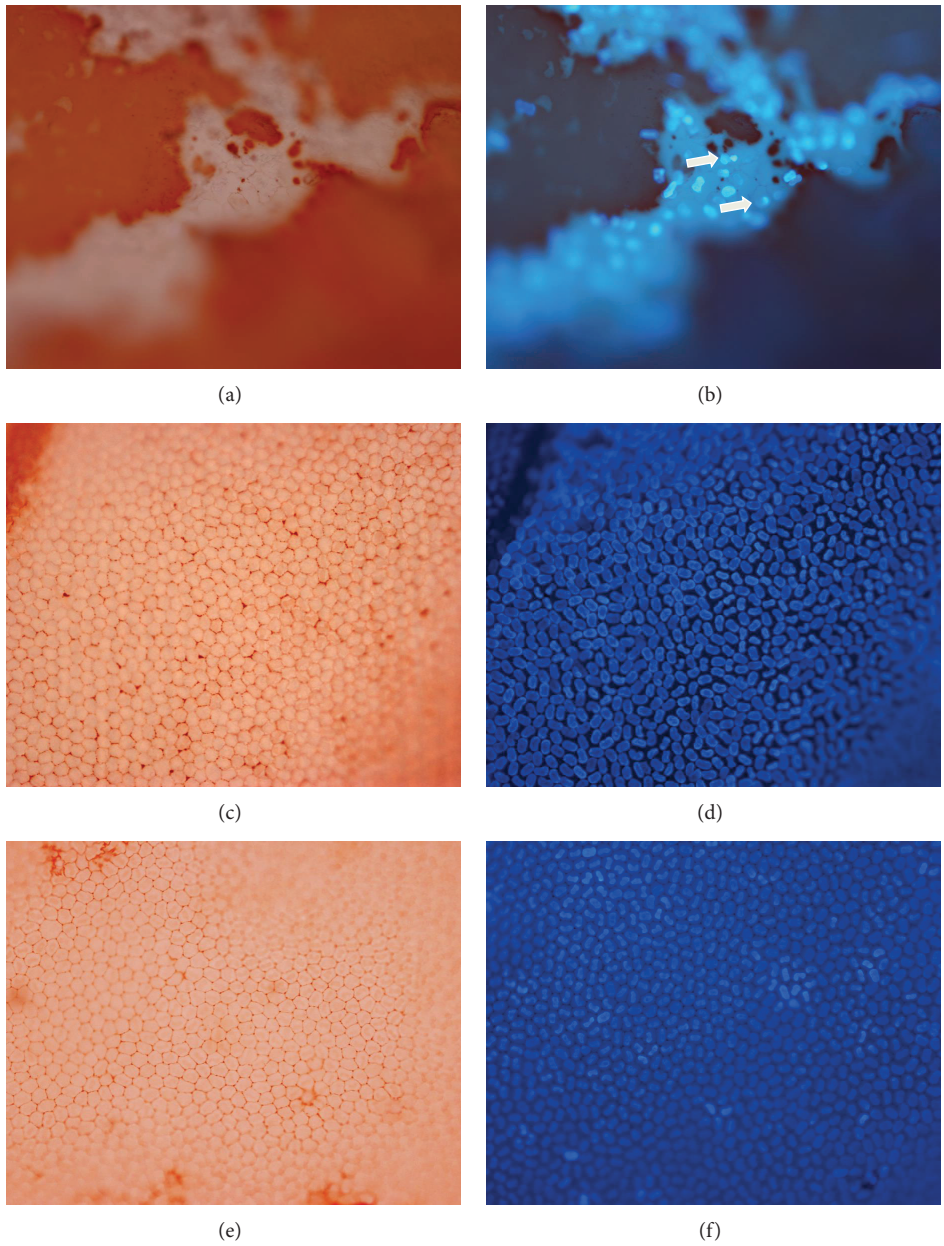

Figure 3: Alizarin Red and Hoechst 33342 staining of the endothelium after femtosecond laser cutting. (a) The endothelial cell borders of corneal buttons in the 50 μm group were not clear, and in some place the endothelial cells were completely lost. (b) Hoechst 33342 staining showed that the nucleus was uneven and shrinking, with many apoptotic cells present in the 50 μm group. ((c) and (e)) The endothelial cell borders of the 150 μm group and the control group were clear and had a normal hexagonal structure. ((d) and (f)) No apoptotic cells could be detected in the 150 μm group or the control group.

in the control group (Figure 5(e)). There were many TUNEL positive endothelium cells and keratocytes in the 50 μm group (Figure 5(b)), but no TUNEL positive endothelium cells were found in the 150 μm group or the control group (Figures 5(d) and 5(f)).

3.6. Statistical Evaluation of Endothelial Cells and Apoptosis. Significant differences were found between the 50 μm group and the 150 μm group ($P < 0.05$) in the endothelial cell counts, the number of apoptotic cells per area as viewed in high magnification, and the number of TUNEL positive cells per area as viewed in high magnification (Figure 6).

4. Discussion

In recent years, split keratoplasties, such as anterior lamellar keratoplasty (LKP) and lamellar posterior keratoplasty (Descemet's stripping automated endothelial keratoplasty), have been used more frequently to replace diseased cornea [13, 14]. Traditionally, the stromal bed or the endothelium

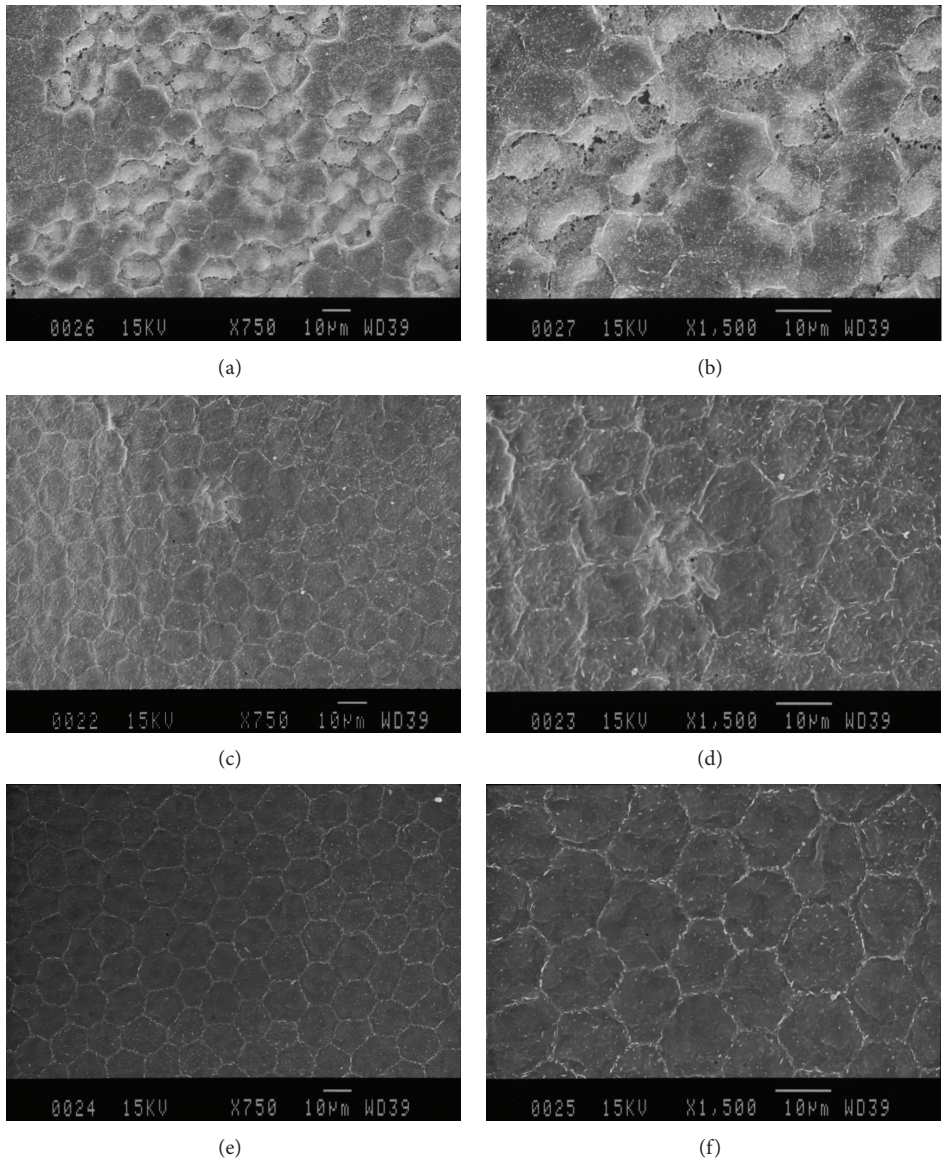

Figure 4: Representative images from scanning electron microscopy (SEM) of endothelial cells in the cutting area after femtosecond laser cutting. ((a) and (b)) The laser created a substantial endothelial damage area in the 50 μm group. The damaged endothelium presented with many small cavities resembling holes in a sponge, and the normal hexagonal structure was destroyed. ((c) and (d)) Only sporadic cells presented with swollen changes in the 150 μm group. ((e) and (f)) No obvious damage was noted in the control group.

grafts were prepared by manual sectioning, and the qualities of the stromal bed were determined by the skills of the surgeon. The use of femtosecond lasers to create a stromal bed had proved to be a viable method, because the lasers can accurately cut the full thickness of the cornea and effectively avoid the possible iatrogenic aberrations associated with microkeratomes [15–17]. Analysis of femtosecond-dissected donor tissues using atomic force microscopy images on a submicron scale proved that the surface quality of posterior cornea is significantly improved when compared with that provided by mechanical microkeratomes [18]. The easy and fast preparation of the stromal bed using femtosecond laser cutting was a remarkable development for lamellar keratoplasty [19, 20].

However, during femtosecond laser cutting, the deposited energy may damage nearby corneal tissue. It has been reported that keratocyte apoptosis and inflammation could occur after femtosecond laser cutting in refractive surgery [21]. If the cutting injury was severe, the endothelium could be damaged during deep lamellar keratoplasty. The effect of femtosecond laser on corneal endothelial health was a main concern when using the femtosecond laser to make a deep lamellar cutting [22–25]. The residual stromal bed may act as a cushion to protect the endothelium from the damage of deposited energy. For anterior lamellar keratoplasty, if the deep corneal stroma was affected, we may need to create a thinner stromal bed. However, making a thin stromal bed will increase the risk of endothelial damage. Until now, we lacked

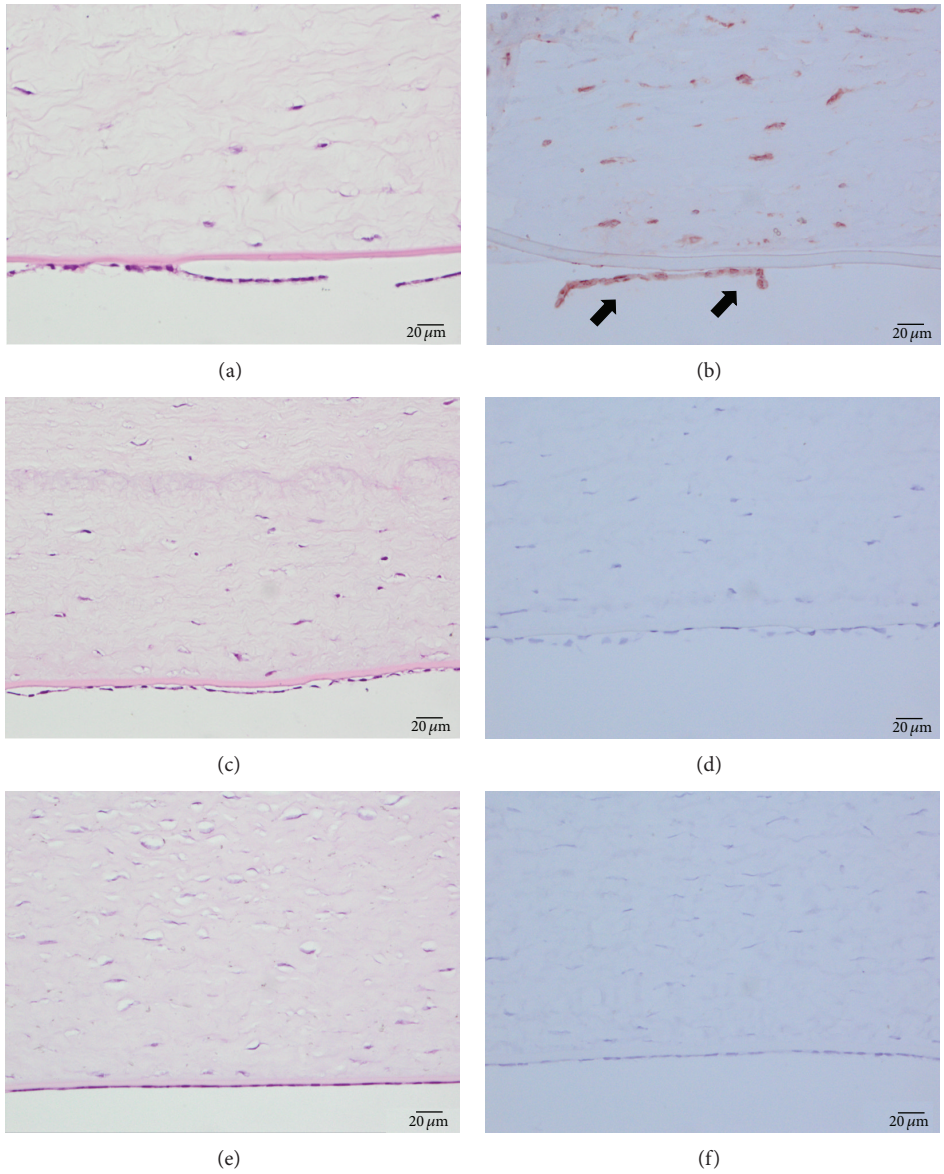

Figure 5: Histological evaluation and TUNEL assay of endothelial cells after femtosecond laser cutting. (a) The corneal stroma was edematous and only a small number of keratocytes and endothelial cells could be found in the 50 μm group. (c) Most of the deep stromal cells and the endothelium of the 150 μm group were intact and only swollen changes could be seen in the 150 μm group. (e) No endothelium damage or swollen changes could be observed in the control group. (b) There were many TUNEL positive cells in the 50 μm group. ((d) and (f)) No TUNEL positive cells were found in the 150 μm group or the control group.

an accurate study to determine whether the anticipated cutting thickness of the FS200 femtosecond laser was stable and what thickness of a residual stromal bed may be safe for lamellar keratoplasty during femtosecond cutting. In the present study, we provide comparative evidence to determine the accuracy of femtosecond laser cutting and the safety of different cutting thickness as we make a more precise stromal bed for deep lamellar keratoplasty.

The accuracy of femtosecond laser cutting depth is very important for guaranteeing the safety of operations. When cutting at 420 μm to 500 μm thickness using a low-pulse energy, high-frequency (LPEHF) femtosecond laser (Ziemer Femto LDV; Ziemer Ophthalmic Systems, Port, Switzerland), Phillips et al. reported that the cutting accuracy was 17 to 54 μm [26]. In our study, when cutting at 293 to 327 μm thickness using the average deviation of the achieved residual bed thickness from the expected target thickness, it did not reach statistical significance, which proved the acceptable cutting ability of FS200 femtosecond laser.

When using a LDV femtosecond laser (energy < 100 nJ) to make a tissue thickness of approximately 70 μm, Phillips et al. reported that there was no endothelial cell damage difference between experimental and control corneas. However, Kimakura et al. [27] reported that the mean ratio of damaged corneal endothelial cells in the group with a remaining depth of 70 μm was significantly higher than that in the group

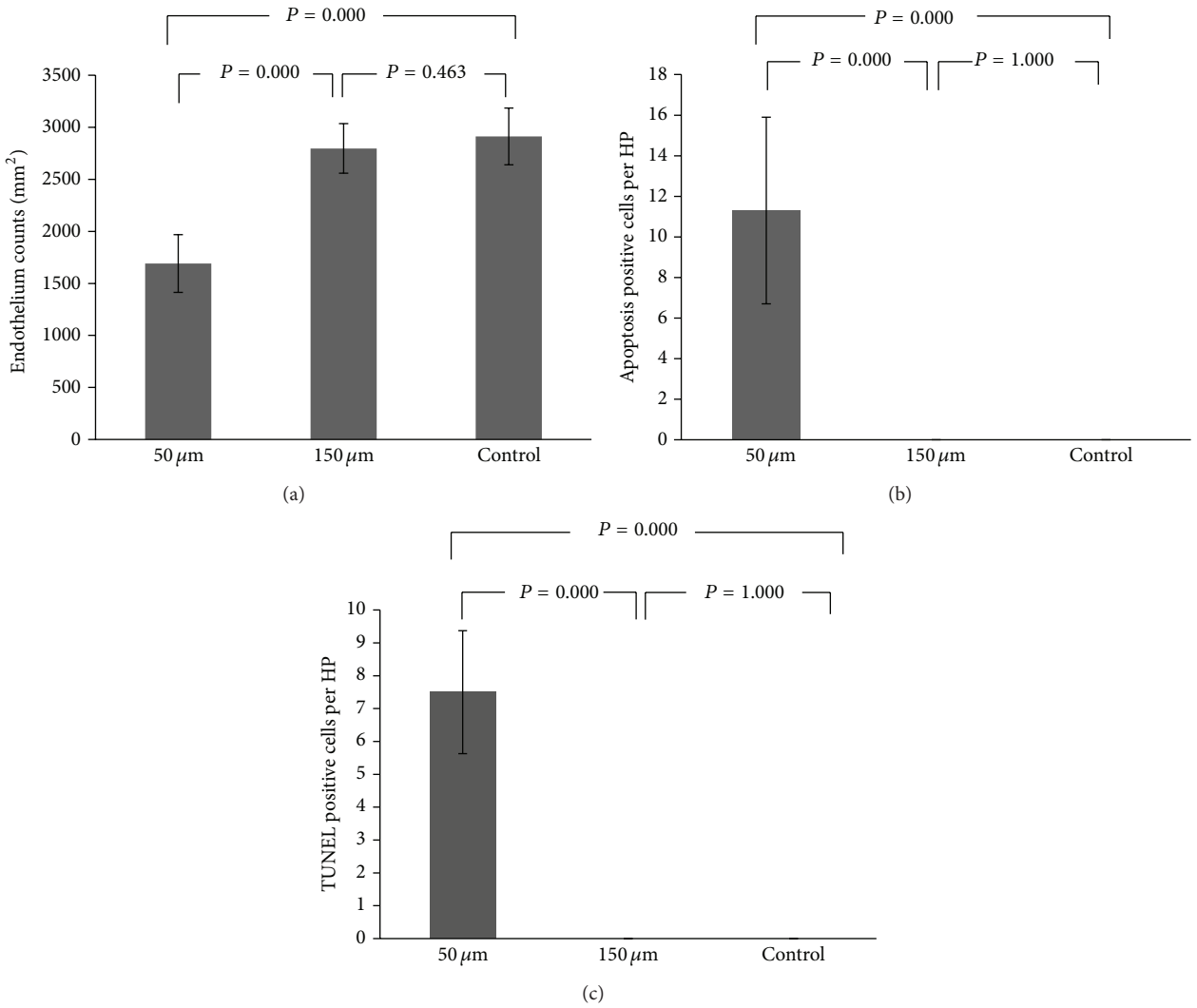

Figure 6: Evaluation of endothelial cells and apoptosis changes after femtosecond laser cutting. Significant differences were found between the 50 μm group and the 150 μm group ($P < 0.05$) including (a) endothelial cell count, (b) the number of apoptotic cells per high power field, and (c) the number of TUNEL positive cells per high power field.

with a remaining depth of 150 μm. The reason may be they used a 150 kHz femtosecond laser (energy 1.50 mJ). In a previous report, when cutting at a greater depth, the irregular stroma could have been caused by the increased scatter and attenuation of laser efficacy [28]. In our study, we could detect more endothelial cell damage and irregular cutting interface in the 50 μm group, but no obvious endothelial cell damage changes and a smooth interface could be found in the 150 μm group. One reason for this result may be more cutting thickness and the thinner stroma left in the 50 μm group; another reason may be more energy exported with the FS200 femtosecond laser (1.0 μJ) than that of LDV femtosecond laser (<100 nJ) during the cutting.

Clinically, a less thick bed and smooth interface play an important role to ensure quality of vision after surgery. The corneal endothelial damage was minor and smooth interface could be found when we prepared 150 μm thickness bed. But perforation occurred in the 50 μm bed rabbits, and more endothelial cells were damaged. This proved that at present femtosecond laser assisted less thick bed preparation may lack safety. A much thicker corneal bed is often difficult to excise lesion, and clinical applications are limited. Therefore, from the viewpoint of safety and clinical application, leaving 150 μm bed may be ideal. But our study involved a limited number of animals, and a larger study or human samples may be needed to further prove the safe stromal bed thickness with femtosecond laser cutting. We used an Allegretto Wavelight FS200 femtosecond laser, and the results may not be applicable for other types of femtosecond laser.

In conclusion, when using a FS200 femtosecond laser assisted anterior lamellar keratoplasty, there was minor endothelium damage with a 150 μm stromal bed, and a more than 150 μm thickness stromal bed design may prevent the damage of corneal endothelium.

Conflict of Interests

The authors declare that there is no conflict of interests regarding the publication of this paper.

Acknowledgments

This work was supported by National Natural Science Foundation of China (81370989), National Basic Research Program of China (2013CB967002), the Science & Technology Development Program of Shandong Province (2012GSF11836), Taishan Scholar Program (20081148), the Natural Science Foundation of Shandong Province (ZR2011HM015), and Shandong Provincial Excellent Innovation Team Program. The funders had no role in study design, data collection, and analysis, decision to publish, or preparation of the paper.

References

[1] D. T. Tan, J. K. Dart, E. J. Holland, and S. Kinoshita, "Corneal transplantation," *The Lancet*, vol. 379, pp. 1749–1761, 2012.

[2] L. Xie, Z. Song, J. Zhao, W. Shi, and F. Wang, "Indications for penetrating keratoplasty in north China," *Cornea*, vol. 26, no. 9, pp. 1070–1073, 2007.

[3] W. Shi, M. Chen, L. Xie et al., "A novel cyclosporine a drug-delivery system for prevention of human corneal rejection after high-risk keratoplasty: a clinical study," *Ophthalmology*, vol. 120, no. 4, pp. 695–702, 2013.

[4] E. I. Wu, D. C. Ritterband, G. Yu, R. A. Shields, and J. A. Seedor, "Graft rejection following descemet stripping automated endothelial keratoplasty: features, risk factors, and outcomes," *American Journal of Ophthalmology*, vol. 153, no. 5, pp. 949.e1–957.e1, 2012.

[5] S. L. Mason, R. M. Stewart, V. R. Kearns, R. L. Williams, and C. M. Sheridan, "Ocular epithelial transplantation: current uses and future potential," *Regenerative Medicine*, vol. 6, no. 6, pp. 767–782, 2011.

[6] J. M. Vetter, C. Butsch, M. Faust et al., "Irregularity of the posterior corneal surface after curved interface femtosecond laser-assisted versus microkeratome-assisted descemet stripping automated endothelial keratoplasty," *Cornea*, vol. 32, no. 2, pp. 118–124, 2013.

[7] S. Heinzelmann, P. Maier, D. Böhringer, C. Auw-Hädrich, and T. Reinhard, "Visual outcome and histological findings following femtosecond laser-assisted versus microkeratome-assisted DSAEK," *Graefe's Archive for Clinical and Experimental Ophthalmology*, vol. 251, no. 8, pp. 1979–1985, 2013.

[8] G. Muñoz, C. Albarrán-Diego, H. F. Sakla, T. Ferrer-Blasco, and J. Javaloy, "Effects of LASIK on corneal endothelium using the 15-kHz IntraLase femtosecond laser," *Journal of Refractive Surgery*, vol. 27, no. 9, pp. 672–677, 2011.

[9] R. I. Angunawela, A. Riau, S. S. Chaurasia, D. T. Tan, and J. S. Mehta, "Manual suction versus femtosecond laser trephination for penetrating keratoplasty: intraocular pressure, endothelial cell damage, incision geometry, and wound healing responses," *Investigative Ophthalmology and Visual Science*, vol. 53, no. 6, pp. 2571–2579, 2012.

[10] M. Chen and L. Xie, "Features of recurrence after excimer laser phototherapeutic keratectomy for anterior corneal pathologies in North China," *Ophthalmology*, vol. 120, no. 6, pp. 1179–1185, 2013.

[11] H. Gao, W. Shi, H. Gong, Y. Wang, Y. Wang, and L. Xie, "Establishment of a murine model of chronic corneal allograft dysfunction," *Graefe's Archive for Clinical and Experimental Ophthalmology*, vol. 248, no. 10, pp. 1437–1445, 2010.

[12] T. Liu, H. Zhai, Y. Xu et al., "Amniotic membrane traps and induces apoptosis of inflammatory cells in ocular surface chemical burn," *Molecular Vision*, vol. 18, pp. 2137–2146, 2012.

[13] R. B. Vajpayee, N. Sharma, V. Jhanji, J. S. Titiyal, and R. Tandon, "One donor cornea for 3 recipients: a new concept for corneal transplantation surgery," *Archives of Ophthalmology*, vol. 125, no. 4, pp. 552–554, 2007.

[14] L. M. Heindl, S. Riss, B. O. Bachmann, K. Laaser, F. E. Kruse, and C. Cursiefen, "Split cornea transplantation for 2 recipients: a new strategy to reduce corneal tissue cost and shortage," *Ophthalmology*, vol. 118, no. 2, pp. 294–301, 2011.

[15] K. N. Klingler, J. W. McLaren, W. M. Bourne, and S. V. Patel, "Corneal endothelial cell changes 5 years after laser in situ keratomileusis: femtosecond laser versus mechanical microkeratome," *Journal of Cataract and Refractive Surgery*, vol. 38, no. 12, pp. 2125–2130, 2012.

[16] M. V. Netto, R. R. Mohan, F. W. Medeiros et al., "Femtosecond laser and microkeratome corneal flaps: comparison of stromal wound healing and inflammation," *Journal of Refractive Surgery*, vol. 23, no. 7, pp. 667–676, 2007.

[17] A. Rousseau, A. Bensalem, V. Garnier et al., "Interface quality of endothelial keratoplasty buttons obtained with optimised femtosecond laser settings," *British Journal of Ophthalmology*, vol. 96, no. 1, pp. 122–127, 2012.

[18] M. Lombardo, M. P. de Santo, G. Lombardo et al., "Surface quality of femtosecond dissected posterior human corneal stroma investigated with atomic force microscopy," *Cornea*, vol. 31, no. 12, pp. 1369–1375, 2012.

[19] S. K. Choi, J. H. Kim, and D. Lee, "The effect of femtosecond laser lamellar dissection at various depths on corneal endothelium in the recipient bed of the porcine eye," *Ophthalmic Surgery, Lasers and Imaging*, vol. 41, no. 2, pp. 255–260, 2010.

[20] L. Buzzonetti, A. Laborante, and G. Petrocelli, "Standardized big-bubble technique in deep anterior lamellar keratoplasty assisted by the femtosecond laser," *Journal of Cataract and Refractive Surgery*, vol. 36, no. 10, pp. 1631–1636, 2010.

[21] F. W. de Medeiros, H. Kaur, V. Agrawal et al., "Effect of femtosecond laser energy level on corneal stromal cell death and inflammation," *Journal of Refractive Surgery*, vol. 25, no. 10, pp. 869–874, 2009.

[22] K. N. Klingler, J. W. McLaren, W. M. Bourne, and S. V. Patel, "Corneal endothelial cell changes 5 years after laser in situ keratomileusis: femtosecond laser versus mechanical microkeratome," *Journal of Cataract & Refractive Surgery*, vol. 38, no. 12, pp. 2125–2130, 2012.

[23] K. Kamiya, A. Igarashi, R. Ishii, N. Sato, H. Nishimoto, and K. Shimizu, "Early clinical outcomes, including efficacy and endothelial cell loss, of refractive lenticule extraction using a 500 kHz femtosecond laser to correct myopia," *Journal of Cataract and Refractive Surgery*, vol. 38, pp. 1996–2002, 2012.

[24] M. Tomita, G. O. Waring, and M. Watabe, "Analysis of corneal endothelial cell density and morphology after laser in situ keratomileusis using two types of femtosecond lasers," *Clinical Ophthalmology*, vol. 6, no. 1, pp. 1567–1572, 2012.

[25] V. V. Mootha, E. Heck, S. M. Verity et al., "Comparative study of descemet stripping automated endothelial keratoplasty donor

preparation by moria cbm microkeratome, horizon microkeratome, and intralase FS60," *Cornea*, vol. 30, no. 3, pp. 320–324, 2011.

[26] P. M. Phillips, L. J. Phillips, H. A. Saad et al., ""Ultrathin" DSAEK tissue prepared with a low-pulse energy, high-frequency femtosecond laser," *Cornea*, vol. 32, no. 1, pp. 81–86, 2013.

[27] M. Kimakura, O. Sakai, S. Nakagawa et al., "Stromal bed quality and endothelial damage after into the deep corneal stroma," *British Journal of Ophthalmology*, vol. 97, no. 11, pp. 1404–1409, 2013.

[28] H. K. Soong, S. Mian, O. Abbasi, and T. Juhasz, "Femtosecond laser-assisted posterior lamellar keratoplasty: initial studies of surgical technique in eye bank eyes," *Ophthalmology*, vol. 112, no. 1, pp. 44–49, 2005.

Hindawi Publishing Corporation
BioMed Research International
Volume 2014, Article ID 748671, 9 pages
http://dx.doi.org/10.1155/2014/748671

Clinical Study

Evaluation of Corneal Deformation Analyzed with Scheimpflug Based Device in Healthy Eyes and Diseased Ones

Michele Lanza,[1,2] Michela Cennamo,[2] Stefania Iaccarino,[2] Carlo Irregolare,[2] Miguel Rechichi,[3] Mario Bifani,[1] and Ugo Antonello Gironi Carnevale[1]

[1] *Multidisciplinary Department of Medical, Surgical and Dental Sciences, Second University of Naples, Via De Crecchio 16, 80100 Napoli, Italy*
[2] *Centro Grandi Apparecchiature, Second University of Naples, Via De Crecchio 16, 80100 Napoli, Italy*
[3] *Santa Lucia Eye Clinic, Via Trieste 71, 00198 Cosenza, Italy*

Correspondence should be addressed to Michele Lanza; mic.lanza@gmail.com

Received 23 April 2014; Revised 4 June 2014; Accepted 9 June 2014; Published 23 June 2014

Academic Editor: Ciro Costagliola

This study was designed to evaluate the correlation between corneal biomechanical and morphological data in healthy eyes, eyes that underwent myopic photorefractive keratectomy (PRK), keratoconus affected eyes, and keratoconus affected eyes that underwent corneal collagen crosslinking (CCC). Complete clinical eye examination of all eyes was followed by tomographic (Pentacam, Oculus, Wetzlar, Germany) and biomechanical (Corvis ST, Oculus, Wetzlar, Germany) evaluation. Differences among Corvis ST (CST) parameters in the different groups have been performed. Linear regression between central corneal thickness (CCT), intraocular pressure (IOP), and anterior corneal curvature measured with Sim'K (KM), versus corneal deformation parameters measured with Corvis ST in the different groups, has been run using SPSS software version 18.0. We evaluated 64 healthy eyes of 64 patients with a mean refractive error of -0.65 ± 1.68 D (measured as spherical equivalent), 17 eyes of 17 patients that underwent myopic PRK for a mean refractive defect of -4.91 ± 2.05 D (measured as spherical equivalent), 16 eyes of 16 patients affected by keratconus (stage 2-3 of Amsler Classification), and 13 eyes of 13 patients affected by keratoconus that underwent CCC. Our data suggest that corneal curvature would have a greater influence on corneal deformation than CCT; in fact KM values are more strongly associated with more CST parameters both about corneal change in shape and both about the corneal ability to come back at original shape.

1. Introduction

Until a few years ago, the corneal parameters that were traditionally studied were central corneal thickness (CCT), corneal curvature (K), and transparency, measured using different devices such as keratometers, autokeratometers, corneal topographies, corneal tomographies, slit lamps, and confocal microscopes. In 2005, Reichert introduced a new instrument, the ocular response analyzer (ORA; Reichert Ophthalmic Instrument, Depew, NY, USA), a device able to measure, in vivo, other corneal properties such as corneal hysteresis (CH) and corneal resistance factor (CRF), using a collimated air pulse to applanate the central cornea [1]. Corneal biomechanical properties measured with ORA have been widely studied in healthy subjects and in patients affected by different kinds of ocular diseases [2–16], so they have today a role in the diagnosis, follow-up, and management of many of them [7, 9, 11]. Different papers, however, showed that CH and CRF are somehow affected by corneal morphological parameters [2, 10, 13, 14, 17, 18], that is, why new kinds of technologies, like optical coherence tomography, are lately utilized in corneal biomechanical evaluation [19–21]. It would be very important to have an accurate evaluation of corneal biomechanics because it would help us in better managing alterations due to a disease (i.e., keratoconus) or to iatrogenic causes (i.e., refractive surgery); moreover, it would help in better measuring the intraocular pressure (IOP), especially in eyes affected by corneal diseases, since the current gold standard, Goldmann applanation tonometry (GAT), has been largely proven to be

affected by corneal properties [6, 9, 12, 22]. The Corvis ST (Oculus, Wetzlar, Germany) (CST) is a new clinical device introduced to investigate corneal deformation properties; it uses an ultrahigh-speed Scheimpflug camera that records the deformation process in 4330 frames/sec along an 8 mm horizontal corneal coverage, while an air puff indentation causes corneal deformation (Figure 1). The ORA, instead, measures corneal shape changes with an electrooptical collimation detector system in the central 3.0 mm diameter area, throughout the 20 millisecond measurement [1].

Repeatability, reproducibility, and correlations between the parameters provided by CST have been studied by Hon and Lam [23] and by Nemeth et al. [24]; other authors evaluated CST in IOP measuring with no analysis of corneal deformation parameters [21, 25–27].

Purpose of our study is to evaluate the corneal behaviour using a Scheimpflug camera in corneas that are very different in their structure and morphology as in healthy eyes, in eyes that underwent myopic PRK, in keratoconus affected eyes, and in keratoconus affected eyes that underwent CCC. This kind of comparison has not been studied in published papers.

2. Materials and Methods

2.1. Subjects Enrolled. The study comprised 64 healthy eyes of 64 healthy subjects with a mean refractive error of −0.65 ± 1.68 D (measured as spherical equivalent), 17 eyes of 17 patients that underwent myopic PRK for a mean refractive defect of −4.91 ± 2.05 D, 16 eyes of 16 patients affected by keratoconus (KC) (stages 2 and 3 of Amsler classification) and 13 eyes of 13 patients affected by keratoconus that underwent CCC. All eyes underwent a complete ophthalmic evaluation and a corneal tomography performed using Pentacam and CST scan, and IOP evaluation with Goldmann applanation tonometry was run at last in order to not create bias in corneal evaluation. PRK and CCC patients were enrolled if they had surgery at least 1 year before. Patients with systemic and/or ocular diseases that could interfere with the corneal evaluation, such as diabetes, connective tissue disorders, dry eye, uveitis, corneal opacities, and glaucoma, were excluded from the study. Subjects wearing contact lenses were asked to stop using them at least 3 days before being evaluated. Details of different groups of patients are summarized in Table 1.

Patients that underwent PRK, enrolled in this study, did not have any complication as regression and haze and were evaluated at least 1 year after surgery, with no refractive and topographic changes from the last follow-up.

KC patients were diagnosed and staged according to Amsler classification (6 were ate stage 1, 8 were at stage 2, and 3 were at stage 3).

CCC was performed with epithelium removal and according to the Dresden Protocol [28] in patients with progressive KC (9 were at stage 2 and 7 were at stage 3 of Amsler classification); these patients were evaluated at least 1 year after treatment and were enrolled only if they did not report any complication.

We have not been able to perform a pre- and posttreatment evaluation in eyes that underwent PRK and CCC because CST has been available in our department only for 1 month.

Table 1: Mean, standard deviation (SD) and range of the parameters in the four groups evaluated in our study.

Parameters	Mean ± SD	Range
Healthy, $n = 64$		
Age (years)	35.21 ± 11.56	From 22 to 81
SE (D)	−0.65 ± 1.68	From −7.0 to 2.5
KM (D)	43.32 ± 1.26	From 40.9 to 45.9
CCT (μm)	553 ± 28.51	From 498 to 631
TP (μm)	551 ± 28.29	From 496 to 627
IOP (mmHg)	16.77 ± 2.31	From 13 to 24
PRK, $n = 17$		
Age (years)	32.39 ± 8.14	From 23 to 48
FU (months)	15.35 ± 1.69	From 13 to 17
KM (D)	40.26 ± 2.38	From 36.1 to 43.9
CCT pupil center (μm)	448 ± 34.33	From 390 to 495
CCT thinnest (μm)	447 ± 34.07	From 389 to 494
IOP (mmHg)	15.71 ± 1.72	From 13 to 19
KC, $n = 16$		
Age (years)	27.38 ± 6.09	From 19 to 37
KM (D)	47.7 ± 2.63	From 43.9 to 53.9
CCT pupil center (μm)	482 ± 52.60	From 426 to 548
CCT thinnest (μm)	459 ± 36.36	From 400 to 531
IOP (mmHg)	14.25 ± 1.89	From 11 to 16
CCC, $n = 13$		
Age (years)	24.44 ± 3.23	From 21 to 29
FU (months)	17.31 ± 1.11	From 15 to 18
KM (D)	47.52 ± 3.45	From 43.6 to 54.5
CCT pupil center (μm)	497 ± 32.59	From 460 to 551
CCT thinnest (μm)	478 ± 39.30	From 421 to 546
IOP (mmHg)	13.65 ± 1.38	From 11.5 to 16.0

SE: Spherical equivalent; FU: follow up from surgery; KM: anterior corneal curvature measured with Sim'K; CCT: central corneal thickness; TP: corneal thinnest point; intraocular pressure (IOP).

2.2. Devices. The Oculus Pentacam is a corneal tomographer utilizing a rotating Scheimpflug camera, largely used by ophthalmologists, and its working principles are well known [29]. For this study the 25 images per scan option were chosen. The parameters provided by Oculus Pentacam that we evaluated in this study were CCT at pupil center and anterior corneal curvature measured with Sim'K (KM).

The Corvis ST (CST) is a noncontact tonometer that measures corneal deformation [23]; parameters included in this study were the following:

(i) Time of Applanation 1 (AT1): time from the start until an air puff causes the corneal flattening (first applanation) as shown in Figure 1,

(ii) Length of Applanation 1 (AL1): length of the flattened cornea in the first applanation as shown in Figure 1,

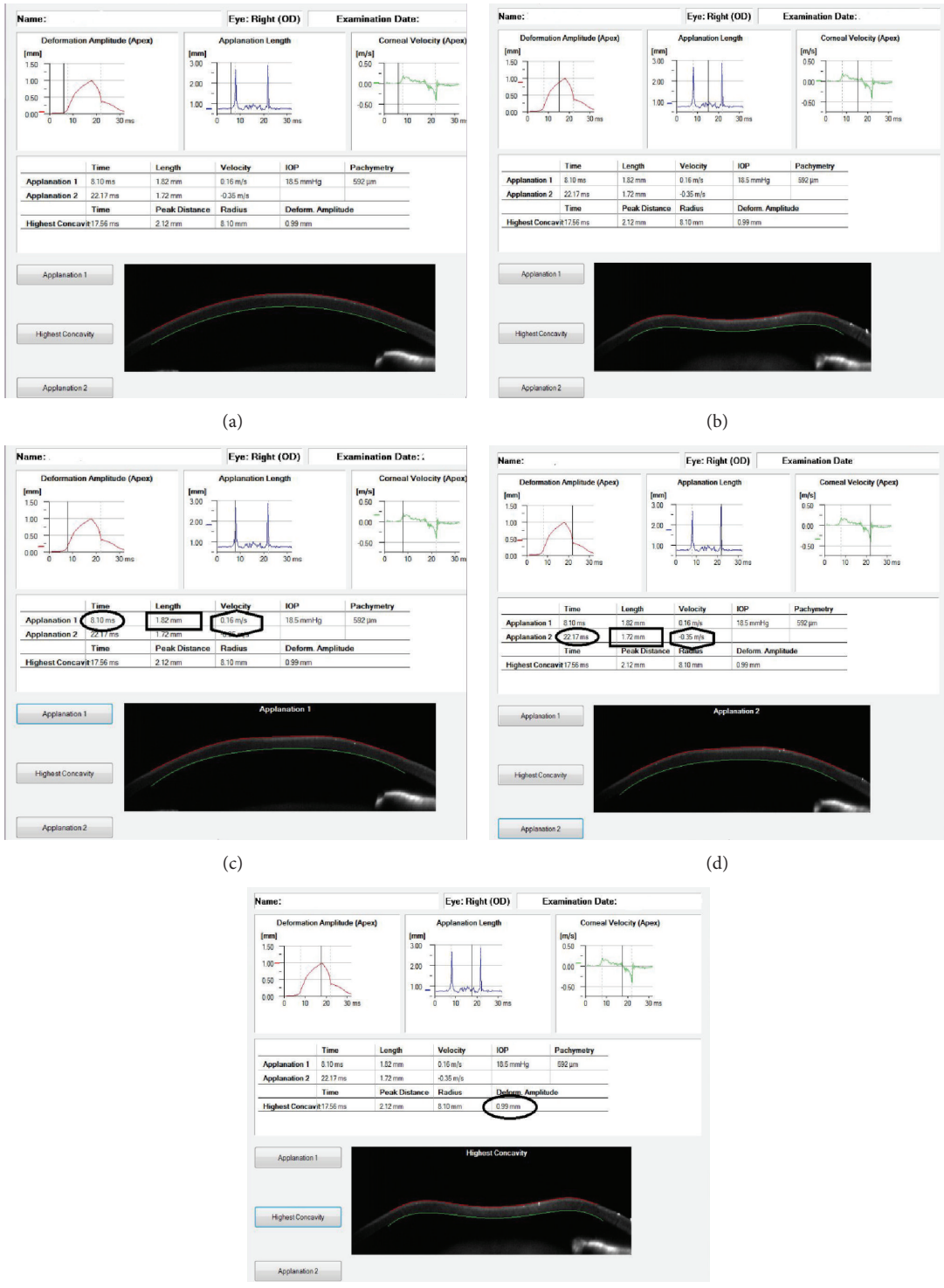

(a) (b)

(c) (d)

(e)

Figure 1: Screenshot of Corvis ST display, showing information recorded immediately upon the air impulse (a); screenshot of Corvis ST display, showing information recorded during the corneal deformation obtained by the air impulse (b); screenshot of Corvis ST display, showing Time of Applanation 1 (ellipse), Length of Applanation 1 (rectangle), Velocity of Applanation 1 (hexagon) at first applanation (c); screenshot of Corvis ST display, showing Time of Applanation 2 (ellipse), Length of Applanation 2 (rectangle), and Velocity of Applanation 2 (hexagon) at second applanation (d); screenshot of Corvis ST display, showing Deformation Amplitude at the highest concavity at corneal apex (ellipse) (e).

(iii) Velocity of Applanation 1 (AV1): velocity of corneal deformation during the first applanation as shown in Figure 1,

(iv) Time of Applanation 2 (AT2): time from the highest concavity until cornea restores its standard curvature,

(v) Length of Applanation 2 (AL2): length of the flattened cornea in the second applanation as shown in Figure 1,

(vi) Velocity of Applanation 2 (AV2): velocity of corneal deformation during the second applanation as shown Figure 1,

(vii) Deformation Amplitude at the Highest Concavity (HCDA): maximum deformation amplitude (from the start to the highest concavity) at the corneal apex as shown in Figure 1.

Three good quality Corvis ST measurements have been taken and every scan has been performed after 5 minutes from the previous one, so as to avoid an underestimation or overestimation of the corneal biomechanical parameters. All subjects started with the Pentacam evaluation and then underwent the CST one, in order to reduce bias in morphological measurements, since the air puff could introduce errors in corneal evaluation if Scheimpflug scan is performed after it. Two different and trained physicians used the two devices (MC used Pentacam and SI used CST) and they were not aware of the results obtained by the other. Despite the fact that all patients underwent bilateral evaluation, only the right eye results were included in the statistical analysis in order to eliminate any potential intrasubject effect that may occur if both eyes of the same patient were considered.

2.3. Statistical Analysis. The fulfilment of the data requirements for parametric analysis (normality, homogeneity of variance) was assessed by specific tests (Kolmogorov-Smirnov, Levene). All groups were compared with one-way factorial analysis of variance (ANOVA) for each parameter, followed by post hoc test LSD for single comparison. Moreover, the correlations among KM, CCT, IOP, and corneal deformation parameters measured with CST were evaluated using parametric (Pearson) test. For all tests the level of significance was set at $P < 0.05$. All analyses were performed using SPSS software version 18.0 (IBM Corp. Armonk, New York).

The study was performed in accordance with the ethical standards stated in the 1964 Declaration of Helsinki and approved by the local clinical research ethics committee; informed consent was obtained from all subjects before examination.

3. Results

Age and main corneal parameters of the four groups are summarized in Table 1.

Correlation between CST and Pentacam parameters are summarized in Table 2. In particular in healthy eyes AT1 show positive correlations with pachymetry and IOP and negative ones with KM. Similar correlations with IOP and KM are also present in KC and CCC groups. Also in the PRK group correlation with IOP is positive while that with KM becomes positive. AV1 shows a positive correlation with KM and a negative one with IOP in healthy and CCC groups. AT2 shows a positive correlation with KM and a negative correlation with pachymetry and IOP in the healthy group; the positive correlation with KM and the negative one with IOP are also present in the CCC group. In the PRK and KC groups AT2 is negatively correlated with IOP values. For AL2 there is only a negative correlation with KM in the healthy group. AV2 is correlated positively with pachymetry and IOP and negatively with KM in healthy and CCC groups. Positive correlations with KM and IOP are present in the PRK group. In the KC group AV2 is negatively correlated with KM values. HCDA shows a positive correlation with KM and a negative one with pachymetry and IOP in the healthy group. Similarly positive correlations with KM and negative ones with IOP are present in KC and CCC groups while negative correlations with KM and IOP appear in the PRK group.

The significant variations of corneal deformation parameters recorded in the different groups are summarized in Table 3 and Figures 2–6. In particular IOP values in healthy and post-PRK groups were statistically higher than the ones found in KC and post-CCC groups as shown in Table 3 (one

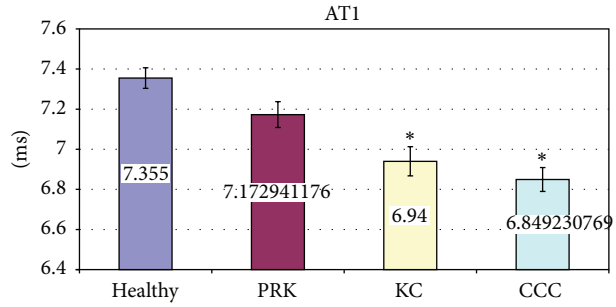

Figure 2: Comparison of Time of Applanation 1 (AT1) in healthy, postphotorefractive keratectomy (PRK), affected by keratoconus (KC) and postcorneal collagen cross-linking (CCC) subjects. Values are presented as mean ± standard error. Stars indicate significant differences ($P < 0.05$).

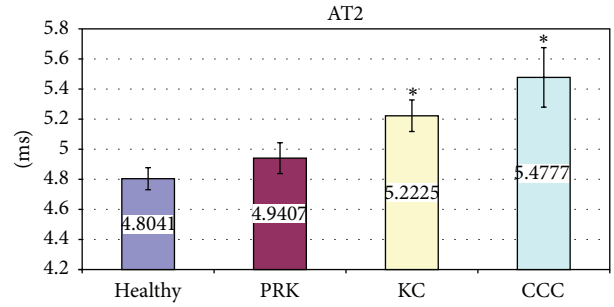

Figure 3: Comparison of Time of Applanation 2 (AT2) in healthy, post-PRK, KC, and post-CCC subjects. Values are presented as mean ± standard error. Stars indicate significant differences ($P < 0.05$).

Table 2: Pearson's parametric correlations among CST and Pentacam parameters in the four groups evaluated in our study. In bold significant results.

		HEALTHY			PRK			KC			CCC		
		KM	CCT	IOP	KM	CCT	IOP	KM	CCT	IOP	KM	CCT	IOP
AT1	Pearson correlation	**−0.371**	**0.442**	**0.932**	**0.690**	0.354	**0.997**	**−0.609**	0.474	**0.998**	**−0.570**	0.263	**0.994**
	P (2-tailed)	**0.022**	**0.005**	**0.000**	**0.002**	0.163	**0.000**	**0.012**	0.064	**0.000**	**0.042**	0.386	**0.000**
	N	38	38	64	17	17	17	16	16	16	13	13	13
AL1	Pearson correlation	−0.089	−0.006	0.005	−0.170	0.412	−0.063	0.003	0.111	0.475	0.178	0.019	−0.458
	P (2-tailed)	0.597	0.970	0.969	0.515	0.101	0.810	0.991	0.682	0.063	0.561	0.951	0.116
	N	38	38	64	17	17	17	16	16	16	13	13	13
AV1	Pearson correlation	**0.407**	−0.151	**−0.580**	−0.184	0.356	−0.261	0.478	−0.320	0.042	**0.650**	−0.016	**−0.561**
	P (2-tailed)	**0.011**	0.367	**0.000**	0.479	0.160	0.311	0.061	0.227	0.878	**0.016**	0.959	**0.046**
	N	38	38	64	17	17	17	16	16	16	13	13	13
AT2	Pearson correlation	**0.451**	**−0.329**	**−0.580**	−0.459	−0.399	**−0.812**	0.429	−0.423	**−0.655**	**0.886**	−0.486	**−0.691**
	P (2-tailed)	**0.005**	**0.043**	**0.000**	0.086	0.141	**0.000**	0.097	0.103	**0.006**	**0.000**	0.092	**0.009**
	N	38	38	64	15	15	15	16	16	16	13	13	13
AL2	Pearson correlation	**−0.327**	0.250	−0.011	0.152	0.173	0.383	−0.351	0.262	−0.174	−0.467	0.184	0.279
	P (2-tailed)	**0.045**	0.130	0.930	0.561	0.507	0.129	0.182	0.327	0.518	0.108	0.547	0.355
	N	38	38	64	17	17	17	16	16	16	13	13	13
AV2	Pearson correlation	**−0.512**	**0.326**	**0.581**	**0.579**	−0.025	**0.728**	**−0.621**	0.374	0.258	**−0.816**	**0.584**	**0.802**
	P (2-tailed)	**0.001**	**0.046**	**0.000**	**0.024**	0.931	**0.002**	**0.010**	0.154	0.334	**0.001**	**0.036**	**0.001**
	N	38	38	64	15	15	15	16	16	16	13	13	13
HCDA	Pearson correlation	**0.541**	**−0.440**	**−0.786**	**−0.546**	−0.155	**−0.838**	**0.718**	−0.383	**−0.715**	**0.852**	−0.463	**−0.894**
	P (2-tailed)	**0.000**	**0.006**	**0.000**	**0.024**	0.552	**0.000**	**0.002**	0.143	**0.002**	**0.000**	0.111	**0.000**
	N	38	38	64	17	17	17	16	16	16	13	13	13

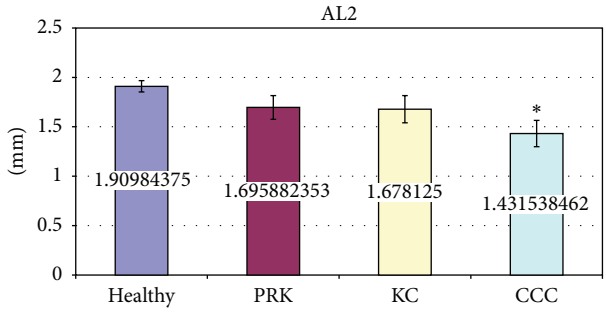

Figure 4: Comparison of Length of Applanation 2 (AL2) in healthy, post-PRK, KC, and post-CCC subjects. Values are presented as mean ± standard error. Stars indicate significant differences ($P < 0.05$).

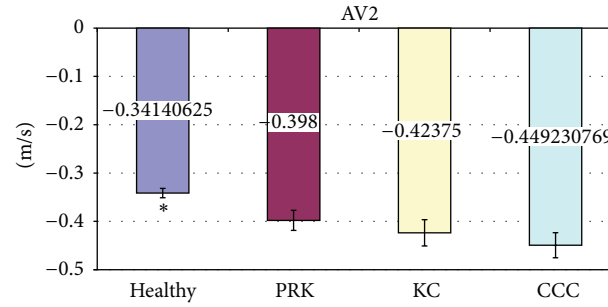

Figure 5: Comparison of Velocity of Applanation 2 (AV2) in healthy, post-PRK, KC, and post-CCC subjects. Values are presented as mean ± standard error. Stars indicate significant differences ($P < 0.05$).

way ANOVA: F: 12.14, $d.f.$: 3/109, $P < 0.000$). Post hoc LSD test gave significant differences between the KC and the healthy group (−15.0%, $P < 0.000$), the CCC and the healthy group (−18.6%, $P < 0.000$), the KC and the PRK group (−9.3%, $P < 0.047$), and the CCC and the PRK group (−13.1%, $P < 0.009$). Similarly AT1 values in healthy and post-PRK groups were statistically higher than the ones found in KC and post-CCC groups as shown in Figure 2 (one way ANOVA: F: 11.02, $d.f.$: 3/109, $P < 0.000$). Post hoc LSD test gave significant differences between the KC and the healthy group (−5.6%, $P < 0.000$), the CCC and the healthy group (−6.9%, $P < 0.000$), and the CCC and the PRK group (−4.5%, $P < 0.016$). Conversely AT2 values in healthy and post-PRK groups were statistically lower than the ones recorded in KC and post CCC groups as shown in Figure 3 (one way ANOVA: F: 6.93, $d.f.$: 3/107, $P < 0.000$). Post hoc LSD test gave significant differences between the KC and the healthy group (+8.7%, $P < 0.009$), the CCC and the healthy group (+14%, $P < 0.000$), and the CCC and the PRK group (10.9%, $P < 0.013$). AL2 was significantly higher in the healthy eyes group than in the others as shown in Figure 4 (one way ANOVA: F: 4.28, $d.f.$: 3/109, $P < 0.007$). Post hoc LSD test gave a significant difference only between the CCC and the healthy group (−25%, $P < 0.001$). Even AV2 was significantly

Table 3: Mean, standard deviation and range of the Corvis ST parameters in different groups evaluated in our study.

Parameters	Mean ± SD	Range
Healthy, $n = 64$		
Time of Applanation 1 (AT1) (ms)	7.36 ± 0.41	From 6.9 to 9.1
Length of Applanation 1 (AL1) (mm)	1.75 ± 0.27	From 1.3 to 2.3
Velocity of Applanation 1 (AV1) (m/s)	0.15 ± 0.04	From 0.0 to 0.2
Time of Applanation 2 (AT2) (ms)	4.80 ± 0.59	From 3.4 to 6.0
Length of Applanation 2 (AL2) (mm)	1.91 ± 0.46	From 1.0 to 2.7
Velocity of Applanation 2 (AV2) (m/s)	−0.34 ± 0.08	From −0.5 to −0.1
Deformation Amplitude at the highest concavity (HCDA) (mm)	1.02 ± 0.10	From 0.7 to 1.3
PRK, $n = 17$		
Time of Applanation 1 (AT1) (ms)	7.17 ± 0.27	From 6.9 to 7.7
Length of Applanation 1 (AL1) (mm)	1.87 ± 0.37	From 1.3 to 2.6
Velocity of Applanation 1 (AV1) (m/s)	0.17 ± 0.09	From 0.1 to 0.5
Time of Applanation 2 (AT2) (ms)	4.94 ± 0.40	From 4.2 to 5.6
Length of Applanation 2 (AL2) (mm)	1.70 ± 0.50	From 1.1 to 2.7
Velocity of Applanation 2 (AV2) (m/s)	−0.40 ± 0.08	From −0.5 to −0.3
Deformation Amplitude at the highest concavity (HCDA) (mm)	1.03 ± 0.11	From 0.8 to 1.2
KC, $n = 16$		
Time of Applanation 1 (AT1) (ms)	6.94 ± 0.29	From 6.4 to 7.3
Length of Applanation 1 (AL1) (mm)	1.66 ± 0.33	From 1.2 to 2.4
Velocity of Applanation 1 (AV1) (m/s)	0.17 ± 0.03	From 0.1 to 0.3
Time of Applanation 2 (AT2) (ms)	5.22 ± 0.42	From 4.6 to 5.9
Length of Applanation 2 (AL2) (mm)	1.68 ± 0.55	From 0.9 to 2.4
Velocity of Applanation 2 (AV2) (m/s)	−0.42 ± 0.11	From −0.6 to −0.2
Deformation Amplitude at the highest concavity (HCDA) (mm)	1.12 ± 0.16	From 0.8 to 1.5
CCC, $n = 13$		
Time of Applanation 1 (AT1) (ms)	6.85 ± 0.22	From 6.5 to 7.2
Length of Applanation 1 (AL1) (mm)	1.69 ± 0.28	From 1.3 to 2.2
Velocity of Applanation 1 (AV1) (m/s)	0.17 ± 0.04	From 0.1 to 0.2
Time of Applanation 2 (AT2) (ms)	5.48 ± 0.71	From 4.6 to 6.8
Length of Applanation 2 (AL2) (mm)	1.43 ± 0.48	From 0.9 to 2.4
Velocity of Applanation 2 (AV2) (m/s)	−0.45 ± 0.09	From −0.6 to −0.3
Deformation Amplitude at the highest concavity (HCDA) (mm)	1.19 ± 0.14	From 1.0 to 1.5

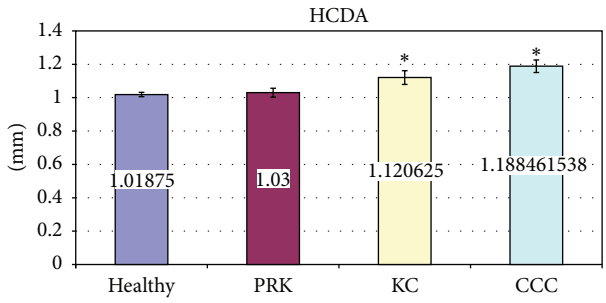

Figure 6: Comparison of Deformation Amplitude at the highest concavity (HCDA) in healthy, post-PRK, KC, and post-CCC subjects. Values are presented as mean ± standard error. Stars indicate significant differences ($P < 0.05$).

higher in the healthy eyes group than in others as shown in Figure 5 (one way ANOVA: F: 8.83, $d.f.$: 3/107, $P < 0.000$). For the healthy eyes group, post hoc LSD test gave significant differences versus PRK (−16.6%, $P < 0.022$), KC (−24.1%, $P < 0.001$), and CCC (−31.6%, $P < 0.000$). Finally HCDA in healthy and post-PRK groups was statistically lower than the one found in KC and post-CCC groups as shown in Figure 6 (one way ANOVA: F: 9.31, $d.f.$: 3/109, $P < 0.000$). Post hoc LSD test gave significant differences between the KC and the healthy group (+10.0%, $P < 0.003$), the CCC and the healthy group (+16.7%, $P < 0.000$), the KC and the PRK group (+8.8%, $P < 0.031$), and the CCC and the PRK group (+15.4%, $P < 0.000$).

4. Discussion

It is well known that the study of the biomechanical properties of the cornea is important for the diagnosis and follow-up of several ocular conditions. Many papers evaluate corneal parameters measured using ORA [1–16]. Corvis ST, the first noncontact tonometer incorporating Scheimpflug technology, has recently been introduced as a clinical device

in ophthalmology to measure both IOP and corneal deformation properties [23, 24, 27].

Changes in corneal deformation are related not only to corneal structure organization and to IOP, but also to corneal biomechanics [6]; biomechanical properties measured by ORA provided information that are not always unanimous [2, 10, 13, 17, 18]. It would be very important to better understand corneal behaviour during shape modifications and corneal biomechanical properties, and this information could be used in different fields such as the following:

(i) having more precise values of IOP, especially in case of eyes affected by corneal disease or in ones that underwent a shape change, as happens after corneal refractive surgery,

(ii) better understanding the evolution of corneal degenerative diseases like keratoconus, in which we observe a change both in shape and in biomechanics [4, 10],

(iii) better screening corneas undergoing refractive surgery in order to avoid complications like ectasia.

There are limitations to this study that should be noted, first, the limited number of participants per group and we did not evaluate the corneal parameters before and after treatment as PRK and CCC but CST has been available in our department only for 1 month so we did not have time to collect these data.

AT2 values, as provided by CST, are the total of milliseconds calculated from the start of deformation until the flattened cornea rebounds from its highest concavity, reaching the second applanation.

In order to achieve a better understanding of corneal shape-changing process, we used the value obtained subtracting AT2, provided by the device, to AT1 (time from the start until an air puff causes the first corneal applanation). In this way, we obtained the time needed by the cornea to come back to a flat position after reaching the maximum deformation (HCDA) and, in our opinion, this value provides us a better idea of the time taken by the cornea to come back to its original shape after a deformation.

AT2 in fact, as you can read on CST display, is the total time from the start of the analysis, so if we had studied this parameter, our analysis about the difference between the corneal resistance to external modification and the capability of the cornea to return to its original shape after a deformation may have been biased.

According to our data, healthy and post-PRK eyes showed higher AT1 and lower AT2 compared to KC eyes and post-CCC eyes.

Corneas that are affected by KC, even if they underwent CCC, seem to be easier to applanate, compared to healthy and post PRK ones, so they show a lower resistance to deformation; moreover, it seems like they take more time to return to the applanation position and so recover the original shape. We noted with interest that corneas after PRK did not show the same values, as if the corneal thinning they underwent did not influence much their behaviour compared to healthy corneas.

It is well known that both KC and post-PRK corneas have morphological and structural differences with healthy ones; according to our data it is possible to imagine that KC induces greater changes in corneal structure that make the cornea easier to modify not only in relation to the thinning it shows; moreover, these changes prevent reaching the original shape after modifications due to external factors.

The higher deformation that KC and post CCC corneas could have is confirmed by the higher values of HCDA observed, compared with healthy and post-PRK ones.

According to our data, KM shows a significant correlation with some of the CST parameters analyzed (AT1, AT2, VA2, and HCDA) whereas CCT does not show a significant correlation in the post-PRK, KC, and post-CCC groups.

KM and CCT show a significant correlation with AT1, AT2, VA2, and HCDA in healthy corneas.

This could mean that KM influences more the deformation than corneal thickness does, in diseased corneas. This influence, however, does not seem to be the same in the four groups studied, AT1 showed values negatively correlated to KM in healthy, KC and post-CCC corneas show, indicating a higher difficulty in applanating flatter corneas whereas in eyes that underwent PRK we observed the opposite correlation.

Previous data suggest that KC and post-CCC corneas seem to be easier to modify in shape, so it is simple to imagine that the higher the corneal curvature is in healthy eyes, the less the time it takes to applanate them. In eyes after PRK, however, we observe the opposite tendency so the flatter the cornea is, the easier it is to applanate; a possible explanation is that the tissue ablation after myopic PRK makes corneas weaker to external deformations. So the greater the flattening is (meaning a higher treatment), the faster you can achieve the corneal applanation.

Interestingly, we did not observe the same correlations between CST parameters and CCT.

IOP values are directly correlated with AT1 and AV2 and inversed correlated with AV1, AT2, and HCDA in every group analyzed. Only in KC eyes AV2 is directly related but without significant value. These results mean that the resistance that IOP apply to deformation and the help that it lends in restoring the original corneal shape are effective in healthy corneas, KC ones, and ones after PRK and after CCC. The not significant value observed in AV2-IOP correlation in KC eyes could be due to two factors.

(1) The small number of KC group biased the analysis.

(2) IOP could not influence the corneal speed to come back at its original shape after a deformation, but this characteristic could depend from some other structural properties.

Our data support the hypothesis that corneal thinning is not the only factor that can explain the changes in corneal behavior we observe in affected corneas, and we know that biomechanic properties have an important role [1–7] but till now we could study it only with two parameters using only one device [1–7]. Values provided by CST in different groups we studied let us think that corneal deformation induced by KC (such as corneal curvature and thinning) is deeper and

affects more the whole cornea making it easier to deform, compared to corneal deformation induced by PRK.

5. Conclusions

Although our results need to be confirmed in further studies with a larger population, they seem to be very interesting: according to our data, corneal deformation detected by CST is related much more to the corneal curvature than to the corneal thickness, especially in diseased corneas. This means that, in corneal disease screening, KM should be more important than CCT. Moreover, our study provides differences in CTS parameters in the groups analyzed and these values could be used to recognize healthy corneas, diseased ones, and borderline ones. Further studies are needed to better understand if CTS could be usefully used in clinical practice to screen eyes undergoing refractive surgery, eyes with KC at early stage, ectatic corneas, or other corneal diseases.

Conflict of Interests

The authors declare that there is no conflict of interests regarding the publication of this paper.

References

[1] D. A. Luce, "Determining in vivo biomechanical properties of the cornea with an ocular response analyzer," *Journal of Cataract and Refractive Surgery*, vol. 31, no. 1, pp. 156–162, 2005.

[2] S. Franco and M. Lira, "Biomechanical properties of the cornea measured by the Ocular Response Analyzer and their association with intraocular pressure and the central corneal curvature," *Clinical and Experimental Optometry*, vol. 92, no. 6, pp. 469–475, 2009.

[3] J. S. Pepose, S. K. Feigenbaum, M. A. Qazi, J. P. Sanderson, and C. J. Roberts, "Changes in corneal biomechanics and intraocular pressure following LASIK using static, dynamic, and noncontact tonometry," *American Journal of Ophthalmology*, vol. 143, no. 1, pp. 39.e1–47.e1, 2007.

[4] D. Ortiz, D. Piñero, M. H. Shabayek, F. Arnalich-Montiel, and J. L. Alió, "Corneal biomechanical properties in normal, post-laser in situ keratomileusis, and keratoconic eyes," *Journal of Cataract and Refractive Surgery*, vol. 33, no. 8, pp. 1371–1375, 2007.

[5] J. Kerautret, J. Colin, D. Touboul, and C. Roberts, "Biomechanical characteristics of the ectatic cornea," *Journal of Cataract & Refractive Surgery*, vol. 34, no. 3, pp. 510–513, 2008.

[6] J. Liu and C. J. Roberts, "Influence of corneal biomechanical properties on intraocular pressure measurement: quantitative analysis," *Journal of Cataract and Refractive Surgery*, vol. 31, no. 1, pp. 146–155, 2005.

[7] A. Kotecha, "What biomechanical properties of the cornea are relevant for the clinician?" *Survey of Ophthalmology*, vol. 52, no. 6, pp. 109–114, 2007.

[8] J. M. Martinez-De-La-Casa, J. Garcia-Feijoo, A. Fernandez-Vidal, C. Mendez-Hernandez, and J. Garcia-Sanchez, "Ocular response analyzer versus Goldmann applanation tonometry for intraocular pressure measurements," *Investigative Ophthalmology and Visual Science*, vol. 47, no. 10, pp. 4410–4414, 2006.

[9] N. Terai, F. Raiskup, M. Haustein, L. E. Pillunat, and E. Spoerl, "Identification of biomechanical properties of the cornea: the ocular response analyzer," *Current Eye Research*, vol. 37, no. 7, pp. 553–562, 2012.

[10] V. Hurmeric, A. Sahin, G. Ozge, and A. Bayer, "The relationship between corneal biomechanical properties and confocal microscopy findings in normal and keratoconic eyes," *Cornea*, vol. 29, no. 6, pp. 641–649, 2010.

[11] C. W. McMonnies, "Assessing corneal hysteresis using the ocular response analyzer," *Optometry and Vision Science*, vol. 89, no. 3, pp. E343–E349, 2012.

[12] A. Kotecha, A. Elsheikh, C. R. Roberts, H. Zhu, and D. F. Garway-Heath, "Corneal thickness- and age-related biomechanical properties of the cornea measured with the ocular response analyzer," *Investigative Ophthalmology and Visual Science*, vol. 47, no. 12, pp. 5337–5347, 2006.

[13] A. Narayanaswamy, R. S. Chung, R. Wu et al., "Determinants of corneal biomechanical properties in an adult Chinese population," *Ophthalmology*, vol. 118, no. 7, pp. 1253–1259, 2011.

[14] B. M. Fontes, R. Ambrósio Jr., R. S. Alonso, D. Jardim, G. C. Velarde, and W. Nosé, "Corneal biomechanical metrics in eyes with refraction of −19.00 to +9.00 D in healthy Brazilian patients," *Journal of Refractive Surgery*, vol. 24, no. 9, pp. 941–945, 2008.

[15] N. Kara, H. Altinkaynak, O. Baz, and Y. Goker, "Biomechanical evaluation of cornea in topographically normal relatives of patients with keratoconus," *Cornea*, vol. 32, no. 3, pp. 262–266, 2013.

[16] N. G. Congdon, A. T. Broman, K. Bandeen-Roche, D. Grover, and H. A. Quigley, "Central corneal thickness and corneal hysteresis associated With glaucoma damage," *American Journal of Ophthalmology*, vol. 141, no. 5, pp. 868–875, 2006.

[17] S. Shah, M. Laiquzzaman, I. Cunliffe, and S. Mantry, "The use of the Reichert ocular response analyser to establish the relationship between ocular hysteresis, corneal resistance factor and central corneal thickness in normal eyes," *Contact Lens and Anterior Eye*, vol. 29, no. 5, pp. 257–262, 2006.

[18] D. Touboul, C. Roberts, J. Kérautret et al., "Correlations between corneal hysteresis, intraocular pressure, and corneal central pachymetry," *Journal of Cataract and Refractive Surgery*, vol. 34, no. 4, pp. 616–622, 2008.

[19] D. Alonso-Caneiro, K. Karnowski, B. J. Kaluzny, A. Kowalczyk, and M. Wojtkowski, "Assessment of corneal dynamics with high-speed swept source Optical Coherence Tomography combined with an air puff system," *Optics Express*, vol. 19, no. 15, pp. 14188–14199, 2011.

[20] C. Dorronsoro, D. Pascual, P. Pérez-Merino, S. Kling, and S. Marcos, "Dynamic OCT measurement of corneal deformation by an air puff in normal and cross-linked corneas," *Biomedical Optics Express*, vol. 3, no. 3, pp. 473–487, 2012.

[21] J. Hong, J. Xu, A. Wei et al., "A new tonometer-the corvis ST tonometer: clinical comparison with noncontact and goldmann applanation tonometers," *Investigative Ophthalmology and Visual Science*, vol. 54, no. 1, pp. 659–665, 2013.

[22] M. J. Doughty and M. L. Zaman, "Human corneal thickness and its impact on intraocular pressure measures: a review and meta-analysis approach," *Survey of Ophthalmology*, vol. 44, no. 5, pp. 367–408, 2000.

[23] Y. Hon and A. K. C. Lam, "Corneal deformation measurement using scheimpflug noncontact tonometry," *Optometry and Vision Science*, vol. 90, no. 1, pp. e1–e8, 2013.

[24] G. Nemeth, Z. Hassan, A. Csutak, E. Szalai, A. Berta, and L. Modis Jr., "Repeatability of ocular biomechanical data measurements with a scheimpflug-based noncontact device on normal corneas," *Journal of Refractive Surgery*, vol. 29, no. 8, pp. 558–563, 2013.

[25] A. Smedowski, B. Weglarz, D. Tarnawska, K. Kaarniranta, and E. Wylegala, "Comparison of three intraocular pressure measurement methods including biomechanical properties of the cornea," *Investigative Ophthalmology & Visual Science*, vol. 55, no. 2, pp. 666–673, 2014.

[26] T. Huseynova, G. O. Waring IV, C. Roberts, R. R. Krueger, and M. Tomita, "Corneal biomechanics as a function of intraocular pressure and pachymetry by dynamic infrared signal and scheimpflug imaging analysis in normal eyes," *American Journal of Ophthalmology*, vol. 157, no. 4, pp. 885–893, 2014.

[27] L. Reznicek, D. Muth, A. Kampik, A. S. Neubauer, and C. Hirneiss, "Evaluation of a novel Scheimpflug-based non-contact tonometer in healthy subjects and patients with ocular hypertension and glaucoma," *British Journal of Ophthalmology*, vol. 97, no. 11, pp. 1410–1414, 2013.

[28] G. Wollensak, E. Spoerl, and T. Seiler, "Riboflavin/ultraviolet-a-induced collagen crosslinking for the treatment of keratoconus," *The American Journal of Ophthalmology*, vol. 135, no. 5, pp. 620–627, 2003.

[29] N. Rosa, M. de Bernardo, M. Borrelli, M. L. Filosa, and M. Lanza, "Effect of oxybuprocaine eye drops on corneal volume and thickness measurements," *Optometry and Vision Science*, vol. 88, no. 5, pp. 640–644, 2011.

Hindawi Publishing Corporation
BioMed Research International
Volume 2014, Article ID 140461, 5 pages
http://dx.doi.org/10.1155/2014/140461

Clinical Study

Outcome of Corneal Collagen Crosslinking for Progressive Keratoconus in Paediatric Patients

Deepa Viswanathan,[1] Nikhil L. Kumar,[1,2] and John J. Males[1,3]

[1] *Australian School of Advanced Medicine, Macquarie University, Sydney, NSW 2109, Australia*
[2] *Sydney Adventist Hospital Clinical School, The University of Sydney, Sydney, NSW 2076, Australia*
[3] *Sydney eye hospital, The University of Sydney, Sydney, NSW 2000, Australia*

Correspondence should be addressed to Deepa Viswanathan; viswamdeepa@gmail.com

Received 19 February 2014; Revised 22 May 2014; Accepted 22 May 2014; Published 11 June 2014

Academic Editor: Ciro Costagliola

Purpose. To evaluate the efficacy of corneal collagen crosslinking for progressive keratoconus in paediatric patients. *Methods*. This prospective study included 25 eyes of 18 patients (aged 18 years or younger) who underwent collagen crosslinking performed using riboflavin and ultraviolet-A irradiation (370 nm, 3 mW/cm^2, 30 min). *Results*. The mean patient age was 14.3 ± 2.4 years (range 8–17) and mean followup duration was 20.1 ± 14.25 months (range 6–48). Crosslinked eyes demonstrated a significant reduction of keratometry values. The mean baseline simulated keratometry values were 46.34 dioptres (D) in the flattest meridian and 50.06 D in the steepest meridian. At 20 months after crosslinking, the values were 45.67 D ($P = 0.03$) and 49.34 D ($P = 0.005$), respectively. The best spectacle corrected visual acuity (BSCVA) and topometric astigmatism improved after crosslinking. Mean logarithm of the minimum angle of resolution (logMAR) BSCVA decreased from 0.24 to 0.21 ($P = 0.89$) and topometric astigmatism reduced from mean 3.50 D to 3.25 D ($P = 0.51$). *Conclusions*. Collagen crosslinking using riboflavin and ultraviolet-A is an effective treatment option for progressive keratoconus in paediatric patients. Crosslinking stabilises the condition and, thus, reduces the need for corneal grafting in these young patients.

1. Introduction

Keratoconus is a degenerative corneal disorder charecterised by corneal thinning, conical protrusion, irregular astigmatism, and visual impairment [1]. Keratoconic eyes have an altered corneal biomechanical profile and appear to be more elastic and less rigid than normal eyes [2]. Keratoconus usually manifests during adolescence and early adulthood. Young patients are at risk for faster disease progression and corneal grafting often becomes necessary for visual rehabilitation [3].

Corneal collagen crosslinking (CXL) is a recently introduced treatment for addressing progressive keratoconus. It is a minimally invasive procedure and the only option that halts or slows disease progression. Riboflavin and ultraviolet-A induce crosslinking through photopolymerization of collagen mediated by reactive oxygen species and, thus, increase corneal biomechanical rigidity and biochemical resistance [4–6].

Several clinical studies have demonstrated that CXL effectively slows keratoconus progression in adult eyes [7–13]. Recently, CXL has been recommended as an optimal intervention for progressive Keratoconus affecting the paediatric population [14–17].

Therefore CXL could potentially reduce the need for corneal grafting in these young individuals. This is particularly relevant as paediatric patients have a greater risk of corneal transplant rejection [17]. We observed favourable results after CXL in adult eyes [13] and this study aims to evaluate its efficacy in treating progressive keratoconus affecting paediatric subjects.

2. Materials and Methods

Twenty five eyes of 18 patients (5 females, 13 males) with progressive keratoconus underwent CXL and were enrolled in this prospective study. Only patients who completed

a minimum of 6 months follow-up after the procedure were included. The institutional ethics committee approved the study and parents provided informed consent prior to treatment.

2.1. Inclusion Criteria. Patients aged less than 18 years with progressive early to moderate keratoconus (grades I to III according to the Amsler-Krumeich classification) with a minimum corneal thickness of at least 400 microns were included [18]. Indications for treatment included an increase in steep keratometry of 1.00 dioptre (D) or more in 1 year, deterioration in visual acuity, and the need for new contact lens fitting more than once in 2 years. Exclusion criteria were advanced keratoconus with stromal scarring, corneal thickness less than 400 microns, corneal hydrops, severe dry eye, corneal infections, previous ocular surgery, and autoimmune diseases.

2.2. Tests and Evaluation. Soft contact lenses were discontinued for a minimum of 3 days and rigid-gas permeable and hard lenses were discontinued for minimum of 2 weeks before preoperative eye examination. Evaluation of visual acuity, manifest refraction, corneal topography, and corneal pachymetry was performed preoperatively and postoperatively in all subjects. The logMAR BSCVA was obtained using the early treatment of diabetic retinopathy study chart (ETDRS). Manifest refraction was performed and the manifest refraction spherical equivalent (MRSE) was analysed. Corneal topography and corneal thickness measurements (pachymetry) were performed using a noncontact rotating Scheimpflug camera (Pentacam, Oculus Inc., Germany).

2.3. Crosslinking Technique. Corneal collagen crosslinking was performed using 0.1% riboflavin (in 20% dextran T 500) and ultraviolet A (UVA) irradiation (370 nm, 3 mW/cm^2, 30 min) under sterile conditions. The UV-X 1000 machine (IROC Innocross AG, Zurich, Switzerland) and the Innocross-R riboflavin isotonic solution (riboflavin 5-phosphate (0.1%) plus 20% Dextran T500 in 2 ml syringes) were used. The procedure was performed under general anaesthesia in very young patients and under topical anaesthesia in older patients. After anaesthesia, a lid speculum was inserted and the corneal epithelium was soaked with 20% alcohol for 40 seconds. The epithelial tissue was then removed in a 9.0 mm diameter area with a cellulose surgical spear to allow penetration of riboflavin into the corneal stroma. Thereafter, the photosensitizer 0.1% riboflavin was applied (2 to 3 drops every 3 minutes) to the cornea for 30 minutes before irradiation to allow sufficient saturation of the stroma.

Corneal soaking of riboflavin was assessed and then the central 8.0 mm cornea was exposed to UVA light (wavelength of 370 nm and irradiance of 3 mW/cm^2) for 30 minutes. Throughout the UVA exposure, riboflavin solution was instilled (2 to 3 drops every 3 minutes). Upon completion of treatment, the eye was washed with balanced salt solution and antibiotic eye drops (ofloxacin 0.3%) and steroid eye drops (dexamethasone 0.1%) were applied. A bandage contact lens was placed in the eye until complete reepithelialization.

Table 1: Pre- and postcrosslinking data for treated eyes.

Parameter	Pre-CXL	Post-CXL	P value
BSCVA (logMAR)	0.24 ± 0.19	0.21 ± 0.13	0.89
MRSE (dioptres)	−5.66 ± 3.47	−4.71 ± 3.11 D	0.71
$K1$ (dioptres)	46.34 ± 3.13 D	45.67 ± 3.31 D	0.03
$K2$ (dioptres)	50.06 ± 3.84 D	49.34 ± 3.18 D	0.005
Topometric astigmatism (dioptres)	3.50 ± 1.36 D	3.25 ± 1.79 D	0.51

BSCVA: best spectacle corrected visual acuity, logMAR: logarithm of the minimum angle of resolution, MRSE: manifest refraction spherical equivalent, $K1$: mean simulated keratometry value in the flattest meridian, and $K2$: mean simulated keratometry value in the steepest meridian.

Subsequent follow-up examinations were performed at 1 week and thereafter at 1, 6, 12, 18, and 24 months and annually thereafter. The BSCVA, corneal topography, and central corneal thickness (CCT) were recorded at each visit.

2.4. Statistical Analysis. The changes in simulated keratometry values in the flattest meridian (*K1*) and the steepest meridian (*K2*), topometric astigmatism, manifest refraction, and BSCVA were analysed to evaluate the effect of crosslinking treatment. This was performed by subtracting each parameter at the respective follow-up examination from the preprocedure value. Postprocedure data was available for all 25 eyes. Statistical evaluation was performed by SPSS software version 19. The paired t-test was used to evaluate the differences in the different parameters between pre- and postprocedure values and a P value of ≤0.05 was considered to be statistically significant.

3. Results

The mean patient age was 14.3 ± 2.4 years (range 8–17 years); there were 5 females and 13 males. The risk factors for Keratoconus development in the patient population included eye rubbing in 58.8% patients and atopy in 47.10% patients. The outcomes after crosslinking at mean follow-up of 20.1 ± 14.25 months (range 6–48 months) are shown in Table 1.

Visual Acuity. The mean logMAR BSCVA improved by 0.02 ± 0.19 ($P = 0.89$) at mean 20-month follow-up after CXL.

Manifest Refraction. There was a reduction in mean spherical equivalent from −5.66 ± 3.47 D to −4.71 ± 3.11 D ($P = 0.71$) in treated eyes at mean follow-up of 20 months.

Corneal Topography. There was a significant reduction in keratometry values following crosslinking. The mean simulated keratometry value in the flattest meridian (*K1*) reduced by 0.66 ± 1.38 D ($P = 0.03$) and the mean simulated keratometry value in the steepest meridian (*K2*) reduced by 0.72 ± 1.17 D ($P = 0.009$) at 20-months follow-up.

There was a decrease in topometric astigmatism by 0.20 ± 1.44D ($P = 0.51$) after crosslinking. Figure 1 shows the difference in *K2* between pre- and post-CXL treated eyes at mean 20-month follow-up. Corneal curvature was either

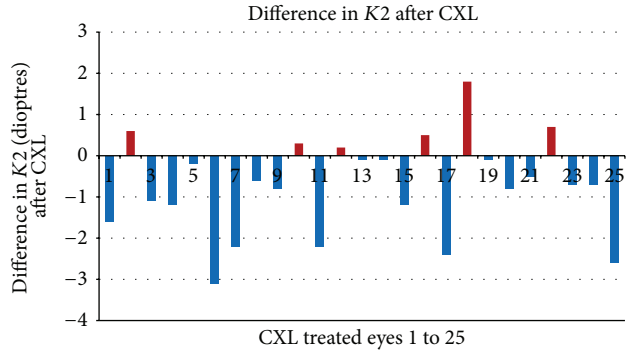

Figure 1: Difference in *K2* between pre- and post-CXL treated eyes.

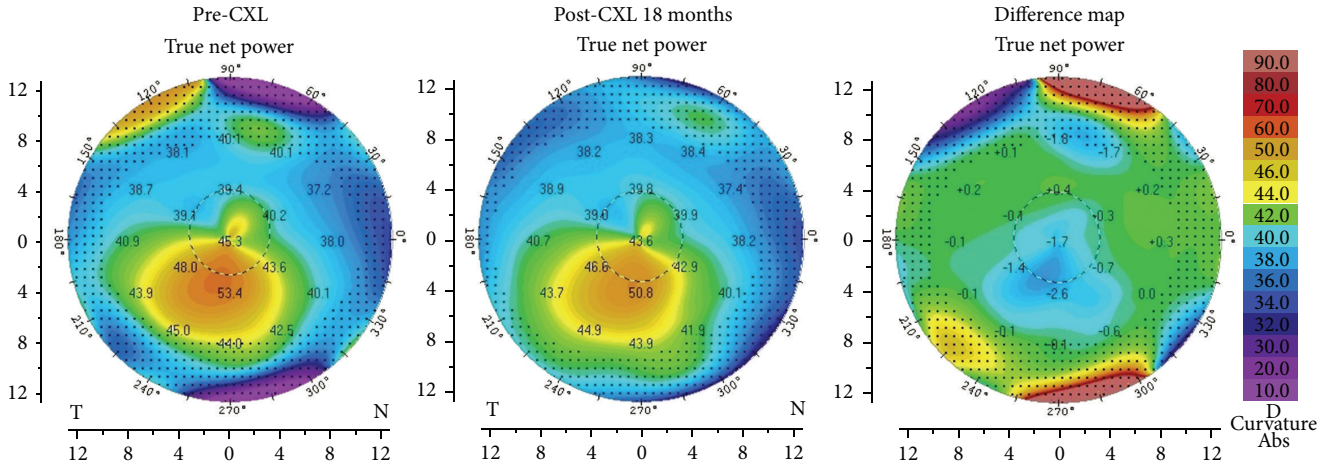

Figure 2: Corneal topography showing a reduction in keratometry after CXL.

reduced or remained stable (within 0.5 D of pre-CXL *K2*) after CXL in 88% (22/25) eyes.

Corneal topography of a crosslinked eye is shown in Figure 2. At 18 months after CXL, there was a reduction in *K2* by 1.8 D in the treated eye. No serious complications like infections or stromal scarring were noted in this series.

4. Discussion

We assessed the topographic, refractive, and visual outcomes of corneal UV collagen crosslinking in a cohort of paediatric patients with progressive keratoconus. At 20 months after crosslinking, there was a mean reduction in simulated keratometry values by 0.66 D in the flattest meridian and by 0.72 D in the steepest meridian. This was associated with an improvement in visual acuity and topometric astigmatism, although these improvements were not statistically significant.

Collagen crosslinking involves a photopolymerization reaction that induces biochemical and microstructural changes within the corneal stroma [4–6]. These include the generation of stiffer collagen fibrils and a rearrangement of corneal lamellae within the matrix [19, 20]. These structural and biomechanical changes after crosslinking result in a regression of corneal curvature and improved shape thus stabilising keratoconus and preventing further progression.

We had previously reported favourable results after collagen crosslinking in adult Keratoconic eyes consistent with other published studies [8–13]. Similar to our adult cohort, this study included only patients who had completed a minimum of 6 months follow-up after CXL. This is based on previous long term studies that reported an initial worsening of corneal curvature followed by subsequent flattening and stabilisation after CXL [9, 11].

In recent times, the age limit for CXL has lowered considerably [14–16]. In this study, the youngest patient was 8 years old and to the best of our knowledge is the youngest patient reported to undergo crosslinking. Vinciguerra et al. evaluated the long term outcome of CXL for progressive keratoconus in different age groups, including 49 eyes of patients aged below 18 years [21]. Interestingly, their results indicated better functional and morphologic outcomes in young adults (age 18–39 years) as compared to the paediatric age group.

Arora et al. conducted a prospective contralateral case control study and included 15 eyes of 15 keratoconic patients that underwent CXL [17]. The criteria for performing CXL were not documented progressions, but the advanced keratoconus status in the fellow eye. At 1 year after CXL, significant

improvements were noted in logMAR BSCVA and apical keratometry. In comparison, CXL was performed only on progressive paediatric keratoconic eyes in the current study and albeit a longer follow-up, significant improvements were noted only for keratometry values and not for BSCVA.

Magli et al. recently compared the efficacy of transepithelial CXL (TE-CXL) to conventional epithelium-off CXL in paediatric patients [22]. At 12-month follow-up, they observed that TE-CXL had similar efficacy, but was less painful and had fewer complications than epithelium-off CXL. Similarly, Salman performed a prospective case control study on the efficacy and safety of TE-CXL in children and reported satisfactory results [23]. In the current study, crosslinking was performed using the epithelium-off technique and no serious complications were noted.

In their series of paediatric crosslinking, Caporossi et al. report worsening in terms of topographic and pachymetic data in 4.6% of eyes; however the term "worsening" is not defined [16]. We observed worsening of the steep keratometry value (*K2*) by more than 0.5 D in 3 crosslinked eyes. However, an increase in *K2* exceeding 1 D occurred in only 1 eye which was not associated with a decrease in BSCVA. We presume that this reflects the fast rate of keratoconus progression in paediatric eyes. Therefore, earlier studies have suggested a closer follow-up schedule for children with keratoconus to rapidly identify deterioration.

This study demonstrates that collagen crosslinking can result in a significant reduction in corneal curvature and can stabilise progressive keratoconus in patients younger than 18 years. These encouraging results emphasize the need for early treatment in these young patients to prevent them from unnecessarily undergoing corneal grafting. The optimal timing of intervention however remains debatable with some authors suggesting crosslinking at diagnosis of keratoconus without awaiting disease progression [24].

Conflict of Interests

No conflicting relationship exists for any author.

References

[1] Y. S. Rabinowitz, "Keratoconus," *Survey of Ophthalmology*, vol. 42, no. 4, pp. 297–319, 1998.

[2] C. Edmund, "Assessment of an elastic model in the pathogenesis of keratoconus," *Acta Ophthalmologica*, vol. 65, no. 5, pp. 545–550, 1987.

[3] S. W. Reeves, S. Stinnett, R. A. Adelman, and N. A. Afshari, "Risk factors for progression to penetrating keratoplasty in patients with keratoconus," *American Journal of Ophthalmology*, vol. 140, no. 4, pp. 607–611, 2005.

[4] E. Spoerl, G. Wollensak, and T. Seiler, "Increased resistance of crosslinked cornea against enzymatic digestion," *Current Eye Research*, vol. 29, no. 1, pp. 35–40, 2004.

[5] M. Kohlhaas, E. Spoerl, T. Schilde, G. Unger, C. Wittig, and L. E. Pillunat, "Biomechanical evidence of the distribution of cross-links in corneastreated with riboflavin and ultraviolet a light," *Journal of Cataract and Refractive Surgery*, vol. 32, no. 2, pp. 279–283, 2006.

[6] G. Wollensak, E. Spoerl, and T. Seiler, "Stress-strain measurements of human and porcine corneas after riboflavin-ultraviolet-A-induced cross-linking," *Journal of Cataract and Refractive Surgery*, vol. 29, no. 9, pp. 1780–1785, 2003.

[7] F. Raiskup-Wolf, A. Hoyer, E. Spoerl, and L. E. Pillunat, "Collagen crosslinking with riboflavin and ultraviolet-A light in keratoconus: long-term results," *Journal of Cataract and Refractive Surgery*, vol. 34, no. 5, pp. 796–801, 2008.

[8] C. Wittig-Silva, M. Whiting, E. Lamoureux, R. G. Lindsay, L. J. Sullivan, and G. R. Snibson, "A randomized controlled trial of corneal collagen cross-linking in progressive keratoconus: preliminary results," *Journal of Refractive Surgery*, vol. 24, no. 7, pp. S720–S725, 2008.

[9] P. Vinciguerra, E. Albè, S. Trazza et al., "Refractive, topographic, tomographic, and aberrometric analysis of keratoconic eyes undergoing corneal cross-linking," *Ophthalmology*, vol. 116, no. 3, pp. 369–378, 2009.

[10] D. S. Grewal, G. S. Brar, R. Jain, V. Sood, M. Singla, and S. P. S. Grewal, "Corneal collagen crosslinking using riboflavin and ultraviolet-A light for keratoconus. One-year analysis using Scheimpflug imaging," *Journal of Cataract and Refractive Surgery*, vol. 35, no. 3, pp. 425–432, 2009.

[11] A. Caporossi, C. Mazzotta, S. Baiocchi, and T. Caporossi, "Long-term results of riboflavin ultraviolet a corneal collagen cross-linking for keratoconus in Italy: the siena eye cross study," *American Journal of Ophthalmology*, vol. 149, no. 4, pp. 585–593, 2010.

[12] D. P. S. O'Brart, E. Chan, K. Samaras, P. Patel, and S. P. Shah, "A randomised, prospective study to investigate the efficacy of riboflavin/ultraviolet A (370 nm) corneal collagen cross-linkage to halt the progression of keratoconus," *British Journal of Ophthalmology*, vol. 95, no. 11, pp. 1519–1524, 2011.

[13] D. Viswanathan and J. Males, "Prospective longitudinal study of corneal collagen cross-linking in progressive keratoconus," *Clinical and Experimental Ophthalmology*, vol. 41, no. 6, pp. 531–536, 2013.

[14] N. Soeters, A. Van der Lelij, R. van der Valk, and N. G. Tahzib, "Corneal crosslinking for progressive keratoconus in four children," *Journal of Pediatric Ophthalmology and Strabismus*, vol. 2148, pp. e26–e29, 2011.

[15] P. Vinciguerra, E. Albé, B. E. Frueh, S. Trazza, and D. Epstein, "Two-year corneal cross-linking results in patients younger than 18 years with documented progressive keratoconus," *American Journal of Ophthalmology*, vol. 154, no. 3, pp. 520–526, 2012.

[16] A. Caporossi, C. Mazzotta, S. Baiocchi, T. Caporossi, R. Denaro, and A. Balestrazzi, "Riboflavin-UVA-induced corneal collagen cross-linking in pediatric patients," *Cornea*, vol. 31, no. 3, pp. 227–231, 2012.

[17] R. Arora, D. Gupta, J. L. Goyal, and P. Jain, "Results of corneal collagen cross-linking in pediatric patients," *Journal of Refractive Surgery*, vol. 28, no. 11, pp. 759–762, 2012.

[18] G. Wollensak, E. Spoerl, and T. Seiler, "Riboflavin/ultraviolet-A-induced collagen crosslinking for the treatment of keratoconus," *American Journal of Ophthalmology*, vol. 135, no. 5, pp. 620–627, 2003.

[19] J. H. Krumeich and J. Daniel, "Live-epikeratophakia and deep lamellar keratoplasty for stage-related treatment of keratoconus," *Klinische Monatsblatter fur Augenheilkunde*, vol. 211, no. 2, pp. 94–100, 1997.

[20] E. Spoerl, M. Huhle, and T. Seiler, "Induction of cross-links in corneal tissue," *Experimental Eye Research*, vol. 66, no. 1, pp. 97–103, 1998.

[21] R. Vinciguerra, M. R. Romano, F. I. Camesasca et al., "Corneal cross-linking as a treatment for keratoconus: four-year morphologic and clinical outcomes with respect to patient age," *Ophthalmology*, vol. 120, no. 5, pp. 908–916, 2013.

[22] A. Magli, R. Forte, A. Tortori, L. Capasso, G. Marsico, and E. Piozzi, "Epithelium-off corneal collagen cross-linking versus transepithelial cross-linking for pediatric keratoconus," *Cornea*, vol. 32, no. 5, pp. 597–601, 2013.

[23] A. G. Salman, "Transepithelial corneal collagen crosslinking for progressive keratoconus in a pediatric age group," *Journal of Cataract and Refractive Surgery*, vol. 39, no. 8, pp. 1164–1170, 2013.

[24] N. Chatzis and F. Hafezi, "Progression of keratoconus and efficacy of corneal collagen cross-linking in children and adolescents," *Journal of Refractive Surgery*, vol. 28, no. 11, pp. 753–758, 2012.

Hindawi Publishing Corporation
BioMed Research International
Volume 2014, Article ID 292139, 8 pages
http://dx.doi.org/10.1155/2014/292139

Research Article

Trehalose-Based Eye Drops Preserve Viability and Functionality of Cultured Human Corneal Epithelial Cells during Desiccation

Aneta Hill-Bator,[1] Marta Misiuk-Hojło,[1] Krzysztof Marycz,[2] and Jakub Grzesiak[2]

[1] *Department of Ophthalmology, Medical University Wroclaw, Borowska 213, 50-556 Wroclaw, Poland*
[2] *Electron Microscopy Laboratory, University of Environmental and Life Sciences in Wroclaw, Kozuchowska 5b, 51-631 Wroclaw, Poland*

Correspondence should be addressed to Jakub Grzesiak; grzesiak.kuba@gmail.com

Received 28 February 2014; Revised 21 May 2014; Accepted 23 May 2014; Published 8 June 2014

Academic Editor: Ciro Costagliola

This paper presents the evaluation of cytoprotective ability of trehalose-based eye drops in comparison with commercially available preparations during the experimental desiccation of cultured human corneal epithelial cells. Cultured human corneal epithelial cells (hCEC) underwent incubation with 7 different, commercially available medicaments used commonly in dry eye syndrome treatment, followed by desiccation trial performed on air under the flow hood for 5, 15, 30, and 45 minutes. Cell viability was quantified by live/dead fluorescent assay, while the presence of apoptotic cells was estimated by immunofluorescent staining for active caspase 3 protein. The preservation of membrane functions was evaluated using neutral red staining, while the preservation of proper morphology and phenotype was determined by fluorescent staining for actin filaments, nuclei, and p63 protein. The trehalose-based eye drops showed the highest efficiency in prevention of cell death from desiccation; moreover, this preparation preserved the normal cellular morphology, functions of cell membrane, and proliferative activity more effectively than other tested medicaments.

1. Introduction

Dry eye syndrome is a wide spread disease, caused by environmental influence or organism's function disorders. These different grounds allowed dividing it on three types: simple dry eyes (SDE), autoimmune positive dry eyes (ADE), and Sjogren's syndrome (SS) [1]. Inadequate quantity of tears or pathologic composition of them puts up the superficial part of eyes on adverse conditions. Dry corneal epithelium is exposed to rubbing, leading to scar formation, irritation, and inflammation. It leads to various occurrences, including squamous metaplasia, corneal neovascularization, or thinning, among others [2]. In the tears of patients suffering dry eye syndrome, the presence of proinflammatory cytokines, such as interleukin-6 and tumor necrosis factor-alpha, is very common [3]. In case of ADE and SS, also the autoaggressive immunoglobulins causing additional inflammatory and allergic reactions can be found [4]. Different grounds limit the general therapy to symptomatic treatment of disorder's outcomes. Therefore, lack or deficiency of tears can be settled by lubricating the cornea with external preparations. There are many types of commercially available medicaments composed of various substances, which prevent the loss of moistness, promoting the wound healing or decreasing the inflammation. However, the mechanisms of their action are often connected with their water retention ability, like in hyaluronian- or carboxymethylcellulose-based preparations. The last investigations revealed a disaccharide named trehalose, which has been described as a protective factor for various cells [5]. It is a nonreducing disaccharide present in many prokaryotic and eukaryotic organisms, which plays a role as the source of energy and carbon. In plants and yeasts it also occurs as the signaling molecule with the ability of cell protection, mainly from desiccation, dehydration, extreme temperatures, or oxidation [6]. Experiment performed by Guo et al. showed that human primary fibroblasts transfected with adenovirus vector for induction of trehalose synthesis could be maintained alive in the dry state for up to five days [7]. Therefore, this molecule could be found as potential medicament in dry eye syndrome.

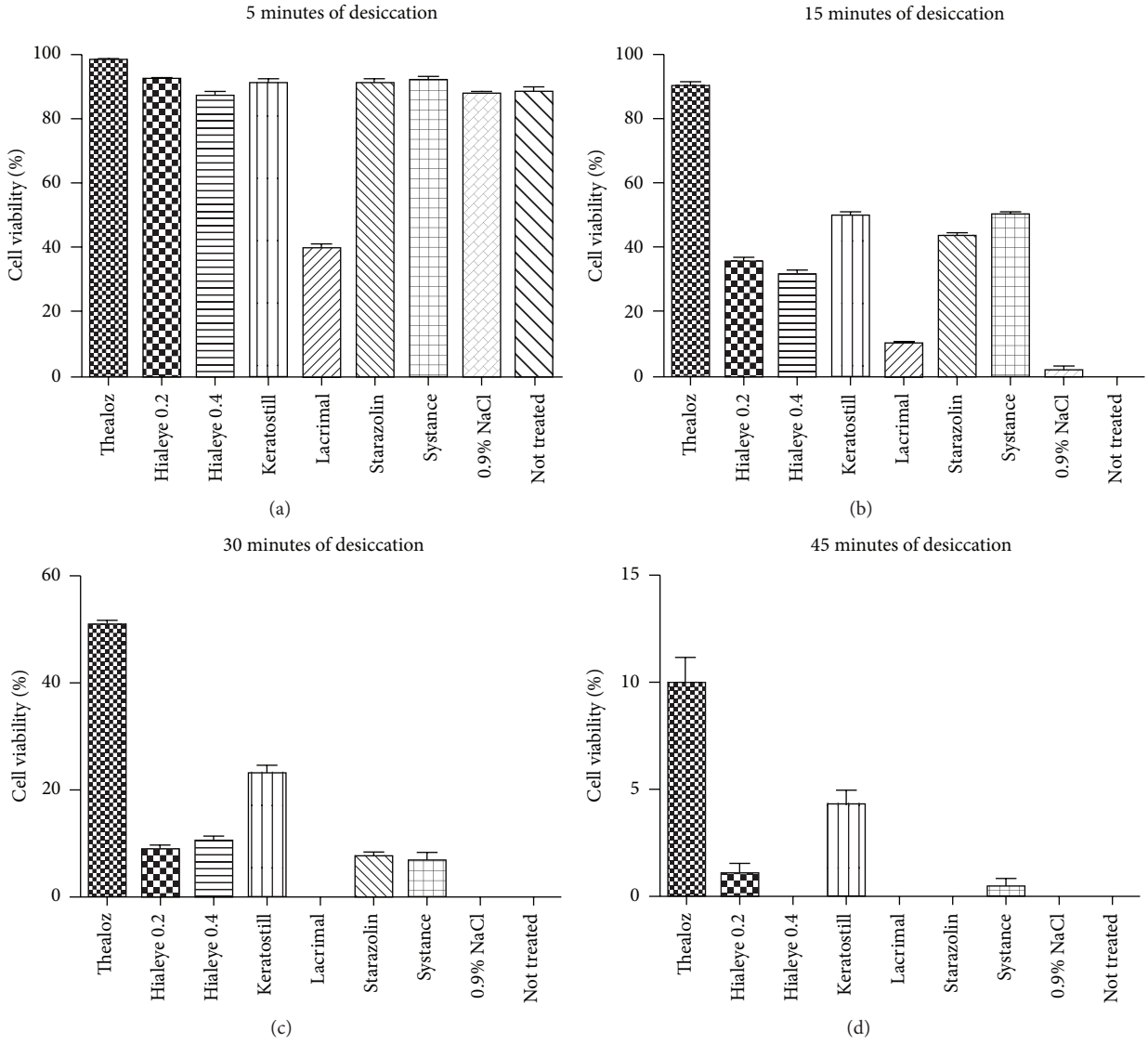

Figure 1: The results of live/dead assay made after 5, 15, 30, and 45 of desiccation, shown as percentage of living cells with standard deviation marked.

In the first experiments, applications of trehalose solution prevented the corneal epithelial cells from dying after drying during *in vitro* experiment [8]. As the natural cause of things, dry eye syndrome-treating preparations containing the trehalose occurred for commercial use. Therefore, we decided to compare the trehalose-based eye drops available on European market with six other, commonly used in clinical practice in a laboratory experiment. The efficiency in preservation of the viability and function of human corneal epithelial cells (hCEC) was evaluated during desiccation trials performed using *in vitro* cell culture model. Cells cultured as monolayer were dried by putting on air without any medium or liquid, pretreated before with medicaments encountered to this research, with respect to normal saline, and not treated control [9]. Cells were then analyzed for vitality by live/dead fluorescent staining and active caspase 3 detection and functionality by p63 protein detection and neutral red staining.

Tested preparations differed in composition and in the mechanism of protection, so substantial differences in results should be expected. Besides the trehalose sample, preparations were based on common viscoelastic substances known for keeping the moistness, like polyvinyl alcohol, hyaluronic acid, or methylcellulose. All results revealed trehalose-based medicament as the most effective in preventing the negative outcomes in hCEC cultures resulting from desiccation trials.

2. Materials and Methods

2.1. Cell Culture. Cell lines and all reagents used in this research were obtained from Life Technologies. 2 vials of frozen human corneal epithelial cells (5×10^5 cells/vial) were thawed and plated in T-25 flasks in Serum-Free Corneal Epithelium Medium at a concentration of 1.5×10^5 per T-25 flask. Prior to plating, the tissue culture flasks were coated

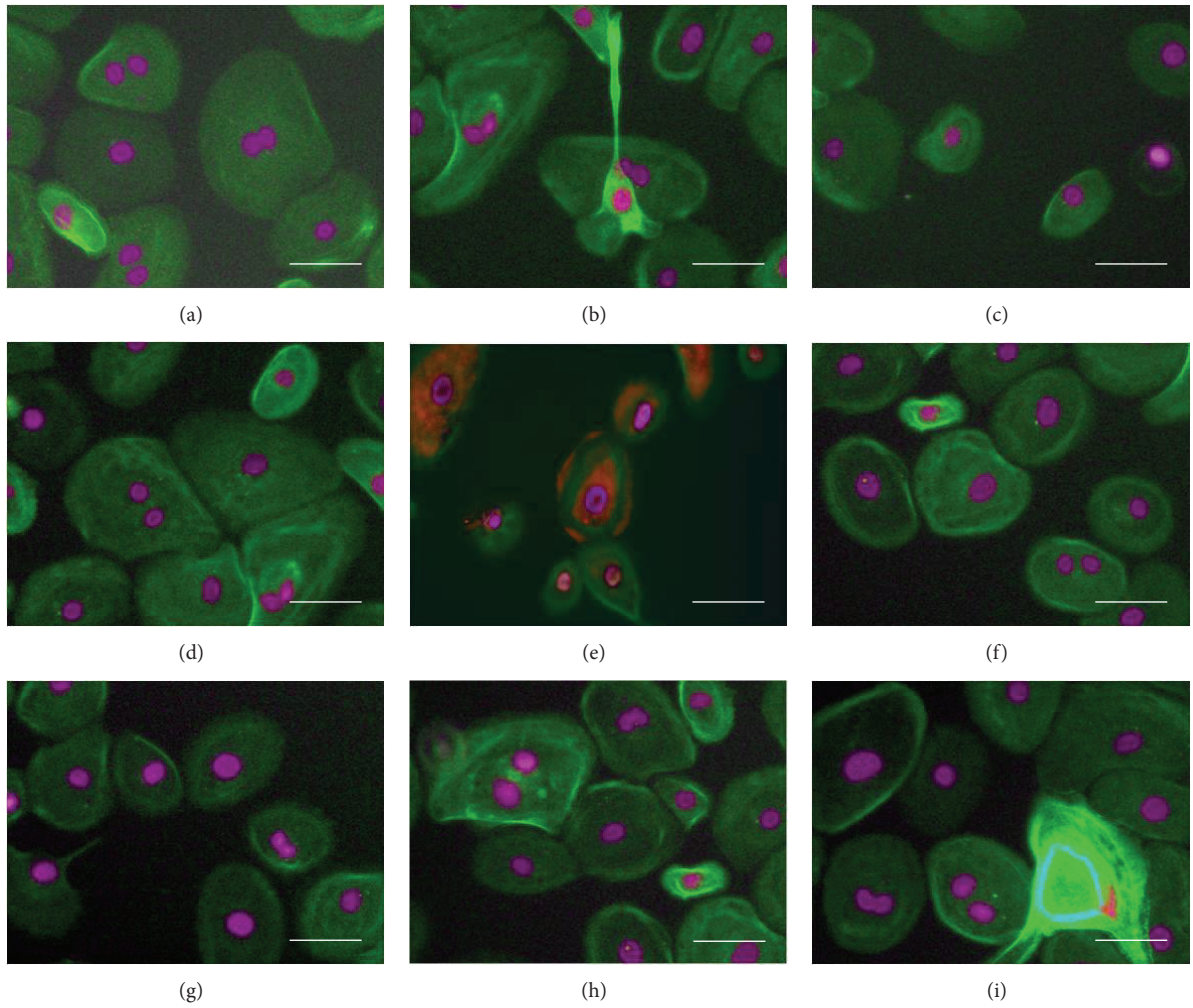

Figure 2: Immunocytochemical staining for active caspase 3 (red), actin (green), and nuclei (violet) in corneal epithelial cells after the treatment with tested preparations and 15 minutes of desiccation. Only in sample treated with Lacrimal (e) apoptotic cells were present; (a) Thealoz, (b) Hialeye 0.2, (c) Hialeye 0.4, (d) Keratostill, (e) Lacrimal, (f) Starazolin, (g) Systane, (h) 0.9% NaCl control, and (i) not treated control; magnification 200x; scale bar = 40 um.

with collagen for increasing the cell attachment. So prepared cultures were maintained in 37°C/5%CO_2/95% humidity until cells reached almost full confluency (5–7 days). Culture medium was changed every 48 hours. Confluent cultures were trypsinized with TrypLE Express and the cells were split to collagen-precoated, chambered coverslips at a concentration of 1×10^4 cells/cm^2. After cells adhered properly, they underwent experiments.

2.2. Eye Drops Application. The eye drops preparations for comparative analysis with Thealoz were chosen based on their commercial availability and popularity in patients. Additionally, they were chosen for different composition and preservatives included. The trade names, producers, and general compositions are shown in Table 1.

Epithelial cell monolayers were washed with warm normal saline and covered with seven kinds of preparations for five minutes ($n = 3$) in 37°C/5%CO_2/95% humidity. Control samples were treated with normal saline or not treated. After the incubation, preparations were discarded and the coverslips were put on air under the fume hood without any liquid for 5, 15, 30, and 45 minutes. In the next step they underwent evaluation of viability and functionality.

2.3. Live/Dead Assay. After the desiccation trial, cultures were stained with live/dead assay kit. Briefly, they were washed with PBS and incubated with fluorescent dyes (red propidium iodide indicated dead cells and green calcein-AM live cells) for 15 minutes. After that, dyes were discarded, layers washed with PBS and covered with Fluoromount (Sigma) to avoid bleaching. After staining, cells were examined under AxioObserver A1 inverted, fluorescent microscope (Zeiss). The number of live and dead cells was evaluated by manual counting of every repeat of every sample. The results were averaged and analyzed for statistical significance of differences between the Thealoz and other preparations using one-way analysis of variance (one-way ANOVA test), with

Table 1: Trademarks, producers, and components of tested eye drops. Data based on information provided by the producer.

Preparation (producer)	Composition
Thealoz (Thea)	3% trehalose; sodium chloride; trometamol; hydrochloric acid; water for injections
Hialeye 0.2 (Blaufarma)	0.2% sodium hyaluronate; disodium phosphate; sodium dihydro orthophosphate; sodium chloride; sodium edetate; benzalkonium chloride; water for injections
Hialeye 0.4 (Blaufarma)	0.4% sodium hyaluronate; disodium phosphate; sodium dihydro orthophosphate; sodium chloride; sodium edetate; benzalkonium chloride; water for injections
Keratostill (Bruschettini S.R.I.)	0.3% hydroxypropyl methylcellulose; dexpanthenol; EDTA; dibasic sodium phosphate; deionized water; cetrimide 0.01%
Lacrimal (WZF Polfa)	Polyvinyl alcohol; 12-water disodium phosphate; sodium dihydrophosphate monohydrate; sodium chloride; benzalkonium chloride; deionized water
Starazolin hydrobalance (Polpharma OTC)	0.1% sodium hyaluronate; sodium chloride; sodium orthophosphate; sodium tetraborate stabilized with phosphonic acid
Systane (Alcon)	Polyethylene glycol 400; polypropylene glycol; hydroxy propylene guar; sorbitol; aminomethyl propanol; boric acid; potassium chloride; sodium chloride; 0.001% polidronium chloride

Bonferroni posttest determining the statistical significance of differences between all other preparations (GraphPad Prism, GraphPad Software).

For detection of apoptotic cells, immunocytochemical staining for active caspase 3 was applied. Prior to fixation, cells were allowed to give a response on desiccation trial by incubating them in medium and 37°C/5%CO_2/95% humidity for one hour. After incubation, cells were washed with PBS and fixed with 3.7% cold paraformaldehyde for 10 minutes. After fixation, cells were triple washed in PBS with 1% FBS and permeabilized with Triton X-100 (0.1% in PBS) for 15 minutes at room temperature. In the next step, cells were triple washed and incubated with primary antiactive caspase 3 antibody produced in rabbit for one hour in 37°C/5%CO_2/95% humidity, followed by triple washing and incubation with secondary anti-rabbit IgG-atto-594 antibody for one hour in 37°C/5%CO_2/95% humidity. After triple washing, cells were incubated with phalloidin-atto-488 dye for visualization of f-actin and DAPI for nuclei staining. Cells were triple washed, covered with fluoromount, and observed in fluorescent, inverted microscope. The documentation was made using Cannon PowerShot Camera.

2.4. Functionality Test. For functionality test, samples desiccated for 15 minutes were chosen, in view of optimal cell number obtained from viability assay. Cells were evaluated for the presence of p63 protein by immunofluorescent staining. After desiccation trials, cells were washed in PBS, covered with medium, and incubated in 37°C/5%CO_2/95% humidity for one hour. In the next step, cells were washed with PBS, fixed with 3.7% cold paraformaldehyde for 10 minutes at room temperature, triple washed in PBS, and permeabilized with Triton X-100 (0.1% in PBS) for 15 minutes. After triple washing, cells were incubated with primary anti-p63 antibody produced in rabbit for one hour at 37°C/5%CO_2/95% humidity, followed by triple washing and incubation with secondary anti-rabbit IgG-atto 594 for one hour at 37°C/5%CO_2/95% humidity. After triple washing, cells were incubated with phalloidin-atto-488 dye for visualization of f-actin and DAPI for nuclei staining. Cells were triple washed, covered with fluoromount, and observed in fluorescent, inverted microscope. The documentation was made using digital Cannon PowerShot Camera. Cells were evaluated for p63 presence or absence and localization of detected protein.

For evaluation of cell membrane function, neutral red staining was applied. After desiccation trials, cells were washed in PBS and incubated in medium at 37°C/5%CO_2/95% humidity for one hour. In the next step cells were incubated with neutral red dye for 15 minutes, washed triple times in PBS, and observed and documented using inverted microscope and digital camera. Cells were evaluated for visible dye uptake, which indicates the proper cellular membrane function.

3. Results

3.1. Live/Dead Assay. After application of different eye drops and desiccation trials, substantial differences in cell viability could be noticed between particular preparations. After 5 minutes of desiccation, similar results from 6 preparations were obtained. The samples treated with Thealoz showed the statistically higher viable cell number ($P < 0.01$) than 0.9% NaCl control-treated samples. Lacrimal samples showed the lowest cell number prominently different from other results. After 15 minutes of desiccation, Thealoz samples showed the highest effectiveness in preventing cell death ($P < 0.01$), while the remaining preparations could be ordered from more to less efficient: Keratostill, Starazolin,

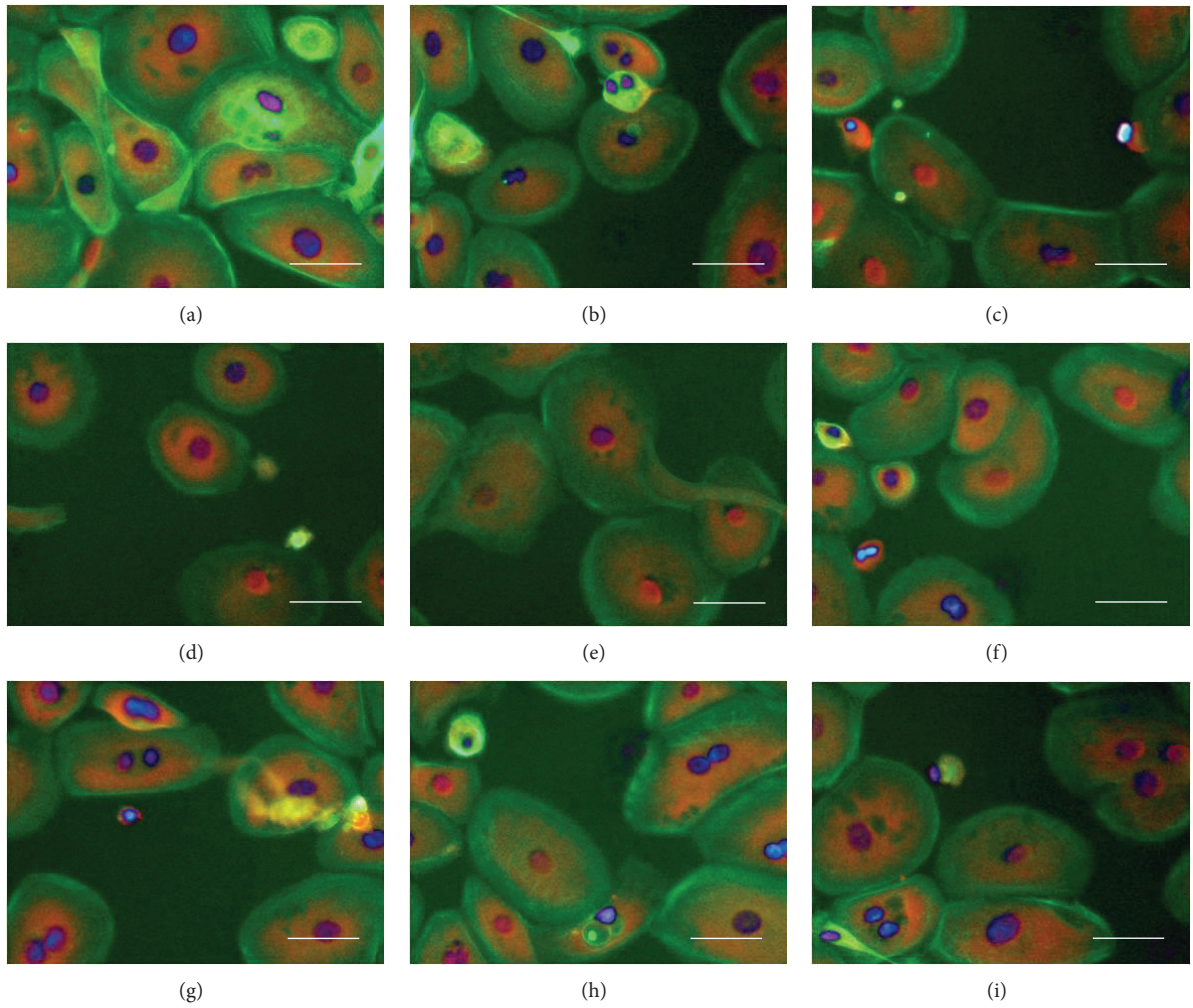

Figure 3: Immunocytochemical stainings for p63 (red), actin (green), and nuclei (blue/violet) in corneal epithelial cells after the treatment with tested preparations and 15 minutes of desiccation. The presence of p63 protein in nuclei and cytoplasm is prominent in all tested cells; (a) Thealoz, (b) Hialeye 0.2, (c) Hialeye 0.4, (d) Keratostill, (e) Lacrimal, (f) Starazolin, (g) Systane, (h) 0.9% NaCl control, and (i) not treated control; magnification 200x; scale bar = 40 um.

Systane, Hialeye 0.2 and Hialeye 0.4, and Lacrimal as the least efficient, respectively; statistically no significant differences were obtained between two pairs of preparation: Keratostill and Systane and between Hialeye 0.2 and 0.4 ($P > 0.05$). After 30 minutes of desiccation, Thealoz was still the most effective ($P < 0.01$). The second most effective preparation was determined as Keratostill, while the Hialeye 0.2 and 0.4, Starazolin, and Systane showed similar results ($P > 0.05$), slightly less effective than Keratostill. In Lacrimal samples no viable cell could be noticed. After 45 minutes of desiccation, the only viable cells were detected in Thealoz and Keratostill samples. The difference between these two samples and 0.9% NaCl control was statistically significant ($P < 0.01$). Detailed results are shown in Table 2 and Figure 1.

Interestingly, the only apoptotic cells were detected in Lacrimal samples, with prominently visible active caspase 3 and characteristic changes in cellular morphology determined by actin filaments and in nuclei structure (Figure 2(e)).

3.2. Functionality Test. Microscopic observations revealed cells with characteristic, epithelial morphology with actin organized smoothly without visible filaments, keeping cells in round shape. Evaluation of p63 protein presence showed its proper localization in every sample also in 0.9% NaCl and not treated control (Figures 3(a)–3(i)).

However, the neutral red staining showed different effects of applied eye drops on cellular membrane functionality and endosomal transportation system. In samples treated with Thealoz and Keratostill, the neutral red dye uptake was prominent (Figures 4(a) and 4(d), resp.). In the remaining samples, cells did not stain which indicated the loss of cellular membrane function (Figures 4(b)-4(c) and 4(e)–4(i)).

4. Discussion

Dry eye syndrome is a chronic disease, which can be induced by various factors. Therefore, any general treatment has not

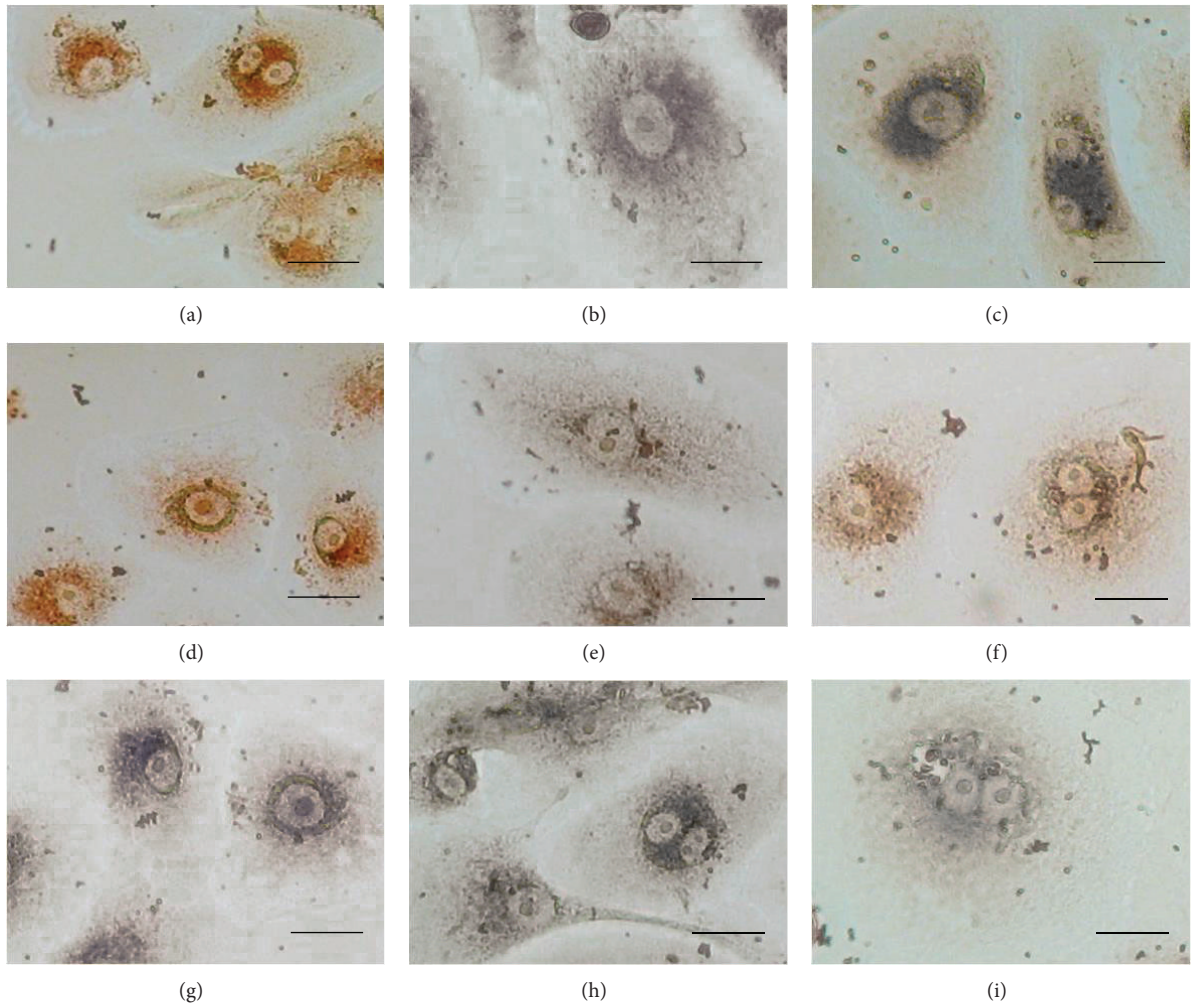

Figure 4: The neutral red staining of corneal epithelial cells after treatment with tested preparations and 15 minutes of desiccation. Only in cells treated with Thealoz (a) and Keratostill (d) a dye uptake may be observed. In the remaining samples only slight or no reaction was noticed. (a) Thealoz, (b) Hialeye 0.2, (c) Hialeye 0.4, (d) Keratostill, (e) Lacrimal, (f) Starazolin, (g) Systane, (h) 0.9% NaCl control, and (i) not treated control; magnification 400x; scale bar = 20 um.

been elaborated yet, although there are preparations that help in keeping the eye in moistness. The most of available preparations are based on hyaluronic acid (HA) or carboxymethylcellulose (CMC). The protection mechanism of hyaluronian-based eye drops is connected with HA's natural lubricating ability, by both binding the water and adsorbing to the ocular surface without allergic reactions [10]. CMC is the main compound of artificial tear drops. It is a high-molecular-weight polysaccharide with mucoadhesive properties, which allow the preparation for prolonged residence time on the ocular surface. It has been shown that application of CMC onto damaged cornea significantly enhances the wound healing process, although the mechanism of this action remains unclear [11]. Due to the discovery of the trehalose's antidehydrating nature, it was concluded that it may help in dry eye syndrome. This disaccharide not only protects cells from desiccation, but also is able to preserve the cell membrane and membrane proteins from deactivation or denaturation, as it was shown by others [6]. We state that this feature of trehalose is the most important advantage, resulting in highest cell survival ratio and maintenance of cell membrane function. In our research, one preparation was based on CMC derivate-the hydroxypropyl methylcellulose (Keratostill). The live/dead assay showed Keratostill, after the Thealoz, as the most effective in cell death prevention. Additionally, these particular eye drops together with Thealoz were able to preserve the function of cellular membrane and retain the intracellular transportation system, which was indicated by neutral red staining. Thus we conclude that this preparation has also the capacity to protect cell membranes during desiccation; however, the mechanism is still uncovered. On the other hand, preparations containing other active agents resulted in less cell survival ratio and even induced apoptosis (Lacrimal). This preparation is based on polyvinyl alcohol, commonly used in artificial tears, which possess high oxygen barrier properties [12, 13]. Basing on the fact that epithelial cells obtain the oxygen directly from atmospheric air not from blood, we conclude that these outstanding

Table 2: Results from live/dead assay at all time points, shown as mean percentage of living cells, with standard deviation (st. dev.), max and min, and *P* value in comparison to 0.9% NaCl control.

(a)

	5 min					15 min				
	Mean [%]	St. dev.	Max	Min	*P* value	Mean [%]	St. dev.	Max	Min	*P* value
Thealoz	98.77	0.45	99.2	98.3	<0.01	90.65	2.05	92.1	89.2	<0.01
Hialeye 0.2	92.63	0.75	93.4	91.9	<0.05	35.1	2.26	36.7	33.5	<0.01
Hialeye 0.4	87.37	2.34	89.1	84.7	ns	32.1	0.28	32.3	31.9	<0.01
Keratostill	92	1.1	93.1	90.9	ns	50.05	3.04	52.2	47.9	<0.01
Lacrimal	40.1	1.34	41.2	38.6	<0.01	10.25	1.48	11.3	9.2	<0.01
Starazolin	91.53	1.62	93.3	90.1	ns	44.05	0.35	44.3	43.8	<0.01
Systane	92.9	0.36	93.2	92.5	<0.05	50	0.28	50.2	49.8	<0.01
0.9% NaCl	88.43	1.17	89.7	87.4		2.4	1.13	3.2	1.6	
Not treated	89.63	1.12	90.6	88.4		0	0	0	0	

(b)

	30 min					45 min				
	Mean [%]	St. dev.	Max	Min	*P* value	Mean [%]	St. dev.	Max	Min	*P* value
Thealoz	51.75	1.48	52.8	50.7	<0.01	10.25	2.76	12.2	8.3	<0.01
Hialeye 0.2	8.15	0.35	8.4	7.9	<0.01	0.6	0.85	1.2	0	ns
Hialeye 0.4	11.2	1.55	12.3	10.1	<0.01	0	0	0	0	ns
Keratostill	23.5	2.83	25.5	21.5	<0.01	4.45	1.77	5.7	3.2	<0.01
Lacrimal	0	0	0	0	ns	0	0	0	0	ns
Starazolin	7.85	0.35	8.1	7.6	<0.01	0	0	0	0	ns
Systane	6.85	3.32	9.2	4.5	<0.01	0.6	0.85	1.2	0	ns
0.9% NaCl	0	0	0	0		0	0	0	0	
Not treated	0	0	0	0		0	0	0	0	

results of Lacrimal could be caused by the lack of oxygen. While the Thealoz is preservatives-free, we conclude that these significant differences in cytoprotective ability between preparations may also result from the presence of particular preservatives, like benzalkonium chloride (BAK, in Hialeye and Lacrimal) or polidronium chloride (Polyquad, PQ in Systane). As it was shown by others, BAK induces cell death and arrests cell growth even at low concentration [14, 15]. The cytotoxic effect of PQ can also be noticed, although it seems to be much less prominent when compared to BAK [16]. Interestingly, the preparation Hialeye 0.2 was more effective than Hialeye 0.4 only after 5-minute desiccation trial, which has the concentration of HA two times greater. We suspect that in Hialeye 0.4, besides the higher concentration of HA there is also a higher concentration of BAK, although such information was not provided by the producer. Finally, the expression of p63 protein was not altered in any sample. This molecule is connected with proliferation and stratification of CEC progenitors [17, 18], so we conclude that none of preparation has the negative influence on normal corneal regeneration.

In conclusions, the preparation based on trehalose showed the highest effectiveness in preventing cell death from desiccation and in keeping the function of cellular membranes, in comparison to other eye drops. Additionally, we confirmed that different preservatives have different negative effect on cell function and viability, as it was shown by others. Therefore, the trehalose-based, preservative-free eye drops are the advanced medicament for dry eye syndrome disease.

Conflict of Interests

The authors declare no commercial association and no conflict of interests regarding this research and paper.

References

[1] K. Tsubota, I. Toda, Y. Yagi, Y. Ogawa, M. Ono, and K. Yoshino, "Three different types of dry eye syndrome," *Cornea*, vol. 13, no. 3, pp. 202–209, 1994.

[2] B. Miljanović, R. Dana, D. A. Sullivan, and D. A. Schaumberg, "Impact of dry eye syndrome on vision-related quality of life," *The American Journal of Ophthalmology*, vol. 143, no. 3, pp. 409–415, 2007.

[3] K.-C. Yoon, I.-Y. Jeong, Y.-G. Park, and S.-Y. Yang, "Interleukin-6 and tumor necrosis factor-α levels in tears of patients with dry eye syndrome," *Cornea*, vol. 26, no. 4, pp. 431–437, 2007.

[4] M.-A. Javadi and S. Feizi, "Dry eye syndrome," *Journal of Ophthalmic and Vision Research*, vol. 6, no. 3, pp. 192–198, 2011.

[5] S. B. Leslie, E. Israeli, B. Lighthart, J. H. Crowe, and L. M. Crowe, "Trehalose and sucrose protect both membranes and proteins in intact bacteria during drying," *Applied and Environmental Microbiology*, vol. 61, no. 10, pp. 3592–3597, 1995.

[6] A. D. Elbein, Y. T. Pan, I. Pastuszak, and D. Carroll, "New insights on trehalose: a multifunctional molecule," *Glycobiology*, vol. 13, no. 4, pp. 17R–27R, 2003.

[7] N. Guo, I. Puhlev, D. R. Brown, J. Mansbridge, and F. Levine, "Trehalose expression confers desiccation tolerance on human cells," *Nature Biotechnology*, vol. 18, no. 2, pp. 168–171, 2000.

[8] T. Matsuo, "Trehalose protects corneal epithelial cells from death by drying," *British Journal of Ophthalmology*, vol. 85, no. 5, pp. 610–612, 2001.

[9] K. Paulsen, S. Maile, J. Giebel, and F. Tost, "Lubricating agents differ in their protection of cultured human epithelial cells against desiccation," *Medical Science Monitor*, vol. 14, no. 6, pp. PI12–PI16, 2008.

[10] P. Aragona, V. Papa, A. Micali, M. Santocono, and G. Milazzo, "Long term treatment with sodium hyaluronate-containing artificial tears reduces ocular surface damage in patients with dry eye," *British Journal of Ophthalmology*, vol. 86, no. 2, pp. 181–184, 2002.

[11] Q. Garrett, P. A. Simmons, S. Xu et al., "Carboxymethylcellulose binds to human corneal epithelial cells and is a modulator of corneal epithelial wound healing," *Investigative Ophthalmology and Visual Science*, vol. 48, no. 4, pp. 1559–1567, 2007.

[12] Y. Sultana, R. Jain, M. Aqil, and A. Ali, "Review of ocular drug delivery," *Current Drug Delivery*, vol. 3, no. 2, pp. 207–217, 2006.

[13] J. D. Nelson and R. L. Farris, "Sodium hyaluronate and polyvinyl alcohol artificial tear preparations. A comparison in patients with keratoconjunctivitis sicca," *Archives of Ophthalmology*, vol. 106, no. 4, pp. 484–487, 1988.

[14] M. de Saint Jean, F. Brignole, A.-F. Bringuier, A. Bauchet, G. Feldmann, and C. Baudouin, "Effects of benzalkonium chloride on growth and survival of Chang conjunctival cells," *Investigative Ophthalmology and Visual Science*, vol. 40, no. 3, pp. 619–630, 1999.

[15] S. P. Epstein, M. Ahdoot, E. Marcus, and P. A. Asbell, "Comparative toxicity of preservatives on immortalized corneal and conjunctival epithelial cells," *Journal of Ocular Pharmacology and Therapeutics*, vol. 25, no. 2, pp. 113–119, 2009.

[16] D. A. Ammar, R. J. Noecker, and M. Y. Kahook, "Effects of benzalkonium chloride- and polyquad-preserved combination glaucoma medications on cultured human ocular surface cells," *Advances in Therapy*, vol. 28, no. 6, pp. 501–510, 2011.

[17] L. Chenzuo and J. Murube, "P63 staining on human ocular surface," *Sociedad Canaria de Oftalmologia*, vol. 14, pp. 15–19, 2003.

[18] M. Senoo, F. Pinto, C. P. Crum, and F. McKeon, "p63 is essential for the proliferative potential of stem cells in stratified epithelia," *Cell*, vol. 129, no. 3, pp. 523–536, 2007.